P.D.
539.7
G 326
v 4, No 4

POWER REACTOR TECHNOLOGY

A Quarterly Technical Progress Review

Prepared for DIVISION of TECHNICAL INFORMATION,
U. S. ATOMIC ENERGY COMMISSION, by GENERAL NUCLEAR ENGINEERING CORP.

ILLINOIS STATE LIBRARY
DEC 19 1961
Documents Deposit

September 1961

● VOLUME 4

● NUMBER 4

TECHNICAL PROGRESS REVIEWS

To meet the needs of industry for concise summaries of current atomic developments, the Atomic Energy Commission is publishing this series, Technical Progress Reviews. Issued quarterly, each of the reviews digests and evaluates the latest findings in a specific area of nuclear technology and science.

The four journals published in this series are:

Nuclear Safety, W. B. Cottrell, editor, R. A. Charpie, advisory editor, and associates, Oak Ridge National Laboratory

Power Reactor Technology, Walter H. Zinn and associates, General Nuclear Engineering Corporation

Reactor Core Materials (covering solid material developments), R. W. Dayton, E. M. Simons, and associates, Battelle Memorial Institute

Reactor Fuel Processing, Stephen Lawroski and associates, Chemical Engineering Division, Argonne National Laboratory

Each journal may be purchased ($2.00 per year for subscription and individual issues $0.55) from the Superintendent of Documents, U. S. Government Printing Office, Washington 25, D. C. See back cover for remittance instructions and foreign postage requirements.

The views expressed in this publication do not necessarily represent those of the United States Atomic Energy Commission, its divisions or offices, or of any Commission advisory committee or contractor.

Availability of Reports Cited in This Review

Unclassified AEC reports are available for inspection at AEC depository libraries and are sold by the Office of Technical Services, Department of Commerce, Washington 25, D. C. Some of the reports cited are not available owing to their preliminary nature; however, the information contained in them will eventually be made available in formal progress or topical reports.

Unclassified reports issued by other Government agencies or private organizations should be requested from the originator.

Unclassified British and Canadian reports may be inspected at AEC depository libraries. British reports are sold by the British Information Service, 45 Rockefeller Plaza, New York, N. Y.; Canadian reports (AECL series) are sold by the Scientific Document Distribution Office, Atomic Energy of Canada, Ltd., Chalk River, Ontario, Canada.

Classified U. S. and foreign reports identified in this journal as Classified may be purchased by properly cleared Access Permit Holders from the Division of Technical Information Extension, U. S. Atomic Energy Commission, P. O. Box 1001, Oak Ridge, Tenn. Such reports may be inspected at classified AEC depository libraries.

POWER REACTOR TECHNOLOGY

A REVIEW OF RECENT DEVELOPMENTS

Prepared for DIVISION of TECHNICAL INFORMATION,
U. S. ATOMIC ENERGY COMMISSION,
by GENERAL NUCLEAR ENGINEERING CORP.

● SEPT. 1961

● VOLUME 4

● NUMBER 4

foreword

This quarterly review of reactor development has been prepared at the request of the Division of Technical Information of the U. S. Atomic Energy Commission. Its purpose is to assist interested organizations in the task of keeping abreast of new results in reactor technology for civilian application.

Power Reactor Technology contains reviews of selected recently published reports that are judged noteworthy, in the fields of power-reactor research and development, power-reactor applications, design practice, and operating experience. It is not meant to be a comprehensive abstract of all material published during the quarter, nor is it meant to be a treatise on any part of the subject. However, related articles are often treated together to yield reviews having some breadth of scope, and from time to time background material is added to place recent developments in perspective.

The intention is to cover the various areas of reactor development from the general viewpoint of the reactor designer rather than from the more detailed points of view of specialists in the individual areas. To whatever extent the coverage of *Power Reactor Technology* may occasionally overlap the fields of the other Technical Progress Reviews, the overlaps will be motivated by this objective of viewing current progress through the eyes of the reactor designer.

A degree of critical appraisal and some interpretation of results are often necessary to define the significance of reported work. Any such appraisals or interpretations represent only the opinions of the reviewers and the editor of *Power Reactor Technology*, who are General Nuclear Engineering Corporation personnel. Readers are urged to consult the original references in order to obtain all the background of the work reported and to obtain the interpretation of the results given by the original authors.

W. H. ZINN, President
J. R. DIETRICH, Vice President and Editor
General Nuclear Engineering Corporation

Issued quarterly by the U. S. Atomic Energy Commission. Use of funds for printing this publication approved by the Director of the Bureau of the Budget on November 1, 1960.

contents

Foreword

1 I ECONOMICS

1 New Uranium Prices
2 Costs of Nuclear Power
7 Small Plant Studies
10 References

11 II REACTOR PHYSICS

11 Critical and Exponential Experiments
13 Evaluation of Criticality Hazards
14 Doppler Effect
17 References

19 III HEAT TRANSFER

19 Liquid Metals
19 Conduction
20 Spray Cooling
25 Boiling Water: Burnout
28 Two-Phase Flow
29 References

31 IV DYNAMICS AND SAFETY: PRESSURE-WAVE PROPAGATION IN STEAM-WATER MIXTURES

32 V SHIELDING

32 Dose-Rate Calculations of Air-Scattered Gamma Radiation
32 Radioisotope Data
33 References

34 VI INSTRUMENTATION

34 In-Core Instrumentation
36 New Instrument Developments
36 References

37 VII FUEL CYCLES: THORIUM

37 Reactivity Transient in Irradiated Thorium
37 Long-Term Reactivity Changes in Irradiated Thorium
38 References

39 VIII CONTROL-ROD MATERIALS

39 Reactivity Worth
41 Effects of Burnup on Reactivity Worth
42 Corrosion and Radiation Effects on Borides
43 Operating Experience with Control-Rod Materials
46 References

47 IX STEAM-CYCLE EFFICIENCY

50 X DESIGN PRACTICE

50 Recent ASME Boiler Code Nuclear Code Cases
51 British Requirements for Inspection and Design of Primary Circuits and Pressure Vessels of Nuclear Power Plants
54 Valves for the Hallam Reactor
54 The Dresden Nuclear Power Station
68 References

69 XI OPERATING EXPERIENCE

69 Yankee
70 Leakage of Pumps and Valves for D_2O Reactors
73 Design Modifications to the Sodium Reactor Experiment
75 References

76 XII ORGANIC-MODERATED REACTORS

84 XIII FAST BREEDERS

97 INDEX, VOLUME 4

Errata

Through an editing error, the March 1961 issue of *Power Reactor Technology* (Vol. 4, No. 2, page 73) stated that the Carolinas-Virginia Pressure Tube Reactor (CVTR) is being financed by the AEC. Only the research and development program for this "third round" heavy-water-cooled and -moderated reactor is being financed by the AEC. Except for certain use charges on fuel and D_2O, all capital costs and operating expenses of the reactor and its associated steam plant will be borne by Carolinas Virginia Nuclear Power Associates, Inc. (CVNPA). The nuclear steam plant is located on a site at Parr, S. C., leased by CVNPA from the South Carolina Electric and Gas Company. Steam from the plant will be sold to the South Carolina Electric and Gas Company for use in the generation of electricity in its adjacent conventional turbogenerator plant. CVNPA is a nonprofit corporation sponsored by the following companies: Carolina Power and Light Company, Duke Power Company, South Carolina Electric and Gas Company, and Virginia Electric and Power Company.

* * * * *

In the March 1961 issue of *Power Reactor Technology* (Vol. 4, No. 2, page 19), the units in Table IV-7 should read as follows:

Dynamic viscosity, lb/(ft)(sec) $\times 10^6$,
at indicated pressure

Section I ECONOMICS

New Uranium Prices

The AEC has reduced its base prices for enriched and depleted uranium[1,2] by amounts said to be consistent with the price of $8 per pound for U_3O_8 in natural-uranium concentrates, which was established under the AEC domestic purchase program for the period Apr. 1, 1962, to Dec. 31, 1966. The new price schedule went into effect on July 1, 1961. It will apply to material leased or sold under domestic and foreign arrangements in the future and also, where appropriate, to material now under lease.

The changes in the price schedule for enriched and depleted material are those that would be expected to occur, as a result of a change in the cost of feed material, on the basis of the theory of the isotope separation process (see the December 1960 issue of *Power Reactor Technology*, Vol. 4, No. 1, pages 3 to 5). The percentage reduction in price varies from 63 per cent for depleted material of 0.40 per cent U^{235} content to 40 per cent for material of near-natural enrichment to 20 per cent for highly enriched material of 90 per cent U^{235} content. The decrease in the percentage price reduction with the increase in enrichment occurs because the cost of the feed material contributes a lesser fraction of the product cost—and the cost of isotope separation contributes a greater fraction—as enrichment of the product increases. However, the amount of feed required per gram of U^{235} in the product increases with product enrichment, and therefore the absolute price reduction per gram of U^{235} in the product also increases with enrichment. The absolute reduction ranges from $1.29 per gram of contained U^{235} at 0.4 per cent enrichment to $2.21 in the natural enrichment range to $3.32 at 90 per cent enrichment. The new price schedule, per gram of contained U^{235}, and the price reduction are plotted in Fig. I-1. The previous price schedule was discussed in the December 1957 and March 1960 issues of *Power Reactor Technology*, Vol. 1, No. 1, pages 1 to 3, and Vol. 3, No. 2, pages 19 and 20.

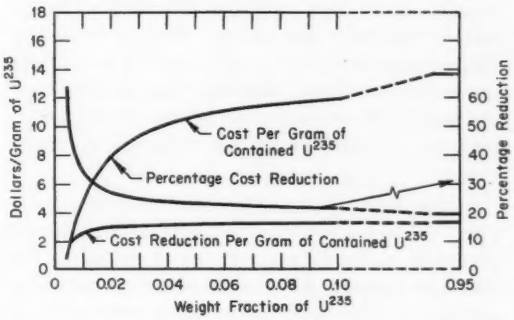

Fig. I-1 New base-charges[2] for enriched uranium as UF_6.

Simultaneously with the reduction in base prices, the use-charge rate was increased from 4 to 4.75 per cent per year to take account of increases in the cost of money to the U. S. Government. This amounts to an increase of about 19 per cent; therefore the net effect on use charges of the increase in rate and the decrease in base price will be nearly zero for highly enriched reactors, whereas the reactors of lower enrichment will benefit slightly in this respect.

The revised price schedule does not extend to U^{233} and plutonium; prices for these materials remain at the levels previously established for the period through June 30, 1963. The announcement of the revised schedule does state, however, that if the fuel values of U^{233} and plutonium were related to the new uranium prices, they would drop from $15 to $12 per gram, and from $12 to $9.50 per gram, respectively. The an-

nouncement also states that the Commission is considering the transition measures that would be necessary over a period of time if a change were made from Government to private ownership of special nuclear material.

The effect of the new uranium prices on net reactor fuel costs will vary with the fuel enrichment and with the neutron economy of the reactor. The greatest absolute benefit will occur in the case of a reactor using "fully" enriched fuel, which will amount to a fuel cost reduction of 0.6 mill/kw-hr. For water-moderated reactors using enrichments in the approximate range 1.5 to 3.5 per cent, it appears that the fuel cost reductions may range from about 0.3 to 0.5 mill/kw-hr (so long as the plutonium buy-back price remains unchanged). The larger savings are usually associated with the reactors of higher fuel enrichment and poorer neutron economy. These reductions will reflect mainly reductions in net burnup cost, although they will include the effects of net reduction of use charge, which will be significant in the lower enrichment range.

In the special case of natural-uranium reactors, the price revision will amount to a strong increase in the attractiveness of extending fuel lifetime through the use of slight enrichment. Before the revision, there was a step increase from the open-market price of natural uranium to the Government price for uranium of very slight enrichment. The revision practically eliminates that step; indeed, one can now use uranium of 1.1 per cent enrichment for about the same cost as the previously scheduled cost of natural uranium.

It seems unlikely that, as power-reactor designers take account of the new prices, the net effect will be simply a change in fuel burnup and inventory charges. Rather, new economic design points will be found in which the lower uranium costs will be exploited to decrease the costs due to "nonnuclear" components and materials, probably at the expense of neutron economy and basic fuel utilization.

Costs of Nuclear Power

Reference 3 is a review of the components of the total cost of nuclear power generation, of the factors affecting those components, and of the costs for nuclear plants now in operation, under construction, or planned. Since the report itself is highly condensed, a comprehensive summary would not serve a useful purpose; the following discussion confines attention to a few of the most interesting points. Reference to the report is recommended for those who have more than a casual interest in the subject.

Table I-1 gives the construction costs for several reactors, broken down into categories based on the classification for nuclear plants in the revised System of Accounts published by the Federal Power Commission (*Federal Register*, May 14, 1959). Not included are costs of research and development, training, nuclear fuel, fuel fabrication, electric substations, and transmission lines. The names of most of the categories are reasonably self-explanatory. The category "reactor plant equipment" includes the moderator, if the moderator is purchased. The D_2O cost is included for CANDU ($59 per kilowatt) but not for the Carolinas-Virginia plant. The category "miscellaneous power plant equipment" includes such items as cranes and hoisting equipment; compressed-air and cleaning systems; furniture; communications, fire-extinguishing, and station-maintenance equipment; laboratory, test, and weather instruments; and service-water-treatment systems. "Additional indirect construction costs" include items, prior to and during construction, such as: design, engineering, field superintendence, inspection, accounting, purchasing, taxes, insurance, contributions, and fees; also the expenses of operating during the initial test period, to the extent that they are not compensated by operating revenue.

The costs given in Table I-1 have been converted in Table I-2 to costs per kilowatt of electrical capacity. From the two tables one would conclude that the number of plants built and under construction is still too small to support useful generalizations on total construction costs; but the cost breakdowns are informative and reveal some differences between specific reactors which are probably incidental and not characteristic of the reactor types.

The fabrication costs of the first cores for a number of reactors are tabulated in Table I-3. For the oxide cases, at least, these figures show a rather definite downward trend with time. They also give some indication as to fabrication-cost differences between steel- and Zircaloy-jacketed oxide elements; however, when steel is used for jacketing, there is a tendency to use

Table I-1 REPORTED CONSTRUCTION COSTS BY MAJOR CATEGORIES FOR SPECIFIC NUCLEAR POWER PLANTS[3]

Plant type and name	Land and land rights	Structures and improvements	Reactor plant equipment	Turbo-generator and accessory equipment	Misc. power plant equipment	Interest during construction	Additional indirect construction costs	Contingencies	Escalation	Total
				Millions of dollars						
Pressurized water										
SM-1	[a]	1.4	1.3	0.87	0.04	[b]	0.3	[c]	[c]	3.9
Shippingport	[d]	14.6	18.8	9.8	2.3	2.3[b]	25.1[e]	[c]	[c]	72.9
Yankee	0.2	6.8	13.0	8.8	0.2	3.0	13.4[f]	←6.6→		52.0*
SELNI (Italy)	←9.5→		18.5	←11.4→		←17.0→				56.4
Indian Point	0.4	24.1	30.0	24.9	0.4	5.1	4.6	[g]	[g]	89.5
Boiling water										
EBWR[h]	[a]	1.2	1.9	1.0	0.1	[b]	0.4	[c]	[c]	4.6
BONUS	0.3	1.8	2.9	1.7	0.3	0.1[b]	2.5	2.7	0.4	12.7[i]
Elk River	[d]	1.8	4.2	1.7[j]	0.05	[b]	4.5	[k]	[k]	12.2
Humboldt Bay	[a]	2.9	8.8	5.2	0.3	←2.3→		[g]	[d]	19.5[l]
Big Rock Point	0.15	6.0	11.1	5.6	0.5	1.8	1.0	0.5	[m]	26.7
Pathfinder	0.4	3.1	7.6	6.4	0.3	[d]	0.9	2.0	1.1	21.8
SENN (Italy)	0.6	4.0	23.6	7.7	0.8	8.8	13.0	1.1	3.6	63.2
Gas cooled										
EGCR	[a]	8.0	10.6	2.8[n]	0.1	[b]	7.6	1.5	[d]	30.6†
Peach Bottom	0.4	2.6	14.1	5.4	0.7	1.2	3.4	[g]	[g]	27.8
Florida[o]	0.3	4.5	9.3[p]	4.2	0.4	2.0	3.9	2.1	1.9	28.6
Heavy water cooled										
Carolinas-Virginia	0.05	3.1	10.7[p]	0.9[q]	0.3	1.4	0.6[r]	[d]	0.6	17.7
CANDU (Canada)	0.9	5.0	22.9[s]	13.2	3.3	9.2	14.2	8.6	4.2	81.5
Organic										
Piqua[t]	0.0035[u]	2.8	2.8	3.2	0.5	[b]	1.5	0.2	0.8	11.8
Sodium graphite										
SRE	[d]	1.9	4.5	2.0	0.2	[b]	[d]	[c]	[c]	8.6
Hallam	0.1	7.1	17.5	10.1	2.2	0.6[b]	5.0	0.4	[v]	43.0[w]
Fast breeder										
EBR-II[x]	[a]	7.5	9.0	3.0	0.5	[b]	3.6	1.7	[y]	25.3
Fermi	0.9	8.6	21.0	8.2	2.1	2.2	11.9[z]	1.4	[g]	56.3

[a] Cost of land and land rights has not been included when the plant is located at a pre-existing site.

[b] Interest during construction has not been included in this table for the AEC portion of construction costs.

[c] Not applicable, since plant construction has been completed and actual costs are given for the other items.

[d] Not available.

[e] Includes $2.9 million for net cost of preliminary operation.

[f] Includes $3.2 million for startup and one year of test operation.

[g] Included by distribution among other categories.

[h] Does not include $2.1 million for recent modifications to increase the capacity to 100 Mw(t).

[i] Recent information indicates a total construction cost of $12.1 million

[j] Includes cost of pre-existing turbine-generator.

[k] AEC portion (75 per cent) of costs shown under other categories is based on ceiling amount of AEC contract with manufacturer.

[l] Based on prices in first quarter of 1958. Recent information indicates a total construction cost of $20.6 million.

[m] Costs given are ceiling amounts under the contract.

[n] Includes $0.25 million as remaining book value of a pre-existing turbine-generator.

[o] Based on design using fuel elements clad with stainless steel. Work is now being done on beryllium cladding.

[p] Does not include cost of heavy water, which is to be leased.

[q] Does not include cost of pre-existing turbine-generator.

[r] Includes start-up cost of $0.2 million.

[s] Includes $11.7 million for heavy water, helium, and organic fluids.

[t] Includes turbogenerator unit rated at 33 Mw(e) and complete structure for an additional turbogenerator unit, although the gross capacity of the plant as designed is only 12.5 Mw(e).

[u] Cost of the site proper, not including a surrounding buffer zone.

[v] Cost given for reactor plant equipment includes $0.5 million for escalation.

[w] Recent information indicates a total construction cost of $45 million.

[x] Does not include $7.1 million for fuel-cycle facility. Recent information indicates an increase of $1.3 million in the total cost of the EBR-II.

[y] Some contracts are fixed cost while others are subject to escalation; construction is over 75 per cent complete.

[z] Obtained by subtracting the other categories listed for Fermi from the total of $56.3 million. The latter amount is the total plant cost minus the costs of research and development and fuel-element fabrication, as given in the Fourth Semiannual Financial Report of the Power Reactor Development Co. Included is $0.8 million for nonnuclear testing and employee training but not the cost of nuclear testing.

* Recent information indicates a total construction cost of about $46 million.

† Construction cost has been re-estimated at $40.6 million

Table I-2 CONSTRUCTION COSTS PER UNIT CAPACITY FOR SPECIFIC NUCLEAR POWER PLANTS*

Plant		Land and land rights	Structures and improvements	Reactor plant equipment	Turbo-generator and accessory equipment	Misc. power plant equipment	Interest during construction	Additional indirect construction costs	Contingencies	Escalation	Total†
Type and name	Net elec. megawatts	Dollars per net electrical kilowatt									
Pressurized water											
Yankee	110–136	1.8–1.5	62–50	118–95	80–64	1.9–1.5	27–22	122–98	←60–49→		470–380
SELNI (Italy)	176	←54→		105	←65→		←96→				320
Indian Point	255	1.5	95	118	98	1.8	20	18			350
Boiling water											
BONUS	16.3	18.4	112	178	106	16	7	156	159	25	780
Elk River	22		80	191	75	2.3		204			550
Humboldt Bay	48.5		59	182	108	5.9	←47→				400
Big Rock Point	48.5–72.8‡	3.1–2.1	125–83	228–152	116–78	11–7	37–25	20–14	10–7		550–370
Pathfinder	62	7.3	49	123	104	4.8		14	32	17	350
SENN (Italy)	150	4.0	27	157	51	5.3	59	87	7	24	420
Gas cooled											
Peach Bottom	40	11.0	65	351	136	18	30	85			700
Florida	50.5	6.3	89	185	83	7	39	78	41	37	570
Heavy water cooled											
Carolinas-Virginia	17	2.7	181	628	54	17	85	37		36	1040
CANDU (Canada)	200	4.4	25	114	66	17	46	71	43	21	410
Organic											
Piqua	11.4	0.3	250	241	280	43		129	19	74	1040
Sodium graphite											
Hallam	75–87	1.6–1.3	95–81	233–201	135–116	29–25	7.6–6.5	67–58	5–4		570–490
Fast breeder											
Fermi	91–143	9.7–6.2	95–60	231–147	91–58	23–15	24–15	129–82	16–10		620–390

* Plants are those listed in Table I-1 with the same footnotes applying, except that primarily experimental plants are not included. The numbers in Table I-2 have been computed from the original data rather than from the rounded figures in Table I-1.

† Rounded to the nearest $10/kw. As stated in footnotes of Table I-1, recent information indicates somewhat different total costs of construction for Yankee, BONUS, Humboldt Bay, and Hallam.

‡ Net capacity of Big Rock Point has been estimated for purposes of this report at 97 per cent of gross capacity.

Table I-3 FIRST CORES FOR POWER REACTORS[3]

Fuel type and nuclear plant	Diameter or thickness of fuel element, in.[a]	U^{235} assay, %	Uranium[b] in reactor, kg	Fabrication cost of uranium,[b] $/kg
Uranium oxide, zircaloy clad				
Shippingport, blanket	0.465	0.71	12,790	560
Carolinas-Virginia	0.50	2.0	3,280	510
Dresden	0.563	1.5	52,600	190
Humboldt Bay	0.563	2.0	13,840	190
SENN	0.563	2.0	41,400	140
BONUS, boiler	0.500	1.85	2,550	140[c]
Uranium oxide, stainless steel clad				
Yankee	0.340	3.4	20,840	200
EGCR	0.32 × 0.75[d]	2.55	9,860	150
BONUS, superheater	0.542	3.5	1,630	125[c]
Florida	0.57	1.68	15,800	87
Big Rock Point[e]	0.388	3.2	7,690	
Saxton	0.343	3.7	1,270	
Uranium oxide-stainless steel cermet, stainless steel clad				
SM-1	0.030[f]	93	24	4,600[g]
McMurdo Sound	0.5	93	31	8,380
Vallecitos	0.025[f]	93	24	
Pathfinder, superheater	0.458 × 0.512 and 0.672 × 0.726[d]	93	37	[h]
Uranium oxide aluminum clad				
Pathfinder, boiler	0.418	1.8	6,500	[h]
Uranium & thorium oxide, stainless steel clad				
Indian Point	0.304	93	16,280[i]	435
Elk River	0.452	93	4,000[j]	105
Uranium & thorium oxide, in graphite				
Peach Bottom	3.5	93	1,390[k]	680
Uranium metal, stainless steel clad				
SRE	0.79	2.78	3,000	100
Uranium alloys, zircaloy clad				
Shippingport, seed 2 (U-Zr)	0.069[f]	93	97	26,000
Fermi, core (U-Mo)[l]	0.158	25.6	1,900	640
EBWR (U-Zr-Nb)	0.24[f]	1.44[m]	5,500	144
Uranium alloys, stainless steel clad				
Hallam (U-Mo)	0.66	3.6[n]	27,600	110
Fermi, blanket (U-Mo)	0.443	0.35	37,580	48
EBR-II, core (U-fissium)	0.174	48.6	350	
Uranium alloy, aluminum clad				
Piqua (U-Mo-Al)	3.11 × 4.10 and 4.14 × 5.13[o]	1.94	6,550	89

[a]Outer diameter of clad rod, unless otherwise noted.

[b]Includes thorium for Indian Point, Elk River, and Peach Bottom.

[c]Assumed by reactor designer.

[d]Inner and outer diameters of tube.

[e]Twelve of the 143 rods per bundle have a diameter of 0.338 in. and a U^{235} assay of 2.8 per cent.

[f]Thickness of plate.

[g]Cost of fabrication at Oak Ridge. A similar core being procured commercially will cost about twice as much.

[h]Total fabrication cost for Pathfinder fuel elements in the boiler and superheater is estimated at $950,000, not including research, development, and testing.

[i]Includes 15,100 kg of thorium.

[j]Includes 3820 kg of thorium.

[k]Includes 1190 kg of thorium.

[l]The first core will have an additional cladding of stainless steel.

[m]Of the 114 fuel assemblies, 8 contain normal uranium.

[n]A few of the fuel elements have a U^{235} assay of 3.45 per cent.

[o]Inner and outer diameters of finned tubes.

elements of smaller diameter. The reference notes that the charges for fuel-element fabrication on which standard fuel-cycle costs are based in the arrangement with Euratom are $100 and $140 per kilogram of uranium, respectively, for steel and Zircaloy jacketing (for uranium enrichments ≦ 3 per cent).

ues of fuel cost are probably about as low as can be expected for the reactor type. It is evident that quite long exposures are necessary to bring the fuel cost down to an attractive range. For example, the estimated cost of 3.16 mills/kw-hr at an average fuel exposure level of 15,000 Mwd/metric ton of uranium, although en-

Table I-4 ESTIMATED FUEL-CYCLE COSTS[3] FOR A YANKEE TYPE PRESSURIZED-WATER REACTOR*

(In Mills per Kilowatt-Hour)

Irradiation level, Mwd/metric ton of U	Initial U^{235} assay, %	Fuel-element fabrication	Transport	Chemical processing and conversion	U^{235} burnup†	Pu credit	Use charge†	Total
2,500	2.38	5.96	0.60	2.21	2.85	−1.37	0.75	11.00
5,000	2.55	2.98	0.30	1.19	2.55	−1.26	0.52	6.18
7,500	2.73	1.98	0.20	0.85	2.40	−1.20	0.46	4.69
10,000	2.90	1.49	0.15	0.66	2.29	−1.07	0.44	3.96
12,500	3.10	1.19	0.12	0.55	2.20	−1.04	0.43	3.45
15,000	3.27	0.99	0.10	0.48	2.15	−0.99	0.43	3.16
20,000	3.63	0.74	0.07	0.38	2.05	−0.91	0.45	2.78
25,000	3.98	0.60	0.06	0.33	1.98	−0.86	0.47	2.58

*The reactor physics calculations were made under the Fuel Cycle Study Project at the Massachusetts Institute of Technology.

†The burnup cost and the use charge are computed on the basis of the uranium price schedule in effect before July 1, 1961, and the use charge is based on the rate of 4 per cent per annum.

In Table I-4 the fuel-cycle costs for a Yankee type reactor are estimated for various average exposure levels. They are based on an assumed fabrication cost of $100 per kilogram and on chemical processing and conversion costs of $33.90 per kilogram of uranium, including losses, plus $1.74 per gram of plutonium. The well-known benefits of high fuel exposure in reducing the effects of fabrication and processing costs are demonstrated. There is also a smaller, but noticeable, decrease in the U^{235} burnup cost with exposure level as the fraction of energy supplied by plutonium fission increases. As might be expected, this cost decrease is nearly compensated by the loss of plutonium revenue, and the net burnup cost does not change rapidly with exposure above about 5000 Mwd/ton.

Although the purpose of Table I-4 is to show the effect of fuel exposure level, the absolute values of the fuel costs are also interesting. The assumptions (other than the uranium prices) entering the fuel cost estimates appear to be, if anything, optimistic rather than pessimistic for the near future. Consequently, the absolute values of fuel cost are probably about as low as can be expected for the reactor type. It is evident that quite long exposures are necessary to bring the fuel cost down to an attractive range. For example, the estimated cost of 3.16 mills/kw-hr at an average fuel exposure level of 15,000 Mwd/metric ton of uranium, although encouraging relative to nuclear fuel costs that have been experienced in the past, is still no lower than the fossil-fuel cost in a medium-cost fuel area. If the assumption is made that a modern fossil-fuel plant will have an over-all efficiency (including stack losses) of 35 per cent, then the 3.16-mill/kw-hr figure would correspond to a heat energy cost of about 32 cents per million Btu. The new uranium prices will, however, decrease the nuclear fuel cost significantly. For the 15,000-Mwd/metric ton of uranium case, the reduction of fuel burnup cost will apparently amount to about 0.48 mill/kw-hr, and a small reduction in use charge, of about 0.05 mill/kw-hr, will also occur. The total estimated fuel cost would then decrease to 2.63 mills/kw-hr. If the plutonium buy-back price were reduced from $12 to $9.50 per gram, about 0.2 mill/kw-hr would be added to this new total fuel cost.

Reference 3 gives Table I-5 as a summary of relative power costs from fossil-fuel plants and nuclear plants of the pressurized- or boiling-water types. The plants considered are privately owned, and they have capacities in the 150-

Table I-5 TYPICAL POWER-COST RANGES[3] FOR 150-Mw(e) PLANTS

	Nuclear plant	Fossil-fuel plant
Construction cost per net electrical kilowatt	$300 to $400	$150 to $200
Plant factor	80 to 70%	80 to 70%
Costs, mills/kw-hr:		
Fixed charges on construction cost	6.5 to 10.0	3.0 to 4.5
Fuel costs	3.5 to 5.5*	2.0 to 4.0†
Operation and maintenance	1.0 to 2.0	0.5 to 1.0
Total generating cost	11.0 to 17.5	5.5 to 9.5

*Includes cost of fuel cycle and fixed charges on investment in fuel fabrication, on the basis of schedules and rates in effect before July 1, 1961.

†Based on fossil-fuel costs of 20 to 40 cents per million Btu and a plant heat rate of 10,000 Btu per net electrical kilowatt-hour.

Mw(e) range. The ranges of costs given are intended to correspond to typical ranges rather than to maximum ranges. It appears that the nuclear plant costs exceed those of the fossil-fuel plants, on the average, in all categories of the cost breakdown. The greatest potential for cost reduction is, of course, in the area of construction costs, simply because those costs constitute the biggest item in the total. Basically, however, it is in the area of fuel costs that the nuclear plant can hope to better the fossil-fuel performance, and any long-range program aimed toward competitive nuclear power must consider fuel cost reduction as an important goal.

The reference summarizes data on the geographical variation of fossil-fuel costs and of installed steam electrical capacity in the United States. The most feasible areas for nuclear competition are probably those in which the fossil-fuel costs are high and in which the population density is sufficiently high to support the construction of rather large-capacity units. The reference states that about 9½ per cent of the total capacity in the United States is in plants of at least 300-Mw(e) capacity, with fuel costs over 35 cents per million Btu. In 1959 there were 23 such plants: eight were in New York, five were in Pennsylvania, three were in Massachusetts, two each were in New Jersey, Maryland, and California, and one was in Connecticut.

Small Plant Studies

As a continuation of the studies sponsored by the AEC Division of Reactor Development, for the establishment of a long-range program for civilian power reactor development, a series of studies was made during 1960 which covered power plants in the lower power ranges. Cost estimates for various types of plants having gross electrical outputs of 12.65 and 44 Mw were made by several different contractors. The power cost estimates were normalized by Kaiser Engineers, who also carried out a study of power costs from conventional plants in the same capacity ranges. The results of these studies are summarized in references 4 and 5.

The studies covered the reactor types listed in Table I-6, on the basis of current technology. In addition, heavy-water reactors and helium-cooled graphite-moderated reactors (EGCR and HTGR types) were studied as "near term potential" plants. The cost estimates were made on the assumption of 80 per cent plant factor; estimates were made using two different sets of economic ground rules, one applicable to plants operated by investor-owned utility companies and the other applicable to plants operated by REA-financed public utility systems. The more important differences between these two sets of ground rules are evident in the power cost breakdown (Table I-7).

The major design characteristics of the "current technology" plants used for the estimates in the 44-Mw(e) range are given in Table I-6. The normalized results of the estimates are summarized in Table I-7. It is no great surprise that the total power cost estimates are lowest for the boiling-water reactor in this power range. It is, however, surprising that the pressurized-water reactor does not compare more favorably with some of the other reactors. It is particularly surprising that the unit capital cost per net kilowatt should be almost $100 higher for the pressurized-water reactor than for the two sodium-cooled reactors. These results probably point up the fact that, although something can be done to normalize the cost estimates made by various designers on different specific designs, it is very difficult to ensure that the same degree of optimism or pessimism shall be used by the several designers in arriving at those specific designs for which the cost estimates are to be made.

Table I-6 SUMMARY OF PRINCIPAL PLANT CHARACTERISTICS FOR 44-Mw(e) POWER COST ESTIMATES[4]

	Current status nuclear power plants, 44 Mw(e) (Gross)				
	Pressurized-water reactor	Boiling-water reactor	Organic-cooled reactor	Sodium-graphite reactor	Sodium-cooled fast reactor
HEAT BALANCE					
Total reactor power, Mw(t)	150	133	135	123	130
Gross turbine power, Mw(e)	44.0	44.0	44.0	44.0	44.0
Net plant power, Mw(e)	41.6	42.0	40.9	41.8	41.6
Net plant efficiency, %	27.7	31.6	30.3	34.0	32.0
TURBINE CYCLE CONDITIONS					
Throttle pressure, psia	580	950	825	1,265	865
Throttle temperature, F	482	540	600	850	770
Condensing pressure, in. Hg abs	1.5	1.5	1.5	1.5	1.5
Final feed-water temperature, F	350	369	380	405	310
REACTOR DESCRIPTION					
REACTOR VESSEL					
Inside diameter, ft	7.5	10.25	9.4	14.8	5.9
Inside height, ft	28.7	28.5	28.0	30.9	23.5
Operating pressure, psia	2,150	1,000	120	Atmospheric	59
REACTOR CORE					
Total uranium loading kg U	11,150	10,650	8,680	4,960	638
Specific power, kw(t)/kg U	13.5	12.5	15.3	24.8	204
Power density, kw(t)/cu ft	940	850	912	215	6,440
Initial U-235 enrichment, wt.%	3.95	2.5	2.53	2.81	93
Final U-235 enrichment, wt.%	2.73	1.64	1.68	1.91	83.1
Fuel exposure, Mwd/metric ton (avg)	13,000	9,000	8,000	8,000	220,000 (25% burnup)
REFLECTOR or BLANKET					
Material	H_2O	H_2O	Organic	Graphite	U-Mo & UO_2
MODERATOR					
Material	H_2O	H_2O	Organic	Graphite	
COOLANT					
Material	H_2O	H_2O	Organic	Sodium	Sodium
Outlet temperature, F	565	546	635	945	900
Inlet temperature, F	511	539	590	615	600
FUEL ELEMENTS					
Fuel material	UO_2	UO_2	U-10 Mo	U-10 Mo	UO_2-SS Cermet
Geometry	Rod	5" x 5" sq	Sq plate	Rod	Plate
Clad material	304 SS	SS	Al	SS	347 SS
Maximum clad temperature, F	650	566	750	960	950
FUEL ASSEMBLIES					
Total number	52	256	80	76	135
Elements per assembly	110	25	22-plates	30	20
REACTOR CONTROL					
Absorber material	Ag-In-Cd	Boron-SS	Gd_2O_3	Gd-Sm oxide	B_4C
Number of control elements	18	24	13	9	10
Type of drive	Magnetic Jack	Rack & Pinion	Roller Nut	Ball & Screw	Rack & Pinion

Table I-7 SUMMARY OF CAPITAL AND POWER GENERATION COSTS 44-Mw(e) (GROSS) CURRENT STATUS NUCLEAR POWER PLANTS[4]

Description	Pressurized-water reactor	Boiling-water reactor	Organic-cooled reactor	Sodium-graphite reactor	Sodium-cooled fast reactor
CAPITAL COST	Amount	Amount	Amount	Amount	Amount
Direct construction cost					
20 Land and land rights	$ 100,000	$ 100,000	$ 100,000	$ 100,000	$ 100,000
21 Structures and improvements	2,739,000	2,475,000	2,229,000	1,614,000	2,327,000
22 Reactor plant equipment	8,510,000	5,238,000	4,970,000	7,358,000	6,497,000
23 Turbine-generator unit	3,180,000	3,665,000	3,079,000	2,803,000	2,798,000
24 Accessory electric equipment	734,000	691,000	721,000	793,000	856,000
25 Miscellaneous power plant equipment	206,000	206,000	217,000	204,000	205,000
Total direct construction cost	$15,469,000	$12,375,000	$11,316,000	$12,872,000	$12,783,000
Indirect construction cost					
General and administrative, 14%	$ 2,166,000	$ 1,733,000	$ 1,584,000	$ 1,802,000	$ 1,790,000
Engineering, design and inspection, 16%	2,820,000	2,257,000	2,064,000	2,348,000	2,332,000
Start-up cost, 4-1/2 months operation and maintenance	185,000	174,000	243,000	180,000	180,000
Contingency, 10%	2,060,000	1,654,000	1,521,000	1,720,000	1,708,000
Interest during construction, 5.4%	1,240,000	987,000	900,000	1,020,000	1,010,000
Total indirect construction cost	$ 8,471,000	$ 6,805,000	$ 6,312,000	$ 7,070,000	$ 7,020,000
Coolant/moderator - initial charge			62,000	58,000	17,000
TOTAL CAPITAL COST	$23,940,000	$19,180,000	$17,690,000	$20,000,000	$19,820,000
Net plant rating, kw(e)	41,600	42,000	40,910	41,800	41,600
UNIT CAPITAL COST PER NET kw	$ 575	$ 457	$ 432	$ 478	$ 476
POWER GENERATION COST	Mills per net kw-hr	Mills per net kw-hr	Mills per net kw-hr	Mills per net kw-hr	Mills per net kw-hr
Investor owned public utility					
Fixed charges					
Capital cost, 14%	11.5	9.1	8.6	9.6	9.5
Working capital, 12.5%	0.4	0.3	0.2	0.2	0.6
Interim replacements, 0.3%	0.2	0.2	0.2	0.2	0.2
Nuclear insurance	0.7	0.7	0.7	0.7	0.7
Total fixed charges	12.8	10.3	9.7	10.7	11.0
Operating cost					
Operation and maintenance	1.7	1.6	2.3	1.6	1.7
Nuclear fuel cycle					
Fabrication	1.2	1.3	1.2	1.6	1.8
Shipping	0.2	0.2	0.3	0.2	0.2
Depletion	2.3	2.0	2.3	2.2	2.7
Reprocessing	0.6	0.7	0.8	0.7	1.0
AEC use charge	0.7	0.4	0.3	0.2	1.3
Plutonium credit	(0.7)	(0.8)	(0.7)	(0.5)	(1.5)
Total fuel cycle cost	4.3	3.8	4.2	4.4	5.5
Total operating cost	6.0	5.4	6.5	6.0	7.2
TOTAL POWER GENERATION COST	18.8	15.7	16.2	16.7	18.2
REA financed public utility					
Fixed charges					
Capital cost, 6.4%	5.3	4.1	3.9	4.4	4.3
Working capital, 3.7%	0.1	0.1	0.1	0.1	0.2
Interim replacements, 0.3%	0.2	0.2	0.2	0.2	0.2
Nuclear insurance	0.7	0.7	0.7	0.7	0.7
Total fixed charges	6.3	5.1	4.9	5.4	5.4
Operating cost					
Total operating cost	6.0	5.4	6.5	6.0	7.2
TOTAL POWER GENERATION COST	12.3	10.5	11.4	11.4	12.6

References

1. AEC to Revise Charges for Enriched and Depleted Uranium, AEC Press Release, May 29, 1961.
2. *Federal Register*, May 30, 1961.
3. Costs of Nuclear Power, USAEC Report TID-8531, January 1961.
4. Study of Nuclear Power Plants Capital and Power Generation Costs, 44 and 12.65 MWE (Gross), for United States Atomic Energy Commission, San Francisco Operations Office, Berkeley, California, USAEC Report TID-8533, Kaiser Engineers, Oakland, California, Oct. 31, 1960.
5. Study of Conventional Steam Power Plants Capital and Energy Costs, 44,000 and 12,650 KW (Gross), for United States Atomic Energy Commission, San Francisco Operations Office, Berkeley, California, USAEC Report TID-8532, Kaiser Engineers, Oakland, California, Aug. 1, 1960.

Section II

REACTOR PHYSICS

Critical and Exponential Experiments

A semiempirical method for calculating reaction rates in uranium-graphite heterogeneous systems has been suggested in reference 1. The method utilizes a comparison of experimental flux traverses and calculated flux distributions to supply an empirical adjustment to the analytic neutron temperature. The exclusion of epithermal effects in the preliminary hardened cross-section calculation resulted in a rather high effective neutron temperature. However, an epithermal correction, determined by means of a P_3 calculation between 0.1 and 10 ev, was used to satisfactorily reduce the originally calculated hardened cross section.

Measurements[2] have been made in large exponential graphite, natural-uranium, water-cooled piles (8 ft long and 6 to 10 ft wide) to investigate the effect of pile size on the measured material buckling and extrapolation distance. Two lattice spacings were used: $8\frac{3}{8}$ in. in both the 8- by 6- and the 8- by 8-ft piles and $14\frac{9}{16}$ in. in the 8- by 10-ft pile. The experiments were performed using four sources which were either split in location or clustered together.

An exponential pile has been used to determine criticality constants for 2.6 per cent enriched UO_2 cylinders in light-water lattices at Hanford Atomic Products Operation.[3] Bucklings and extrapolation lengths were determined for three different hexagonal lattice arrangements with annular fuel tubes (inside diameter: 0.820 cm; outside diameter: 1.791 cm). In each lattice array, measurements were taken with and without acrylic resin rods filling the center void of the fuel rods. In addition, measurements[4] of criticality, buckling, and extrapolation lengths were made for 2.00 per cent enriched uranium rods in light water. For these hexagonal lattice arrays, fuel rods (0.600 in. in diameter) were encased in thin-walled ($\frac{1}{32}$ in.) acrylic resin tubes, and the assemblies were completely reflected by light water.

An experiment,[5] using clusters of seven rods, was performed in the Physical Constants Test Reactor (PCTR) to determine the infinite multiplication factor, k_∞, and the thermal utilization factor, f, in a natural-uranium graphite assembly. Because k_∞ was less than unity for this assembly, the usual PCTR method of poisoning the cell to reduce k_∞ to unity could not be used to determine its multiplication. The reference describes three alternate ways of making the determination, and the results are compared. In the process, two arrays, one of natural-enrichment rod clusters and one of 1.007 wt.% enriched rod clusters, were used in the graphite moderator with a 7-in. cluster lattice spacing. The rods, 0.925 in. in diameter, were enclosed in aluminum jackets (inside diameter: 0.940 in.; outside diameter: 1.002 in.).

As a part of the Multi-region Reactor Lattice Studies Program, a number of critical experiments[6] have been performed at the Westinghouse Reactor Evaluation Center. These experiments were used to investigate basic multiplying characteristics, flux distributions, and, to a lesser degree, rod worths for light-water-moderated, UO_2-fueled assemblies. Groups of three differently enriched (1.6, 2.7, and 3.7 wt.% U^{235}) fuel rods with stainless-steel cladding were employed to obtain a comparison of multiregion versus single-region assemblies. The geometry was cylindrical for the majority of these investigations wherein a pitch of 0.493 in. and two moderating water-to-uranium ratios, 4.5:1 and 2.5:1, were used. A three-region square core with a moderating water-to-uranium ratio of 2.5:1 and a pitch of 0.418 in. was also investigated. Some of the same experimental

arrangements were further used to measure the microscopic parameters with which it was possible to infer values of: ρ^{28}, the ratio of epicadmium to subcadmium capture in U^{238}; δ^{25}, the ratio of specific activation of a U^{235} foil due to neutrons of epicadmium energies to the specific activation due to thermal neutrons; and δ^{28}, the ratio of fissions in U^{238} to those in U^{235}.

Two critical experiments[7] which represent the initiation of the Spectral Shift Control Reactor critical and exponential investigations were performed with a 4 per cent enriched UO_2–light water lattice. Criticality, buckling, and thermal disadvantage factors were determined for two cases: (1) a clean assembly and (2) a boric acid-poisoned assembly. The stainless-steel-clad (outside diameter: 0.475 in.; wall thickness: 0.0155 in.) UO_2 rods were arranged in a square lattice (metal-to-water ratio of 1) with a lattice pitch of 0.595 in.

Prior to operation of the SNAP Experimental Reactor (SER) at full power and temperature, the assembly was run at power ratings of 1 watt or less in order to investigate its fundamental behavior and obtain measurements[8] of various basic physics parameters. Some of the specific areas of investigation were: critical mass, control-drum calibrations, reflector material worths, temperature coefficients, U^{235} foil activations, and reactivity mappings external to the reflector and reactivity worths of material distribution in the core. The SER has a beryllium internal reflector between the hexagonal fuel-element array and the cylindrical core vessel and a beryllium external reflector outside the core vessel. The 0.975-in.-diameter fuel elements are zirconium-uranium, enriched to 93 per cent U^{235} and clad in stainless steel with a ceramic outer coating. When the SER is run as a power reactor, it is NaK cooled; however, for these low-power experiments, the coolant was not present.

Critical experiments[9] using UO_2-fueled light-water-moderated lattices have been performed to investigate criticality, power distribution, lattice parameters, and reactivity coefficients both in boiler and integral boiler-superheater type assemblies. The boiler fuel rods (0.445 in. in diameter) were 1.85 per cent enriched and clad in aluminum. The superheater fuel elements (0.500 in. in diameter) were 3.40 wt.% enriched and clad in stainless steel. For the experiments involving only boiler elements, slab type geometry was used with lattice pitches of 0.625 and 0.884 in. In the case of the integral boiler-superheater experiment, a superheater assembly with a pitch of 1.094 in. was sandwiched between boiler blankets having a pitch of 0.625 in. The experimental arrangement used to supply water to the superheater assembly was built in such a manner that it was possible either to flood or to void all or some of the superheater elements. The specific lattice parameters measured were the inverse of the disadvantage factor and the ratio of the total to the epicadmium neutron captures in U^{238}. These parameters were to be used to determine the thermal utilization factor (f) and the resonance escape probability (p).

To aid in the development of the gas-cooled Mobile Low-Power Reactor, criticality studies[10] were performed using the ML-1-1B critical assembly. This experimental array has a lead side reflector with a variable-pitch hexagonal lattice of 61 fuel assemblies. An individual fuel assembly was made up of 19 pins (18 of these contained UO_2-BeO pellets, and the 19th was the central flux-shaping poison pin) arranged in a hexagonal array. The 18 pins were nonuniform in fuel content, wherein the 12 pins having the lower mass of fuel were used to form the outer row of the hexagon and 6 of the 7 pins having the higher fuel mass formed the inner hexagon row; the final high-fuel-mass pin served as the poisoned central flux-shaping pin. The fuel was clad in Hastelloy X. There was a stainless-steel insulation liner (outside diameter: 1.50 in.; wall thickness: 0.012 in.) around the hexagon formed by the pins, and each entire assembly was enclosed by a stainless-steel pressure tube (outside diameter: 1.804 in.; wall thickness: 0.020 in.). In some of the experiments, copper strips wrapped around the assembly insulation liner simulated a burnable poison, whereas stainless-steel strips, also wrapped around the liner, were used as poison shims. The experiments yielded information concerning the following parameters: critical fuel loading, general and localized flux and power distributions, and general and detailed reactivity effects.

Three critical experiments[11] which used plutonium-enriched uranium mixtures were employed to make substitution measurements. The results of these measurements were then applied in a calculation of the number of fission neutrons released when a Pu^{240} nucleus is fissioned by a

2-Mev neutron. Three 1.6-kg balls of plutonium with different isotopic concentrations of Pu^{239} were used to provide three sets of experimental data. Each ball was surrounded by a sufficient quantity of oralloy (93.2 wt.% enriched uranium) to ensure criticality with a spherical natural-uranium reflector. The material substitution processes were ones of interchange between equal masses of plutonium with different known isotopic concentrations of Pu^{239} and, in order to provide a reactivity balance, of a corresponding interchange of equal masses of oralloy and natural uranium. The experiment and subsequent analysis yielded a value of

$$\bar{\nu}(Pu^{240}, 2\ \text{Mev}) = 3.32 \pm 0.14$$

The TRX critical assembly was recently used to measure[12] the resonance fission integrals of U^{235}, Pu^{239}, and Pu^{241}, relative to the resonance capture integral of Au^{197}, by means of the cadmium-ratio method. Uranium metal rods (0.387 in. in diameter), enriched to 1.3 wt.% U^{235}, served as the fuel in a light-water-moderated lattice with a pitch of 0.711 in. The central fuel rod and the first two interior hexagon rows were removed from the hexagonal core in order to provide a central irradiation area (approximately 3.2 in. in diameter) for the experiments. Below 25 kev, a very nearly $1/E$ epicadmium flux spectrum was calculated for the central part of the assembly. By the use of subsequent fission-activation corrections, a pure $1/E$ spectrum was assumed for the energy region of experimental interest. For a 0.5-ev cutoff energy, the following values of the resonance fission integrals were obtained: U^{235}, 274 ± 11 barns; Pu^{239}, 327 ± 22 barns; and Pu^{241}, 557 ± 33 barns.

The resonance capture integrals of U^{238} in UO_2 and uranium metal rods (0.387 in. in diameter), both of which were enriched to 1.3 wt.% U^{235}, have been measured[13] in the TRX critical facility. The effective U^{238} resonance integral for the UO_2 rods was found to be 1.30 ± 0.02 times that of the effective U^{238} resonance integral in the uranium metal rod. By substituting aluminum and zirconium for the oxygen in the UO_2 rods and obtaining similar resonance measurements, it was further determined that 0.15 of the 0.32 excess in the UO_2 effective resonance integral was due to oxygen moderation. The remaining 0.15 ± 0.02 excess was found to be attributable to the lower U^{238} atom density in the UO_2 rods.

Evaluation of Criticality Hazards

The Nuclear Safety Guide, TID-7016, was first published in unclassified form in 1957. During the intervening years, as more empirical information and operating experience became available, certain of the values originally thought to provide a given safety factor were found to need revision of a conservative nature. Thus, in order to update and in some instances expand the information provided therein, a revision[14] of the Guide was issued in 1961.

The 1961 version of the Guide is divided into three sections: (1) the nuclear safety problem, (2) recommended nuclear safety limits, and (3) application to processing plants. The first section consists, in part, of a general qualitative discussion aimed at acquainting the reader with some of the factors affecting potential criticality in compositions containing fissionable materials. This discussion is followed by a table giving conservatively safe geometries and concentrations of the three most commonly encountered fissionable isotopes: U^{235}, U^{233}, and Pu^{239}. The second section provides, in graph and table form, detailed characteristics for individual systems, excluding reactor type compositions. These detailed characteristics are combination values of mass and geometry which incorporate safety factors of 2.3 and 1.3, respectively. The third section begins with precautionary statements regarding possible critical conditions in processing operations. This discussion is followed by several constructive examples wherein the results of Section 2 are applied in dealing with problems commonly encountered in processing plants. Consideration is also given to the determination of safe mass limits and container volumes for slightly enriched fuel elements.

The present edition of the Guide constitutes a useful source of information for the preparation of safety procedure manuals covering processing, handling, and storage operations.

In order to better define potentially critical concentrations and geometries in homogeneous compositions of uranium and hydrogen, such as those occurring in chemical processing operations, a significant amount of experimental information has been correlated[15] with the results of calculations using previously derived empirical formulas. In this correlation the experimental data were taken from systems of closely packed compacts of uranyl fluoride and uranyl nitrate, wax, and water. The empirical formulas

were used to derive critical masses and volumes for reflected spherical, infinite cylindrical, and slab geometries. The calculations and subsequent correlations were parameterized on the bases of variable enrichments and hydrogen-to-U^{235} atomic ratios.

In the fall of 1959 a symposium, conducted under the auspices of the Health and Safety Branch, United Kingdom Atomic Energy Authority, was convened to treat the problem of criticality as it might occur in chemical processing and storage. Prior to the meeting, an introductory report[16] on the fundamental aspects of criticality was issued. This paper developed and explained, sometimes in limited fashion, the parameters which define, affect, and provide control of criticality.

Subsequent to the meeting, a series of eight lectures presented were collected and printed.[17] The first of these lectures was a review of nuclear physics as applied in the generation of the nuclear constants necessary for criticality type calculations. The next four lectures were concerned with the following theoretical considerations: behavior of neutrons in matter and criteria for critical size; factors affecting criticality, interaction, and storage; and transport containers. These four lectures were, in part, an expansion and refinement of the material contained in reference 16. The final three lectures in the series dealt specifically with criticality problems associated with metal systems, the chemical aspects of criticality, and design considerations leading to criticality safety.

Reference 18 treats the problem of potential interaction between individually safe assemblies, containing fissionable materials, that may be placed close enough to each other to form a critical array. Some of the more prominent theoretical and empirical approaches used to investigate potential criticality in arrays are discussed, and in some instances the results of such methods are compared with experimental data. Although the authors do not make any specific recommendations favoring one method over another, they do suggest that, if time and economics permit, an analysis of a given criticality problem should be made using two of the methods independently. For anyone concerned with assembly storage problems, the detailed techniques presented in this reference would serve as recommended starting points for specific safety analyses.

Doppler Effect

A comprehensive review of the experimental and theoretical work on the Doppler effect in thermal reactors is presented in reference 19. Three different techniques have been used for measuring the Doppler coefficient: (1) activation experiments; (2) small-sample reactivity experiments; and (3) complete-lattice reactivity experiments. The experiments are reviewed in the reference with particular attention to the inherent sources of errors and difficulties of interpretation of experimental results. A discussion is presented of the Breit-Wigner, Doppler-broadened resonance line shape, which is the underlying basis for theoretical analyses of the Doppler effect. The general calculational procedures used for determination of the temperature dependencies of the volume and the surface terms of the effective resonance integral are briefly outlined. The theoretical and experimental work on the radial dependence of the Doppler effect in a lump is briefly given along with a discussion of the temperature-dependence of the Doppler effect. A previous review of resonance absorption and the Doppler effect was given in the December 1960 issue of *Power Reactor Technology*, Vol. 4, No. 1.

In uranium bars in the size range of practical interest, experiment and theory agree that the Doppler coefficient increases very slowly with increasing surface-to-mass ratio (S/M) of the lump. This effect is caused by an increase in the contribution of lower-energy resonances to the Doppler effect and is also in agreement with the theoretical interpretation of the radial dependence of the Doppler effect in a lump. Most experiments have not been sufficiently accurate to give a conclusive experimental indication of the temperature-dependence of the Doppler coefficient; theory predicts an approximate $T^{-1/2}$ variation. Evaluation of the Doppler coefficient for the case of nonuniform temperature distributions over the volume of the lump presents a practical problem for which no experimental work, and only very little theoretical work, is available.

The brief survey of reference 19 is quite complete in scope, and adequately points up the basic theoretical and experimental difficulties involved in obtaining a better understanding of the Doppler effect as related to the pertinent variables. A list of references is included which

historically traces the development of the work on Doppler-broadening effects.

The experimental values of the Doppler coefficient, α (fractional increase in resonance capture per °C), have a spread many times their quoted errors. (This was previously pointed out in the March 1960 issue of *Power Reactor Technology*, Vol. 3, No. 2, pages 31 and 32.) For example, for $S/M \sim 0.1$ cm^2/g, experimental values of α range from 0.9×10^{-4} to 3.0×10^{-4}/°C. Reference 19 suggests that some of the disagreement in α is due to differences in the slowing-down spectra in the various experiments. An attempt is made in the reference to estimate the different spectra and to correct the measured α values (only order-of-magnitude correction is possible because of difficulties of estimating spectra) so as to obtain the Doppler coefficient α_0 appropriate to a $1/E$ spectrum. It is to be noted that α_0 is not necessarily the coefficient to use in a reactor, inasmuch as the slowing-down spectrum actually existing at the rods is determined by the lattice compositions and geometries. Table II-1* presents the values of the uranium metal Doppler coefficient α arrived at in the various experiments and, in addition, the values of α_0 as deduced by application of a spectrum-correction factor. The spread in the corrected values for α_0 is smaller than that for α but is nevertheless still unsatisfactory. The values are for the temperature range of approximately 300 to 600°K.

Table II-1 URANIUM METAL EXPERIMENTAL DOPPLER COEFFICIENTS AND SPECTRUM CORRECTIONS[19]

Method	Reference	S/M, cm^2/g	α, 10^{-4}/°C	α_0, 10^{-4}/°C
Activation	Mitchell	0	1.5	
	Egiazarov	2.14	3.1	
		0.214	2.1	1.9
		0.053	1.6	1.4
	Rodeback	0.117	0.9 ± 0.2	
	Pearce	0.084	1.0 ± 0.2	1.0
	Hellstrand et al.	0.08	1.35 ± 0.10	1.35
		0.27	1.56 ± 0.10	1.56
Reactivity, small sample	Pearce and Walker	0.066	1.1 ± 0.2	1.1
	Small	0.100	2.24 ± 0.14	1.89
		0.147	2.17 ± 0.22	1.80
		0.169	2.30 ± 0.18	1.93
		0.376	2.93 ± 0.58	2.48
		0.399	3.59 ± 0.36	3.14
	Davis	0.062	1.74 ± 0.2	1.54
	Chernick and Kunstadter	0.076	1.1	
Reactivity, full lattice	Borst		1	
	Leslie	0.076	1.9	
	Adyasevich	0.063	1.95	
	Panasyuk		1.4 ± 0.25	
	BNL-113	0.076	1.5	
	Chernick and Kunstadter	0.076	1.5	

The experimental α values for UO_2, thorium metal, and ThO_2 are summarized in Table II-2.* No spectrum or thermal-expansion corrections have been made. (Thermal-expansion effects are generally one order of magnitude smaller than the Doppler effect.) The values are for the temperature range of approximately 300 to 600°K. The experimental α values for thorium do not increase with S/M, as in the case of uranium, because the resonance structure of tho-

*Tables II-1 and II-2 are reprinted here by permission from the *Journal of Nuclear Energy: Part A, Reactor Science*.[19]

Table II-2 EXPERIMENTAL α VALUES[19] FOR UO_2, Th, AND ThO_2

Material	Experiment	α, 10^{-4}/°C	S/M, cm^2/g
UO_2	Creutz	2.7	0
		1.6	0.177
		1.8	0.297
	Mitchell	0.88	0.18
	Hellstrand et al.	1.59 ± 0.10	0.14
		1.68 ± 0.10	0.23
		2.00 ± 0.12	0.48
		2.0 ± 0.2	Cluster
Th	Rodeback	2.8 ± 0.3	0.189
	Pearce	3.8 ± 0.2	0.140
	Pettus	3.1 ± 0.4	0.284
			0.148
	Small	3.9 ± 0.3	0.253
		3.9 ± 0.3	0.276
		2.6 ± 0.5	0.653
ThO_2	Pettus	3.8 ± 0.2	0.796
			0.767
			0.528
			0.292

rium does not have as many low-lying levels as U^{238}. The weak dependence of thorium on S/M is consistent with the results obtained on the radial dependence of the Doppler effect.

A theoretical analysis of the Doppler effect in fast-neutron reactors is reported in reference 20—wherein a number of the assumptions and approximations used in earlier theoretical works are studied—and additions and improvements are introduced in the analytical treatment. Theoretical and experimental work has indicated the Doppler temperature coefficient of reactivity to be almost negligibly small in fast-neutron reactors. However, because of its importance to reactor safety, particularly with regard to the design factors which affect the sign and magnitude of the coefficient, a more complete knowledge of the Doppler effect remains an important consideration in fast-neutron reactor-physics analyses. Reference 20 is a useful and rather comprehensive presentation of the theoretical approach and contains the important basic references adequately documented.

Three theoretical studies of the Doppler effect in fast-neutron reactors have been published. Goertzel et al.[21,22] give the general principles of the statistical theory that forms the foundation of most of the work presented in reference 20. Lane et al.[23] present the theory in somewhat greater detail, devote considerable effort to evaluation of the resonance parameters, and give a quantitative estimate of the effect, including both s- and p-waves. In 1957 Bethe[24] improved the calculation substantially by utilizing to a greater extent the available data on low-energy resonance parameters and high-energy average cross sections.

A number of experiments[25,26,27] that have been carried out for fast reactors are not sensitive enough, except for a single U^{238} experiment,[25] but they do provide a means of establishing an upper limit to the magnitude of the effect. The one U^{238} experiment gives results comparable to the calculations of Bethe.

Reference 20 evaluates the Doppler effect at several neutron energies from 1 to 200 kev instead of restricting attention to an energy of 100 kev, as in earlier work. In the earlier work it was rationalized that the neutron energy spectrum in fast reactors drops off rapidly below 100 kev and that the Doppler effect itself drops off rapidly above 100 kev, with the result that most of the net Doppler coefficient originates from neutrons of energies near 100 kev. Such an assumption turns out to be quite good for very small fast reactors (such as Experimental Breeder Reactor No. 1) which contain a large fraction of U^{235}. However, for the larger, more dilute, fast power reactors, the analysis of reference 20 shows that the neutron-spectrum drop-off below 100 kev is not fast enough to offset the rapidly increasing Doppler effect associated with the low-energy resonances. The basic method of Goertzel et al. was found to be invalid for treatment of the energy range below 30 kev, and a different method was developed in reference 20 for this energy range.

Table II-3 COMPOSITION OF ENRICO FERMI REACTOR USED IN DOPPLER CALCULATIONS[20]

Material	Vol. fraction
U^{235}	0.0612
U^{238}	0.1657
Molybdenum	0.0472
Zirconium	0.0382
Stainless steel	0.2591
Sodium	0.4286

Calculations of the Doppler temperature coefficient of reactivity for the Enrico Fermi fast-breeder reactor are reported in reference 20. The reactor composition used in the calculations is given in Table II-3; it is for a particular fuel

loading considered for use in the Enrico Fermi reactor, and may be slightly different from the actual composition finally used. The calculations give a contribution to the Doppler coefficient of reactivity due to the U^{238} of $-2.0 \times 10^{-6}/°C$ at 550°F. It was further deduced that the positive contribution to the reactivity coefficient due to the U^{235} is about eight times smaller than the calculated U^{238} effect, thus making it about $+0.3 \times 10^{-6}/°C$, for a net reactivity coefficient of $-1.7 \times 10^{-6}/°C$.

General conclusions arrived at in reference 20 as a result of the theoretical work are:

1. There is little chance that a practical fast reactor will ever be designed which will prove to have a large positive Doppler coefficient. This statement is based on the fact that a large positive coefficient requires: (*a*) a large concentration of U^{235} (relative to U^{238}), and (*b*) an appreciable fraction of the neutron-flux spectrum well below 50 kev. These two requirements are, however, mutually exclusive, at least so long as U^{238} is used as the principal diluent.

2. Some of the fast-reactor types currently under consideration by Atomic Power Development Associates (fuel mixtures of plutonium and uranium oxide with appreciable stainless-steel structural material and sodium as the coolant) will have negative Doppler coefficients of reactivity that are large enough ($\sim -10 \times 10^{-6}/°C$) to be of great importance to reactor safety. Any fast power reactor that has a large volume fraction of U^{238} in the core can be forced to have a large negative Doppler coefficient by including in the core a small amount of an efficient moderator such as zirconium hydride.

3. The dependence of $\delta k/\delta T$ on temperature has previously been approximated by use of the proportionality $\delta k/\delta T \propto T^{-3/2}$. This approximation is a rather poor one if a large fraction of the Doppler effect comes from neutrons below 10 kev. In this case, it is necessary to actually evaluate $\delta k/\delta T$ as a function of temperature.

4. Since most of the Doppler effect comes from the low-energy tail of the neutron-flux spectrum, inelastic scattering can be ignored except in very small fast reactors that have very few neutrons below 50 kev.

5. The ratio of U^{238} to U^{235} atoms for zero net Doppler effect (i.e., the balance point) can be quite different for two different fast reactors because of differences in the neutron-flux energy spectra.

References

1. D. E. Wood, The Effects of Neutron Temperature and Epithermal Flux on Lattice Cell Flux Traverses, in Nuclear Physics Research Quarterly Report for July, August, September, 1960, USAEC Report HW-67219, pp. 67–74, Hanford Atomic Products Operation, Oct. 20, 1960.
2. G. W. R. Endres and D. E. Wood, Investigation of Extrapolation Lengths for Graphite Uranium Lattices, in Nuclear Physics Research Quarterly Report for July, August, September, 1960, USAEC Report HW-67219, pp. 75–93, Hanford Atomic Products Operation, Oct. 20, 1960.
3. T. J. Powell, Exponential Measurements with 2.6 Per Cent Enriched Uranium Dioxide Rods in Water Lattices, in Nuclear Physics Research Quarterly Report for July, August, September, 1960, USAEC Report HW-67219, pp. 100–103, Hanford Atomic Products Operation, Oct. 20, 1960.
4. R. C. Lloyd and E. D. Clayton, Critical Approach and Exponential Measurements with 2.00 Per Cent Enriched Uranium Rods in Light Water, in Nuclear Physics Research Quarterly Report for July, August, September, 1960, USAEC Report HW-67219, pp. 104–109, Hanford Atomic Products Operation, Oct. 20, 1960.
5. E. Z. Block and D. E. Wood, Measurements of Negative k_{ex} for a Graphite Uranium Lattice in the PCTR, USAEC Report HW-67179, Hanford Atomic Products Operation, Dec. 1, 1960.
6. Ira H. Coen, Multi-Region Reactor Lattice Studies Quarterly Progress Report for the Period October to December 31, 1960, USAEC Report WCAP-1428, Westinghouse Electric Corp., Atomic Power Dept., Jan. 30, 1961.
7. N. L. Snidow et al., Task 1—Critical Experiments, in Spectral Shift Control Reactor Basic Physics Program, Quarterly Technical Report Number 2, October–December, 1960, USAEC Report BAW-1218, pp. 3–15, Babcock and Wilcox Co.
8. F. H. Clark et al., Physics Measurements on the SNAP Experimental Reactor (SER), USAEC Report NAA-SR-5619, Atomics International, Jan. 30, 1961.
9. J. S. Crudele et al., Studies of Low Enriched Cores Containing Simple Nuclear Superheat Elements. Part I, Critical Experiments, USAEC Report CEND-121, Combustion Engineering, Inc., Nuclear Div., Feb. 1, 1961.
10. J. W. Ray et al., ML-1-1B Critical-Assembly Studies, USAEC Report BMI-1501, Battelle Memorial Institute, Feb. 21, 1961.
11. D. M. Barton et al., Critical Masses of Composites of Oy and Pu-239-240 in Flattop Geometry, USAEC Report LAMS-2489, Los Alamos Scientific Laboratory, December 1960.

12. J. Hardy, Jr., et al., The Resonance Fission Integrals of U^{235}, Pu^{239}, and Pu^{241}, *Nuclear Sci. and Eng.*, 9(3): 341–345 (March 1961).
13. G. G. Smith et al., Experimental Studies of U^{238} Resonance Neutron Capture in UO_2 Fuel Rods, *Nuclear Sci. and Eng.*, 9(4): 421–429 (April 1961).
14. Goodyear Atomic Corporation, Nuclear Safety Guide 1961, revised by Subcommittee 8 of the American Standards Association Sectional Committee N6 and Project 8 of the American Nuclear Society Standards Committee, USAEC Report TID-7016(Rev. 1), 1961.
15. B. G. Owen, An Empirical Correlation of the Experimental Data on Homogeneous Critical Assemblies of Uranium and Hydrogen of All Enrichments, British Report PGR-97(R), 2nd Edition, November 1960.
16. E. R. Woodcock, Fundamentals of Criticality Control, British Report AHSB(S)-R15, 1961.
17. E. D. Pendlebury et al., Lectures on Criticality, British Report AHSB(S)-R4, 1961.
18. R. T. Ackroyd et al., Methods of Calculation for Interacting Arrays, With Special Reference to Storage Problems, British Report DEGR-336(R), United Kingdom Atomic Energy Authority, 1961.
19. R. M. Pearce, The Doppler Effect in Thermal Reactors, *J. Nuclear Energy: Pt. A, Reactor Sci.*, 13(3/4) (January 1961).
20. R. B. Nicholson, The Doppler Effect in Fast Neutron Reactors, Report APDA-139, Atomic Power Development Associates, Inc., June 1960.
21. G. Goertzel, An Estimation of Doppler Effect in Intermediate and Fast Neutron Reactors, *Proceedings of the International Conference on the Peaceful Uses of Atomic Energy, Geneva, 1955*, Vol. 5, pp. 472–476, United Nations, New York, 1956.
22. H. Feshbach et al., *Nuclear Sci. and Eng.*, 1(1): 4–19 (March 1956).
23. A. M. Lane et al., An Estimation of the Doppler Effect in Fast Neutron Reactors, British Report AERE-T/M-137, July 1956.
24. H. A. Bethe, Atomic Power Development Associates, Inc., Mar. 11, 1957. (Unpublished)
25. A. R. Baker and T. A. J. Jaques, A Measurement of the Contribution of the Doppler Effect to the Temperature Coefficient of Reactivity in a Fast Reactor, British Report AERE-R/M-168, June 1958.
26. W. Y. Kato and D. K. Butler, Measurement of the Doppler Temperature Effect in an EBR-I Type Assembly, USAEC Report ANL-5809, Argonne National Laboratory, July 1958.
27. R. T. Frost et al., Measurement of Doppler Temperature Coefficient in Intermediate and Fast Assemblies, *Proceedings of the Second United Nations International Conference on the Peaceful Uses of Atomic Energy, Geneva, 1958*, Vol. 12, pp.79–83, United Nations, New York, 1958.

Section III

HEAT TRANSFER

Liquid Metals

The use of orifices to partition flow in power reactors is a common design practice. The development of a variable orifice for the Hallam Nuclear Power Facility (HNPF) is described in reference 1. The installation is unusual because the variable orifice is to be operated from outside the reactor and presumably during power operation.

Several different orifices were designed and tested; the one selected for the HNPF is illustrated in Fig. III-1. The orifice plate has a

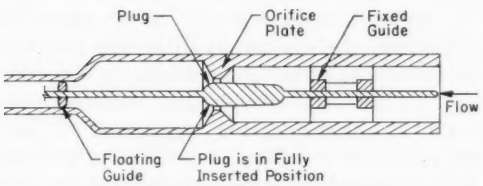

Fig. III-1 Variable orifice, type II, for control of the exit temperature of the coolant from each fuel channel of HNPF.[1]

minimum diameter of 2.2 in., whereas the maximum diameter of the plug is about 2.078 in. The effect of orifice plug position on coolant-channel exit temperature is shown in Fig. III-2. The orifice will possibly be located at the exit end of each fuel channel, incorporated in the fuel-element hanger tube. No details are given for the drive mechanisms and associated components.

Conduction

The subject of heat conduction in a solid that is pierced by coolant channels was discussed in

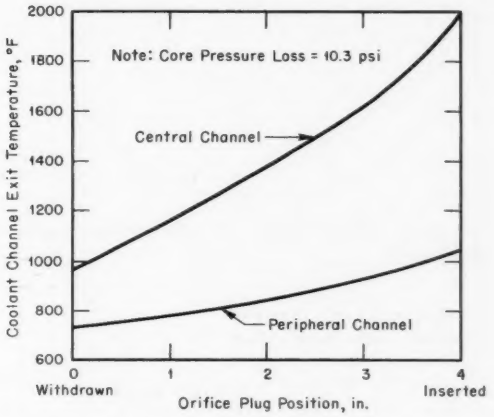

Fig. III-2 Exit temperature of HNPF coolant channel with type II variable orifice.[1]

the March 1961 issue of *Power Reactor Technology*, Vol. 4, No. 2, page 13. A Los Alamos report[2] extends the use of harmonics to the geometry indicated in Fig. III-3. Two applications are considered: (1) outer surface insulated and heat generation, and (2) outer surface at T_0 with no heat generation. Convection cooling of the holes is allowed in the first case, and the coolant-hole temperature is assigned a value of zero for the second case. The solutions are not expressed in closed form, and the usual complexities of harmonic functions are exhibited; the problem was coded for a large digital machine, and the results are presented graphically for various numbers and sizes of coolant holes and for several values of the Biot modulus. The authors[2] discuss the application of other boundary conditions (e.g., thermal radiation on the outer surface); they discuss the case wherein a central hole is present and the extension to consideration of a thin cladding on the surface of the coolant holes.

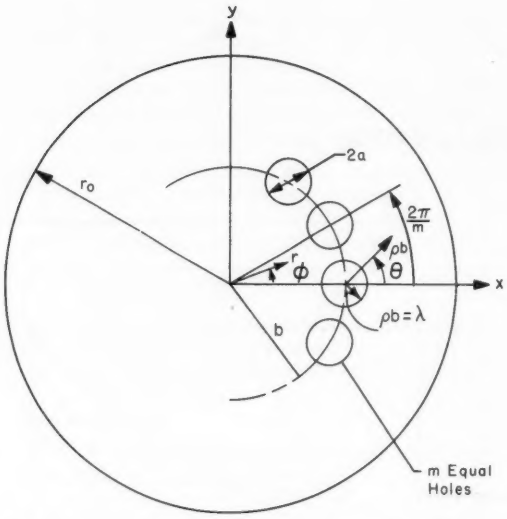

Fig. III-3 Cross section of cylinder with indicated geometry.[2]

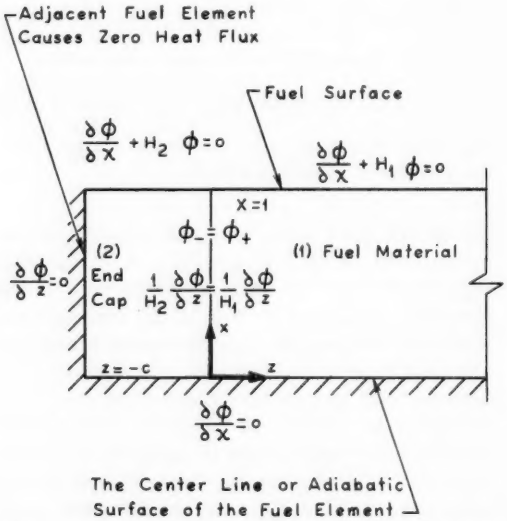
Adjacent Fuel Element Causes Zero Heat Flux
Fuel Surface
$\frac{\partial \phi}{\partial x} + H_2 \phi = o$
$\frac{\partial \phi}{\partial x} + H_1 \phi = o$
X=1
$\phi_- = \phi_+$
(2) End Cap
(1) Fuel Material
$\frac{\partial \phi}{\partial z} = o$
$\frac{1}{H_2}\frac{\partial \phi}{\partial z} = \frac{1}{H_1}\frac{\partial \phi}{\partial z}$
x
z=-c
z
$\frac{\partial \phi}{\partial x} = o$
The Center Line or Adiabatic Surface of the Fuel Element

Fig. III-4 Boundary-value problem for fuel-element end-cap temperatures.[3]

The temperature distribution in reactor fuel-element end caps is treated in reference 3. A plate or thin tubular geometry is considered; Fig. III-4 illustrates the boundary-value problem and associated geometrical considerations. Although series solutions result, it is shown that the first term is a good approximation for end caps about as long as the fuel-plate thickness for a Zircaloy-2-clad uranium element.

Spray Cooling

The spray-cooled reactor concept was discussed in the December 1960 issue of *Power Reactor Technology*, Vol. 4, No. 1, pages 74 to 77; this discussion should be reviewed for background information. Although spray cooling is a form of two-phase heat transfer, it will be treated separately herein since the spray-cooled reactor design is quite different from a design employing nucleate boiling.

It is not unusual to design a conventional boiling-water reactor to produce exit voids of about 50 per cent, which correspond to exit qualities of less than about 10 per cent, for pressures up to 1500 psia. This ensures that the two-phase flow is in the "bubble" regime, where stable flow occurs. (Flow regimes were discussed in the March 1961 issue of *Power Reactor Technology*, Vol. 4, No. 2.) At higher void fractions the flow regime changes to alternate slugs of liquid and vapor which fill the pipe—this is the slug-flow regime. At still higher void fractions, annular flow occurs, wherein a water film is present around the periphery of the heated channel with vapor flowing in the central regions. As the water film disperses, the channel is filled with vapor that is entraining small liquid drops. In the British literature the annular-flow regime is often called the climbing film region and the latter wet-steam flow regime is often called the spray-flow or liquid-dispersed region. As the small liquid drops evaporate, the vapor commences to superheat. These various regimes have been pictured in Fig. 14 of reference 4. The boundary between the annular and spray region is not necessarily a distinct one since in annular flow the central vapor core may entrain some of the liquid and in spray flow the walls may support a thin film of liquid. The spray-cooled-reactor concept avoids operation in the slug-flow regime where unstable conditions may exist; a typical spray-cooled channel at 800 psia is expected to operate between an inlet quality of 20 per cent and an outlet quality of 60 per cent.[5]

Some qualitative considerations are pertinent to a comparison of heat transfer in the bubble- and annular-flow regimes. Figure III-5* illustrates that the spray-cooled reactor may op-

*Figure III-5 is reprinted here by permission from the United Kingdom Atomic Energy Authority.[5]

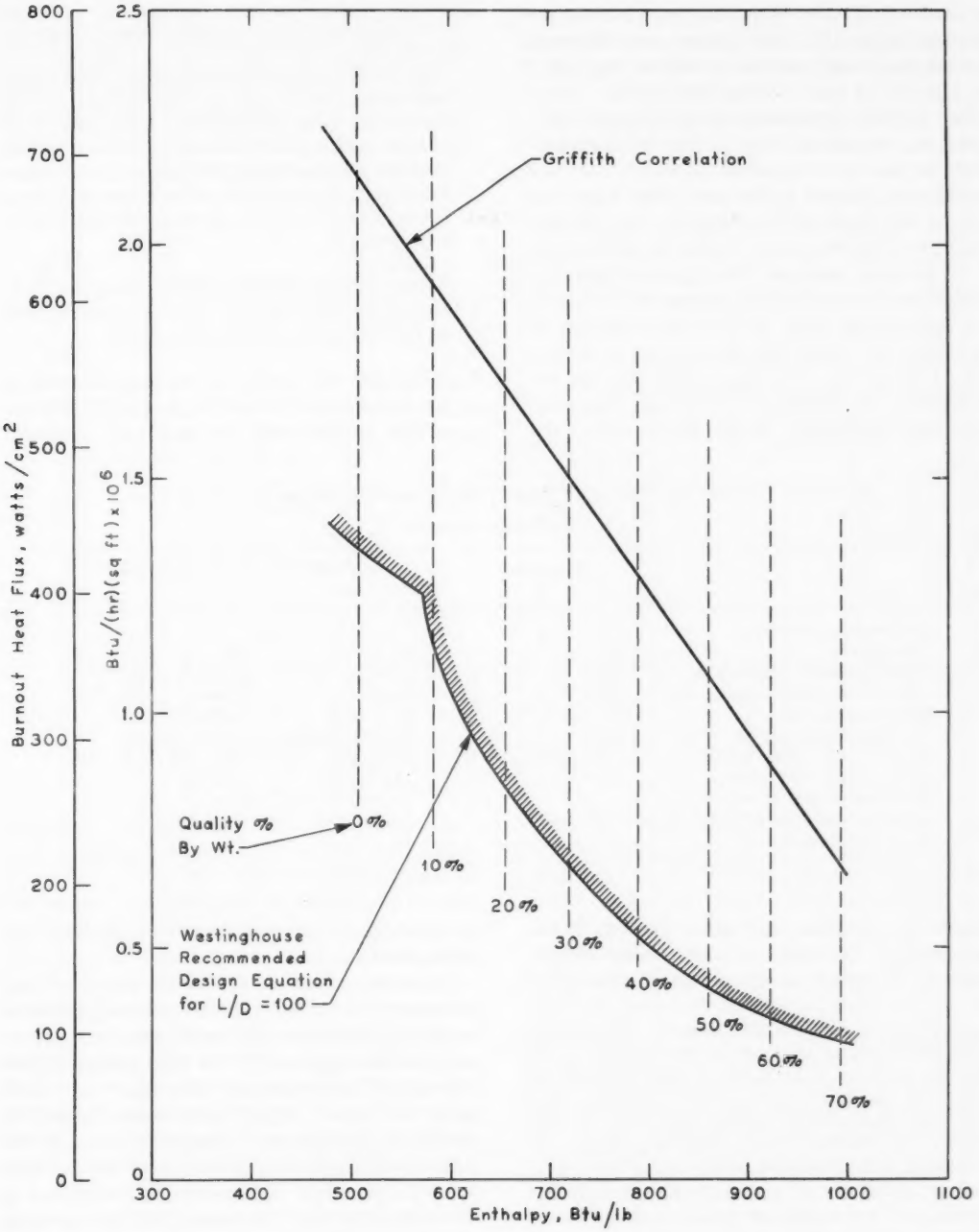

Fig. III-5 Quality burnout heat-flux data at 800 psia.[5]

erate closer to burnout for a given heat flux since the burnout curve falls quite rapidly as the enthalpy of the two-phase mixtures increases. High film coefficients are obtained. The Westinghouse curves shown[6] in Fig. III-5 are Eqs. VI-13 and VI-14 of WAPD-188.

The British experimental results are contained in references 7 to 9. The detailed correlations will not be presented because they are of primary interest to the specialist; a discussion of the various flow regimes and general behavior of the two-phase system is believed to be of general interest. The experimental apparatus was essentially a heated rod enclosed in a transparent tube. A controlled mixture of dry steam and water was admitted to the bottom of the test section of the apparatus that was instrumented to measure appropriate temperatures and pressures. Table III-1* shows the ranges of variables that were studied. Three mechanisms[7] of heat transfer were distinguished, as given in the following excerpt.*

Region I—Nucleate boiling region. This region was characterized by the formation of steam at the heating surface in the form of bubbles which are detached and dispersed in the flowing water. Heat transfer under these conditions appears to be governed by the laws of surface nucleate boiling.

Region II—Forced convection region. In a critical range of the dryness fraction, the increased velocity of the two-phase mixture induced by the vapourization process is sufficient to suppress the nucleate boiling mechanism, and above this point heat transfer becomes governed by the forced convective process.* Here, the water may be considered as the dispersed phase and the steam the continuous phase since the total volume is composed almost entirely of steam.

Region III—Liquid deficient regime. The forced convective process continues until at some critical value of the dryness fraction the heat transfer coefficient suddenly diminishes from a very high value to a value near to that expected for heat transfer to dry steam by forced convection. This is accompanied by a sharp rise in the heating surface temperature.

*Reprinted here by permission from the United Kingdom Atomic Energy Authority.

*This may be considered as an extension of the forced-convective process observed by McNelly and Coulson in the climbing film region.

Correlations are given for the nucleate boiling region and forced-convective, heat-transfer region film coefficients; no data are presented for the liquid-deficient region because the experimental accuracy was poor.

Table III-1 RANGE OF VARIABLES STUDIED, USING THE EXPERIMENTAL APPARATUS[9]

(Steam-Water System)

	Run series A	Run series B	Run series C
Test-section geometry:			
Length, in.	29	29	29
Heater outside diameter, in.	0.375	0.375	0.623
Glass tube inside diameter, in.	0.551	0.551	0.866
Inlet pressure, psia	35.2–20.5	35.0–21.9	34.6–15.3
Heat flux, Btu/(hr)(sq ft)	126,840	63,420–126,840	31,710–158,550
Mass flow rate, lb/(hr)(sq ft)	1.12×10^5–2.17×10^5	2.17×10^5	5.15×10^4–2.06×10^5
Steam quality, wt.% steam	17.5–58.9	12.8–52.3	0–54.6
Experimental heat-transfer coefficients, Btu/(hr)(sq ft)(°F)	3,730–10,060	3,990–9,580	1,498–8,214
No. of experiments	5	16	77

Experimentation on air-water mixtures was accomplished to study film thickness, entrainment, and pressure drop in the annular and dispersed flow regions.[8,9] The film thickness was determined by measuring the conductivity of the water (to which copper nitrate was added) by means of two probes through the wall of the 1.25-in.-ID 10-ft-long plastic test-section flow tube. Entrainment was measured at the exit of the test section by "skimming off" the climbing film with a knife edge and then passing the liquid-dispersed phase and the climbing film phase to cyclones. In addition, two other test sections were utilized which were instrumented only for pressure-drop determinations. Since

measurements of film thickness, pressure drop, and entrainment were available for analyses, the most interesting data are those taken with the more highly instrumented test section. The entrainment data, for example, allow the average liquid-dispersed phase density to be determined for use in computing static heads. The pressure-drop data were analyzed by the techniques of Lockhart and Martinelli[10] and Chenoweth and Martin.[11] Analyses by Calvert and Williams[12] and by Anderson and Mantzouranis[13] were examined as to their ability to predict water-film thickness, and the work of Wicks and Dukler[14] was used for correlation of the entrainment data. The Chenoweth and Martin correlation was found to be more accurate than that of Lockhart and Martinelli; however, it should be noted that the pressure drop was found to be a function of the method of introducing the liquid phase in the channel, and this conclusion is valid only when jet type injection is utilized. The Calvert-Williams and Anderson-Mantzouranis analyses both use velocity distributions in the liquid film to predict the liquid flow rate from a knowledge of the film thickness and pressure drop. Calvert and Williams assumed a laminar and a turbulent layer, whereas Anderson and Mantzouranis included a buffer layer. Qualitative agreement was obtained between the Bennett and Thornton data,[8] and deviations were tentatively explained as being caused by acceleration/deceleration effects associated with interchange of droplets between the gas core and the liquid film and/or the collapse of surface waves of the liquid film. The Wicks and Dukler correlation was in qualitative agreement with the data.

An Argonne National Laboratory report is on the subject of heat transfer to a mist (or spray) flow.[15] A steam-water mixture at nominal pressure was injected into an electrically heated 1-in.-ID copper tube, 4 ft in length. Flow rates and heat flux were adjusted so that transition from annular mist to the liquid-dispersed phase could be studied. After a detailed review of the literature, an analytical model was developed which uses several simplifying assumptions. The development of the model is quite straightforward, and both mass- and heat-transfer coefficients are used; the model is then used to study the region between annular-mist flow and superheated-steam flow. Figure III-6 shows a typical wall-temperature profile predicted by the model. The film coefficient in the annular-flow region has been assumed to be very high, and $T_w - T_b$ approaches zero.* In the annular-flow region the rate of diffusion of droplets to the wall may be greater than or equal to the rate at which they are evaporated, and a film of

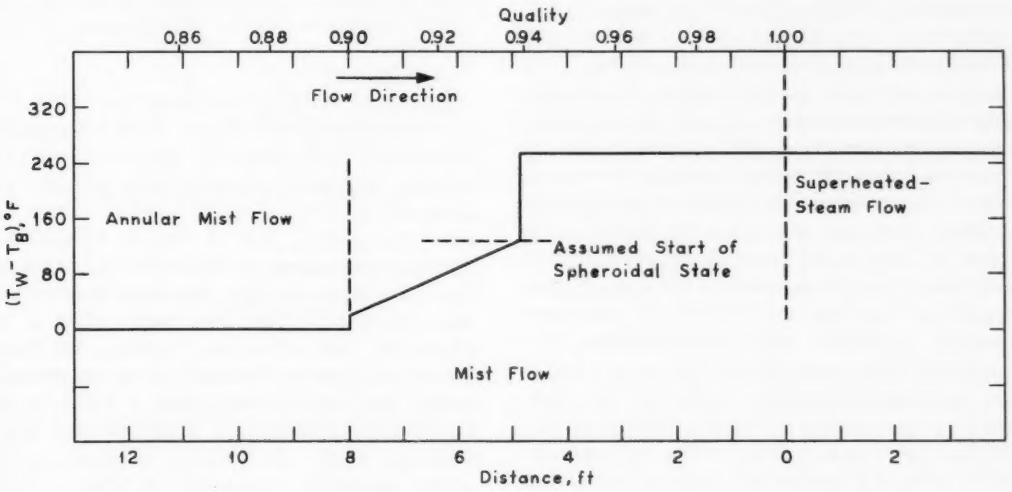

Fig. III-6 Wall temperature predicted by simplified model with spheroidal effect.[15]

*T_w is the wall temperature, and T_b is the bulk temperature of the two-phase mist.

liquid is maintained at the wall. At the axial distance, where the annular film disappears, it can be noted that a discontinuity is present in the curve. The discontinuity is not always present, however, and the case is illustrated where, for example, the annular film had been formed in an entrance section prior to the start of heating and where the rate of diffusion of droplets to the wall is insufficient to keep the wall temperature near saturation just downstream from the point where the film disappears. Another discontinuity, which is created by assuming the onset of the "spheroidal state," exists approximately midway in the mist-flow regime. This condition can best be visualized as the experiment of pouring droplets of water on a hot surface; under certain conditions the droplet is separated from the plate by a vapor layer, and evaporation is slow. The change to a low heat-transfer coefficient results in the discontinuity shown in Fig. III-6. Conduction and other effects would tend to smooth out the temperature discontinuities, and Fig. III-6 is an idealized example containing both discontinuities. Experimental data were taken, and it was found that the general behavior shown by Fig. III-6 could be reproduced. A rather interesting result was noted when an electronic spray analyzer which utilized a probe was used to detect the presence of an electrostatic charge induced on droplets of water. It was discovered that water droplets existed in the stream of superheated vapor at the test-section exit. This departure from equilibrium was not included in the model assumptions. Some of the conclusions[15] are quoted:

1. Two distinct types of heat transfer to a mist flow are possible, depending upon whether the wall temperature is above or below a critical value for the spheroidal state. For the former case the heat transfer coefficients are almost identical to those of dry steam at the same flow rate. For the latter case the heat transfer coefficients are approximately 3 to 6 times the dry steam coefficients. The latter type of heat transfer exists only with certain flow condition and heat flux combinations. High heat fluxes and/or high qualities tend to make the spheroidal state exist. Preheating of the tube wall before injection of water can cause the spheroidal state to exist for conditions where it normally would not. Fluctuations in the flow conditions can cause severe temperature fluctuations in the tube wall as the type of heat transfer changes in a certain region.

2. It appears that equilibrium does not exist between the droplets and vapor in the mist region, and considerable superheating of the vapor or part of the vapor seems to occur even when drops are present. For this reason heat transfer coefficients for a mist should probably not be based on $(T_{wall} - T_{sat})$, as this leads to coefficients for mists that are lower than those for dry steam at equivalent flow conditions.

3. Very high heat transfer coefficients were found for annular-mist flow [of the order of 5,000 Btu/(hr)(ft^2)(°F)]. It appears that if all of the moisture in a stream could be kept on the wall, then high coefficients could be maintained for very high qualities.

Additional work in this country is being done by General Electric's Atomic Power Equipment Department (GE-APED) in connection with the nuclear superheat project. This project was discussed in the June 1961 issue of *Power Reactor Technology*, Vol. 4, No. 3. Preliminary data are presented in reference 16, and a design of a once-through superheat reactor has been prepared.[17] The data were taken in the GE-APED Heat-Transfer Facility; the high-quality data were obtained in an electrically heated test section employing a 0.625-in.-OD heated rod enclosed in a pressure tube with a resulting 0.120- or 0.060-in. annulus. Appropriate pressure, temperature, and voltage-measuring equipment monitored the experimental conditions. The range of variables included pressures from 800 to 1400 psia, flow rates from 0.7 to 1.9×10^6 lb/(hr)(sq ft), and steam qualities from 20 to 100 per cent. The method of operation was to establish the desired flow and inlet subcooling and to increase the test-section power until a wall temperature reached 1000°F, at which time the power would be reduced manually or automatically. Traces of the various wall temperatures revealed varying degrees of stability in the transition region between nucleate and film boiling. If the temperature fluctuations are "small" (no quantitative limits are given), the transition is "smooth," whereas, if divergent oscillations are present, the transition is "sudden." Heat-transfer coefficients for a smooth transition are given in Fig. III-7. Although reference 16 states that "The wall temperatures within this acceptable operating zone can then be obtained from measured heat transfer coefficient," it would appear that the scatter of data in Fig. III-8 would force a conservative calculation for steam qualities

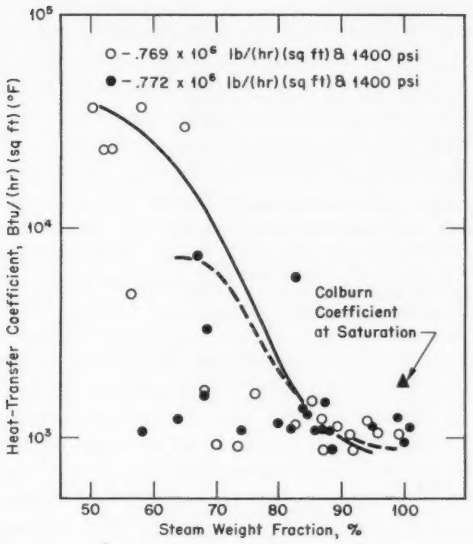
○ – .769 x 10⁶ lb/(hr)(sq ft) & 1400 psi
● – .772 x 10⁶ lb/(hr)(sq ft) & 1400 psi
Colburn
Coefficient
at Saturation
Heat-Transfer Coefficient, Btu/(hr)(sq ft)(°F)
Steam Weight Fraction, %

Fig. III-7 Typical heat-transfer coefficients for smooth transition.[16]

in the transition region from 50 to about 80 per cent. Film-boiling coefficients for smooth temperature transitions are shown in Fig. III-8. The scatter in the 1400-psi data shown in Fig. III-7 is not apparent at the other pressures in Fig. III-8, although transition presumably would occur somewhere in roughly the same quality region as for 1400 psi.

Boiling Water: Burnout

The Nuclear Development Corporation of America (NDA) is engaged in a review of existing data on burnout in an attempt to achieve a better correlation of burnout heat fluxes for the regions of interest in heavy-water boiling reactors. As a first step, experimental forced-convection quality burnout data have been compiled and put on Datatron tape for machine processing. The sources of data are shown in Table III-2. Reference 18 contains the data in tabular form, and should be valuable to the reader in

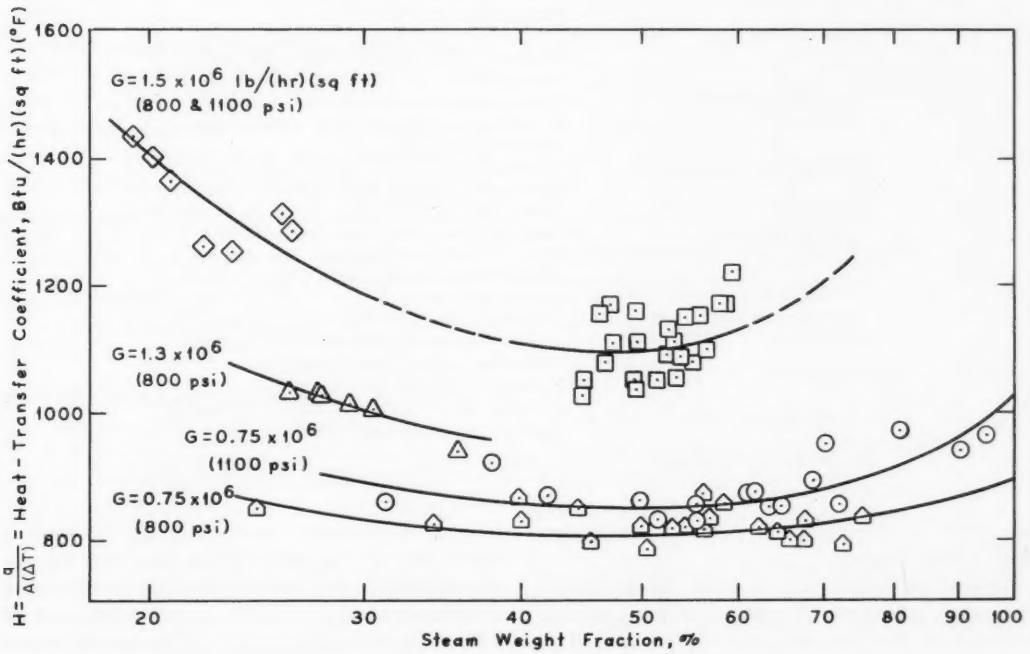

Fig. III-8 Film-boiling coefficients for runs with smooth temperature transitions.[17] ○, 0.75×10^6 lb/(hr)(sq ft) and 1100 psi. △, 1.3×10^6 lb/(hr)(sq ft) and 800 psi. ◇, 1.5×10^6 lb/(hr)(sq ft) and 800 psi. □, 1.5×10^6 lb/(hr)(sq ft) and 1100 psi. ⌂, 0.75×10^6 lb/(hr)(sq ft) and 800 psi. Heater tube: types 304, 316, and 347 stainless steel, 0.625 in. in outside diameter, 40 in. long. Annular flow: 0.865 in. in outside diameter × 0.625 in. in inside diameter = 0.120-in. annulus. Resistance heating: a-c voltage.

Table III-2 BURNOUT DATA SOURCES[20]

NDA Indexes	Source
1 through 1227	R. A. DeBortoli et al., Forced-Convection Heat Transfer Burnout Studies for Water in Rectangular Channels and Round Tubes at Pressures Above 500 psia, Report WAPD-188, October 1958
1228 through 1347	W. H. Lowdermilk and W. F. Weiland, Some Measurements of Boiling Burnout, Report NACA RME54K10, February 1955
1348 through 1449	W. H. Jens and P. A. Lottes, Two-Phase Pressure Drop and Burnout Using Water Flowing in Round and Rectangular Channels, Report ANL-4915, October 1952
1450 through 1471	J. A. Clark and W. M. Rohsenow, Local Boiling Heat Transfer to Water at Low Reynolds Numbers and High Pressure, Report NP-4112, July 1952
1472 through 1495	A. E. Galson and E. E. Polomik, Burnout Data Applicable to Boiling Water Reactors, ANS Paper, June 1957
1496 through 1593	M. A. Styrikovich and L. E. Faktorovich, Effect of Tube Length on the Magnitude of Critical Heat Flow with Forced Convection of Steam-Water Mixtures, *Soviet Phys. Doklady*, 3 (3): 518–520 (1958)
1594 through 1732	R. J. Weatherhead, Critical Heat Flux (Burnout) in Small Diameter Tubes at 2000 psia, ANL Memo, December 1958
1733 through 1738	H. F. Dobel et al., In-Pile Heat Transfer Burnout Tests at MTR, Report WAPD-LSR(1M)-2, August 1955
1739 through 1740	A. Weiss, Results of Final High Heat Flux Tests at 2000 psia on Parallel Flow Rods, Report WAPD-TH-478, 1959
1741 through 1756	A. E. Galson and E. E. Polomik, Burnout Data Applicable to Boiling Water Reactors, ANS Paper, June 1957
1757 through 1777	A. Cicchitti et al., Two-Phase Cooling Experiments: Pressure Drop Heat Transfer and Burnout Measurements, Report CISE-71, November 1959
1778 through 1861	N. A. Dolezhal et al., Uranium-Graphite Reactor with Superheated High Pressure Steam, *Proceedings of the Second United Nations International Conference on the Peaceful Uses of Atomic Energy, Geneva, 1958*, Vol. 8, p. 398, United Nations, New York, 1958

that many of the pertinent data are available under a single cover.

Theoretical study of burnout mechanisms continues. Reference 19 postulates that burnout is caused by the disappearance of the liquid film when the two-phase mixture is flowing in the spray-annular flow regime. Differential material and energy balances on the liquid film are written and integrated over the boiling length. Diffusion of water droplets from the mist, or spray, to the water film is treated by the use of a mass-transfer coefficient, as was done in reference 15. Liquid leaves the film by re-entrainment, and a re-entrainment coefficient is incorporated. Subcooling or superheating of either phase is neglected, an assumption which may be questioned in view of the results published in reference 15. Functional forms are assumed for the re-entrainment and mass-transfer coefficients, yielding relations with a number of adjustable constants which are evaluated from actual burnout data. Although this

technique may raise questions as to the empirical nature of the resulting correlation, the comparison of the derived equation with the Bettis uniform and nonuniform (hot-patch) heat-flux tests shows agreement within about ±20 per cent. Reference 20 assumes a burnout model of fog flow, and postulates that burnout occurs when "... the heat flux becomes greater than that needed for the complete evaporation of all liquid droplets which diffuse to the wall."[20] The authors also speculate that this diffusion of liquid droplets may be a controlling mechanism in low-quality and subcooled burnout. Mass and heat balances are utilized to arrive at a basic equation relating burnout heat flux to the mass-transfer coefficient. The principal assumption utilized appears to be the neglect of axial and eddy slip; a comparison is made of the mass-transfer coefficients predicted from the basic equation with the value of ½ times the friction factor, which results from the analogy between mass and momentum transfer. The agreement is termed "remarkable" in view of the assumptions made in the derivations of the basic equation.

An interesting statistical treatment of burnout for round tubes and uniform heat flux is contained in reference 21. Although data from several experimental groups are studied, the analysis of the 2000-psia data contained[6] in WAPD-188 will serve for illustrative purposes. An often-used WAPD-188 correlation[6] is given below:

$$\phi_{BO}/10^6 = 0.28(H_{BO}/10^3)^{-2.5} (1 + G/10^7)^2 \, e^{-0.0012L/D} \qquad (1)$$

where ϕ_{BO} = burnout heat flux, Btu/(hr)(sq ft)
H_{BO} = enthalpy at burnout location, Btu/lb
G = mass flow rate, lb/(hr)(sq ft)
L = distance from inlet to burnout point, ft
D = diameter of tube, ft

Reference 21 shows a plot of the calculated burnout values using Eq. 1 versus the observed burnout values of the data from which Eq. 1 was derived and notes that the equation correlates the data with an average 95 per cent confidence range of $\pm 0.556 \times 10^6$ Btu/(hr)(sq ft). A regression analysis was applied to the same data to yield the following equation:

$$\begin{aligned}\frac{\phi_{BO}}{10^6} = {} & 2.38835 - 0.14903T + 1.86056G \\ & - 7.87565L + 1.03569D + 0.07294T^2 \\ & - 0.17787G^2 + 5.85628L^2 \\ & - 0.23087TG - 0.22685D^2 \\ & - 0.00814T^3 - 0.04715GL \\ & + 0.00686G^3 - 1.32195L^3 \\ & + 0.179194TG^2 \end{aligned} \qquad (2)$$

where T = °F/100, D = inches (10), G = (lb × 10^{-6})/(hr)(sq ft), and L = inches/10. In Eq. 2, T is the inlet temperature and L is the heated length of the tube. The 95 per cent confidence range was found to be $\pm 0.234 \times 10^6$ Btu/(hr)(sq ft). The authors consider this reduction in the 95 per cent confidence range to be significant. Another equation derived by regression analysis, and similar to Eq. 2, was presented to correlate the 500- to 2750-psia data given in WAPD-188 from MIT, ANL, Bettis, Battelle, and UCLA; this is shown as Eq. 3.

$$\begin{aligned}\frac{\phi_{BO}}{10^6} = {} & 0.78400 - 0.47962T + 0.91581P \\ & + 1.33762G - 4.09246L + 2.60341D \\ & + 0.11501T^2 - 0.54502P^2 \\ & - 0.14804G^2 + 0.95825L^2 \\ & + 0.09933TP - 0.20015TG \\ & - 0.34693D^2 - 0.01258T^3 \\ & + 0.11052PG + 0.22063PL \\ & - 0.31924PD - 0.11436GL \\ & + 0.10575GD + 0.01732LD \\ & + 0.07398P^3 + 0.00643G^3 \\ & - 0.02242L^3 + 0.01384TG^2 \end{aligned} \qquad (3)$$

and the symbols are defined as follows: T = °F/100, P = psia/1000, G = (lb × 10^{-6})/(hr)(sq ft), L = inches/10, and D = inches (10). In reference 21, Eq. 3 is termed "Formula No. 8." The ranges of the variables used in the derivation of Eq. 3 are:

D = 0.075 to 0.306 in.
G = 0.17 to 7.79×10^6 lb/(hr)(sq ft)
L = 6 to 27.4 in.
P = 500 to 2750 psia
T = 72 to 644°F

A review of reference 21 by W. R. Gambill, Oak Ridge National Laboratory, and an author's closure have been published in a subsequent issue of *Nuclear Science and Engineering*.[22] One of the main points raised by Gambill is the inclusion of the diameter term in Eq. 3, and he cites work done at Savannah River and two pieces of Russian literature which suggest that the diameter effect is of importance only when the size of the channel approaches the size of the bubbles. The authors of reference 21 agree that the diameter term may be false, but state that they have done a regression analysis on the rectangular-channel data in reference 6; a similar effect of plate spacing was found to be significant. Bettis, however, according to Susskind,[23] has revised the WAPD-188 rectangular-channel correlation, and the channel spacing term has been dropped in the latest Bettis correlation. The revised correlation is of the form

$$\phi/10^6 = Ae^{-BL}(H/H^*)^{-(C+DL)} \qquad (4)$$

In Eq. 4, A, B, C, D, and H^* are constants that depend on pressure and the particular enthalpy and channel-length range of interest. The range of data for Eq. 4 is as follows:[23]

Pressure:	800 to 2000 psia
Mass velocity, $G/10^6$	> 0.025 lb/(hr)(sq ft)
Fluid enthalpy at DNB:	500 to 1000 Btu/lb
Channel length to DNB:	Up to 72 in. (for pressures > 1850 psia, values of L = 72 in. may be used for lengths between 72 and 96 in.)
Channel spacing:	0.050 to 0.250 in.

The data scatter ±35 per cent with respect to Eq. 4, however, and apparently not all the variables have been taken into account.

In his discussion of reference 21, Gambill cites Russian literature that indicates the lack of a diameter effect for tubular test sections from 0.157 to 0.473 in. in inside diameter. Other Russian data,[24] however, do not substantiate this. Experiments were conducted with tubes 0.118 and 0.323 in. in inside diameter; the following are the quoted results:[24]

> We carried out three experiments (p = 40 and 80 atmos, w = 8 m/sec) with a tube of diameter 3 mm [0.118 in.*]. The values of q_{cr} obtained in these experiments were much higher than those in experiments with a tube of 8.2 mm [0.323 in.*]. The influence of the dimensions of the channel on the values of q_{cr} for low pressures was also established in [reference 25†]. In contradistinction to this it was concluded in [references 26 and 27] that for $p \geq 100$ atmos, q_{cr} was independent of the diameter of the tube (for $4 \leq d \leq 12$ mm) [0.157 in. to 0.473 in.*]. The values of q_{cr} obtained for p = 180–210 atmos in channels formed from tubes with a minimum distance between them of 1 mm [0.0394 in.*] were, according to [reference 28], the same as for a single tube.

Two-Phase Flow

Reference 29 is a survey of the literature on flow patterns existing in two-phase flow through ducts. Thirty-five reports are cited, and the basic horizontal and vertical flow patterns for gas-liquid two-phase mixtures are discussed. In the area of vapor-liquid flow in vertical tubes, only natural-circulation boiling has been studied, and, of the references cited in the review,[29] the most recent one is dated 1940. No studies of flow patterns for forced-circulation boiling were found in the literature surveyed in reference 29. The author concludes that the relation between two-phase pressure drop and two-phase flow patterns has not been thoroughly explored. In addition, it is concluded that little work appears to have been done on the stability of two-phase flow patterns.

The application of mixing-length theory to predict two-phase flow phenomena is presented in reference 30. Since details of the application are somewhat specialized, only the conclusions[30] are quoted:

1. The density and velocity distributions are of the power type and their exponent varies with total liquid Reynolds number, mean fluid density, and channel geometry. The calculated profiles are much more curved than in single-phase flow and agree with the density distributions measured by Petrick.
2. The two-phase pressure drop in horizontal flow is a function of total liquid Reynolds number and mean fluid density. In vertical flow, it also depends upon the equivalent total liquid velocity head.

---

*Added by editor.

†The reference numbers have been changed to be compatible with the reference numbers appearing in this Review.

3. The ratio of two-phase pressure drop to total liquid pressure drop decreases as the total liquid Reynolds number increases, or as the channel geometry changes from horizontal to vertical or from pipe to parallel plates. Available low and high pressure data in horizontal and vertical channels confirm the predicted trends.

4. Good agreement is obtained between test and analytical two-phase pressure losses at high flow and mean fluid density. The predicted values are, however, low at reduced flow and mean fluid density. This discrepancy is attributed to the approximate treatment presently used near the channel wall. Improved solutions patterned after those of single-phase flow with variable fluid properties are expected to improve the correlation between tests and analysis.

5. According to the present analysis, local slip must exist between liquid and gas at every position in the flow channel.

6. The proposed model reduces a two-phase problem to an equivalent one in single-phase flow. As such, it can be extended to predict such effects as film boiling, entry length, and heat transfer in two-phase flow.

References

1. C. J. Baroczy et al., Development of a Variable Orifice for HNPF Fuel Channels, USAEC Report NAA-SR-5369, Atomics International, May 1, 1961.
2. J. C. Rowley and J. B. Payne, Steady-State Temperature Solution for a Heat-Generating Circular Cylinder Cooled by a Ring of Equal Holes, USAEC Report LA-2486, Los Alamos Scientific Laboratory, Dec. 1, 1960.
3. K. R. Merckx, Temperature Distributions of Reactor Fuel Element End Caps, USAEC Report HW-64161(Rev.), Hanford Atomic Products Operation, January 1961.
4. Argonne National Laboratory, A Study of the Variation of Steam Velocity in Vertical Boiling Channels, Report of Work Done by General Nuclear Engineering Corp. Under ANL Subcontract, USAEC Report ANL-6251, Argonne National Laboratory, November 1960.
5. J. G. Collier, Suggested Design Methods for the Application of Spray Evaporation to a Steam Cooled Heavy Water Moderated Reactor, British Report AERE-M-707, November 1960.
6. R. A. DeBortoli et al., Forced-Convection Heat Transfer Burnout Studies for Water in Rectangular Channels and Round Tubes at Pressures Above 500 psia, USAEC Report WAPD-188, Westinghouse Electric Corp., Bettis Atomic Power Laboratory, October 1958.
7. J. A. R. Bennett et al., Heat Transfer to Two Phase Gas-Liquid Systems, Steam-Water Mixtures in the Liquid-Dispersed Region in an Annulus, British Report AERE-R-3159, November 1959.
8. J. A. R. Bennett and J. D. Thornton, Pressure-Drop Data for the Vertical Flow of Air-Water Mixtures in the Climbing-Film and Liquid-Dispersed Regions, British Report AERE-R-3195, December 1959.
9. J. G. Collier and G. F. Hewitt, Data on the Vertical Flow of Air-Water Mixtures in the Annular and Dispersed Flow Regions, British Report AERE-R-3455, August 1960.
10. R. W. Lockhart and R. C. Martinelli, *Chem. Eng. Progr.*, 45: 39 (1939).
11. J. M. Chenoweth and M. W. Martin, *Petrol. Refiner*, 34: 151 (1955).
12. S. Calvert and B. Williams, *A.I.Ch.E. Journal*, 1: 78–86 (1955).
13. G. H. Anderson and B. G. Mantzouranis, *Chem. Eng. Sci.*, 12: 109–126 (1960).
14. M. Wicks and A. E. Dukler, Entrainment and Pressure Drop in Concurrent Gas-Liquid Flow–I. Air-Water in Horizontal Flow, University of Houston, Texas. (Unpublished)
15. J. D. Parker and R. J. Grosh, Heat Transfer to a Mist Flow, USAEC Report ANL-6291, Argonne National Laboratory, January 1961.
16. General Electric, Nuclear Superheat Project Fifth Quarterly Progress Report, July–September 1960, USAEC Report GEAP-3581, September 1960.
17. R. T. Pennington, Steam-Cooled Reactor Evaluation. Study of 300 Mw(e) Once-Through Superheater Reactor, USAEC Report GEAP-3633, General Electric Co., Atomic Power Equipment Dept., January 1961.
18. H. Firstenberg et al., Compilation of Experimental Forced-Convection, Quality Burnout Data with Calculated Reynolds Numbers, USAEC Report NDA-2131-16, Nuclear Development Corp. of America, June 30, 1960.
19. H. S. Isbin et al., A Model for Correlating Two-Phase, Steam-Water, Burnout Heat-Transfer Fluxes, *J. Heat Transfer*, 83(2): 149 (May 1961).
20. K. Goldmann et al., Burnout in Turbulent Flow—A Droplet Diffusion Model, *J. Heat Transfer*, 83(2): 158 (May 1961).
21. R. T. Jacobs and J. A. Merrill, The Application of Statistical Methods of Analysis for Predicting Burnout Heat Flux, *Nuclear Sci. and Eng.*, 8(6): 480–496 (December 1960).
22. W. R. Gambill, Re: The Application of Statistical Methods of Analysis for Predicting Burnout Heat Flux, and R. T. Jacobs and J. A. Merrill, Re: The Application of Statistical Methods of Analysis for Predicting Burnout Heat Flux—Rebuttal, *Nuclear Sci. and Eng.*, 10: 92–93 (May 1961).
23. H. Susskind, A Survey of Bulk-Boiling Studies in Pressurized Water Reactor Systems, USAEC Report BNL-636, Brookhaven National Laboratory, August 1960.

24. I. T. Alad'ev et al., Burnout Heat Flux for Flow of Water in Pipes, *Soviet J. At. Energy*, 6(1): (January 1959).
25. V. S. Chirkin and V. P. Yukin, *Zhur. Tekh. Fiz.*, 26(7): 1542 (1956).
26. B. A. Zenkevich and V. I. Subbotin, *Soviet J. At. Energy*, 3(8): 149 (1957).
27. B. A. Zenkevich, *Soviet J. At. Energy*, 4(1): 74 (1958).
28. B. A. Zenkevich et al., *Soviet J. At. Energy*, 4(4): 370 (1958).
29. J. H. Vohr, Flow Patterns of Two-Phase Flow — A Survey of Literature, USAEC Report TID-11514, Columbia University, Dec. 15, 1960.
30. S. Levy, Prediction of Two-Phase Flow from Mixing Length Theory, USAEC Report GEAP-3628, General Electric Co., Atomic Power Equipment Dept., Dec. 27, 1960.

Section IV

DYNAMICS AND SAFETY: PRESSURE-WAVE PROPAGATION IN STEAM-WATER MIXTURES

The understanding of the propagation of sound and pressure waves in steam-water mixtures may have several applications in the study of water-moderated reactors: in determining pressure pulses associated with accidents or malfunctions, in interpreting transient pressure measurements, and possibly in the theory of boiling-water reactor stability.

A study of the propagation of pressure waves in mixtures of water and steam has been performed by the Armour Research Foundation. The analytical and experimental methods used in the study, as well as the results obtained, are presented in reference 1. Some of the conclusions reached are summarized below.

1. The velocity of propagation of small-amplitude sound waves in mixtures of water and steam is very low, and is less in the mixture than in either of the constituents. The theoretical sound velocity is given as a function of steam quality in Fig. IV-1 for several different pressures and the corresponding saturation temperatures. The theory is derived on the assumptions that the pressure amplitude is too small to cause condensation of all the steam and that the frequency of the sound wave is low enough that thermodynamic equilibrium is maintained, on effectively an instant-by-instant basis, at all points in the system.

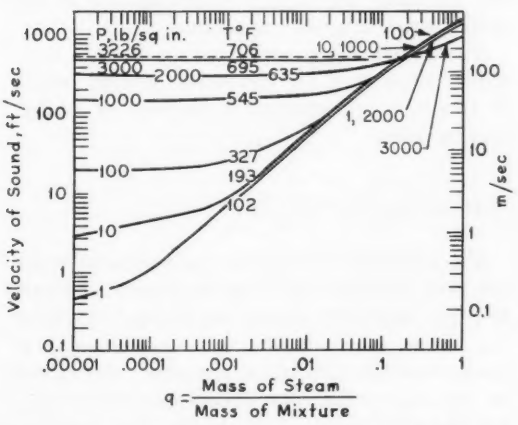

Fig. IV-1 Velocity of sound as a function of steam quality.[1]

2. If boiling water is subjected to large-amplitude pressure waves, the steam will be completely eliminated. If the pressure differential is only large enough to barely condense all the steam, the wave propagation velocity is low, or nearly equal to the small-amplitude sound-wave speed.

3. As a large-amplitude wave moves through boiling water, condensing the steam as it proceeds, the rate of rise of pressure decreases. A true shock wave is not propagated. However, the condensing, or driving, pressure produces a velocity in the condensed fluid. When the moving condensed phase reaches a region of no bubbles, very high-amplitude pressure pulses are generated. Peak pressures in the pulses are an order of magnitude greater than the original driving pressure, and the amplification is apparently due to the formation of a water hammer.

The reference points out that the pressure-wave propagation characteristics of a liquid-vapor mixture, in which the masses of the phases will change with the changing pressure, are quite different from the characteristics of a liquid-gas mixture, in which no condensation occurs. Obviously, caution should be used in simulating steam-water mixtures by air-water mixtures, as is sometimes attempted.

Reference

1. H. B. Karplus, Propagation of Pressure Waves in a Mixture of Water and Steam, USAEC Report ARF-4132-12, Armour Research Foundation, Illinois Institute of Technology, January 1961.

Section V

SHIELDING

Dose-Rate Calculations of Air-Scattered Gamma Radiation

In hazards analyses a difficult but often necessary calculation is that of finding the scattered gamma dose rate outside the containment building from a hypothetical release of fission products inside the building. This estimation has been especially difficult at large distances because experimental and analytical data have not been available. For an unshielded containment building, the unscattered or direct-beam dose rate is greater than the scattered dose rate to a distance of about 100 yd. If a direct-beam shield is included in the building design to reduce the dose rate in the vicinity of the building, the scattered dose rate originating from the unshielded portion, usually the top, can and often does become the controlling contribution to the total dose rate at and beyond the boundary of the exclusion area.

The only information previously available[1] was a set of Monte Carlo results for source-detector separation distances up to 100 ft. These results include the single- and multiple-scattered gamma-ray flux and dose rate, in an infinite medium of air, for several monodirectional source angles and for several monoenergetic source energies. The actual scattering geometry in practical cases usually consists of a semi-infinite region of air with a ground interface; at small separation distances the assumption of an infinite medium of air is a good approximation.

The exclusion radius for a power reactor is ordinarily much larger than 100 ft, and the need for data applicable to longer distances has been acute. A recently published paper[2] gives the results of Monte Carlo calculations of gamma fluxes and dose rates for distances of 180 to 1500 yd. The tabular results are for point isotropic monoenergetic sources of 0.5, 1.0, 2.0, 4.0, and 6.0 Mev in an infinite medium of air of sea-level density of 1.293×10^{-3} g/cm^3. The results include the angular and energy distribution at the detector, as well as the angular distribution of the dose rate. Included in the tables are the unscattered flux and dose rates. Again, the practical geometry of interest is usually a semi-infinite medium of air with a ground interface. Direct application of the results to this case should overestimate the dose rate at the detector, but by no more than a factor of 2. In any case, the new data represent a very helpful contribution to the practical calculation of dose rates at large distances. It should be kept in mind that the results are not applicable when the source is partially shielded, since the partial shielding destroys the isotropic requirement of the source. At more expense, the calculations could be done for monodirectional sources; they were originally done for atomic bomb studies, and, for this purpose, the angular and energy distributions at the detector are of more importance.

If the dose rates are required for air densities other than the sea-level density, which is likely, a transformation derived by Zerby[3] may be used.

Radioisotope Data

A compilation of data for many radioisotopes has been published by a United Kingdom Atomic Energy Authority Research Group.[4] Included are some isotopes of particular interest in power-reactor activation analysis. The tables in the report list, for each reported isotope, the mode of decay, the half life, the energies of the radiation emitted, the thermal-neutron

cross sections—both absorption and activation—the specific activities for several irradiation times in a thermal flux of 10^{12} neutrons/(cm^2)(sec), and the transition percentages (where available). The latter are of particular interest to the shield designer.

The activation cross section is not reported for single isotopes, as in BNL-325, but its magnitude is based on the natural element. That is, the activation cross section of the single isotope is multiplied by the abundance of the isotope in the natural element.

The specific activities were calculated using the 2200-m/sec cross section. Therefore the appropriate temperature and neutron distribution should be applied to attain the correct specific activity.

References

1. R. E. Lynch et al., A Monte Carlo Calculation of Air-Scattered Gamma Rays, USAEC Report ORNL-2292(Vols. 1–5), Oak Ridge National Laboratory, Oct. 7, 1958.
2. M. B. Wells, A Monte Carlo Calculation of Gamma-Ray and Fast-Neutron Scattering in Air, in OCDM-NRDL Shielding Symposium Proceedings, October 31–November 1, 1960, Report NP-10038, pp. 308–395, Office of Civil and Defense Mobilization and Naval Radiological Defense Laboratory.
3. C. D. Zerby, Radiation Flux Transformation as a Function of Density of an Infinite Medium with Anisotropic Point Sources, USAEC Report ORNL-2100, Oak Ridge National Laboratory, Oct. 22, 1956.
4. R. A. Allen et al., Radioisotope Data, British Report AERE-R-2938, January 1961.

Section VI

INSTRUMENTATION

In-Core Instrumentation

Throughout the history of nuclear reactors, there has been an interest in instrumentation to measure various reactor-core performance characteristics such as coolant-flow distribution, neutron-flux distribution, fuel-cladding leakage, coolant-temperature variations, fuel temperature, and fuel-cladding temperature. In order to measure many of these characteristics with the desired precision and resolution, an appropriate detector must be mounted in the reactor core. Such detector placement is, however, fraught with very difficult problems. Chief among these have been the inability of the detectors to withstand the environmental conditions of high radiation intensity and high temperature, the necessity of a large number of pressure-vessel penetrations, and the requirement for a large number of detectors to gather information of the desired scope and detail. Three strong incentives have preserved a continuing effort to develop satisfactory in-core instrumentation. These are: (1) the necessity for ensuring against spatial oscillations of the power density in very large cores, (2) the economic incentive to maintain flat distributions of power and of fuel burnup in order to increase the average power density and the average fuel life, and (3) an incentive to locate failed fuel elements during power operation, since it is extremely difficult to locate the failure when the reactor is shut down. In a recent symposium on power-reactor in-core instrumentation, a number of in-core instrumentation problems and solutions were presented and discussed. The minutes[1] of this meeting are discussed below.

Two divergent viewpoints on the future of in-core instrumentation were presented. One held that in-core instrumentation should be placed primarily in reactor experiments and prototypes in order to gain design information and that little or no in-core instrumentation would be used in most large power-producing reactors. A second viewpoint held that with large cores the economic incentives tend to force the use of in-core instrumentation, and it was predicted that, once satisfactory instruments are available, there will be a gradual atrophying of out-of-core instrumentation for reactor control and that ultimately all reactor control will be based on in-core measurements. Positions between these two extremes are, of course, possible. It was pointed out that, for example, with present instrument costs and the requirement for a large number of in-core instruments, the possible fuel savings just about equal the added cost of the in-core instruments. The validity of this estimate depends, of course, upon the life expectancy of in-core instruments, which now appears to be roughly the same as that of a single fuel loading.

The major portion of the meeting was taken up with informal reports of what various groups are now using as in-core instrumentation. Table VI-1 summarizes these reports in terms of solutions and partial solutions to the two main core-monitoring problems, i.e., measurement of power distribution and detection and location of failed fuel elements. The reactors are listed in the order in which the reports were delivered. Reference to the table shows that there is considerable variation in both the extent of in-core instrumentation used and in the techniques applied.

Several speakers pointed out that the choice of failed-element detection and location systems depends upon whether the fuel cladding is bonded to the fuel. With unbonded fuel it is observed that a sudden rush of gaseous fission products

Table VI-1 IN-CORE INSTRUMENTATION IN USE OR PLANNED

Reactor	Purpose of instrument	
	Measurement of power distribution	Failed-element detection and location
Shippingport	Fuel-wire activation flux mapping; flow nozzles and DP cells on certain instrumented fuel assemblies; thermocouples measure both inlet and outlet coolant temperature on some fuel assemblies	Delayed-neutron measurement on sample stream from each assembly
Indian Point	None	No location equipment planned; detection equipment not reported
N.S. *Savannah*	Thermocouples to measure exit fluid temperature on some fuel assemblies	No location equipment planned; detection equipment not reported
Savannah River Plant reactors	Stainless-steel wire activation flux mapping; neutron thermometer*; gamma thermometer; gamma ion chambers	Low-energy gamma monitoring of sample stream from each fuel channel; charged-wire precipitation of gas is used to some extent
PM-1 (Sundance, Wyo.)	One fuel assembly is instrumented	Not reported
CVTR	Resistance thermometer and venturi flowmeter in each of 42 pressure tubes	Iodine gamma monitor on cation column for detection; sample from each tube is drawn through anion column and scintillation detector cell for location
Yankee	One core quadrant has a flux-mapping wire and an exit coolant temperature thermocouple for each fuel assembly	Not reported
Hanford reactors	Wire-activation flux mapping; gamma ion chambers	Gross gamma monitor capable of monitoring each fuel channel
PRTR	Flow venturis for each channel; exit coolant temperature resistance thermometer on each channel	Gross gamma monitor capable of monitoring each fuel channel
EBWR	Wire-activation flux mapping; special fuel assemblies will have turbine type flowmeter and fuel-meat temperature thermocouples	Not reported
Dresden	64 in-core neutron ion chambers	Gamma-ray spectroscopy of off-gas from air ejectors is used for detection; 44 sampling lines, each seeing 11 fuel elements, are used for location determination
OMRE	Thermocouples measure outlet coolant temperature on each fuel channel; some flow instruments are planned for the fourth core	Not reported
Piqua	Not reported	Delayed neutron monitoring of sample line from each coolant channel for location; similar system on main coolant channel is used for detection
SRE	Thermocouples measure outlet coolant temperature on each fuel channel	None
EGCR	Pneumatic temperature sensors measure outlet coolant temperature on each fuel channel; other devices were being considered but had not been decided upon at the time of the meeting	Charged wire-gas precipitator monitors sample line from each coolant channel
GCRE-I	Outlet coolant temperature is measured by thermocouples at each pressure tube in the core; some special fuel assemblies are highly instrumented	Fission-product "sniffer" line is provided for each coolant channel; detector selection was not reported

*Owing to success of the gamma ion chamber, development of the neutron thermometer has been discontinued at SRP.

accompanies a fuel rupture. In this case a fission-product detector designed to detect these gases appears to be most effective. On the other hand, with bonded cladding, the fission products released are primarily recoil particles, and the rate of release is dependent upon the power level and the size of the failure area. In this case a delayed-neutron monitor is frequently found to yield the greatest signal-to-noise ratio obtainable.

New Instrument Developments

Several new instrument developments of interest to the power-reactor designer have recently been reported. Included in these are a high-temperature, radiation-tolerant preamplifier; a new in-core neutron-flux monitor; and an alpha-particle contamination monitor.

In connection with its aircraft nuclear propulsion activities, the General Electric Company developed a pulse preamplifier[2] which has been tested and found to operate successfully at a temperature of 540°F. Further, the chamber has operated a total of 1530 hr in the west animal tunnel of the Graphite Reactor at ORNL. During this time there was a total of 1366 hr of high-level irradiation. The integrated exposure was 2.52×10^{15} nvt. During this exposure a gain change of only about 0.5 db was observed. The nominal gain of the preamplifier is about 40 db. Further tests at higher irradiation levels are planned.

The coaxial cable used with this preamplifier is of interest. The cable consisted of a stranded nickel-plated center wire with a surrounding dielectric of braided Fiberglas, a double-shield braid of nickel-plated copper, and an outer covering of silicone-impregnated Fiberglas. Its characteristics at high temperature were found to be very satisfactory. At 95 per cent relative humidity, the insulation resistance was found to drop to a marginal value, but operation of the cable-preamplifier combination at this humidity level was considered satisfactory.

References

1. Proceedings of the Power Reactor In-Core Instrumentation Meeting, Washington, D. C., April 28-29, 1960, USAEC Report TID-7598, March 1961.
2. E. M. Palmer, Final Program Report for the 542°F Temperature and Radiation Tolerant Pulse Preamplifier, USAEC Report APEX-549, General Electric Co., Aircraft Nuclear Propulsion Department, March 1959. (Classified).

Section VII

FUEL CYCLES: THORIUM

Reactivity Transient in Irradiated Thorium

Thorium that has been subjected to neutron irradiation will experience a reactivity transient that may last for several months. This transient is due mainly to the decay of Pa^{233} to U^{233}, with a 27.4-day half life; there may also be effects of the decay of U^{233} and U^{235} fission products present in quantities which are functions of the neutron-flux level of the irradiation and of the irradiation time. The principal mechanisms for the formation of the higher isotopes can be described by the following scheme (isotopic composition of natural thorium is 100 per cent Th^{232}):[1]

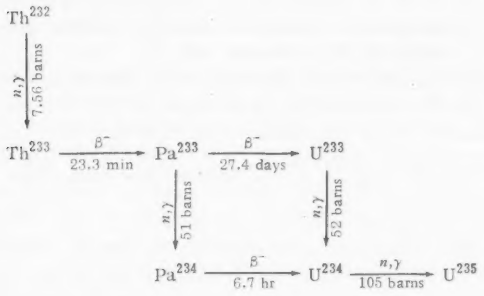

The preceding half lives and thermal cross sections are based on values in the second edition[1,2] of BNL-325.

Analytical studies of the reactivity transient in irradiated thorium are reported in references 3 and 4. Reference 3 also reports the measurements of reactivity variation with time for two thorium slugs of the Savannah River type, which had been irradiated at a thermal-neutron-flux level of about 2.5×10^{13} nv for about 49 days. The slugs had been in the Materials Testing Reactor (MTR) for three irradiation cycles. The variation of reactivity in the slugs was measured in the Reactivity Measurement Facility (RMF) (located in the MTR canal), starting at 3.22 hr after removal from the MTR and continuing for 161 days. Previous work at the MTR had shown that this level of irradiation of Th^{232} produces very little U^{235}—less than 0.1 per cent of the produced U^{233}. Analysis of these measurements indicated that the effect of U^{233} fission products (even the short-term transient due to the buildup and decay of Xe^{135}) was negligible; therefore the observed reactivity transient is attributed, within experimental accuracy, to the decay of Pa^{233} to U^{233}. On the basis of this result, reference 3 also discusses the practicality of using thorium as a monitor of large neutron flux (integrated).

The net production of U^{233} and Pa^{233} in one of the slugs during irradiation was estimated to be 0.167 mg/g of Th^{232} and 0.367 mg/g of Th^{232}, respectively. Additional measurements are reported in reference 4, involving a pair of Savannah River type thorium slugs, which were irradiated in the MTR for an estimated 2.5×10^{20} nvt at an estimated flux of 1.8×10^{14} nv, and a pair of Hanford type thorium slugs, which were irradiated for an estimated 6.6×10^{20} nvt at an estimated flux of 2.0×10^{13} nv. The variation of reactivity in the slugs (following irradiation) was measured in the RMF. Analysis of these data verifies the earlier work reported in reference 3; namely, the long-term transient is due to the decay of Pa^{233} to U^{233}.

Long-Term Reactivity Changes in Irradiated Thorium

Reference 5 describes measurements of the long-term reactivity changes in irradiated thorium samples and discusses the analysis of

the results. This work is part of a joint United Kingdom–Canadian program. The reactivity effects of thorium cartridges were measured in the GLEEP reactor at Harwell, England, before and after the cartridges were irradiated in the NRX reactor at Chalk River, Canada. The cartridges were subjected to a maximum irradiation of 1.44 neutrons/kb (1.44×10^{21} nvt) at flux levels of between 0.268×10^{13} and 1.869×10^{13} nv. The aluminum-canned cartridges were 19.08 cm in length and 3.86 cm in diameter, and each contained 1635 g of thorium.

The long-term reactivity changes are due to the formation of U^{233} and U^{235}, to the neutron absorption by the fission products of these two isotopes, and to the absorption by other heavy isotopes produced, such as U^{234} and Pa^{233}; but the predominant factor is the formation of the fissile U^{233}. Allowance was made for the decay of Pa^{233} to U^{233} during the period between removal of the cartridges from the NRX reactor and measurement in the GLEEP reactor.

The buildup of the heavy isotopes and fission products causes a change in the apparent absorption cross section in the thorium when it is measured in the GLEEP reactor, the neutron production by fission having the effect of negative absorption; the change in cross section also changes the neutron flux through the thorium cartridge. After proper calibration, perturbation and oscillator techniques were used to measure the change in apparent cross section of the thorium in the GLEEP reactor.

The measured change in apparent cross section for each cartridge was compared to the theoretical change to be expected from a measurement in the GLEEP reactor. The expected values were calculated using "world" nuclear data and a simplified model of neutron behavior that had been demonstrated in an earlier set of experiments.[6] Agreement between experimental and calculated values was, in general, shown to be within the limit of accuracy of the experiment. However, the reactivity change[1] would be more accurately predicted by this model if the "world" value for eta of U^{233} ($\eta_{23} = 2.28 \pm 0.02$ at 2200 m/sec) were reduced by 1 per cent to 2.26 ± 0.02.

References

1. D. J. Hughes and R. B. Schwartz, Neutron Cross Sections, USAEC Report BNL-325(2nd Ed.), July 1, 1958.
2. D. J. Hughes et al., Neutron Cross Sections, USAEC Report BNL-325(2nd Ed.)(Suppl. 1), Jan. 1, 1960.
3. R. G. Nisle, An Analysis of a Reactivity Transient in Irradiated Thorium, USAEC Report IDO-16513, Phillips Petroleum Co., July 9, 1959.
4. R. G. Nisle and D. A. Millsap, Additional Measurements of the Reactivity Transient in Irradiated Thorium, USAEC Report IDO-16660, Phillips Petroleum Co., Mar. 13, 1961.
5. D. C. C. Gibbs et al., Long Term Reactivity Changes in Irradiated Thorium, British Report AEEW-R-29, November 1960.
6. H. Rose et al., The Use of the Pile Oscillator in Thermal Reactor Problems, *Proceedings of the Second United Nations International Conference on the Peaceful Uses of Atomic Energy, Geneva, 1958*, Vol. 16, p. 34, United Nations, New York, 1958.

Section VIII

CONTROL-ROD MATERIALS

The June 1960 issue of *Power Reactor Technology*, Vol. 3, No. 3, pages 26 to 47, presented a review of the first topical report[1] of the AEC-sponsored research and development program on solid neutron-absorbing materials; the program is being conducted by the Atomic Power Equipment Department of the General Electric Company. The following discussion is concerned largely with results reported during the succeeding year of this program and with operating experience with boron–stainless steel control rods.

Reactivity Worth

Additional materials were tested in the Critical Experiment Facility of the Vallecitos Atomic Laboratory,[2] and the results of relative-worth measurements are listed in Table VIII-1. The materials were used in the form of 3- by 6-in. plates having various thicknesses as recorded in the table. The critical assembly was H_2O moderated; it was fueled with UO_2 pellets, 0.491 in. in diameter, in 0.562-in.-OD aluminum tubes of 30-mil wall thickness. The fuel rods were located on a uniform square lattice, with 0.8-in. spacing between centers; the enrichment was 1.6 wt.% U^{235}. Measurements were made of the reactivity worth of each absorbing plate, bare, and of each plate plus a constant cadmium box enclosing it. The relative worth is expressed, arbitrarily, as the ratio of the reactivity worth of the arrangement in question to the reactivity worth of a 0.200-in.-thick cadmium plate in the cadmium box. The results have been edge corrected to reduce the edge effect to that which would characterize a plate of zero thickness. The equivalent boron surface density is that surface density of natural boron which, if substituted for the sample (bare or in the cadmium box as the case might be), would yield the same reactivity worth. The epithermal effectiveness of each material is illustrated by the cadmium-covered relative worths and by the cadmium-covered equivalent boron surface densities.

Measurements were made on slabs composed of europium hexaboride–copper dispersions, with copper cladding plus a boron–stainless steel outer cladding. These measurements are reported in Table VIII-2. Rows of close-packed stainless-steel tubes containing boron carbide or dysprosium oxide were tested in single rows and in double rows; the results are summarized in Table VIII-3.

Reference 3 contains an analysis of experiments in which a series of gold slabs of several thicknesses were inserted into the core, with and without cadmium shields. The number of neutrons absorbed in the gold is demonstrated to be proportional to the reactivity worth of the rod for both epithermal and thermal absorptions. The analysis indicates that 42 per cent of the epithermally captured neutrons would have been captured thermally in the cadmium. When a two-and-one-half-group diffusion theory[4] is used to calculate the absorptions, it appears that the proper lethargy width for the second group is from 0.6 to about 7 ev, within an estimated factor of 2. The use of a 10^5-ev upper limit for the second group tends to overestimate the worth of second-group absorptions by about 30 per cent. If, however, the epicadmium group transmission probability is normalized to the results of relative-worth experiments, this error is canceled and a wide-lethargy second group may be used for design work.[5]

Table VIII-1 RELATIVE REACTIVITY WORTHS OF VARIOUS CONTROL-ROD MATERIALS[2]

Material	Surface density, g/cm²	Thickness, in.	Relative worth, bare	Relative worth, Cd covered	Equivalent boron surface density, g/cm²	
					Bare	Cd covered
Boron glass	0.0478*	0.101	0.8183	1.0093		
(B_2O_3)	0.1575	0.104	1.0046	1.1112		
	0.0888	0.200	0.9266	1.0617		
	0.3026	0.206	1.0863	1.1838		
	0.4241	0.290	1.1305	1.2181		
	0.0664	0.302	0.8789	1.0349		
	0.02392	0.109	0.6892	0.9802		
	0.01430	0.065	0.5810	0.9510		
	0.03822	0.174	0.8014	1.0100		
Boron carbide	1.5260	0.306	1.2963	1.3666		
(B_4C)	1.0011	0.204	1.2505	1.3255		
Erbium oxide	0.558	0.049	0.5698	0.9789	0.0137 ± 0.0007	0.0290 ± 0.0060
(Er_2O_3)	2.009	0.175	0.8411	1.0171	0.0530 ± 0.0039	0.0530 ± 0.0070
	3.405	0.299	0.9296	1.0668	0.0940 ± 0.0066	0.0950 ± 0.0120
Terbium oxide	1.624	0.125	0.7650	1.0352	0.0347 ± 0.0023	0.0670 ± 0.0084
(Tb_4O_7)	2.287	0.175	0.8411	1.0646	0.0530 ± 0.0039	0.0940 ± 0.0120
LiAl	0.3150	0.058	0.2379	0.9355	0.0026 ± 0.0002	0.0060 ± 0.0051
10.2% Li	0.6614	0.125	0.4193	0.9406	0.0071 ± 0.0004	0.0090 ± 0.0052
6.39% Li^6	0.9976	0.181	0.5091	0.9503	0.0105 ± 0.0006	0.0140 ± 0.0054
	1.3366	0.248	0.5702	0.9580	0.0138 ± 0.0007	0.0165 ± 0.0055
	1.6527	0.306	0.6196		0.0170 ± 0.0008	
LiMg	0.1620	0.050	0.8027	1.0023	0.0425 ± 0.0029	0.0425 ± 0.0065
18.3% Li	0.3162	0.097	0.9147	1.0734	0.0870 ± 0.0060	0.0950 ± 0.0120
73.04% Li^6	0.4788	0.147	0.9862	1.0953	0.1390 ± 0.0105	0.1340 ± 0.0155
	0.6459	0.199	1.0172	1.1284	0.1720 ± 0.0150	0.1900 ± 0.0205
	0.8082	0.249	1.0532	1.1497	0.2220 ± 0.0210	0.2300 ± 0.0240
	0.9771	0.301	1.0697	1.1729	0.2620 ± 0.0260	0.2770 ± 0.0280
Au	1.254	0.026	0.5603	1.0011	0.0120 ± 0.0007	0.0420 ± 0.0066
	2.438	0.050	0.7225	1.0340	0.0280 ± 0.0016	0.0650 ± 0.0083
	3.622	0.075	0.8227	1.0533	0.0480 ± 0.0035	0.0823 ± 0.0105
	4.918	0.101	0.8893	1.0738	0.0720 ± 0.0053	0.1050 ± 0.0130
	7.391	0.153	0.9626	1.1007	0.1180 ± 0.0086	0.1410 ± 0.0165
	9.599	0.198	0.9802	1.1167	0.1330 ± 0.0100	0.1660 ± 0.0185
	12.747	0.263	1.0283	1.1481	0.1878 ± 0.0178	0.2260 ± 0.0235
Ag in Cd	1.268	0.049	0.8860	1.0390	0.0721 ± 0.0069	0.0690 ± 0.0086
79.60 wt.% Ag	2.636	0.102	0.9841	1.0789	0.1370 ± 0.0110	0.0990 ± 0.0124
15.06 wt.% In	3.904	0.151	1.0247	1.0966	0.1820 ± 0.0170	0.1360 ± 0.0157
5.17 wt.% Cd	5.203	0.202	1.0506	1.1152	0.2250 ± 0.0215	0.1650 ± 0.0182
0.04 wt.% Cu	6.471	0.251	1.0821	1.1239	0.2910 ± 0.0290	0.1790 ± 0.0195
+ trace PbAlMg	7.752	0.300	1.0878	1.1289	0.3080 ± 0.0310	0.1890 ± 0.0204

* Surface densities of boron.

Table VIII-2 RELATIVE REACTIVITY WORTHS OF EUROPIUM HEXABORIDE–COPPER SLABS CLAD WITH COPPER PLUS BORON–STAINLESS STEEL[2]

(Density of EuB_6 = 0.355 g/cm³ in Copper Matrix; Density of Boron in Stainless Steel = 0.16 g/cm³ Boron)

Thickness, in.				Relative worth, bare	Relative worth, Cd covered	Equivalent boron surface density, g/cm²	
Total	EuB_6	Cu	S.S.			Bare	Cd covered
0.375	0.285	0.015	0.030	0.965		0.1125 ± 0.0081	
0.293	0.203	0.015	0.030	0.919	1.017	0.0875 ± 0.0060	0.0530 ± 0.0072
0.243	0.203	0.005	0.015	0.902	1.026	0.0780 ± 0.0055	0.0590 ± 0.0076
0.211	0.121	0.015	0.030	0.844	0.994	0.0550 ± 0.0040	0.037[illegible] ± 0.0064

Table VIII-3 RELATIVE REACTIVITY WORTHS OF ROWS OF EIGHTEEN 0.161-IN.-OD STAINLESS-STEEL TUBES, 0.020-IN.-WALL, CONTAINING BORON CARBIDE OR DYSPROSIUM OXIDE RODS[2]

	Relative worth	
	Bare	Cadmium covered
Tubes Containing Rods of Dysprosium Oxide Having Density of 6.48 g/cm³		
Single row	0.932	1.088
Two rows	1.067	
Two rows nested	1.073	
Tubes Containing Rods of Boron Carbide Having Density of 2.34 g/cm³		
Single row	1.090	1.192
Double row	1.232	
Two rows nested	1.239	

Effects of Burnup on Reactivity Worth

One of the important characteristics of a control poison is its rate of change of reactivity worth with exposure to neutron flux. This rate of change depends not only on the thermal microscopic cross section, but also on the degree of self-shielding, the effects of resonances, the spectra in which irradiation and measurement are made, and the absorption cross sections of the isotopes produced by neutron capture.

Small cylindrical samples (1/4 by 2 in.) of several different materials were irradiated in the reflector region of the GETR to exposures between zero and 10^{21} nvt (thermal). About 2 per cent of the absorptions in a $1/v$ absorber was estimated to be above the cadmium cutoff in this location. Most of the materials were diluted in glass to provide samples of different concentration and correspondingly different self-shielding factors. The change in absorption with exposure is shown for three of the materials in Figs. VIII-1 to VIII-3. Theoretical curves are drawn for comparison.

The theoretical curves were calculated using self-shielding factors determined by the equation

$$f(\Sigma_a r) = \frac{1 + 0.3707\ \Sigma_a r + 0.0049\ (\Sigma_a r)^2}{1 + 1.2091\ \Sigma_a r + 0.6802\ (\Sigma_a r)^2} \quad (1)$$

where f is the self-shielding factor, Σ_a is the effective 2200-m/sec cross section, and r is the sample radius. This polynominal fits the results of a series of P_3 calculations of a large cylindrical cell centered about the absorber using Maxwellian averaged cross sections. The burnup equation for a single, absorbing isotope with variable self-shielding is

$$\frac{d\delta_a}{dt} = -\phi_w \delta_a f(\Sigma_a r) \quad (2)$$

where δ_a is the apparent instantaneous microscopic cross section, and ϕ_w is the average flux in the surrounding water. The reactivity

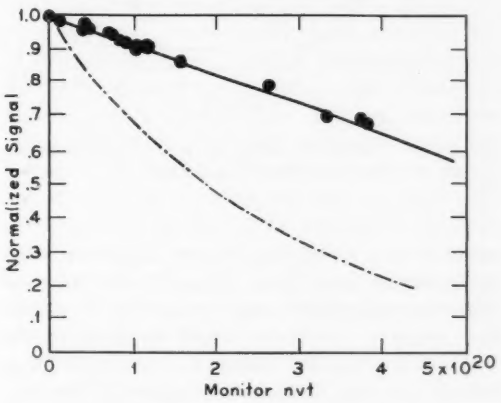

Fig. VIII-1 Change in reactivity worth of boron upon irradiation.[6] ——, theory. ●, data. – – –, unshielded theory.

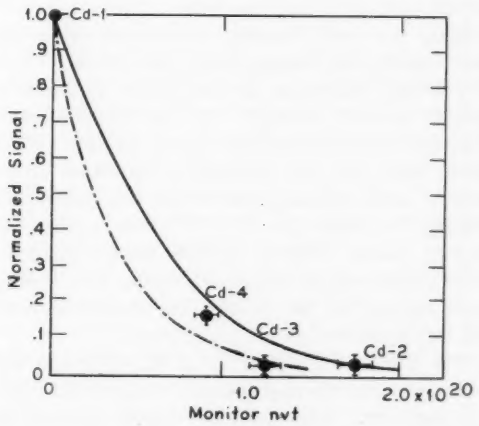

Fig. VIII-2 Change in reactivity worth of cadmium upon irradiation.[6] ——, theory. ⊢●⊣, data. – – –, unshielded theory.

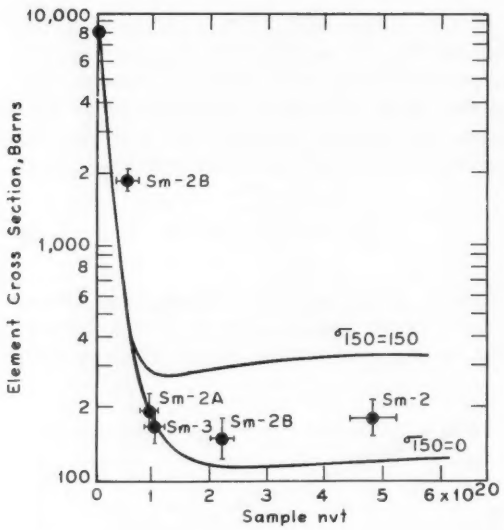

Fig. VIII-3 Change of apparent absorption cross section of samarium upon irradiation.[6] ——, theory. ⊢●⊣, data.

worth of the irradiated material relative to an unirradiated reference sample was obtained from pile-oscillator experiments in the MTR. The relative reactivity worth is equal to the "normalized signal" quoted in Figs. VIII-1 and VIII-2; in Fig. VIII-3 the apparent thermal cross section of the element (samarium) is presented directly in barns.

Figure VIII-1 shows excellent correspondence between the experimental points and the theoretical curve for a $1/v$ absorber. Since the initial self-shielding is large ($\Sigma_a r$ = 1.2, f_0 = 0.423), the self-shielded poison burns up far less rapidly than would unshielded boron.

The high cadmium cross section is due to a single, non-$1/v$ isotope, Cd^{113}, of 20,500 barns. The Maxwellian averaged cross section is 1.3 times that of a $1/v$ absorber of the same 2200-m/sec cross section; therefore the calculated burnup is based on a Cd^{113} cross section of 26,600 barns. Figure VIII-2 shows reasonable agreement between calculated and measured burnup on two points; the discrepancy in the third point is as yet unexplained.

The Sm^{149} cross section of 40,800 barns has a Maxwellian average about 1.5 times that of a $1/v$ absorber. This isotope burns rapidly to leave a residual cross section which slowly increases with subsequent irradiation. The residual cross section depends on the unknown cross sections of Sm^{148} and Sm^{150}. The curves in Fig. VIII-3 are plotted assuming 0 and 150 barns for these isotopes, and they bracket the experimental points at large exposures. The large discrepancy between theory and experiment at 0.5×10^{20} nvt probably indicates that the self-shielding model is inadequate for this very black sample ($\Sigma_a r$ unirradiated = 3.43).

The reference[6] contains curves similar to Figs. VIII-1 to VIII-3 for dysprosium, erbium, europium, lutetium, and silver-indium-cadmium alloy.

Corrosion and Radiation Effects on Borides

The initial phases of the materials-investigation program discussed in reference 7 emphasize rare-earth and metallic borides, to be followed by rare-earth oxides, cadmium-base materials, and dispersion-hardened silver-indium-cadmium alloys. Borides were chosen because, among the boron-bearing materials, they represented a possible method for controlling helium release and damage within the crystal structure, they are a large class of materials with relatively unknown potential, and they can be combined with rare-earth metals.

Corrosion resistance and the effects of radiation are being investigated intensively, whereas materials properties are being studied less intensively.

A variety of borides was subjected to boiling water for periods up to 500 hr. Figure VIII-4 shows the quantities of boron dissolved in water as a function of time. The hexaborides showed excessive solubility, whereas hafnium and zirconium diborides were much less soluble.

A large number of borides were exposed to steam at 400°C for periods up to 500 hr; the results are shown in Table VIII-4. Tetraborides formed a thin, adherent film and were the most oxidation resistant, whereas diborides and hexaborides corroded badly. The hexaborides formed metal borates which appeared very stable in steam. Consequently, the program will now investigate metal and rare-earth borates to establish their ability to withstand a reactor environment.

Compacted boride powders were irradiated to deplete 30 to 100 per cent of the B^{10} atoms present. Postirradiation data are shown in

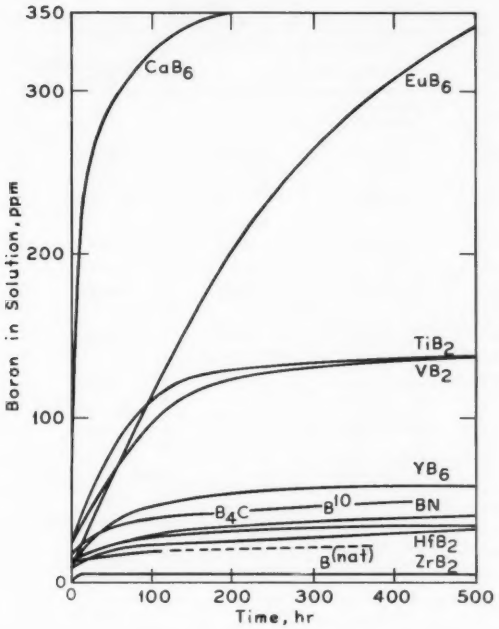

Fig. VIII-4 Solubility of borides in boiling water.[7]

Table VIII-5. The diboride powders showed the highest helium retention; three of the four diborides released less than 15 per cent of the helium produced. The tetraborides, including boron carbide, released 20 to 30 per cent of the produced helium. The hexaborides had virtually negligible helium retention, releasing 70 to 100 per cent.

For conditions in which minimum helium release and maximum integrity of the system are desired, it would appear that the diborides are preferable, since they contain helium well, have good corrosion resistance, and (in the case of hafnium diboride) contain a good resonance absorber. Tetraborides are somewhat less desirable on these counts, and hexaborides appear to be poor materials for this type of application.

Operating Experience with Control-Rod Materials

Operating experience with several types of control rods is summarized in Table VIII-6. Most of the materials have operated satisfactorily for the equivalent of about a year at reactor design power and still longer in elapsed time in a reactor environment. Most of the troublesome or suspicious behavior so far encountered has occurred in boron–stainless steels: in EBWR, in Dresden, in SM-1, and in GETR. The type of rod, its configuration, the type of weld used, the amount and enrichment of boron in the steel, and the integrated irradiation exposure varied over considerable ranges from reactor to reactor in this group. All showed cracks at or near welds and other locations of stress concentration. Cracks were not restricted to locations exposed to large neutron fluxes, and cracking was sometimes difficult to avoid during manufacture. It is well to note, however, that no malfunctions have yet been observed as a result of the cracks.

Two of the initial control rods for the SM-1 suffered cladding cracks as a result of internal helium-gas pressure. The damage was first noted after about one-half of the first core life (after about 380 equivalent full-power days), but it may have occurred earlier.[7]

Examination of the GETR rods after replacement revealed cracking of welds near the tips that joined the 1 per cent B^{10} stainless-steel plates and some cracking of the plates at points of stress concentration.

Of the nine EBWR control rods for core 1, four were fabricated of type 304 stainless steel containing 2 per cent natural boron. Each control rod was fabricated from four angles which were spot-welded together in a cruciform shape. These rods were located in the outermost (corner) rod positions, whereas hafnium control rods were located in the five inner positions. EBWR has been operated to an integrated power of 8800 Mwd, the equivalent of 440 days at full [20 Mw(t)] power. For approximately 10 per cent of the time, the boron–stainless steel control rods were removed completely from the active portion of the core and the reactor was controlled by the hafnium rods. For the remainder of the exposure, the boron–stainless steel rods were partially inserted.

Removal of the rods for core modification has shown that cracking has occurred at a large number (estimated at 60 per cent) of the spot welds.[8] The cracks are semicircular, averaging about $\frac{1}{4}$ in. in length. Some of the cracks from the outermost row of welds extend to the edges of the blades. The cracks appear to be old and are not propagating; but this is not definitely known. A possible explanation of the cracking is that it is due to stresses from the

Table VIII-4 CORROSION OF BORIDES IN 400°C STEAM[7]

SAMPLE	NO.	STARTING PHASES	% THEORETICAL DENSITY	TEST DURATION	APPEARANCE AT TERMINATION	AVERAGE WEIGHT CHANGE AT TERMINATION Mg/Dm^2	PRODUCT PHASES
BORON	A B C	β Rhombohedral Boron	A - 98 B - 97 C - 68	106 Hours	Powdered	———	β Rhombohedral Boron
BORON NITRIDE	A B C	Single Phase Hexagonal BN	A - 95 B - 95 C - 97	106 Hours	Crumbled to small pieces	———	BN
BORON CARBIDE	A B C	$B_4C + C$	A - 100 B - 100 C - 100	490 Hours	Brown - red powder	−8130	B_4C
YTTRIUM TETRABORIDE	A B C	$YB_4 + YB_6$	A - 98 B - 101 C - 118	490 Hours	Little change	+29	$YB_4 + YBO_3$
YTTRIUM HEXABORIDE	A B C	$YB_6 + YB_4$	A - 93 B - 93 C - 96	490 Hours	Slight change, turned pink	−6301	YBO_3
SAMARIUM HEXABORIDE	A B C	SmB_6	A -92 B - 86 C - 77	490 Hours	No change in dimensions, turned white	−4600	$SmBO_3$
EUROPIUM HEXABORIDE	A B C	EuB_6	A - 78 B - 88 C - 99	490 Hours	No change in dimensions, tan colored	−2450	$EuBO_3$
CALCIUM HEXABORIDE	A	CaB_6	A - 90	490 Hours	Little change in dimensions, chalky color	−6270	$CaBO_3$?
VANADIUM DIBORIDE	A B	VB_2 + Trace of VB	A - 92 B - 93	490 Hours	Glassy film, otherwise intact	−2860	$VB_2 + VO_2$ Film + B_2O_3
ZIRCONIUM DIBORIDE	A B C	ZrB_2	A - 94 B - 96.5 C - 87	106 Hours	Crumbled to small pieces and powder	———	ZrB_2 + ZrO_2 (Monoclinic)
HAFNIUM DIBORIDE	A B C	HfB_2 + HfO_2 cubic	A - 78 B - 81 C - 82	490 Hours	Covered with powdery yellow oxide	−12,660	HfB_2 + HfO_2 (Monoclinic)
TITANIUM DIBORIDE	A B C	TiB_2	A - 100 B - 98 C - 99	106 Hours	Covered with powdery yellow oxide	———	TiO_2 TiB_2

Table VIII-5 HELIUM RELEASE DATA FOR BORIDE POWDERS[7]

Sample	Density % Theoretical	% Burnup of B^{10} Atoms (1)	Measure Volume of He Released cm^3	% He Released (2)	Volume H_2 Released	Maximum Estimated Irradiation Temperature °C
B	40	90-100	79	70	———	400
B_4C	70	55-60	22	29	———	400
TiB_2	67	90-100	2.6	3	———	400
ZrB_2	58	90-100	6.0	10	———	400
HfB_2	59	90-100	9.2	14	———	400
VB_2	42	90-100	24	39	35	400
YB_4-00	49	90-100	23.5	30	2.13	400
YB_4-01*	70	90-100	18	19.5	———	400
YB_4-02*	63	90-100	21	25	———	400
YB_6	52	90-100	45	48	———	400
SmB_6	60	30-40	36	100	227	600
EuB_6-01	61	60-70	38	77	———	400
EuB_6-02	53	60-70	34	70	———	400
CaB_6	40	80-90	61	78	———	400

(1) All burnup values are calculated and therefore approximate - analyses will be performed later.

(2) Based on calculated burnup values and measured He volumes.

* These powders contained $YB_6 + YBO_3$ as second and third phases.

Table VIII-6 OPERATING EXPERIENCE WITH CONTROL-ROD MATERIALS IN REACTORS

Reactor	Rod design	Temp., °F	Equivalent days at power	Malfunctions
		B_4C		
OMRE	1¼-in. ϕ tubes	600	300	None
VBWR	Platelets canned	545	20	B_4C erosion
VBWR	Tubes in slab array	545	270*	None
		Hafnium		
EBWR	Cruciform	490	440	Rod stuck during oscillating test
Shippingport	Cruciform	525	325	Hf-to-Zr weld corrosion
		Rare Earth		
SM-1	Flux trap, Eu_2O_3 (38 wt.%) in S.S., S.S. clad	440	200	None
		Boron		
SRE	Stacked rings, 2 wt.% B in Ni	960	125	None
SM-1	Flux trap, 3 wt.% B^{10} in Fe, S.S. clad	440	380	Cladding cracked
EBWR	Cruciform, 2 wt.% B in S.S.	490	440	Semicircular cracks at 60% of spot welds
Dresden	Cruciform, 2 wt.% B in S.S.	545		Cracks at welds throughout length of rod
VBWR	Slab, 1 wt.% B^{10} in S.S.	545	270	None
ETR	Flux trap, 1 wt.% B^{10} in S.S.	140	$\sim 10^{22}$ nvt*	None
GETR	Flux trap, 1 wt.% B^{10} in S.S.	130	$\sim 10^{21}$ nvt (1.2–1.4 at.% burnup)	Weld cracks at tip

* Rods withdrawn during power operation.

welding process. (The control rods were not annealed after fabrication.)

Except for the cracking, the appearance of the blades is good. The blades are covered by a blue-gray oxide coating and some crud deposits, but no gross corrosion is exhibited.

Cracks were discovered in the Dresden control rods when they were removed to check the guide rollers. The Dresden rods were fabricated from 2 per cent borated stainless-steel sheets, butted and welded into a cruciform. The welds are 2½-in. long, spaced 6 in. center-to-center. The cracks are small (¼ to ½ in.). They have appeared at the welds, all along the length of the rods, rather than being concentrated in the sections of the rods exposed to a neutron flux. Although the rods were performing satisfactorily prior to removal, they have been replaced (by cruciform rods made up of B_4C canned in steel tubes) since there is no way to estimate their future performance, and no assurance that the cracking will not spread, especially under severe irradiation. A factor contributing to the decision to replace the rods was that the welds around which the cracks occurred played an important part in the structural integrity of the rods and were subject to significant stresses. The EBWR case was different in that the only function of the spot welds was to hold together the angle sections that formed the cruciform; the welds were not essential to the support of the rod.

The chemical composition of the metal used in the Dresden rods is given in Table VIII-7. The fabrication process consisted of vacuum melting 2000-lb ingots, forging into slabs at 1900°F, and hot and cold rolling to the desired thickness, followed by annealing at 1950°F and

Table VIII-7 COMPOSITION OF DRESDEN CONTROL RODS

Element	Content, %
Chromium	18.00–20.00
Nickel	12.00–14.00
Manganese	2.00 (max.)
Boron (natural)	2.00
Silicon	1.00 (max.)
Carbon	0.05 (max.)
Phosphorus	0.035 (max.)
Sulfur	0.030 (max.)

air cooling. The slabs were fillet welded into a cruciform shape. Both legs of the fillet were butted before welding. Severe cracking during forging and rolling occurred if the nickel content fell below 12 per cent. A double chamfer on the narrow slabs with 100 per cent penetration welds was not satisfactory due to cracking of the base metal near the welds.

Although both EBWR and Dresden control rods were operating satisfactorily at the time of removal, neither had been in the reactor for times or exposures comparable to normally expected fuel-element lifetimes.

Table VIII-8 IMPACT TESTS ON BORON STEELS[1,9]

Alloy	Temp., °F	Nonirradiated, Izod ft-lb	Irradiated, Izod ft-lb	Irradiation, nvt
347	70	15.9	15.6	3×10^{20}
0.5 B^{10}	600	8.4	1.48	3×10^{20}
0.85 B^{10}	600	5.70	0.18	9×10^{20}
1.18 B^{N}	600	1.8	0.66	4.35×10^{20}

The use of boron enriched in B^{10} allows a beneficial lowering of the total boron content in the steel, but the extent of improvement that can be obtained in this way has not yet been established. Tests on enriched and natural boron–stainless steel, irradiated to exposures of 2×10^{20} to 9×10^{20} nvt, are summarized in Table VIII-8, from references 1 and 9. The table shows a large embrittlement effect due to irradiation but is not sufficient to evaluate the effect of boron content plus irradiation.

As has been previously recognized, boron steel has two major shortcomings: (1) the boron content tends to cause the base material to be hard and brittle, and (2) the production of lithium and helium gas on absorption of neutrons causes dislocations in the metal lattice and may lead to further embrittlement, swelling, and cracking. It is not evident, however, that these difficulties are enough to counterbalance its attractive features for many reactor applications, nor that they cannot be largely circumvented by appropriate design measures. Because of the significance of these questions, it is important to know the exact circumstances of the troubles that have been experienced.

References

1. General Electric Co., Vallecitos Atomic Laboratory and Atomic Power Equipment Dept., Survey of the Physics, Metallurgy, and Engineering Aspects of Reactor Control Materials, USAEC Report GEAP-3183, June 12, 1959.
2. W. R. Morgan et al., Relative Effectiveness of Reactor Control Materials (Supplement), USAEC Report GEAP-3201-2(Suppl.), General Electric Co., Vallecitos Atomic Laboratory and Atomic Power Equipment Dept., Jan. 11, 1961.
3. W. L. Morgan and J. L. Russell, Jr., Reactivity vs. Number of Neutrons Captured in Control Materials, USAEC Report GEAP-3616, General Electric Co., Vallecitos Atomic Laboratory and Atomic Power Equipment Dept., Dec. 30, 1960.
4. R. W. Deutsch, Evaluation of a Bank of Slab Type Control Rods, *Nuclear Sci. and Eng.*, 5: 150–155 (1959).
5. D. R. Bach and M. E. Way, The Worth of Single Control Rods in Hydrogenous Reactors, USAEC Report KAPL-1961, Knolls Atomic Power Laboratory, July 28, 1958.
6. J. L. Russell, Jr., et al., Absorber Burnup Experiment Interim Report, USAEC Report GEAP-3617, General Electric Co., Vallecitos Atomic Laboratory and Atomic Power Equipment Dept., Jan. 20, 1961.
7. W. C. Ballowe et al., Status Report on Control Rod Materials Research and Development Program, USAEC Report GEAP-3355-2, General Electric Co., Vallecitos Atomic Laboratory and Atomic Power Equipment Dept., Nov. 14, 1960.
8. Argonne National Laboratory, Reactor Development Program Progress Report, January 1961, USAEC Report ANL-6307, p. 37, Feb. 15, 1961.
9. L. B. Prus et al., Boron–Stainless Steel Alloys, *Nuclear Sci. and Eng.*, 4(3): 415–428 (September 1958).

Section IX

STEAM-CYCLE EFFICIENCY

The steam cycles used in nuclear plants vary over a wide range because of the wide range of the conditions of the generated steam, because of the range of plant capacities, and for other reasons. Table IX-1 from reference 1 gives the net thermal efficiency and the steam conditions for most of the nuclear plants in operation or under design or construction. The net efficiency, of course, has taken account of the power used for coolant circulation and for other plant auxiliary requirements. A general study of the efficiency of various cycles was made some time ago and is reported in reference 2. It was based on turbogenerator units of 100- to 200-Mw capacity, operating at a backpressure of 1.5 in. Hg (absolute), and covered steam conditions ranging from 150-psig saturated steam to 2450-psig steam at 1100°F. However, owing to such a wide range, it could not, of course, include all the possible variations in the steam cycles. If attention is confined to saturated-steam cycles, which are applicable to the pressurized- and boiling-water plants when no superheat is added, it is possible to make a much more detailed survey within this limited area. Such a survey, made in connection with the heavy-water reactor program, is reported in reference 3. Two of the resulting sets of curves are shown in Figs. IX-1 and IX-2. These two sets of curves apply to the two extreme cases of regenerative feed-water heating studied. Figure IX-1 is for the case of no feed-water heating and Fig. IX-2 is for five stages of feed-water heating. In both cases moisture separation was provided by external separators whenever the moisture in the turbine expansion line amounted to as much as 12 to 14 per cent. Certain simplifications were used in the calculations which can best be evaluated from the original report, but the results appear very useful as general

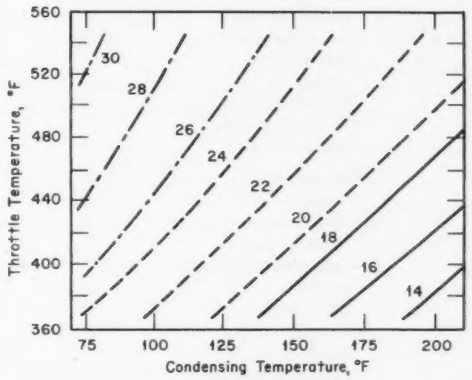

Fig. IX-1 Gross turbine-cycle efficiency for saturated-steam cycles—no feed-water heating.[3] The values shown in the curves are in per cent. — — —, two moisture separators. — — —, one moisture separator. ———, no moisture separator.

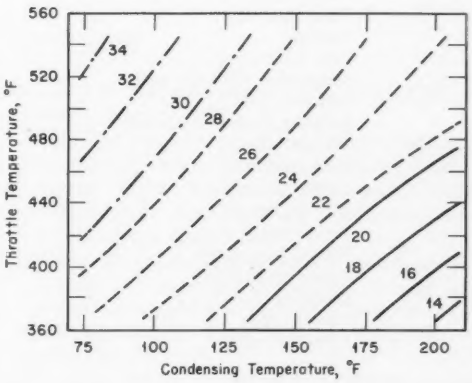

Fig. IX-2 Gross turbine-cycle efficiency for saturated-steam cycles—five stages of feed-water heating.[3] The values shown in the curves are in per cent. — — —, two moisture separators. — — —, one moisture separator. ———, no moisture separator.

Table IX-1 DESIGN VALUES OF EFFICIENCY AND STEAM CONDITIONS FOR SPECIFIC NUCLEAR POWER PLANTS[1]

	Net thermal efficiency, %	Steam conditions at outlet of nuclear steam generator[a]	
		Temp., °F	Pressure, psia
Pressurized water			
McMurdo Sound	14.4	417	300
SM-1	17.9	425	213
Saxton	16.2		300-500
APS-1 (USSR)[b]	16.7	536	178
BR-3 (Belgium)	24.9	471	520
Shippingport	26.0	486	600
Yankee	28.0	467	500
SELNI (Italy)	28.6	467	515
Voronezh (USSR)	25.8	446	470
Indian Point[c]	25.8	449	420
Boiling water			
EBWR	22.5	489	615
Vallecitos	25.0	545	1000
JPDR (Japan)	29.2	529	877
Kahl (West Germany)	25.0	497	663
BONUS[d]	32.6	900	865
Elk River[e]	26.0	505	700
Humboldt Bay	29.8	548	1025
Big Rock Point	31.1	546	1015
Ulyanovsk (USSR)[f]	20.0	446	426
Pathfinder[g]	30.5	825	555
Byeloyarsk (USSR)[h]	33.0	950	1470
SENN (Italy)	29.5	543/469	990/510
Dresden	28.7	543/469	990/510
Gas cooled			
AVR (West Germany)[b]		941	1045
EGCR	26.5	900	1325
AGR (UK)	27.3	860	675
Peach Bottom	34.8	1005	1500
Florida[i]	32.6	950	1465
EDF-1 (France)	20.0	649/421	309/63
Neuglobsow (East Germany)[j]	28.0	454	426
Berkeley (UK)	24.4	612/612	321/77
Bohunice (Czechoslovakia)[f]	25.4	752/356	426/29
Bradwell (UK)	28.2	703/703	770/210
Hunterston (UK)	28.0	700/660	595/165
JAPC (Japan)[b]	27.7	714/687	910/285
EDF-2 (France)	25.0	644/644	473/126
Latina (Italy)	28.4	703/703	770/210
Hinkley Point (UK)	26.4	685/669	665/195
Trawsfynydd (UK)	28.7	720/694	977/319
Dungeness (UK)	32.9	739/743	1418/590
Sizewell (UK)	30.5	736/734	720/305
EDF-3 (France)			
Heavy water cooled			
Carolinas-Virginia[k]		487	605
NPD-2 (Canada)	24.2	448	415
CANDU (Canada)	29.1	482	580

Table IX-1 (Continued)

	Net thermal efficiency, %	Steam conditions at outlet of nuclear steam generator[b]	
		Temp., °F	Pressure, psia
Organic			
Piqua	25.1	550	450
Sodium graphite			
SRE[l]	27.0	825	615
Ulyanovsk (USSR)		932	1320
Hallam	29.5	833	865
Fast breeder			
Dounreay (UK)	16.7	525	200
EBR-II	27.8	840	1315
BN-50 (USSR)		779	426
Fermi	30.3	740	565

[a]For dual-cycle systems, steam conditions are given for both the high- and low-pressure steam generated.

[b]Steam conditions at turbine inlet.

[c]Oil-fired superheater raises the net efficiency to 32.1 per cent, delivering steam at 1000°F and 370 psia.

[d]Includes nuclear superheat. Steam conditions before nuclear superheat are 534°F and 915 psia.

[e]Coal-fired superheater raises the net efficiency to 30.2 per cent, delivering steam at 825°F and 615 psia.

[f]Thermal efficiency given is gross rather than net.

[g]Includes nuclear superheat. Steam conditions before nuclear superheat are 489°F and 615 psia.

[h]Includes nuclear superheat. Steam conditions before nuclear superheat are 644°F and 1580 psia.

[i]Exhaust steam from the high-pressure turbine is returned to the steam generator where it is reheated to 950°F and enters a reheat turbine at a pressure of 215 psia.

[j]Thermal efficiency given is gross rather than net. Steam conditions given are at turbine inlet.

[k]Oil-fired superheater raises the net efficiency to 23.6 per cent, delivering steam at 725°F and 415 psia.

[l]Has operated at steam temperatures up to 1000°F.

guides to the selection of those design variables which affect the steam cycle.

Reference 4 is a study of single pressure steam cycles which is aimed at their application to gas-cooled reactors. Efficiencies are calculated as functions of the reactor coolant inlet and outlet temperatures, with the top and bottom "pinch points" (temperature difference between reactor coolant and steam at steam outlet of superheater and temperature difference between reactor coolant and water at water inlet to evaporator, respectively) as parameters. The calculations have been programmed for the Mercury and IBM-704 computers.

References

1. Costs of Nuclear Power, USAEC Report TID-8531 (Rev.), January 1961.
2. N. A. Beldecos et al., Comparative Performance of Modern Steam Turbine Generator Units for Atomic Power Plants, USAEC Report WIAP-2, Westinghouse Electric Corp., Industrial Atomic Power Group, March 1953.
3. Heavy-Water-Moderated Power Reactors, Engineering and Economic Evaluations. Volume II, Engineering Studies and Technical Data, USAEC Report DP-520, E. I. du Pont de Nemours & Co., December 1960.
4. F. Kay, Single Pressure Steam Cycle Analysis, British Report DEG-131(R), July 1960.

Section X

DESIGN PRACTICE

Recent ASME Boiler Code Nuclear Code Cases

Since the review of codes and practice for nuclear pressure vessels in the March 1961 issue of *Power Reactor Technology*, Vol. 4, No. 2, several revisions of the Nuclear Case Interpretations of the ASME *Boiler and Pressure Vessel Code* have been issued.

Case 1274N-3 permits[1] the use of ferritic steel castings in addition to the austenitic castings conforming to American Society for Testing Materials (ASTM) specification A-356-58T, grade 10, as allowed in Case 1274N-2. The materials listed in this new revision include only ASTM specifications:

- A-216 Carbon steel castings suitable for fusion welding for high-temperature service
- A-217 Alloy steel castings for pressure-containing parts suitable for high-temperature service
- A-351 Ferritic and austenitic steel castings for high-temperature service
- A-352 Ferritic steel castings for pressure-containing parts suitable for low-temperature service

In addition to the normal requirements for these materials, they must be 100 per cent radiographically and magnetic-particle or dye-penetrant inspected, weldability tests must be made, all major discontinuities must be removed and repaired if necessary, and the allowable stress is reduced to 0.95 times the S value given in Table P-7 of Section I of the ASME *Boiler and Pressure Vessel Code*.

Case 1272N-2 requires[2] that material for nonpressure parts, except studs up to $\frac{3}{8}$-in. in diameter, welded to pressure parts of impact-tested material, be of similar impact-tested material if the part is not subsequently stress relieved. The impact-tested material shall extend at least 16 times the weld thickness before other material is attached by welding. If the weld is subsequently stress relieved, other code materials in the P-1 group of Table UCS-23, except SA-53 pipe and those of structural quality, may be used.

Cases 1273N-4 (reference 3) and 1273N-5 (reference 4) incorporate special requirements for nozzles and openings in the pressure shell. These cases require that all nozzles, except for attachment of openings where substantially no piping reactions exist, such as control-rod housings, be attached by full-penetration welds that are 100 per cent radiographed. Opening compensation must be of the integral type and may be made either totally or partially of weld buildup. Reduction of strain raisers is required by the use of rounded corners and fillets with a specified minimum radius or throat. Where partial-penetration welded sleeves are necessary, as in a control-rod housing, and the tolerances will not permit stress relief, provision is made to accommodate this requirement by locating all reinforcement in the shell, providing mechanical means to relieve external bending stress on the weld, and using a proved weld procedure.

Case 1274N-4 permits[5] the use of types 304L and 316L low-carbon stainless steel for construction of nuclear pressure vessels, to be stamped under the rules of Section I.

Case N-11, which is an interpretation of the Code for Pressure Piping,[6] permits the use of standard piping expansion provisions, such as pipe bends, offsets, bellows expansion joints, sliding joints, or swivel joints, so long as they comply with the requirements of American Standards Association (ASA) B31.1-1955, Section 6, Chapter 3, and are of materials recog-

nized by ASA B31.1, as amended by the nuclear code cases.

British Requirements for Inspection and Design of Primary Circuits and Pressure Vessels of Nuclear Power Plants

The similarity between the British[7] and American[8] requirements for design, fabrication, and inspection of pressure components for reactor systems is striking. Both codes are based upon the premise that the safety and reliability of nuclear plants is the primary consideration of design and subjugate considerations of cost to a secondary position.

The outstanding difference between the British and American design standards is the absence of a secondary containment shell in many of the British plants. The Calder Hall type reactors, the plants of the Central Electricity Generating Board and the South of Scotland Electricity Board, and the plants at Latina (in Italy)* and in Japan* are not enclosed within secondary containment buildings. However, the provision or absence of a secondary building does not influence the high standards to which the components of the primary system are constructed.

A recent paper[9] by Pemberton and Crossley gives a detailed discussion of the steps taken by *Lloyd's Register of Shipping* during their surveys of various British reactor plants. They advocate the general principle that only the parts associated with the reactor core should represent advanced practices. The designs of the vessels and components of the primary circuit should be conservative, and materials and fabrication techniques should be recognized and proved where possible.

The sizes and design conditions for the British plants are shown in Table X-1.† An advance that had to be faced was the large size of the pressure parts. This feature accounted for most of the problems encountered during design, fabrication, and inspection of these plants.

Recently, *Lloyd's Register of Shipping* issued "Provisional Requirements for the Survey of Pressure Components for Land-Based Nuclear Installations." This Code requires the designer to consider the following:

1. The containment of radioactive materials.
2. The effects of neutron irradiation on the characteristics of the materials of construction.
3. Accessibility for inspection and maintenance.

Pressure vessels and parts are classed in four main categories: in Category A are the vessels that contain radioactive materials and are subjected to high-level neutron irradiation and are inaccessible for periodic examination and maintenance; in Category B are the pressure parts which contain radioactive materials in service but which can be made available for periodic inspection and maintenance during shutdown; in Category C are the parts that fall within the normal rules of *Lloyd's Register of Shipping* for Class 1 or severe-duty pressure vessels; and in Category D are the emergency steel containment vessels.

Category C is adequately covered by conventional existing codes. Category B vessels require added stringency because of their duty, size, and, in many cases, nonconventional design features. For vessels in this category it is required that the design pressure exceed the maximum working pressure by 10 per cent. Provision is made for more extensive examination and testing of materials, welding procedures, welder tests, etc. Stress relieving and pressure testing may not be conventional and may need special study in order that the inspection and testing schedule can be designed to ensure that the vessel is, in all ways, suitable for its contemplated service.

The reactor vessel and its branches (up to and including the first shutoff valves) are in Category A and require the greatest care in design, fabrication, and inspection. In addition to the design requirements of Category B, it is required that (1) stress-concentration factors be kept to a minimum; (2) compensation for openings be of the integral and balanced type; (3) butt-welded joints be used whenever possible and be arranged for the best possible radiography; (4) after fabrication is completed, materials, including weld metal, be of the right type and in their optimum condition; and (5) any internal insulation be of proved efficiency and care be

* Also designed by British firms.

† Table X-1 is reprinted here by permission from the *Journal of the British Nuclear Energy Conference*.[9]

Table X-1 NUCLEAR POWER STATIONS PLANT PARTICULARS[9]

Item	*Nominal design pressure*, lb/in²	*Nominal design temperature*, °F	*Dia. × height*	*Thickness*, in.
Calder Hall— (4 reactors: 4 circuits per reactor)				
Reactor	100	665	37 ft inside dia. × 71 ft 6 in. high	2
Ducting	125	665	54 in. dia.	$\frac{3}{8}$
Heat exchanger	125	665	17 ft 3 in. inside dia. × 73 ft 4 in. high	$1\frac{3}{16}$
Main isolating valves	125	665	54 in. dia.	$1\frac{1}{2}$
Expansion bellows	125	665	54 in. dia.	Convolutions $\frac{1}{4}$
Berkeley— (2 reactors: 8 circuits per reactor)				
Reactor	137·5	645	50 ft dia. × 80 ft high	3
Ducting	137·5	720	60 in. dia.	$\frac{7}{16}$
Heat exchanger	137·5	720	17 ft 6 in. outside dia. × 70 ft high	$1\frac{1}{8}$
Main isolating valves	137·5	720	60 in. dia.	$1\frac{7}{8}$
Expansion bellows	137·5	720	60 in. dia.	Convolutions 3 mm
Bradwell— (2 reactors: 6 circuits per reactor)				
Reactor	146	750	66 ft dia. sphere	3–4
Ducting	146	750	60 in. dia.	$\frac{1}{2}$
Heat exchanger	146	750	19–20 ft inside dia. × 92 ft 4 in. high	$1\frac{9}{16}$
Main isolating valves	146	750	60 in. dia.	$\frac{7}{8}$
Expansion bellows	146	750	60 in. dia.	Convolutions $\frac{1}{4}$
Hunterston— (2 reactors: 8 circuits per reactor)				
Reactor	165	500	70 ft inside dia. sphere	$2\frac{7}{8}$–3
Ducting	165	800	5 ft inside dia.	$\frac{1}{2}$–$\frac{5}{8}$
Heat exchanger	165	800	19 ft 6 in. inside dia. × 73 ft 6 in. high	$1\frac{7}{16}$–$2\frac{1}{8}$
Main isolating valves	165	800	5 ft inside dia.	Body $\frac{7}{8}$–$1\frac{1}{2}$
Expansion bellows	165	750	5 ft inside dia.	Convolutions 3·5 mm
Latina— (1 reactor: 6 circuits)				
Reactor	200	420	66 ft dia. sphere	$3\frac{9}{16}$–$4\frac{3}{8}$
Ducting	200	750	66 in. and 72 in. dia.	$\frac{5}{8}$–$1\frac{1}{16}$
Heat exchanger	200	750	18 ft 4 in. inside dia. × 79 ft high	$1\frac{5}{16}$–$2\frac{3}{16}$
Main isolating valves	200	750	66 in. inside dia.	$1\frac{3}{4}$
Expansion bellows	200	750	60 in. dia.	Convolutions $\frac{5}{16}$
A.G.R.— (1 reactor: 4 circuits)				
Reactor	300	645	21 ft 3 in. dia. × 53 ft high	$1\frac{3}{4}$–$4\frac{3}{8}$
Concentric ducting	Inner duct external pressure 30	645	24 in. inside dia.	$\frac{7}{16}$
	Outer duct internal pressure 300	645	34 in. inside dia.	$\frac{1}{2}$
Heat exchanger	300	645	11 ft dia. × 66 ft high	$1\frac{7}{16}$–$2\frac{1}{2}$
Main isolating valves	300	Hot 1070	24 in. dia.	$1\frac{1}{2}$
	300	Cold 620		
Expansion bellows	None fitted—Thermal expansions taken up by heat exchanger moving on roller supports			
Dragon project— (1 reactor: 6 coolant loops)				
Reactor	350	Metal 662	11 ft 2 in. inside dia.	2
		Gas outlet 1382	6 ft 3 in. inside dia. × 56 in. high	$1\frac{1}{2}$
			2 ft inside dia.	$\frac{3}{4}$
Heat exchanger*	350	662	2 ft 6 in. dia. × 10 ft long	$\frac{7}{8}$
Gas circulators*	350	662	12 in. inside dia. × 3 ft 6 in. long	$\frac{1}{2}$

Note: These Figures are Approximate.

taken to ensure its mechanical integrity. After a review of these categories, with the ASME *Boiler and Pressure Vessel Code* in mind, it is noted that the requirements parallel each other.

In the British plants mild steel has generally been used for the main pressure parts, with the exception of some expansion-joint corrugations. For the reactor vessels at Calder Hall, the steel plates were made from a fine-grained, low-carbon manganese steel, which has good low-temperature notch ductility. The manufacturer investigated the effects of hot-pressing operations on the plate properties for the vessel. It was determined that strict control of the process was necessary to avoid loss of the impact properties. Therefore check tests have been introduced on hot-formed plates, and those which have failed to meet the specifications have had to be restored to normal and retested.

All materials for the pressure parts receive extensive testing. In addition to the normal mechanical tests, weldability and soundness are investigated. All plates for reactor vessels are ultrasonically inspected. Forgings and plates for other components, where operating or welding stresses are predominant through the thickness, are also inspected.

Difficulties have been experienced with the impact properties of forgings, since British forgemasters prefer silicon-killed acid open-hearth steels, and also since the methods of manufacture and the section sizes encountered are not conducive to good impact properties at ambient temperatures. Recently, however, considerable progress has been made toward narrowing the gap between the impact properties for forgings and those for plate materials.

Steels for pressure parts for heat exchangers, ductings, and casings are of normal boiler quality and are tested to recognized specifications. Because of the uncertainties of large castings, blower casings and valve bodies are made of fabrications from boiler-quality plate; although, in the case of the Calder Hall reactors, sufficient time was not available to permit the necessary development work from normal practice, and castings were used.

Even though the heat exchangers are very large and are complex (Category B vessels) they have attracted less attention than the reactor vessel because they are shop-fabricated and proved by normal hydrostatic test. They may be isolated for examination and maintenance during service. Leak tests are used to check the tube elements and their connections.

Site inspection of British plants is particularly important because of the large reactor vessels that are constructed at the site (see Table X-1). A certain amount of plate rectification, due to dimensional inaccuracies, uneven weld shrinkage, etc., is unavoidable. There is usually a great advantage in making a trial assembly of segments, or at least courses, prior to shipping plates to the site. Surveyors will not accept wholesale weld buildup of plate edges to correct undersized plates. Careful selection and positioning of plates can often correct what first appears to be a bad "fit-up," and this should be done prior to welding vertical seams. In fact, no welding of vertical seams is allowed until all plates or panels of a course are assembled. One of the most important duties of the site surveyor is the examination of radiographs and the designation of areas requiring repair. The normal procedure is for the radiographer to provide the radiographs, complete with his interpretation, to the surveyor for final assessment.

Owing to the very large volumes encountered, it is difficult to pressure-test the British reactor vessels and primary systems. The normal practice for smaller vessels is to use water as the pressurizing medium, and this is to be preferred when feasible. Except for the AGR vessel, it has been necessary, however, to use air for all the gas-cooled reactor vessels. Table X-2* shows the test pressure and medium used for each of the various reactor vessels.

Pneumatic tests are hazardous because of the large amount of potential energy stored in the compressed gas. Even though the vessels are built to the highest standards, the following precautions are taken:

1. Strain gauges or brittle lacquers are used as controls.
2. Only the required personnel are allowed on the site.
3. Test personnel are located in safe positions and cannot approach the vessel while it is pressurized.

As in the United States, the British also have some controversy over the minimum test tem-

*Table X-2 is reprinted here by permission from the *Journal of the British Nuclear Energy Conference*.[9]

Table X-2 TEST PRESSURES FOR REACTOR VESSELS[9]

Reactor vessel	Diameter, ft	Dimensions (height), ft	Nominal thickness, in.	Nominal design pressure, psi	Test pressure, psi (test medium)
Calder Hall	37	71 ft 6 in.	2	100	135 (air)
Chapelcross	37	77	2	100	135 (air)
Berkeley	50	80	3	137-5	211 (air)
Bradwell	66		3-4	146	260 (air)
Hunterston	70		$2\frac{7}{8}$ to 3	165	253 (air)
Latina	66		$3\frac{9}{16}$ to $4\frac{3}{8}$	200	306* (water)
AGR	21	53	$1\frac{3}{4}$ to $4\frac{3}{8}$	300	450 (water)

*This test pressure is tentative.

perature of the vessel. However, to date, the majority of the 12 air-pressure-tested vessels have been tested at ambient temperatures. Sound arguments can be proposed also for conforming to recognized requirements and practices for testing and to avoid special deviations such as elevated temperatures.

The normal pressure test is followed by a gas leak test at reduced pressure, usually 10 per cent in excess of design pressure. Where necessary, a vacuum test is also applied.

The results of the strain-gauge readings at Calder Hall, Chapelcross, Bradwell, and Berkeley are of interest. The readings showed the designs to be completely adequate. Minor fabrication deviations caused variations of as much as 50 per cent in the strain concentration factors observed at similar locations on nominally identical vessels. The Berkeley pressure vessel has an improved outlet-duct reinforcement design which reduced the strain concentration significantly relative to that in a similar region on the Calder Hall type reactors.

Periodic inspection is performed on accessible components and has shown that, after four years, the heat exchangers and components of the primary system for the Calder Hall type reactors are in excellent condition, with negligible corrosion effects. There appears to have been no increase in radiation levels due to contamination after the first inspection.

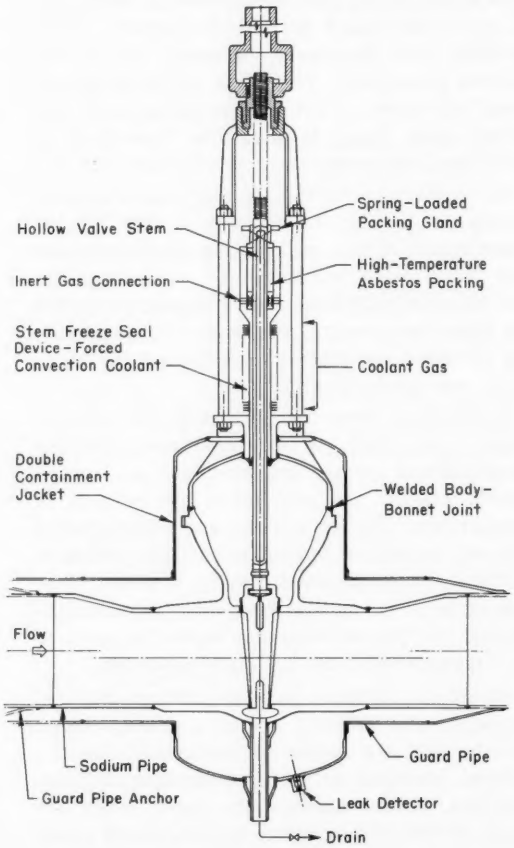

Fig. X-1 Primary sodium blocking valve.[10]

Valves for the Hallam Reactor

As a result of experience gained with the sodium valves in the Sodium Reactor Experiment (SRE), new valve designs have evolved for use in the Hallam Nuclear Power Facility (HNPF).[10]

Leakage across block valve seats in the SRE has been attributed to the large seating surface and to thermal distortion of the valves. The main block valves in the HNPF will have small seating-surface areas and will be of the flexible-wedge disk type shown in Fig. X-1. On closing, the wedge makes contact with the seating surface of the valve, and the further downward motion of the stem causes the wedge to deflect to

accomplish contact over the entire seating surface. Tests conducted on prototype valves, both of the flexible-wedge type and of a split-wedge disk type, disclosed excellent shutoff characteristics, before and after thermal cycling, for both valves.[11]

The small valves used to block and divert sodium flow to various components of the sodium service system will probably be of the flexible-seat type shown in Fig. X-2. After extensive thermal cycling,[12] across-the-seat leakage tests of four 2-in. valves of this type have disclosed no leakage.

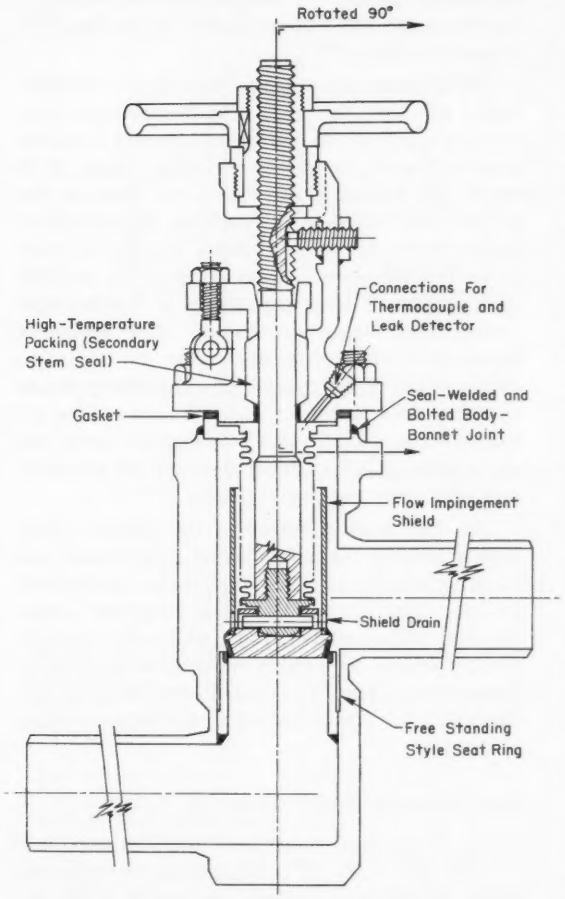

Fig. X-2 Small blocking and diverting valve (bellows stem seal).[10]

The primary sodium system check valves will be swing checks with knife-edge hinge structures rather than conventional pin-in-sleeve type journals. The check valve in the auxiliary heat-transfer system of the SRE tended to stick in the open position when the oxide content of the sodium was relatively high. This sticking was attributed to seizure of the pin-in-sleeve type journal due to an accumulation of oxide deposits. Tests of the prototype of this knife-edge hinge type check valve in sodium of relatively high oxide content indicate that the sticking problem has been solved.[13]

The SRE had no sodium throttling valves and in order to prevent thermal shock to structures in the outlet end of the reactor, eddy-current brakes were used to control the sodium flow after a reactor scram. The eddy-current brake will be eliminated from the sodium system in the HNPF, and a throttling valve will be used to both control and block the sodium flow in the reactor return line. Venturi ball valves were selected for this purpose because they offered the high flow capacity, suitable throttling range, and prospects for a tight shutoff. Two of the prototype Venturi ball valves leaked after they had been thermal cycled. In order to obtain better shutoff characteristics, the geometry of the valve body in the vicinity of the ball seat was revised from a massive section to a "free-standing" nozzle that is concentric with the seat bore. The proportions of the nozzle are calculated to dampen the effect of valve-body distortion on the valve seat. The revised valve is shown in Fig. X-3.

The valve stems of the HNPF will be sealed with nitrogen-cooled freeze seals instead of organic-cooled freeze seals as in the SRE. All the sodium valves except the small valves used for blocking and diverting the sodium flow to components of the sodium service system will have freeze seals. These valves will have bellows stem seals as shown on the valve in Fig. X-2. The freeze seals of the small valves located in lines between the primary heat-transfer system and the sodium service system will be cooled by natural convection of nitrogen. The other valve freeze seals will be cooled by forced convection of nitrogen. A freeze seal that will be cooled by forced convection is shown on the valve in Fig. X-1.

The stem seal is accomplished by solidifying sodium in an annulus that communicates with the valve interior. This annulus is formed by the inside diameter of a finned sleeve and the outside diameter of the valve stem. Ducted nitrogen cools the fins to form the freeze seal. A lantern

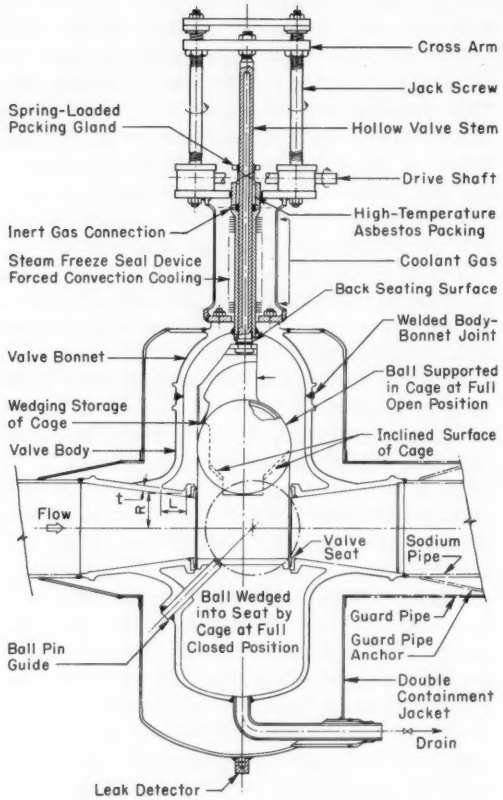

Fig. X-3 Primary sodium throttling valve.[10]

ring and packing arrangement are provided above the freeze section to maintain an inert atmosphere over the seal. This atmosphere is intended to minimize the formation of sodium oxides. The packing also provides an effective seal for the sodium in the event of complete loss of the frozen seal.

The sodium-valve bodies are all of type 304 stainless steel, and the hard-faced material applied to valve trims is Stellite. The valve yokes are of carbon steel, and the stem packing is high-temperature-graphitized asbestos reinforced with Inconel wire.

The Dresden Nuclear Power Station

In the June 1961 issue of *Power Reactor Technology*, Vol. 4, No. 3, the intention was stated of summarizing the design characteristics of new nuclear plants, as they become operative, in some detail. The summary of the Dresden plant is presented below. Although the material would have been more timely if it had been presented earlier, it is still pertinent and useful and belongs in the series of "design practice" summaries. The information was extracted from the Preliminary Hazards Summary Report,[14] Amendments 1, 2, 3, 4, and 6 to the Hazards Summary Report,[15–19] and the Enclosure Section (containment shell description) of the Hazards Summary Report.[20]

The Dresden plant uses a "dual-cycle" boiling-water reactor (Fig. X-4). The large steam drum that receives steam and water directly from the reactor pressure vessel is located some 85 ft above the vessel. Steam from the drum is fed to the first stage of the turbine. Recirculation water from the steam drum is fed to four canned-rotor pumps, each of which is located in a separate loop containing a U-tube type "secondary steam generator," that produces steam by transferring heat from the recirculation water of the reactor to a secondary steam system. This steam is fed to a lower stage of the turbine. Water that is returned from the condenser is proportioned between the primary and secondary reactor circuits.

The two main features of the reactor core design are (1) the use of a fuel enrichment that is quite low (1.5 per cent) for a water-moderated reactor and (2) the use of a relatively large number (80) of control rods, which are hydraulically driven and which must move upward to reduce reactivity. The control-rod features are favorable for power flattening in a boiling-water reactor.

Fuel Elements (Rods) (See Fig. X-5)

The basic fuel is uranium dioxide, enriched to 1.5 per cent U^{235}, fabricated as sintered, solid, cylindrical pellets measuring 0.625 in. in length (0.500 in. for two end pellets in each fuel segment) and 0.498 in. in diameter. Forty-three of these fuel pellets are encased in a tubular Zircaloy-2 jacket to compose a fuel segment with an over-all length of 28 in. The group of 43 pellets in each segment has approximately a ½-in. free expansion space. Four of these 28-in. segments are joined end-to-end by Zircaloy-2 screw connectors to form a 117-in. fuel rod. Fuel-rod alignment is maintained with

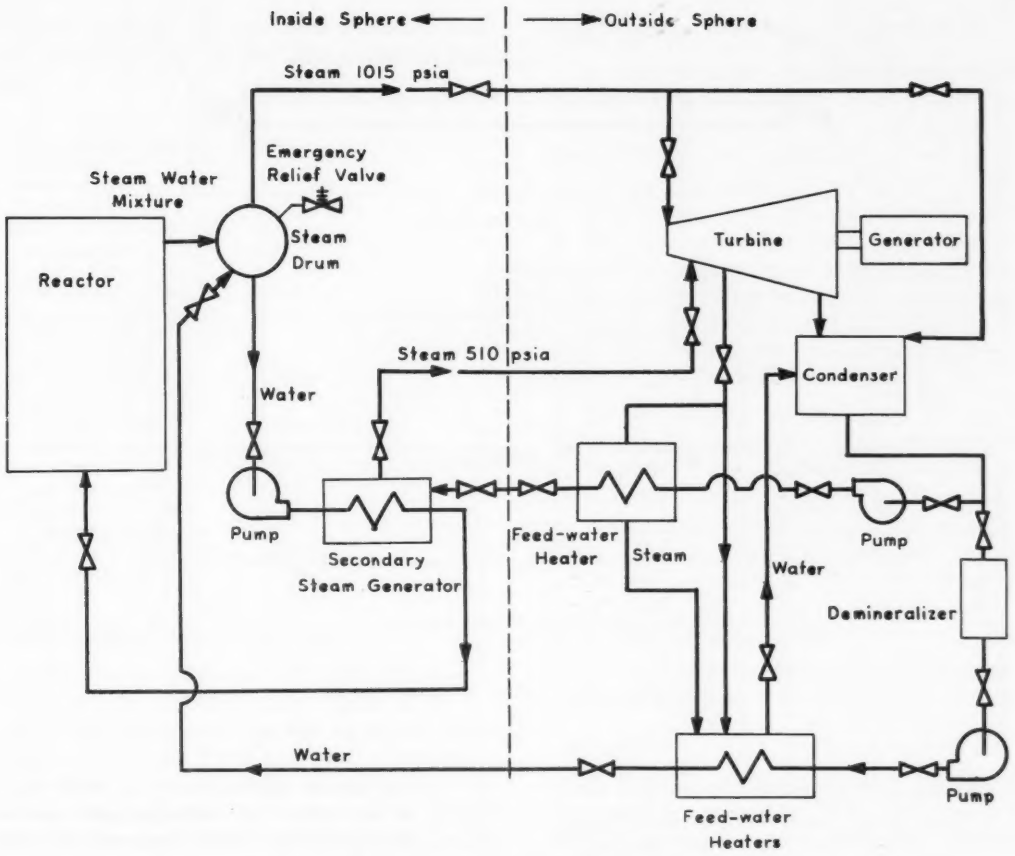

Fig. X-4 Process flow (simplified diagram).[14]

spacer plates (grids) at the joints between segments.

Total number of fuel rods in core	17,547
Total number of fuel segments in core	70,188
Number of fuel-rod positions for source and instruments	21
Fuel-rod length, including connectors	117 in.
Length of UO_2 per fuel rod (cold)	106.5 in.
Outside diameter of fuel jacket	0.567 in.
Pellet dimensions	0.498 in. in diameter × 0.625 in. long
Number pellets per fuel rod	172
Total UO_2 pellets in core	3.018×10^6
Pellet density (minimum average over a fuel segment)	94 per cent of the theoretical density (10.31 g/cm^3)
Jacket	Zircaloy-2, 0.030 in. thick
Jacket thickness-to-diameter ratio	0.0529
Pellet-jacket clearance	0.0045 in. on radius
Additional gas space	Approximately ½ in. per fuel segment or a total of 2 in. per fuel rod (hot)
Filling gas	Helium
End closures	Zircaloy-2 plugs, thoriated tungsten (inert-gas-shielded arc welded)

Fuel Assemblies (See Fig. X-5)

Each fuel-rod assembly consists of a bundle of 36 fuel rods in a square array arranged in six rows of six fuel rods each. The spacing of the 36 fuel rods is maintained by a Zircaloy-2 spacer plate at each of the three screw connector joints along the length of the fuel rods and by tie plates at the upper and lower ends of the fuel rods. The three spacer plates seat on shoulders on the male and female ends of the

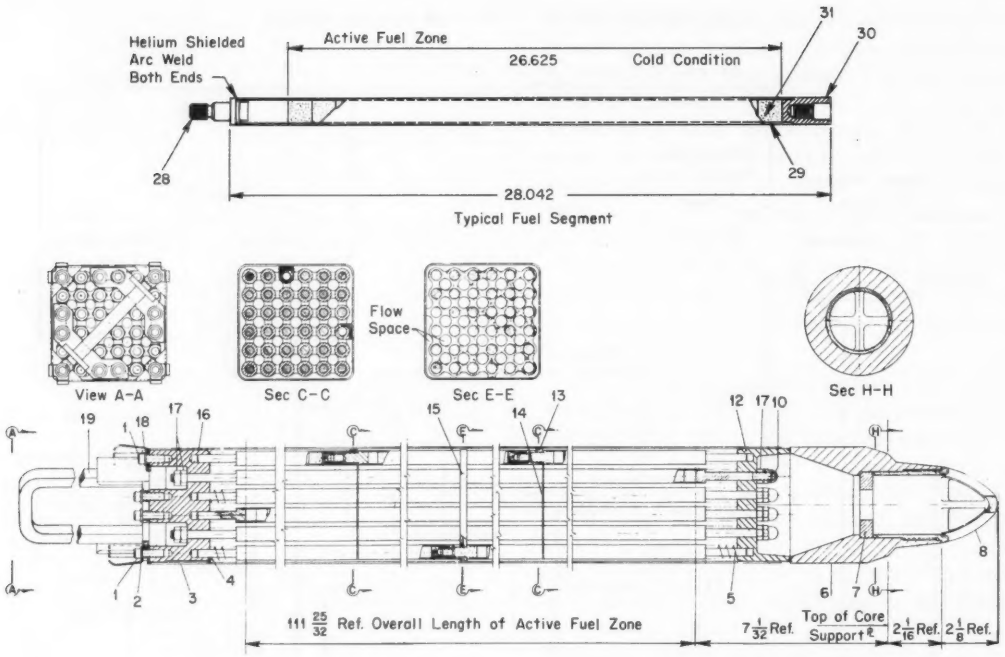

Fig. X-5 Fuel segment and assembly.[14]

fuel-element screw connectors. The upper and lower ends of the fuel rods are fitted with threaded extensions over which cylindrical springs are fitted. The springs are compressed, and the free ends of the fuel-rod extensions are inserted through holes in the upper and lower tie plates; lock nuts are attached to the fuel-rod extension ends to tie the fuel bundle together. The fuel bundle is composed of the 36 fuel rods (four segments per rod, totaling 144 segments), three spacer plates, and the upper and lower tie plates (which compress fuel-rod springs and are held in place by lock nuts).

The fuel bundle is encased in a (replaceable) square 60-mil-thick Zircaloy-2 channel or sheath. The upper end of the upper tie plate is welded to the fuel-bundle sheath. The weld forms the only fixed connection between the sheath and the fuel bundle; this arrangement allows thermal expansion of the bundle relative to the sheath. The fuel rods can expand individually against the compressed cylindrical springs that react against the upper and lower tie plates. All relative thermal expansion between individual fuel rods is referenced from the central spacer plate, which is rigid compared to the other two intermediate spacer plates. The sheath is held in alignment by nodes on the three spacer plates.

A lifting bail, screwed to the upper tie plate, is used to handle the fuel-bundle assembly. Leaf springs are also screwed to each of the four corners of the upper tie plate. These springs facilitate alignment of the fuel-bundle assembly in the core structure. Eight screws fasten the lifting bail, and four screws fasten the leaf springs into the upper tie plate. In line with these 12 screws are 12 fuel-rod extensions that cannot protrude through the upper tie plate and be held in place with lock nuts as in the case of the remaining 24 fuel rods. Instead, 12 holes are drilled partly through the upper tie plate into which these 12 fuel-rod extensions are placed. These holes are drilled extra deep to allow for thermal expansion of the rods. The 12 rods are positioned vertically by cylindrical springs.

Welded to the lower end of the lower tie plate is a transition section that fits into a mating hole in the core support plate. A com-

bination orifice plate (for setting coolant flow) and nosepiece screws into this transition section.

Total number of fuel assemblies	488
Number of fuel rods per assembly	36
Number of fuel segments per assembly	144
Fuel-rod lattice	Square
Lattice pitch	0.710 in.
Approximate diameter of core formed by all 488 assemblies	129-in. circumscribed circle
Inside dimension of fuel-bundle sheath (square)	4.29 in.
Fuel-bundle sheath material	Zircaloy-2
Fuel-bundle sheath wall thickness	0.060 in.
Over-all length of fuel assembly, nose to bail	134¼ in.
Length of fuel zone	112 in.
Active fuel length (cold)	106.5 in.

Control Rods

Eighty boron–stainless steel* cruciform control rods are mounted on the bottom of the reactor. The withdrawn position of these control rods is below the core; therefore reactivity is decreased by their upward movement and increased by their downward movement. During normal operation some rods will act as safety rods in a fully withdrawn position, whereas other rods will be used as shim rods and will usually be partially inserted.

Number	80
Material	2.0 wt.% natural boron in stainless steel
Dimensions	Cruciform, 6.5-in. span × 0.375 in. thick
Active length	102 in.
Spacing to adjacent control rods	9.96 in.
All control rods located in core within	99-in.-diameter circle
Followers	None
Upward motion of rod	Decreases reactivity
Control rods driven from	Below
Expected lifetime	4.5 years at 70 per cent load factor

*See reference 21 for a discussion of the replacement of the boron–stainless steel rods with a compacted boron carbide rod assembly.

Core Structure (See Figs. X-6 and X-7)

The core structure occupies an approximately cylindrical space 120 in. high, within a circumscribed circle 129 in. in diameter. The core assembly is supported on a bottom support plate that rests on a ring girder, which in turn is supported through columns attached to the reactor-vessel bottom. A cylindrical core guide support, which also acts as a thermal shield, rests on the ring girder at the bottom and supports a core upper guide assembly. Fuel assemblies rest on the core bottom support plate and are held in transverse alignment at the top by the core upper guide (Fig. X-7). The core assembly unit thus consists of the cylindrical core guide support, core bottom support plate, core upper guide, and fuel assemblies, all supported through columns to the bottom of the vessel. The cruciform control rods are guided by the sides of the fuel elements. Coolant flow is upward, through the core, making a single pass. There is no recirculation of the core coolant within the reactor vessel (external loops are used for recirculation flow).

Core dimensions	120-in. height within a 129-in. circumscribed circle
Method of supporting fuel assemblies	Bottom support plate and core upper guide
Fuel assembly hold-down	Friction of springs, attached to top of assemblies, bearing on core upper guide assembly
Control rods guided by	Sides of fuel assemblies within core and perforated guide tube between core support plate and vessel bottom
Coolant-flow guides	A diffusion basket assembly at the bottom of the pressure vessel aids in distributing inlet flow to the fuel assemblies. Vortex-shaped turning vanes are centered above the fuel assembly exits and are used to direct the reactor coolant (steam-water mixture) to the outer periphery of the pressure vessel toward the outlet nozzles
Coolant-flow orifices	An orifice plate is screwed into the transition section in the lower extremity of each fuel assembly. The size of each orifice flow opening is dictated by the power requirements of the fuel assembly it serves

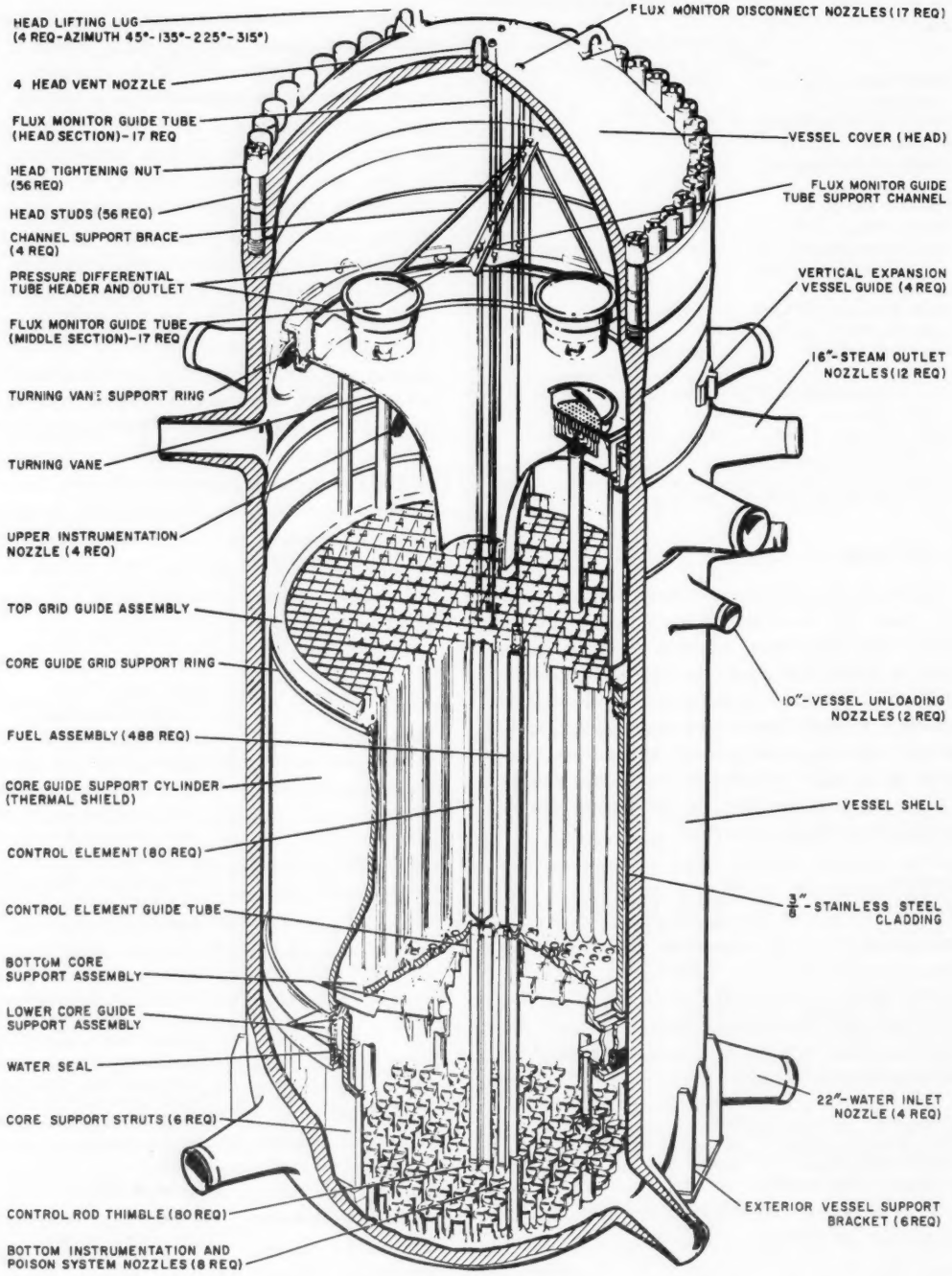
HEAD LIFTING LUG (4 REQ-AZIMUTH 45°-135°-225°-315°)
4 HEAD VENT NOZZLE
FLUX MONITOR GUIDE TUBE (HEAD SECTION)-17 REQ
HEAD TIGHTENING NUT (56 REQ)
HEAD STUDS (56 REQ)
CHANNEL SUPPORT BRACE (4 REQ)
PRESSURE DIFFERENTIAL TUBE HEADER AND OUTLET
FLUX MONITOR GUIDE TUBE (MIDDLE SECTION)-17 REQ
TURNING VANE SUPPORT RING
TURNING VANE
UPPER INSTRUMENTATION NOZZLE (4 REQ)
TOP GRID GUIDE ASSEMBLY
CORE GUIDE GRID SUPPORT RING
FUEL ASSEMBLY (488 REQ)
CORE GUIDE SUPPORT CYLINDER (THERMAL SHIELD)
CONTROL ELEMENT (80 REQ)
CONTROL ELEMENT GUIDE TUBE
BOTTOM CORE SUPPORT ASSEMBLY
LOWER CORE GUIDE SUPPORT ASSEMBLY
WATER SEAL
CORE SUPPORT STRUTS (6 REQ)
CONTROL ROD THIMBLE (80 REQ)
BOTTOM INSTRUMENTATION AND POISON SYSTEM NOZZLES (8 REQ)
FLUX MONITOR DISCONNECT NOZZLES (17 REQ)
VESSEL COVER (HEAD)
FLUX MONITOR GUIDE TUBE SUPPORT CHANNEL
VERTICAL EXPANSION VESSEL GUIDE (4 REQ)
16"-STEAM OUTLET NOZZLES (12 REQ)
10"-VESSEL UNLOADING NOZZLES (2 REQ)
VESSEL SHELL
3/8"-STAINLESS STEEL CLADDING
22"-WATER INLET NOZZLE (4 REQ)
EXTERIOR VESSEL SUPPORT BRACKET (6 REQ)

Fig. X-6 Reactor core and vessel assembly.[22]

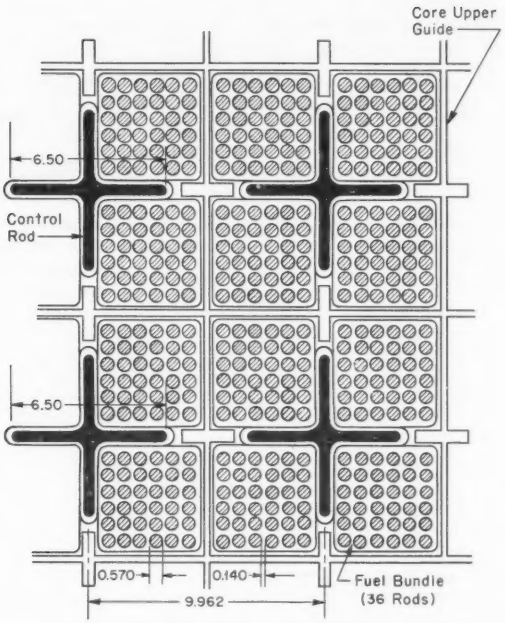

Fig. X-7 Cross section of fuel arrangement.[23]

Fuel and Control Program

The rate of burnup and the burnup status of each fuel assembly in the core are expected to be determined on a continuous basis. Assemblies of approximately equal burnup rate will be handled as a group on refueling or rearrangement. The spread within a group is expected to be ± 5 to 10 per cent of the average for the group. The reactivity status of all assemblies is to be evaluated continuously to assure that sufficient control is available for safety purposes and to assure proper control of the power distribution by rods. The power distribution will also be evaluated continuously to assure that the burnup limitations are not compromised.

When the need for refueling and/or rearrangement of fuel is indicated, or when the group of assemblies with the highest burnup reaches the specified limit, a refueling and/or rearrangement will be scheduled.

Refueling and/or rearrangement frequency	Once or twice per year
New fuel addition at any one refueling	Between 10 and 30 per cent
Average fuel lifetime exposure	10,000 Mwd/ton
Maximum fuel lifetime exposure (for a fuel assembly)	Approximately 10,000 Mwd/ton (dependent upon rearrangement program)
Worth of safety rods (selected control rods which are completely withdrawn during operation)	Approximately 0.01 to 0.08 Δk, depending on reactor conditions
Positions of control rods in fresh operating core (equilibrium Xe and Sm)	Some completely withdrawn (safety rods), some partially inserted and fixed for long periods of time (shims), and some partially inserted and used for certain power changes (control)
Program of rod withdrawal as burnup proceeds	Core power distribution is maintained by continuous programming of the control-rod pattern

Spatial Distribution of Power

Axial flux distribution peaking factor	1.4
Radial flux distribution peaking factor	1.6
Local flux peaking factor	1.36
Overpower trip	1.25
Maximum peaking factor at 125 per cent of rated power	3.81
Flux-flattening method	Programming various control rods as shims (rods kept in a fixed position for long periods of time)
Method of reducing end-cap effect	Burnable poison [dysprosium oxide (Dy_2O_3)] used at end of each fuel segment

Heat Removal

Design limits	Maximum heat flux of 350,000 Btu/(hr) (sq ft) set by maximum fuel centerline temperature of 4900°F with reactor operating at 125 per cent of rated power
Coolant-flow orificing	An orifice plate is screwed into the transition section at the lower extremity of each fuel assembly. Each plate is sized for the flow rate dictated by individual fuel-assembly power output
Average core inlet velocity	4.5 ft/sec
Central assembly inlet velocity	6.8 ft/sec
Central assembly water exit velocity	12.26 ft/sec
Total flow rate through core	2.56×10^7 lb/hr
Primary steam flow	1.405×10^6 lb/hr
Secondary steam flow	1.191×10^6 lb/hr

Average steam quality at core exit (by weight)	0.0517
Reactor operating temperature	546.4°F
Feed-water temperature	405°F
Core inlet temperature	504.7°F
Fraction of heat removed by temperature rise	0.614
Fraction of heat removed by boiling	0.386
Pressure drop across core	7.8 psi
Number of passes	1
Maximum heat flux (at 126 per cent of rated power)	350,000 Btu/(hr)(sq ft)
Average heat flux at rated power	91,820 Btu/(hr)(sq ft)
Average power density in core	28.9 kw/liter
Specific power	11.50 Mw/metric ton of uranium

Pressure Vessel (See Fig. X-6)

Materials	Low-alloy carbon steel, ASTM A302 clad with ASTM A304 (0.06 per cent carbon max.), clad as per ASTM A264
Dimensions:	
Inside diameter	122 in.
Over-all inside height (including top and bottom heads)	489⅝ in.
Shell thickness opposite core	5⅝ in. (including ⅜-in. stainless-steel cladding)
Weight	Approximately 300 tons, including 50-ton top head
Operating pressure	1000 psig
Design pressure	1250 psig
Hydrostatic test pressure	1875 psig
Material between core and vessel	2-in. stainless-steel cylindrical core guide support member, which also functions as a thermal shield, plus 6½ in. of water acting as neutron reflector
Maximum temperature used in design of vessel wall	621°F at outside of vessel wall opposite core
Maximum temperature difference used in design of vessel wall	68°F opposite core

Nozzle schedule:

Title	Nominal size, in.	Quantity	Location
Inlet nozzles	22	4	Bottom head
Outlet nozzles	16	12	About 25 ft above inlets
Unloading nozzles	10	2	About 3½ ft below outlets

Nozzle schedule (continued):

Title	Nominal size, in.	Quantity	Location
Instrument nozzles	10	4	About 3½ ft below outlets
Poison nozzle	4	1	Bottom head
Pressure taps	2	3	About 3½ ft below outlets
Density nozzles	2	2	One about 3½ ft below outlets; one about 2 ft above outlets
Drain nozzles	1½	3	Bottom head
Vent and instrument nozzle	18	1	Top head
Flux-monitoring nozzle	2	9	Top head
Seal vent nozzle	1	1	Top head
Control-rod nozzles	~5	80	Bottom head

Type of heads:	
Bottom	Nearly semihemispherical with radii 81⅜ and 78⅝ in.
Top	Spherical segment with radius 75⅜ in.
Method of holding head on	Fifty-six 5-in.-diameter stud bolts screwed into upper vessel flange and protruding through 29⅛-in. upper head flange
Method of sealing closure	Double-ring gasket compression is aided by heating the 56 stud bolts (which affords tighter closure without exceeding safe bolt tensional stresses)

Reactor Instrumentation and Control

Internal instrumentation:	
Core flux monitor system	Three or four miniature ion chambers in each of 16 fuel assemblies (64 chambers in four planes of 16 ion chambers was a proposed arrangement) provide local power indication, automatic scram (signals from two or more ion chambers required for scram), and rod programming information. These ion chambers are inserted through the reactor-vessel head into guide tubes. A fuel rod is omitted in each of 16 fuel assemblies to accommodate the guide tubes
Failed fuel-element detection	Reactor water, steam, and any associated gases arising from each of the fuel assemblies are sampled through tubes within the vessel and monitored outside the reactor

Nuclear operating instruments and locations:	Two BF_3 proportional counters with logarithmic count-rate meters and recorders. No scram is initiated by these counters. Range is 10^{-9} to 10^{-4} times rated reactor power
Two startup channels	
Three pile-period channels	Three gamma-compensated ionization chambers with a recorder on each. Period shorter than 4 sec causes scram (two out of three channels). Range is 10^{-6} to 10^{-1} times rated power
Six channels for measuring excessive neutron flux	Six gamma-compensated ionization chambers with a recorder on each. Scram at 120 per cent of rated power. Three channels are on each of the two safety system circuits. One channel from each circuit is required for scram. Range is 10^{-5} to 1.5 times rated power
High-radiation-flux channel	One gamma-compensated ion chamber, powered by a battery system, to be used in event all normal sources of power fail. Assures operator that reactor scram is effective and indicates whether liquid-poison system should be used. Range is 10^{-1} to 1.5 times rated power
Neutron source	$\frac{1}{4}$ lb of beryllium with 865 curies of antimony (initially), producing about 10^8 neutrons/sec
Control-rod drives	All hydraulic system, including both slow positioning and scram. Piston and cylinder arrangement. Pressure across piston for slow positioning is 170 psi (200 psi supplied by reactor feed pumps against a 30-psi backpressure). For scram, two accumulators with a capacity of 5.4 gal each are pressurized (by the reactor feed pumps) to supply a pressure of 1300 psi across the piston
Maximum rod withdrawal rate	6 in./sec 0.0029 Δk/sec
Scram time	10 per cent rod travel in 0.6 sec; 90 per cent rod travel in 2.5 sec
Liquid poison system (emergency system)	Sodium pentaborate; 20 sec response time; 0.20 Δk total worth

Worth of control agencies (Δk):	
Total worth of control rods	0.141
Total worth of end-connector poison (dysprosium burnable poison)	0.020
Total worth of control at startup	0.161

Control requirement for:

	Startup, Δk	Equilibrium core, Δk
Temperature defect (excluding Doppler effect)	−0.001*	−0.001*
Doppler effect	0.01	0.01
Steam voids	0.023	0.023
Xenon and samarium	0.04	0.040
Burnup and maneuvering	0.059	0.020
Cold shutdown margin	0.03	0.049
Total	0.161	0.141

*The negative value corresponds to an increase of 0.1 per cent Δk between room temperature and operating temperature. This would seem to imply substantial positive moderator-temperature and void coefficients of reactivity at room temperature. Amendment 1 to the Preliminary Hazards Summary Report states, however, that this is not the case.

Primary Coolant Circuit

(See Figs. X-4 and X-8)

Subcooled water enters the inlet nozzles at the bottom of the reactor vessel, passes through a (perforated) diffusion basket assembly, and enters the bottom of the fuel assemblies. The water then flows upward through the fuel assemblies where heat is added causing it to boil. The entire mixture of steam and water then flows out of the top of the fuel assemblies and is directed by turning vanes to the reactor-vessel outlet nozzles. This mixture flows through the riser pipes to a steam drum, 85 ft above the reactor-vessel outlets, where the water and steam are separated. The steam is passed from the drum directly to the turbine, whereas the water flows through downcomers that feed two lower headers. From these headers the water is fed to four separate loops, each containing a canned rotor pump and a U-tube type vertical (secondary) steam generator. The primary water is thus subcooled below reactor saturation temperature in the steam generators and then enters the reactor inlet nozzles. Steam from the (secondary) steam generators is utilized by a lower turbine stage than steam from the primary steam drum. Condensate from the main condenser is then proportionately fed back to the steam drum and to the shell side of the (secondary) steam generators.

No. of steam drums	1
No. of independent recirculation loops	4 (except for the common steam drum)
No. of steam generators per loop	1

No. of pumps per loop	1
Circulation rate per loop	6.4×10^6 lb/hr
Primary steam flow (from steam drum)	1.405×10^6 lb/hr
Secondary steam flow (from steam generators)	1.191×10^6 lb/hr
Flow velocity in main piping	Approximately 17.2 ft/sec
Method of pressure limitation	10 safety valves (located on steam drum) in parallel having a total capacity of 150 per cent of rated steam flow. Set pressures range from 1205 to 1250 psig
	Two low-capacity (total capacity of 14 per cent of rated steam flow) pilot-operated safety valves located on the primary steam lines
Provisions for shutdown cooling	Normally steam is dumped to the main condenser and to a separate unloading heat-exchanger circuit when reactor water is not boiling. An emergency condenser is used on loss of the main condenser
Type of steam generators	Inverted U-tube type with integral steam separation equipment

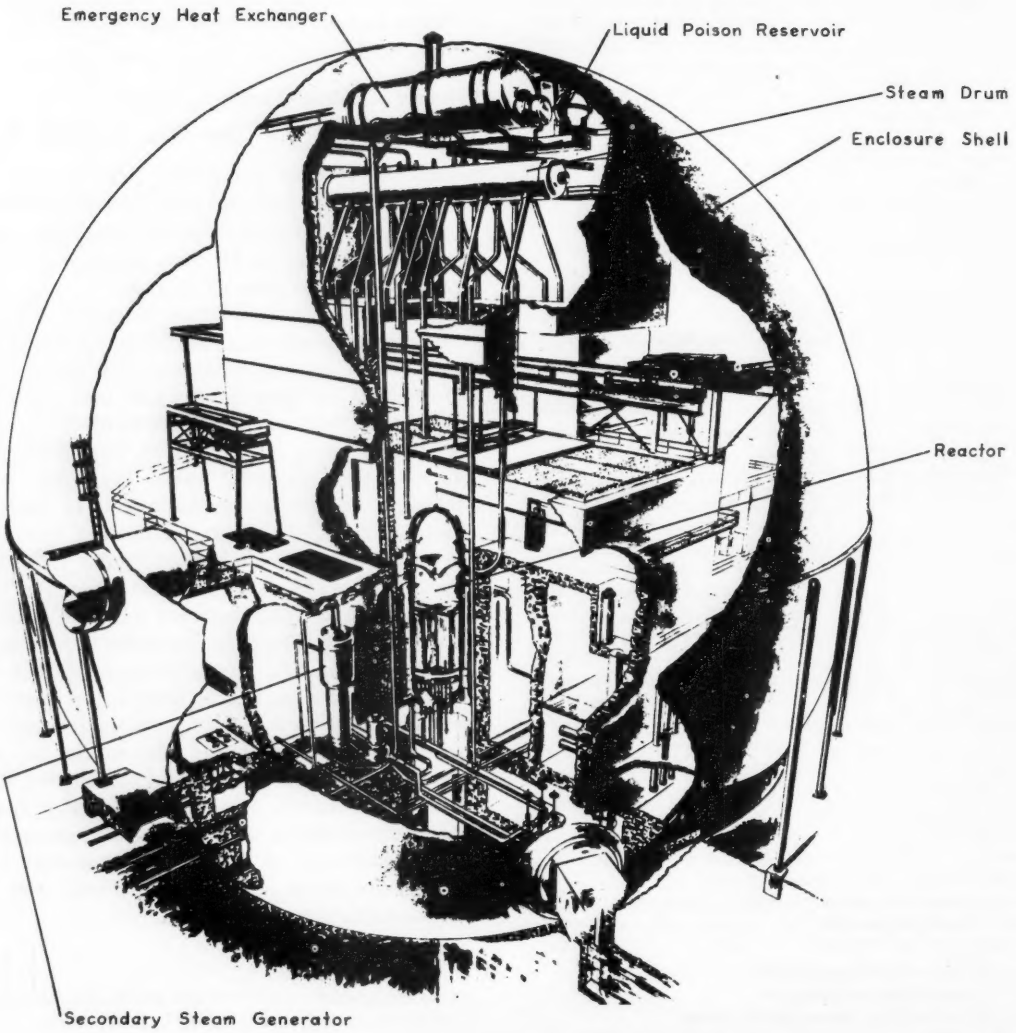

Fig. X-8 Reactor enclosure arrangement.[16]

Construction of steam generator	On primary side, low-alloy steel (ASTM A302) clad with $\frac{3}{8}$-in. A304 stainless steel. Carbon steel ASTM A106 on secondary. 22-in. primary inlet, 18-in. primary outlet, 6-in. feed water, 12-in. steam outlet
Operating pressure of steam generator	1000-psig primary side; 500-psig secondary side
Design pressure of steam generator and steam drum	1250-psig primary side; 1250-psig secondary side (hydro at 1.5 times design pressure)
Steam drum	Approximately 60 ft long × 8 ft in outside diameter, with 1500-cu ft water storage volume with integral steam-separating equipment
Type of main circulating pumps	Canned-rotor
Circulating Δp	7.8 psi across core
Valving of primary loop for secondary steam generators	Two adjacent motor-operated valves in 22-in. inlet leg and two in 18-in. outlet leg of each of the 4 loops
Piping materials:	
From reactor to steam drum, from steam drum to secondary steam generator, and from secondary steam generator to reactor	Stainless steel (ASTM A312 or A358)
Primary steam piping (from steam drum to turbine)	Low-alloy steel (ASTM A155 or A335)
Steam piping from secondary steam generator, feed-water piping, and extraction piping	Carbon steel; carbon steel (ASTM A106)
Emergency condenser, secondary steam generator (secondary side), and feed-water system (except tubes in feed-water heaters which are monel and copper-nickel)	Carbon steel (ASTM A212)
Main-condenser materials:	
Tubes	Phosphorized admiralty
Tube sheets	Muntz metal
Shells	Carbon steel
Hot-well trays and baffles	Stainless steel
Steam drum	Low-alloy (ASTM A302 clad with ASTM A304 (0.06% carbon max.))
Canned-rotor pumps and valves in four primary loops	Stainless steel
Handling of leakage	Pumped to liquid-waste collection tanks, monitored, diluted with main-condenser cooling water, and released to the Illinois River when activity permits

Treatment of Primary System Water

Additives to reduce oxygen content	None; however, deaeration in the main-condenser hot well limits condensate oxygen content to 0.001 vol.%
Handling of radiolytic gases	72.5 scfm of noncondensables removed from condenser by air ejector; held up 5 min for decay of any active gases. 200 cfm of air inleakage from turbine gland seals; held up 105 sec. All 272.5 cfm are mixed with 45,000-cfm building exhaust to 300-ft stack if activity is permissible. Air-ejector exhaust can be isolated from stack but turbine gland exhaust cannot. Provisions are made for transferring held-up radioactive air-ejector gases to another container for long-time holdup
Purity specifications	Reactor circulating water 0.5 ppm maximum total solids, pH 7.2 ± 0.2. Feed-water, condensate, 6 to 8 ppb (10 megohms-cm of resistivity)
Ion exchangers:	
Reactor circulating water	Two purification loops (each equipped with ion-exchanger), each 100,000 lb water/hr capacity. Normal operation, one loop. Resins not regenerated, sluiced directly to waste system when activity builds up
Condensate	Three demineralizer beds, normally two beds used for 3100-gal/min total feed-water flow. Resins regenerated normally but can be sluiced directly to waste system if highly contaminated
Monitoring of water	Batch principle is used. Before disposal of batch of water to river, it is sampled, analyzed, and returned for reprocessing, if necessary. Several points in waste-treatment system are monitored for operating information only. Releasability to river is determined by sampling

Fuel Handling

The expected frequency of fuel handling for refueling and rearrangement of the fuel assemblies is one or two times per year. The top head closure to the reactor vessel is re-

moved (56 bolts) for refueling, and a 139½-in.-diameter opening is provided. Components above the core are removed, and the fuel-handling canal is filled with water. Pole type grapples are used by operators who, by visual guidance, attach grapples to the fuel assemblies (below 40 ft of water) and, with the aid of a crane, lift them from the core. Each assembly is lifted individually from the reactor into a water basin above and is then removed horizontally through the canal to a point near the side of the building containment shell. The fuel is then lowered through a water lock to a level below grade and horizontally into the storage area, outside the containment shell, being kept below water at all times. Provisions are made for the removal of an assembly with a suspected ruptured element by supplying a sealed container which would be placed over the suspected assembly as soon as possible after the reactor vessel is opened. A ventilation exhaust system is used to sweep the canal and other fuel-transporting water surfaces in order to control any released fission gases. All other fuel-handling operations are performed in the fuel building. These include receiving, inspecting, and storing of new fuel; assembling new fuel bundles; and handling spent fuel, which includes stripping of reusable zirconium fuel-assembly sheaths, storing, and preparing for shipping.

Steam Plant

Number of turbines	One
Type	Saturated steam, tandem-compound, dual admission, 1800 rpm; high, intermediate, and divided flow sections; six points of extraction for feed-water heating; exhausting to horizontal, single-pass, divided-water-box condenser
Steam conditions:	
Primary steam (direct from steam drum)	1.41×10^6 lb/hr at 1000 psig, 546.4°F
Secondary steam (from steam generators)	1.18×10^6 lb/hr at 500 psig, 470.1°F
Main condenser	Capable of handling normal steam flow from turbine plus bypassed extraction steam. Also capable of handling 1.9×10^6 lb/hr bypassed primary turbine steam, thus serving as a heat sink for the reactor. Approximately 1.2×10^5 sq ft of surface
Feed-water heaters	Five feed-water heaters serve the primary feed system, and five serve the secondary system. The heaters are of the vertical U-tube type with integral drain coolers
Turbine rating	192,000 kw at 2.5 in. Hg (absolute) exhaust pressure
Reactor thermal power	630 Mw
Gross electrical output (at generator)	180 Mw
Gross efficiency	28.6 per cent
Heat rate (turbine)	11,900 Btu/kw(e)-hr

Plant Arrangement

The reactor and all associated equipment (including the steam supply system) are housed in a 190-ft-diameter spherical steel vapor container. Air-lock type accesses into the vapor container are provided for personnel and equipment. The turbine building houses the control room and power-extraction equipment (turbine, condenser, feed-water heaters, etc.); the fuel building is for storing and handling new and used fuel; the radioactive waste building houses equipment for removing radioactive matter and chemical impurities from contaminated waste water; the access control building contains laboratories, health-monitoring facilities, locker room, and first-aid station. A shop and a warehouse are also provided.

Containment (See Fig. X-8)

The reactor, primary recirculation piping, pumps, steam drum, steam generators, and emergency heat exchanger are located within a spherical steel vapor container, the equator of which is about 56 ft above ground level. Some areas of the vapor container are habitable during normal reactor operation to allow periodic entry for sampling, inspection, and auxiliary equipment maintenance.

Diameter of vapor container	190 ft
Wall thickness	From 1.25 to 1.4 in.
Free volume	2.88×10^6 cu ft
Design pressure	29.5 psig
Basis for design pressure	Design pressure must equal or exceed pressure created by release of all pressurized hot water in the reactor and primary recirculation loop
Pneumatic test pressure	1.25 times design pressure = 37 psig
Basis for pneumatic test pressure	In addition to the design conditions, a nuclear excursion contributes enough energy to melt the UO_2 fuel in the core

	plus a 25 per cent zirconium-water reaction
Maximum leakage rate	0.5 per cent of sphere free volume per day at a pressure of 37 psig
Inspection	All welds are radiographed. Also, a soap bubble check is made during 37-psig pneumatic test
Missile protection	Shield (proposed) for reactor vessel "upper-head explusion accident" consists of a wood "cushion" above the head; the tunnel walls above the head are reinforced concrete. Also, 6½ ft of concrete and 12 in. of steel (proposed) are below the reactor. For minor missiles, woven-cable blast mats at the end of the reactor tunnel were proposed
Doors and other openable penetrations	Personnel and equipment air locks are provided. Any penetrations open during normal operation are closed automatically in event of accident, and interlocks prevent opening of others during operation

Plant Control

During operation, reactor power is controlled automatically over a specified range by means of a turbine governor linked with a reactor pressure regulator. The governor controls secondary steam flow, which changes the subcooling of primary recirculating water. This subcooling change affects the point at which boiling starts along the reactor core axis and causes reactor power to follow turbine demand. The speed governor and pressure regulator are linked together to operate the primary turbine admission valves, the primary steam bypass valves, and the secondary turbine admission valves. The pressure regulator holds reactor-vessel pressure essentially constant by regulating steam flow to the turbine and/or bypass to the condenser. The speed governor admits secondary steam to the turbine to complete the total turbine requirements and control reactor-inlet-water subcooling (which produces a change in reactivity by altering the coolant steam volume) to maintain reactor power at the proper level. When core power is increased automatically by changes in subcooling, the final net steady-state void reactivity content returns to the value present before subcooling occurred, due to the change in heat output of the core. By this means, load control in the range of about 40 to 100 per cent of full load is effected automatically. Control rods are adjusted (rod drives are entirely manual) only to change the operating range (by changing the void reactivity content) or to adjust for xenon-poisoning changes and fuel burnup.

Shielding Criteria and Arrangement

In uncontrolled access areas the dose rate was set at 0.5 mrem/hr. The areas included are the control room and adjacent offices, administration building, access control building, a portion of the shop, warehouse, and outside areas around the process building. In certain areas where continuous occupancy may be required, such as the space above the storage basin in the fuel building, the dose rate was set at 1 mrem/hr. The dose rate for the reactor-enclosure and turbine-building areas requiring periodic entry for sampling, inspection, auxiliary equipment maintenance, etc., is 6 mrem/hr. Areas that are entered infrequently, which include equipment cells that are shut down for maintenance with the plant in operation, are shielded for a dose rate limit of 12 mrem/hr. In determining these dose rate levels, expected entry times in the various areas were related to a working limit of 100 mrem/week. The control room is shielded to reduce the radiation below 0.5 r during the first 8 hr following a "maximum credible accident." Shielded exits would permit personnel in the control room to leave the plant 4 hr after a "maximum credible accident" without being exposed to more than 5 r. Biological radiation-shielding material is standard-density concrete with few exceptions.

Each of the four recirculation loops, including the 22-in. piping, two inlet valves, canned-rotor pump, secondary steam generator, and two outlet valves, is completely enclosed within a concrete wall with side wall thicknesses of 54, 48, and 36 in.; ceiling 54 in.; and floor 33 in. Below the floor is a pipe space, under which is another 48 in. of concrete, totaling 81 in. of concrete between the bottom of the secondary steam generators and any operating working space below. Shield plugs are provided above the steam generators.

Surrounding the reactor is a sand fill approximately 20 ft square in a plan section outside of which is a square concrete annulus about 48 in. thick. Above the reactor head is a vertical fuel-unloading tunnel. The first 27 ft of this tunnel is flooded for fuel unloading.

Surrounding this 27-ft length is a 60-in. annulus of concrete. Above the flooded section the tunnel extends another 27 ft, forming the reactor service crane area, and surrounding this portion is a 30-in. annulus of concrete with a 48-in.-thick ceiling at the top of the tunnel. Another vertical tunnel encases the fuel-unloading tunnel and the primary steam drum, leaving an annulus between the two tunnels of about 8 ft in which the recirculation downcomer pipes from the primary steam drum are run. This outer tunnel wall varies in thickness from 54 in. at the reactor level to 36 in. at the primary steam drum level. Above the primary steam drum the concrete ceiling of this outer tunnel is 24 in. thick. Other shielding walls around equipment spaces average between 48 and 60 in. of concrete.

In the turbine building, shield walls forming the main and secondary steam lines tunnel are about 48 in. thick, and typical equipment shield-wall thicknesses are 54 in. for the feed-water heaters, 48 in. for the air ejectors, 24 in. around the feed pumps, and 48 in. around the condenser.

References

1. Nuclear Code Case 1274N-3, ASME Boiler and Pressure Vessel Code, *Mech. Eng.*, 83(1): 133 (January 1961).
2. Nuclear Code Case 1272N-2, ASME Boiler and Pressure Vessel Code, *Mech. Eng.*, 83(2): 107 (February 1961).
3. Nuclear Code Case 1273N-4, ASME Boiler and Pressure Vessel Code, *Mech. Eng.*, 83(2): 107–110 (February 1961).
4. Nuclear Code Case 1273N-5, ASME Boiler and Pressure Vessel Code, *Mech. Eng.*, 83(4): 107 (April 1961).
5. Nuclear Code Case 1274N-4, ASME Boiler and Pressure Vessel Code, *Mech. Eng.*, 83(2): 110 (February 1961).
6. Nuclear Code Case N-11, ASME Code for Pressure Piping, *Mech. Eng.*, 83(4): 125 (April 1961).
7. Provisional Requirements for the Design, Manufacture, and Testing of Pressure Components of Land-Based Nuclear Installations, *Lloyd's Register of Shipping*, 1960.
8. *Boiler and Pressure Vessel Code:* Section VIII, Unfired Pressure Vessels (as amended by the Nuclear Code Cases), American Society of Mechanical Engineers, New York, 1959.
9. H. N. Pemberton and E. Crossley, Inspection of Primary Circuits and Reactor Pressure Vessels of Nuclear Power Plant, *J. Brit. Nuclear Energy Conf.* 6(2): 79-95 (April 1961).
10. B. Brooks et al., The Selection, Design Modification, and Analysis of Sodium Valves for Hallam Nuclear Power Facility, USAEC Report NAA-SR-5463, Atomics International, Dec. 1, 1960.
11. C. J. Baroczy, Thermal Cycling and Leakage Tests of 12-Inch Valves for Sodium Service, USAEC Report NAA-SR-4947, Atomics International, May 1, 1960.
12. C. J. Baroczy, Thermal Cycling and Leakage Tests of 2-Inch Valves for Sodium Service, USAEC Report NAA-SR-5275, Atomics International, Dec. 1, 1960.
13. R. Cygan, 14-Inch Swing Check Valve Test, USAEC Report NAA-SR-Memo-4934, Atomics International, Feb. 10, 1960.
14. G. Sege, Preliminary Hazards Summary Report for the Dresden Nuclear Power Station, Report GEAP-1044, Commonwealth Edison Co. and General Electric Co., May 1, 1957.
15. Amendment No. 1 to Preliminary Hazards Summary Report for the Dresden Nuclear Power Station, Report GEAP-3009, Commonwealth Edison Co. and General Electric Co., May 1, 1958.
16. D. P. Ebright, Amendment No. 2 to Preliminary Hazards Summary Report for the Dresden Nuclear Power Station, Report GEAP-3053, Commonwealth Edison Co. and General Electric Co., Aug. 22, 1958.
17. J. L. Murray and D. P. Ebright, Amendment No. 3 to Preliminary Hazards Summary Report for the Dresden Nuclear Power Station, Report GEAP-3076, Commonwealth Edison Co. and General Electric Co., Dec. 23, 1958.
18. D. P. Ebright, Part I, Amendment No. 4 to the Preliminary Hazards Summary Report for the Dresden Nuclear Power Station, Report GEAP-3106, Commonwealth Edison Co. and General Electric Co., Feb. 3, 1959.
19. D. P. Ebright, Amendment No. 6 to Preliminary Hazards Summary Report for the Dresden Nuclear Power Station, Report GEAP-3186, Commonwealth Edison Co. and General Electric Co., June 12, 1959.
20. R. C. Thorburn et al., Enclosure Section of the Hazards Summary Report for the Dresden Nuclear Power Station, Report GEAP-0878, Commonwealth Edison Co. and General Electric Co., Jan. 24, 1957.
21. *The Forum Memo to Members*, Atomic Industrial Forum, Inc., 8(4): 30 (April 1961).
22. V. A. Elliott et al., The Dresden Nuclear Power Station, *Proceedings of the Second United Nations International Conference on the Peaceful Uses of Atomic Energy, Geneva, 1958*, Vol. 8, p. 516, United Nations, New York, 1958.
23. V. A. Elliott et al., The Dresden Nuclear Power Station, *Proceedings of the Second United Nations International Conference on the Peaceful Uses of Atomic Energy, Geneva, 1958*, Vol. 8, p. 520, United Nations, New York, 1958.

Section XI

OPERATING EXPERIENCE

Yankee

The main design characteristics of the Yankee Nuclear Power Station were summarized in the June 1961 issue of *Power Reactor Technology*, Vol. 4, No. 3. At the June meeting of the American Nuclear Society, several papers were presented[1–7] covering the initial testing of the plant and the operating experience. The last of these, delivered by Roger J. Coe of the Yankee Atomic Electric Company, described the major lessons learned so far from operation of the plant. The main points of the paper are summarized below. Although the paper necessarily emphasizes the troubles that have been experienced, it is evident that these have been, on the whole, minor and that the performance of the plant and its relative freedom from troubles have been very encouraging.

The experience with flanged gasketed closures on the 2000-psig primary system has been mixed. The reactor-vessel closure, which is sealed by self-energized O-rings, has never leaked, but there have been difficulties with some of the smaller closures. Closures employing Flexitallic type gaskets from one manufacturer have never leaked, whereas those of another manufacturer leaked so badly that seal welding was required. Some difficulty has been experienced with copper flat gasket leakage at the main coolant canned-rotor pumps. This is attributed to differential expansion effects between the stainless-steel motor flange and the carbon-steel closure bolts, and has been circumvented by delaying full pressurization of the system until relatively high temperatures are reached in the circuit. The present conclusion is that, on multiloop pressurized-water reactor plants with loop-isolating valves, it would be most practical to seal weld all valve bonnets and all flanges directly connected to the reactor vessel, except the main reactor closure flange. If quality stop valves are provided in the main coolant loops, then gasketed flanged closures should be used in the loops for equipment that is likely to require maintenance.

It is still believed that hermetically sealed valves are unnecessary, although leakage has occurred in some packed-stem valves. As in the case of gasket leakage, valve leakage appears to vary from manufacturer to manufacturer. It is considered good policy to buy the best quality valves for all installations between the reactor and the loop-isolating valves.

The main coolant pumps have performed well, and this is attributed partly to strict procedures for maintaining positive net suction head and to operating only with gas cushions or with a steam bubble in the main coolant system.

The vertical steam generators have performed well. There has been no primary-to-secondary leakage; steam of reasonable quality is produced; and there has been no problem due to trapped air in the inverted U tubes. There is a problem of getting air out of the isolated loops of the main coolant system, and this affects the chemistry of the coolant for some time after the loop or the system is refilled. This disadvantage is considered a small one relative to the advantages of the vertical type generators.

Experience with the control-rod-drive mechanisms has been excellent, there having been no problems with anything other than minor parts such as external coils and vent plugs. The possibility of high radioactive crud deposition in the drives had been anticipated, but after 3000 effective full-power hours the radioactivity levels at the drives do not appear to be a problem. It appears that in the future the cost of rods and drives will be low enough that the use of boric acid as a cold-shutdown mechanism in lieu of control rods will not be economically

justified. Experience has shown that there are substantial operating costs associated with the use of boric acid, in loss of operational time, dilution time, physics testing time, resin consumption, and in waste-disposal-system processing. The boric acid in the water has not, however, given any problems of water chemistry. Main coolant-water crud levels and the activity levels at main coolant pipes and equipment are low, and components are readily accessible within minutes after shutdown.

The concept of a closed vapor container with limited double-door access has proved favorable. However, the shielding has proved to be adequate for access to the charging floor, the tops of the steam generators, the pressurizer compartment, and the shield tank cavity during full-power operation; and it is anticipated that permission may be asked for entry during operation in order to check for points of system leakage. The methods of finding leakage points, in order of decreasing effectiveness, are: by direct inspection, by means of the vapor-container relative humidity indicator, and by means of the audio listening system. Total leakage can be measured quite accurately by the level drop in the main coolant-system pressurizer.

The elevated-vapor-container concept has the advantages of access to all welded seams, both inside and out, and of convenience in handling heavy equipment during construction; its disadvantages are the higher construction cost of the container itself and added complexity of the fuel-handling system.

Excessive vibration of the turbine occurred at loads of about 90 Mw(e). This problem has been corrected by a major modification of the high-pressure turbine. The experience with the turbine has justified the decision not to pretest the turbine with auxiliary boilers, since the trouble which did occur would not have been evident at a low power level. There have been some troubles with the turbine governing system which involved both the steam-admission valves and the main throttle valves. These difficulties were corrected during a one-week shutdown.

The 68-man staff has been adequate for operating the plant as a power station, although considerable extra work has been occasioned by the demands of public relations, licensing and inspection activities, and the research and development programs, which would not apply for long-term operation.

In summary, it can be said that, of the relatively minor difficulties that have been experienced, almost all have had to do with problems of hardware and are not inherently related to the nuclear nature of the plant. As of May 31, 1961, the plant had produced about 374×10^6 gross kw-hr of electricity, operating at a maximum thermal power of 392 Mw. The over-all load factor from the beginning of electrical production on Nov. 10, 1960, through May 31, 1961, was 63 per cent, well above the estimated load factor for this period. During this period the reactor was at operating temperature and pressure — capable of delivering steam to the turbine — at all times except during one week in February when valve-stem leakage required a shutdown.

Recently the permanent 40-year operating license for the Yankee reactor has been granted for the design-level thermal power of 485 Mw. The new power level will correspond to 145 Mw(e) gross and 136 Mw(e) net plant output.

Leakage of Pumps and Valves for D_2O Reactors

Since D_2O is expensive, the cost of material lost by leakage of valves, pumps, and other components represents an economic penalty to the reactor type. Reference 8 is a report on the leakage rate from the stuffing boxes of four commercially available valves. The valves were tested in a loop by subjecting them to hot, pressurized, deionized, light water. Three of the valves were cycled about 100 times from 1000 psig and 240°C to atmospheric pressure and 70°C, and the valve stems were back-seated and stationary. Only the bonnet-and-stem assemblies were utilized for these tests. A fourth valve was tested by passing water at 260°C and 850 to 1000 psig through the body of the valve and opening and closing the gate 1100 times at 3-min intervals. The four valves tested and their pertinent dimensions are given in Table XI-1. The water leakage was measured by enclosing the valve bonnet-and-stem assembly in a sealed chamber. Dry nitrogen was swept through the chamber to collect the vapor, and the water pickup in the chamber was measured with electric hygrometers. The analytical

Table XI-1 STUFFING BOX AND PACKING DIMENSIONS[8]

Valve description	Stuffing-box OD, in.	Stem OD, in.	Square packing rings		
			Size, in.	No. of rings before heat setting	Total uncompressed height, in.
3/4-in., 600-psig, globe	1 1/8	5/8	1/4	6	1 1/2
3-in., 600-psig, globe	Specified: 1 7/8 Actual: 1.90	1 1/4	5/16	3* and 8†	3 7/16
6-in., 900-psig, gate	2 3/8	1 5/8	3/8	3* and 9†	4 1/2
3-in., 600-psig, gate	1 5/8	1	5/16	3* and 6†	2 13/16

*Below lantern ring.
†Above lantern ring.

Table XI-2 LEAKAGES FROM VALVE ASSEMBLIES WITH STATIONARY, BACK-SEATED STEMS[8]

Valve description	Duration of test cycles*	Average during test	Leakage rate, lb of light water per year					
			Heating phase		Hot phase		Cooling phase	
			Max.	Av.	Max.	Av.	Max.	Av.
3/4-in., 600-psig, globe	80	10	30	13	20	12	8	5
3-in., 600-psig, globe	100	0.09	0.3	0.08	10	0.09	0.6	0.10
6-in., 900-psig, gate	100	0.6	3	0.4	3	1.0	3	0.5

*In a typical 3-hr cycle, the stuffing boxes were heated at 1000 psig for 1 hr, maintained at the maximum temperature (240°C) and maximum pressure (1000 psig) for 1 hr, and then cooled at 1000 psig for 1 hr, at which time the temperature was less than 70°C. At the end of each cycle, the test assemblies were vented to atmospheric pressure.

method was sensitive within 5 per cent to water leakage rates between 0.005 and 50 lb/year.

The valves were slightly modified from the as-received condition prior to testing. The valve stems were polished to reduce wear, and the packing was changed to a braided asbestos yarn containing copper wire for reinforcement and containing a graphite lubricant. The gland bolts were then intermittently tightened, and the valves were heated at 240°C for 24 hr to "heat-set" the packings. Table XI-2 shows the results of the stationary tests. The average leakage from the 3-in. gate valve that was given the dynamic test was reported as 30 lb/year. This average rate increased from a minimum of 17 lb/year at the beginning of the test to a maximum of 50 lb/year at the end of the test. The leakage rate was highest in the open position. Since the reproducibility of the experiment was not determined, the data indicate only the order of magnitude of leakage to be expected.

The Plutonium Recycle Test Reactor (PRTR) requires pumps to deliver about 8400 gal of D_2O per minute at 1115 psig and 479°F. The PRTR is to use low-leakage mechanical seal pumps[9] rather than canned-rotor pumps since the former are available at about 40 per cent of the canned-rotor pump cost. In addition, a flywheel can be incorporated in a mechanical seal pump with relative ease, to provide a degree of emergency pumping power during a power failure. Reference 9 presents the results of various tests on a prototype seal pump and on a spare PRTR primary pump. The prototype seal pump is a 2 1/2-in. discharge, 2 1/2-in. suction, 15-in. impeller, single-volute, single-stage, centrifugal pump, whereas the spare primary pump is an 8-in. discharge, 10 1/2-in. suction, 18-in. im-

peller, double-volute, single-stage, centrifugal pump. The pumps were tested in separate flow loops with water at a nominal pressure of 1000 psi and a nominal temperature of 500°F.

Both pumps incorporated the same type of seal assembly. This assembly is shown schematically in Fig. XI-1. Not shown is a small, auxiliary impeller which is located on the main pump shaft and which circulates the water in the region of the primary seal through a heat exchanger for cooling purposes. The prototype pump operated over 7500 hr in five separate tests, and only one failure occurred. This failure was due to excessive wearing of the seal faces which was caused by the accumulation, in the seal region, of large amounts of corrosion products from the carbon steel test loop. Two other failures were attributed to loss of cooling water and to an improper procedure. Seal leakage for the prototype seal pump was less than 0.1 gal/hr across the high-pressure seal and less than 100 cm^3/day for the water-oil seals. The rotating seal disk in the pumps was made of a material approximating Haynes Stellite No. 1 in composition, and the stationary seal was an impregnated graphite. An improved seal, fabricated for the prototype seal pump, provided for two sets of contact faces in series for the primary seal.

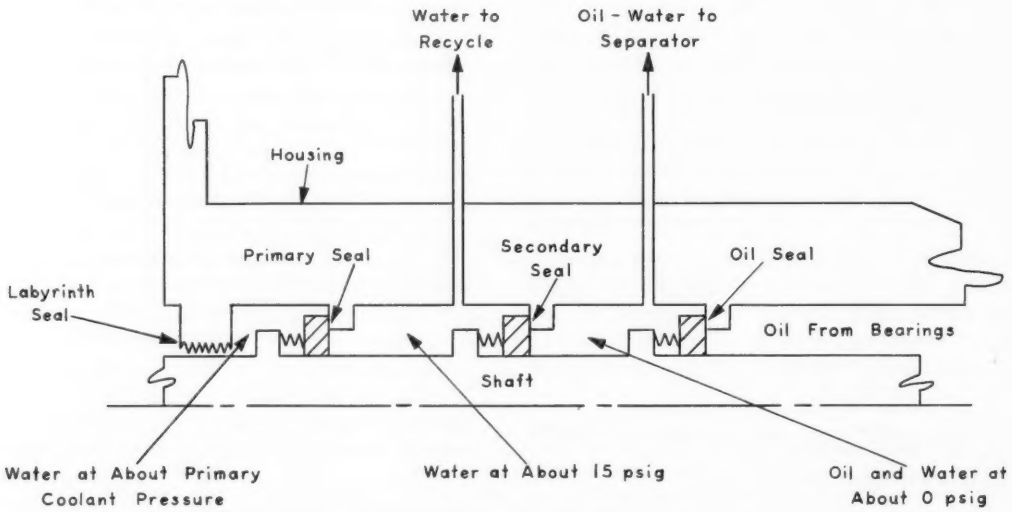

Fig. XI-1 Schematic diagram of mechanical pump seal.

The spare reactor pump was operated for over 5500 hr in its flow loop. The first series of tests proved unsatisfactory in that leakage rates up to 10 gal/hr were observed after relatively short operating times. It was determined that excessive vibration of the pump was probably causing the difficulty, and the following steps were taken to improve the situation:

1. Reduce tolerances in flywheel and impeller bores, and at bearing mountings to provide press fits.
2. Replace the radial bearing just below the flywheel with a 10° contact-angle thrust bearing preloaded with 1000-lb spring force.
3. Replace the gear type couplings with laminated metal flexible couplings.
4. Balance pump motors to within 0.5 oz-in. of imbalance.
5. Balance each assembled pump to less than 1-mil vibration while operating at 1775 rpm.

These modifications were done by the manufacturer at the factory; however, it was necessary to balance the pump while in operation in the test loop at low pressure, since the previous balancing had been done in air. Operation of the modified pump continued for 1584 hr when a motor bearing failed; leakage ranged from 0.001 to 1 gal/hr.

The author concludes that the concept of mechanically sealed circulating pumps is sound for reactor use. Although standard pump manufacturing practices are not satisfactory to give

adequate seal life, the modifications listed above are not particularly expensive; the modifications add roughly an extra 5 per cent to the cost of the unit. Three deviations were demonstrated which could be used to indicate seal-wearing conditions when remote operation prevented observation of the leakage. These deviations are:

1. Increased power requirements.
2. Increased seal temperatures as measured by thermocouples embedded in the graphite seal rings.
3. Decreased flywheel rundown time.

Through continued development it is believed[9] that continuous runs of 5000 hr or more can be achieved at reactor conditions.

Design Modifications to the Sodium Reactor Experiment

The damage to the SRE fuel elements experienced in 1959 has been attributed to blockage of the fuel coolant channels by Tetralin decomposition products. Tetralin, the coolant used in the service cooling system, leaked into the primary system through a small rupture in the shaft freeze seal gland of the main primary system pump. This damage was discussed in the March 1960 issue of *Power Reactor Technology*, Vol. 3, No. 2.

Previously other elements were damaged while being cleaned in the fuel-element wash cell.[10] This damage has been attributed to the violent reaction that resulted from the water wash because greater quantities of sodium than had been anticipated were held up in the fuel bundles.

Reference 10 describes the changes in the service cooling system, the fuel-bundle design, and the fuel washing system which were made to overcome these problems.

Service Cooling System

Tetralin has several disadvantages as a service coolant. Naphthalene, which is one of Tetralin's decomposition products, forms a naphthyl-sodium compound which is very reactive and pyrophoric. Tetralin also forms peroxides on exposure to air. These peroxides are unstable, react violently, and constitute an explosion hazard. Tetralin is also an excellent solvent for rubber, neoprene, and other common gasket materials.

The Tetralin in the service cooling system was replaced by nitrogen, NaK, and kerosene. The nitrogen is used for low heat-flux cooling where ample coolant surface is available. The primary cold traps, plugging meters, and backup valve freeze seals are nitrogen cooled. The nitrogen is at lower pressure than the sodium; thus there can be no leakage of gas into the sodium system. Since nitrogen behaves as an inert gas with sodium, if sodium leaks into a nitrogen coolant annulus, there will be no chemical reaction.

NaK is the new coolant in the bearing housing, case freeze seals, and shaft freeze seals on the sodium-circulating pumps. The use of NaK was required by the high heat flux, low coolant flow area, and the need for a coolant that does not react with sodium.

Kerosene was selected as the coolant for the top reactor shield. NaK and nitrogen were not suitable for this application because of the tube size and materials in the existing coils. The use of an organic coolant in this top shield is permissible because there is a double barrier between the service coolant and the sodium system. Also, kerosene is a saturated organic; therefore it neither forms complex sodium compounds nor forms peroxides that are common to alkyl aromatics such as Tetralin. Although aromatic compounds suffer less radiation damage than other classes of organics, the radiation level in the top shield is such that the difference is not signifi ... n this application. In the event of significant damage after long exposures, the kerosene can be replaced.

Fuel-Element Design

To minimize the possibility of fuel-channel plugging, the radial clearance between the fuel rods was increased from 29 to 162 mils, and two conical screens were installed in the bottom guide hardware of the fuel elements to prevent entrance into the fuel channels of particles larger in diameter than one-third of the radial clearance between fuel rods. To provide this extra clearance, the seven-rod cluster was replaced by an element made of five peripheral rods arranged in a concentric ring around a $\frac{3}{8}$-in.-diameter stainless-steel support rod. This new fuel configuration is shown in Fig. XI-2.

To reduce the potential holdup of sodium and subsequent reactions in the wash cells, the

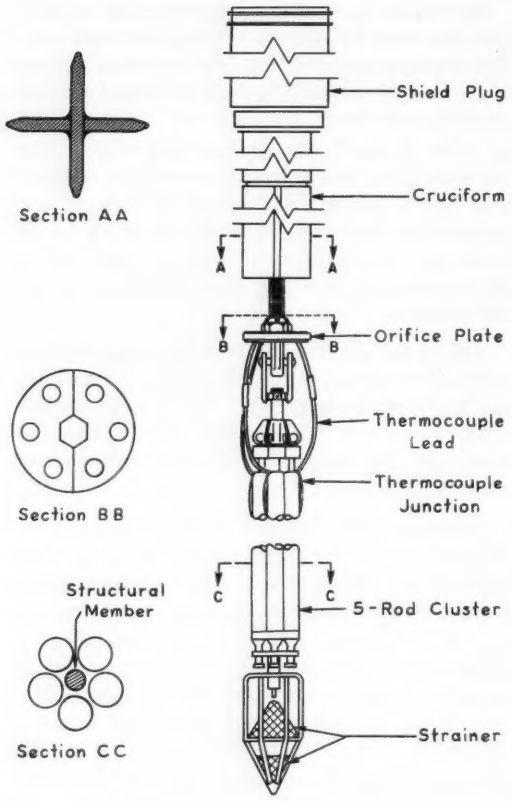

Fig. XI-2 SRE fuel-element configuration.[10]

hanger rod and hold-down tube from the previous design were replaced by a cruciform section.

Fuel Washing System

The fuel washing system used to remove sodium from the core components has been converted from a water to a steam system.

In the past, the sodium was removed from the SRE core components by placing the components in the wash cell, purging the cell with an inert gas, and flooding the cell with water. The water reacted with the sodium on contact, and the gaseous products were vented directly to the radioactive vent system.

The water flooding system was used successfully many times. Then, in October 1958, one of the fuel elements was damaged during the washing process. An investigation was initiated to determine the cause of the damage. In the following months more fuel elements were damaged. During one routine fuel washing, a pressure surge occurred in the wash cell, severely damaged the fuel element, and ejected the shield plug from the cell.

Inspection of the hold-down tube indicated that sodium may have been trapped in the tube. Recent observations have shown the drain holes on other unwashed core components to be completely plugged in the lower section of the hold-down tube. It was calculated that 8 lb of sodium could possibly be retained in this tube.

The potential danger of washing such a tube is increased by trapped sodium being submerged in the rising wash water. Normally, small gram-size chunks will melt quickly in water and react noiselessly while floating on the water. When the sodium is forced under water, audible reports are heard. The geometry of the hold-down tube was such that a jet propulsive force, acting along the axis of the tube, could be produced by the escaping gases which would result from the sodium-water reaction.

Tests were carried out in which 90 to 110 g of sodium in various size chunks were placed in a test rig which duplicated the trapped sodium conditions in the hold-down tube. Shortened dummy fuel rods were placed below the test rig so as to be below the water and thus be subject to the pressure surges when they occurred. A pressure surge of 690 psi was detected during one of the tests. Based on these tests, it is believed that trapped sodium was responsible for the failures that occurred during washing.

Subsequently the hold-down tube was replaced with a cruciform hold-down piece which prevents this trapping of sodium; a steam cleaning process which would eliminate the possibility of submerging the sodium was investigated. These steam cleaning tests showed that large quantities of sodium (125–200 g) could be disposed of without the usual audible reports associated with water washing, that the rate of the reaction could be controlled by the quality of the cleaning steam, and that components in the reaction zone would not be damaged by overheating (one of the main concerns with steam cleaning). A water rinse would be required after the steam cleaning to remove the NaOH film which remains on the components.

A series of initial washings with the new steam system have shown it to be an improved and safe way to clean SRE components.

References

1. A. R. Collier and W. J. Schmidt, Comparison of Yankee Systems Design and Operating Performance, *Trans. Am. Nuclear Soc.*, 4(1): Paper 20–1 (June 1961).
2. J. M. Gallagher and J. E. Howard, Transient Operation of the Yankee Atomic Power Plant, *Trans. Am. Nuclear Soc.*, 4(1): Paper 20–2 (June 1961).
3. J. E. Howard and D. Hunter, Experimental Evaluation of Core Reactivity and Control-Rod Worth, *Trans. Am. Nuclear Soc.*, 4(1): Paper 20–3 (June 1961).
4. H. W. Graves, Jr., and R. F. Janz, Comparison of Prediction with Experiment Reactivity and Control-Rod Worths, *Trans. Am. Nuclear Soc.*, 4(1): Paper 20–4 (June 1961).
5. D. Hunter et al., Evaluation of Reactivity Coefficient in the Yankee Reactor, *Trans. Am. Nuclear Soc.*, 4(1): Paper 20–5 (June 1961).
6. D. Hunter et al., Evaluation of Power Distributions and the In-Core Instrumentation System, *Trans. Am. Nuclear Soc.*, 4(1): Paper 20–6 (June 1961).
7. R. J. Coe, Major Lessons of Operation, *Trans. Am. Nuclear Soc.*, 4(1): Paper 20–7 (June 1961).
8. F. C. Apple, Leakage of Water from Valve Stuffing Boxes, USAEC Report DP-538, Savannah River Laboratory, January 1961.
9. P. A. Scott, PRTR Mechanical Seal Pump Operating Experience, September 1959 Through August 1960, USAEC Report HW-65724(Rev.), Hanford Atomic Products Operation, Sept. 16, 1960.
10. G. E. Deegan et al., Design Modifications to the SRE During FY 1960, USAEC Report NAA-SR-5348(Rev.), Atomics International, Feb. 15, 1961.

Section XII

ORGANIC-MODERATED REACTORS

References 1 through 12 comprise the Proceedings of the Organic-Cooled Reactor Forum, which was held on Oct. 6 and 7, 1960. The references contain status reports on organic-coolant technology,[1] heat-transfer development,[2] process development,[3] fuel-element development,[4] and experimental physics.[5] A brief account of the Organic-Moderated Reactor Experiment (OMRE) operating experience[6] and a description of the Canadian research and development program for organic-cooled reactors[7] are also given. Descriptions are given of: the Piqua nuclear power facility;[9] the Experimental Organic-Cooled Reactor[8] (EOCR), a 40-Mw(t) reactor now under construction at a site adjacent to the OMRE; an intermediate-size prototype design study[10] by Atomics International [50 Mw(e)]; a 300-Mw(e) design study[11] of an organic-moderated plant by Atomics International; and a 150-Mw(e) design study of an organic-cooled deuterium-moderated plant by the Canadian General Electric Company.[12] Some of the items of more general interest from the status reports are discussed below. It may be helpful to consult the review of organic-moderated reactors in the September 1958 issue of *Power Reactor Technology*, Vol. 1, No. 4, pages 42 to 51.

One of the fundamental considerations in the use of an organic coolant or moderator is its rate of radiolytic decomposition in the reactor. The products of such decomposition are radiolytic gases, which evolve from the organic liquid, and high-boiler (HB) compounds — organic compounds having boiling points higher than those of the original constituents of the organic liquid — which remain in the liquid unless removed by distillation. The rate of production of HB compounds decreases as the concentration of the HB compounds in the liquid is al-

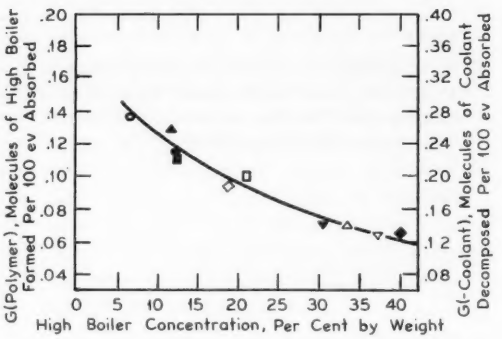

Fig. XII-1 Decomposition rate of OMRE coolant.[1] Tests at constant HB content: ▲, 11.6 per cent HB, 667°F; ■, 12.2 per cent HB, 600°F; ●, 12.1 per cent HB, 600°F; ▼, 30.6 per cent HB, 600°F; and ◆, 40.9 per cent HB, 600°F. Tests at changing HB content: ○, miscellaneous reactor tests at 450 to 675°F; □, 12 to 30 per cent HB, 600°F; △, 31 to 36 per cent HB, 600°F; ▽, 34 to 41 per cent HB, 600°F; and ◇, 7.6 to 30 per cent HB, 500°F.

Table XII-1 TYPICAL CHEMICAL COMPOSITION OF OMRE COOLANT[1]

	Core 1 (5-21-58), wt.%	Core 2 (7-5-59), wt.%
Low boilers*	0.9	0.7
Diphenyl	12.3	5.7
Orthoterphenyl	24.7	28.8
Metaterphenyl	19.7	22.5
Paraterphenyl	3.7	2.8
Intermediate boilers†	8.7	9.7
High boilers‡	30.0	29.8

* Components in the volatility range greater than that of diphenyl and through benzene.

† Components in the volatility range between diphenyl and the HB fraction.

‡ Components less volatile than the least volatile major component (paraterphenyl).

lowed to build up; however, because of the increase in viscosity and decrease in the heat-transfer capability of the organic, there is a practical limit to the HB content which can be tolerated. Figure XII-1 is an experimental curve showing the rate of formation of HB compounds as a function of their concentration in the organic liquid. These measurements were made during OMRE operation with core 1. Reference 1 states that the rates observed during operation with core 2 were substantially the same: 53.0 lb/Mwd for core 2 as compared to 51.0 lb/Mwd for core 1, at 30 per cent HB concentration. The rate of formation of HB compound is given in terms of the *G* factor, or *G* (polymer), the number of molecules of HB formed per 100 ev of radiation energy absorbed. An average molecular weight of 460 is assumed for the HB. The *G* factor is also given in the figure for the rate of "decomposition" of the coolant. Typical comparisons of the OMRE coolant composition during operation with core 1 and core 2 are given in Table XII-1.

Reference 1 states that the value of 53.0 lb/Mwd for the organic decomposition rate in OMRE core 2 is equivalent to 28.3 lb/Mw-hr of radiation energy actually absorbed in the organic liquid. The reference also states that extrapolation of these data to a full-scale power reactor predicts an HB formation rate of 27 lb/Mwd(t) of reactor operation, at an HB concentration of 30 per cent, along with a gas generation rate of 8 scf/Mwd(t). This extrapolation is based on the assumption of equal damage per unit of energy absorbed from ionizing radiation, regardless of whether the radiation consists of fast neutrons, gammas, or electrons. The lower rate of decomposition in the full-scale reactor,

Table XII-2 SUMMARY[1] OF TEMPERATURE-DEPENDENT PROPERTIES OF COMMERCIAL TERPHENYL MIXTURE*

Property	Temp., °F	HB content, wt.% 0	10	20	30	100
Density, liquid, g/cm^3	600	0.874	0.884	0.896	0.907	0.982
	700	0.827	0.839	0.851	0.864	0.952
	800	0.777	0.791	0.804	0.818	0.922
Vapor density, g/cm^3	650	0.001				
	700	0.004				
	800	0.012				
Hydrogen density, atoms/cm^3 × 10^{-22}	600	3.20	3.22	3.25	3.27	3.41
	700	3.03	3.06	3.09	3.12	3.31
	800	2.84	2.88	2.92	2.95	3.21
Viscosity, centipoises	600	0.32	0.41	0.53	0.70	7.8
	700	0.23	0.29	0.38	0.49	4.1
	800	0.18	0.22	0.28	0.37	2.4
Enthalpy, base 300°F, Btu/lb	600	154				
	700	207				
	800	262				
Specific heat, Btu/(lb)(°F)	600	0.530	0.522	0.515	0.507	
	700	0.542	0.533	0.524	0.515	
	800	0.555	0.545	0.534	0.524	
Thermal conductivity, Btu/(hr)(ft)(°F)	600	0.0660	0.0660	0.0660	0.0660	
	700	0.0635	0.0635	0.0635	0.0635	
	800	0.0610	0.0610	0.0610	0.0610	
Latent heat of vaporization, Btu/lb	600	124.7				
	700	120.4				
	800	113.8				
Vapor pressure, psia	600	4.0	3.9	3.7	3.5	
	700	13.2	12.5	12.0	11.0	
	800	35.5	33.7	32.0	29.7	
Surface tension, dynes/cm	600	19.2				
	700	15.4				
	800	11.8				

* Available as both Santowax R and Santowax OMP. A typical composition of Santowax R is as follows (wt.%): orthoterphenyl, 10; metaterphenyl, 49; paraterphenyl, 26; and higher boiling components, 11.3. The Santowax OMP has the same terphenyl isomer ratio as the Santowax R with the higher boiling components removed.

Table XII-3 SUMMARY[1] OF MISCELLANEOUS PROPERTIES OF COMMERCIAL TERPHENYL MIXTURE*

Property	HB content, wt.%				
	0	10	20	30	100
Final melting point, °F	312	303	292	278	230
Boiling point, °F	713	739	728	713	
Flash point, °F	375				
Flame point, °F	460				
Threshold temperature, °F	835				
Auto-ignition temperature, °F	1148				
Critical temperature, °F	1210				
Critical pressure, psia	506				
Critical density, g/cm^3	0.298				
Heat of combustion, cal/g at 20°C	9604	9598	9593	9589	
Latent heat of fusion, cal/g	21				

* Available as both Santowax R and Santowax OMP. A typical composition of Santowax R is as follows (wt.%): orthoterphenyl, 10; metaterphenyl, 49; paraterphenyl, 26; and higher boiling components, 11.3. The Santowax OMP has the same terphenyl isomer ratio as the Santowax R with the higher boiling components removed.

relative to the OMRE, results from the higher relative concentration of fuel in the large reactor and the consequent absorption of a greater fraction of the radiation energy in the fuel.

Reference 1 gives data on specific heat, thermal conductivity, viscosity, melting point, vapor pressure, and critical constants for various organics, both unirradiated and irradiated, of interest as reactor coolants. A summary of some of the data for Santowax is given in Tables XII-2 and XII-3. The density and viscosity of irradiated polyphenyls are treated in detail in reference 13. Reference 1 also gives chemical properties of the organics, their decomposition products, and their impurities.

Results are reported[1] of a screening test to find attractive alternate organic coolants. These tests were made by irradiating samples in stainless-steel capsules, at 580 and 750°F, in the Materials Testing Reactor (MTR) gamma facility. The results are summarized in Table XII-4 in terms of relative values for G (gas) and G (polymer). The first two entries in the table, the alkylphenanthrene refinery stream from petroleum and the anthracene oil fraction of coal tar are considered promising. Both of these liquids are commercially available in very large quantities, are liquid at room temperature, and are less volatile than the commercial terphenyl mixture. Table XII-5 gives the results of a comparison of decomposition rates for alkylphenanthrenes and terphenyls under electron bombardment at high temperature. The behaviors under irradiation appear to be comparable. Reference 1 states that the pyrolytic threshold temperature for the alkylphenanthrenes is about 730°F, about 90°F below that of the terphenyls.

A search has also been under way for inhibitors that might reduce the rate of decomposition of the polyphenyl coolants. Four additives were found that produced reductions of 15 to 25 per cent in the decomposition rate; however, the additives are expensive compounds, and work in the area of inhibitors has been deemphasized.

Reference 3 summarizes the status of development of process systems, most of which have to do with handling and disposing of decomposition products. Systems are included for: removal of impurities from the coolant, separation of HB, disposal of HB by burning, degasification of coolant, disposal of decomposition gases, and water disposal. Much of this work was previously reviewed in the March 1961 issue of *Power Reactor Technology*, Vol. 4, No. 2.

Investigation[1] of the fouling of fuel elements and other heat-transfer surfaces by film deposits has indicated that the films are built up from particulate matter in the coolant. These deposits typically consist of submicron particles of inorganic material surrounded by insoluble (in the coolant) organic material. The report states that organic and inorganic insoluble materials are hardly ever observed to exist independently, either as insoluble particles in the coolant or as film deposits. Iron is the major cation of the inorganic materials. In film deposited within the reactor, the iron is usually bound as the percarbide, $Fe_{20}C_9$ (or Fe_2C), although some of the iron, perhaps 10 per cent, is probably in the form of oxides. Bench tests have been made on pyrolytically induced fouling to determine the relative importance of various factors on the rate of fouling-film deposition. For these tests the temperature of the heated surface was in the range 850 to 1050°F to produce rapid fouling. The amount

Table XII-4 RESULTS OF SCREENING TEST EVALUATION[1] OF NEW COOLANTS AT 580°F

New coolant	Relative *G* (gas)	Relative *G* (polymer)	Price, $/lb
Alkylphenanthrenes (refinery stream)	10.4	0.60	0.05–0.08*
Anthracene oil (coal tar hydrocarbons, mainly aromatic)	0.86	0.70	0.032
Creosote oil (coal tar hydrocarbons, 80% aromatics)	5.2	1.5	0.027
Whole PAP (a mixture of polyalkylpyridines)	26.0	1.4	0.16
Quinoline residues (coal tar base fraction)	14.6	4.5	0.026
Heat-stable oil (petroleum naphthene fraction, stabilized with an additive)	58	0.7	0.13
Kaydol (a petroleum naphthene fraction)	46.0	2.0	0.11
Isopropyl Santowax OM	7.2	0.83	
Ditolylethane	40.0	4.0	
Heat-transfer fluid (a hydrogenated mixture of glycerides of fatty acids from fish oils)	Very large	Caked	

* Depends on sulfur content, price is for 100 ppm.

Table XII-5 ELECTRON IRRADIATION OF ALKYLPHENANTHRENES[1] AT 750°F (1-MEV ELECTRONS)

Dose, g/watt-hr	Concentration, %	Radiolytic gas formation rate		Radiolytic polymer formation rate, g/watt-hr	Total radiolytic decomposition rate, g/watt-hr
		ml (STP)/watt-hr	g/watt-hr		
		Alkylphenanthrenes			
13.6	16.3			0.0124	
18.2	17.4	2.52	0.00162	0.0096	0.0112
18.5	15.2	1.97	0.00127	0.0082	0.0095
30.6	25.6	2.04	0.00132	0.0084	0.0097
40.7	27.5	1.22	0.00081	0.0068	0.0076
		*Terphenyls**,†			
13.6	16.4	0.20	‡	0.0121	0.0121
18.2	20.3	0.17		0.0111	0.0111
18.5	20.5	0.17		0.0113	0.0113
30.6	30.1	0.15		0.0099	0.0099
40.7	35.7	0.15		0.0088	0.0088

* W. G. Burns et al., The Effect of Fast Electrons and Fast Neutrons on Polyphenyls at High Temperatures, *Proceedings of the Second United Nations International Conference on the Peaceful Uses of Atomic Energy, Geneva, 1958*, Vol. 29, p. 266, United Nations, New York, 1958.

† E. L. Colichman and Raymond Fish, Pyrolytic and Radiolytic Decomposition Rate Studies on Ortho-, Meta-, and Para-terphenyls, USAEC Report NAA-SR-1287, North American Aviation, Inc., May 15, 1955.

‡ The gas from the terphenyls does not contribute significantly to the weight of terphenyls decomposed.

of film deposited was found to correlate with the inorganic ash content of the coolant (Fig. XII-2). Reference 1 also states that, since the inorganic content of the coolant has been shown to be mostly associated with insoluble particulates larger than 0.22 μ, the correlation suggests strongly that the removal of the inorganic and organic material comprising these larger particulates will reduce the fouling rate in the OMRE coolant to acceptably low values.

Reference 2 gives data on film buildup under conditions of forced convection and subcooled nucleate-boiling heat transfer. The data were obtained from 15 long-term heat-transfer experiments, varying in duration from 100 to 3600 hr. The buildup of the film is measured in terms of a film thermal resistance (r), defined in terms of heat-transfer quantities, as follows:

$$\frac{T_w - T_b}{q} = \frac{1}{U} = \frac{1}{h} + r$$

where

T_w = the surface temperature of the metal cladding, °F

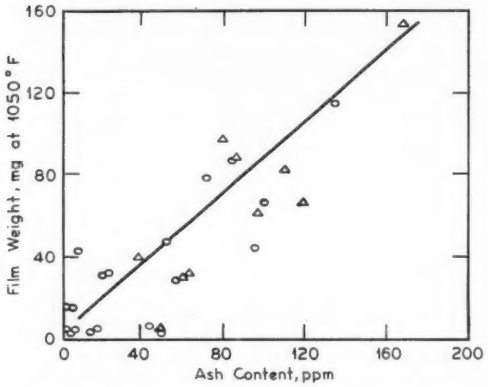

Fig. XII-2 Correlation of fouling film weight with ash content for all coolants tested.[1] Δ, OMRE coolant "as is." ○, treated coolant.

T_b = the bulk temperature of the coolant at that point, °F

q = the heat flux at the same point, Btu/(hr)(sq ft)

U = the maximum over-all heat-transfer coefficient, Btu/(hr)(sq ft)(°F)

h = local heat-transfer coefficient, Btu/(hr)(sq ft)(°F)

r = film resistance, $[\text{Btu/(hr)(sq ft)(°F)}]^{-1}$

Figure XII-3 shows the value derived from the measurements for r extrapolated to 1 yr of operation as a function of the initial temperature of the heat-transfer surface. The value of r increases exponentially with the initial surface temperature and decreases as the flow velocity is increased. These experiments were made with OMRE coolant containing 30 per cent HB compounds. Reference 2 states that Santowax OMP, which had been carefully distilled in glass, showed two orders of magnitude less fouling than the OMRE coolant in the pyrolytic capsule fouling test. The reference also states that the removal of substantially all magnetic particles by means of a magnetic filter, filtration using an Alsop asbestos filter, and deaeration with a nitrogen sparge all reduce fouling by approximately 75 per cent.

Reference 6 describes the experience with fuel-plate fouling in the OMRE (see also the review in the September 1960 issue of *Power Reactor Technology*, Vol. 3, No. 4, pages 66 and 67). According to reference 6 the evidence indicates that the fission-product beta-particle current flowing into the coolant channel is a significant factor in promoting the migration of

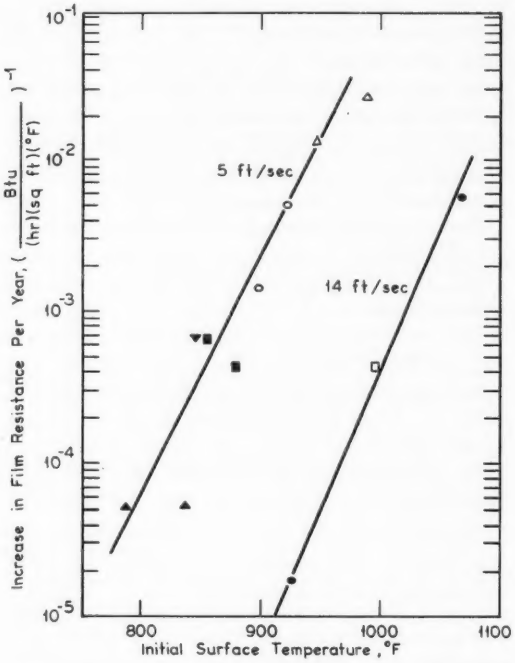

Fig. XII-3 Expected increase in film resistance[2] with OMRE coolant containing 30 per cent HB.

Run No.	Duration, hr	Velocity, ft/sec
○, ext. forced convection No. 3	304	5
Δ, ext. forced convection No. 5	172	5.8
□, ext. forced convection No. 6	165	14
▼, ext. boiling No. 3	558	5
■, ext. boiling No. 4B	313	10
▲, ext. boiling No. 6	2970	5
●, ext. forced convection No. 7	456	14

inorganic-based particulate material to the surface of the fuel plates and in retaining it on the surface for a period sufficient to radiolyze its organic fraction in place.*

*E. G. Lowell, Atomics International, states that more information has become available with respect to the transportation of particles to the fuel-plate surface. "Present theory, however, gives more weight to Brownian movement and diffusion as means of transporting particles to the fuel element surface. The principal effect of the beta current is thought to be increased residence time for the particles. W. E. Parkins, Surface Film Formation in Reactor Systems, NAA-SR-6048, Atomics International, Jan. 30, 1961."[14]

Reference 15, prepared by the Civilian Reactors Evaluations and Planning Branch of the AEC Division of Reactor Development, and Consultants, is an evaluation of the fuel-element fouling problem in the OMRE, and covers observations and conclusions based on OMRE developments through May 1960. This reference is in agreement with reference 1 in concluding that the fouling on OMRE fuel-element surfaces is due primarily to the presence of significant amounts of inorganic particulate matter in the coolant. A further conclusion is that the inorganic contamination in OMRE is due principally to rust that forms when the reactor system is opened to air and moisture. Major fouling of some of the OMRE fuel elements was caused by deposition of this particulate matter, and one of the OMRE experimental test elements (designated HB-1, high-burnup element) melted during testing in the OMRE, owing to plugging of the small coolant channels by large particles in the coolant. Actual fouling of the heat-transfer surfaces (significant film deposition) was not observed on the aluminum-clad, low-enrichment, OMR type elements. The particulate matter was found to be composed of an agglomeration of minute particles which consisted of a dense inner crystalline nucleus, about 0.2 μ or less in size, surrounded by a layer up to approximately 0.1 μ thick of less dense material. The inner nucleus was found to consist primarily of $Fe_{20}C_9$, whereas the less dense material was an insoluble, highly polymerized, organic film with an unusually high carbon-to-hydrogen ratio of approximately 2 to 1.

Another film of a less serious type of fouling, which built up on some of the OMRE fuel elements, was characteristically rather smooth and was deposited in such a thin layer that the flow in the coolant channels was not significantly diminished. This smooth film was composed of essentially the same kind of minute particles that caused gross plugging of other elements. The difference of behavior, leading to serious fouling in some cases and smooth thin films in others, was attributed to the variation in fuel-element location relative to the available fission-product beta-particle current as mentioned in reference 6. It was observed that the submicron iron carbide fouling particles did not acquire additional organic coatings after the layer thickness reached about 0.1 μ but that their tendency to agglomerate increased their fouling ability. Reference 15 states, however, that deposition of the agglomerated particles, as they are circulated by the organic coolant, does not lead to gross fouling rates. Radiation (fission-product beta-particle current) variations with location were determined to be the major differences between slightly and badly fouled fuel plates. The validity of the beta-current theory was strengthened when it was observed that, at the inlet end of the fuel plate, the film deposits coincided with the outline of the fuel within the plate and, at the outlet ends, the film deposits extended beyond the fuel, gradually decreasing to nothing. To account for this phenomenon, the charging of the coolant by beta particles was compared with the charging of an electrical condenser. As further evidence of the beta-current contribution to fouling, it was observed that heavy fouling deposits in the OMRE fuel elements were found only on the fuel plates themselves and on the inside surfaces of fuel-element boxes, whereas the film formation rate on the outside of the boxes was considerably lower (the outside surfaces were exposed to the same coolant flow as the inside). Although the neutron and gamma radiation on both sides of the fuel boxes is roughly the same, the beta density is greatly diminished by the thickness of the fuel-element box.

Once the agglomerated particles are deposited on fuel-assembly surfaces, they are subject to a continuous radiation exposure, and polymerization of the organic-coated particulate matter proceeds rapidly. Another characteristic of the gross fouling buildup[15] was attributed to flaking of deposits from the organic film layer once it becomes rather thick; this could expose a roughened or porous surface in which the circulating organic liquid could lie stagnant. Stagnation of the liquid organic coolant increases pyrolytic as well as radiolytic decomposition, and would result in a further film buildup. The contribution to film buildup by pyrolytically decomposed organic liquid, however, is not expected to be significant for surface temperatures below 1000°F, and presently contemplated organic-reactor designs do not exceed this limit.

In reference 15 the origin of the majority of coolant impurities was traced to rust (caused by water or dissolved oxygen in the system) from the carbon steel reactor system piping. This rust is subsequently removed by the hot polyphenyls and is introduced into the coolant stream where it then accumulates the organic

film. As a result of the deleterious effect caused by rust in the system, it is concluded that design, construction, operation, and maintenance practices must be carefully reviewed and altered in order to reduce to a practical minimum the particulate fouling of the fuel coolant-flow channels of organic-cooled systems. Such corrective measures will include reduction of the air and water content in the coolant to a low value, inert atmosphere handling of the fuel, and an additional cleanup system for particulates. The proposed new cleanup system for OMRE core 3 is designed to reduce the particulate content in the coolant to 10 ppm before startup and to keep it below that level during operation.

Reference 2 gives results of heat-transfer tests conducted in various laboratories (Atomics International, Harwell, Naval Research Laboratory, and Canadian General Electric) on unirradiated polyphenyls (Santowax, diphenyl, and isopropyl diphenyl), all of which were correlated to within ±20 per cent by the Dittus-Boelter equation. Figure XII-4 shows a similar

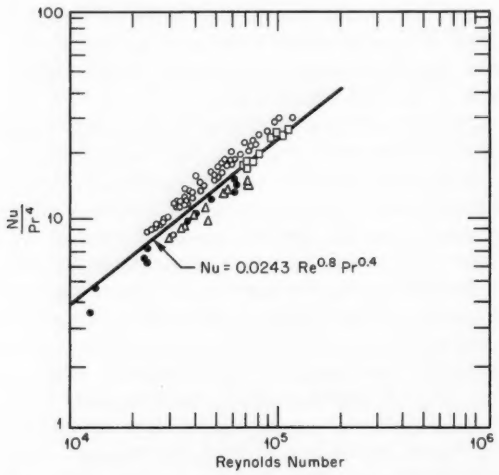

Fig. XII-4 Comparison of irradiated OMRE coolant heat-transfer data with the Dittus-Boelter correlation.[2]

correlation for measurements on various samples of irradiated OMRE coolant. The slope of the line is the same as that used for the correlation of the unirradiated data. The scatter of the irradiated data is approximately ±25 per cent.

For nucleate-boiling heat transfer, the major variables are stated[2] to be wall superheat and the physical properties of the coolant. Fluid velocity is stated to have little effect, and there is little difference whether the bulk temperature of the coolant is below or at saturation temperature. The Levy correlation[16] has shown the best agreement for Santowax OM, OMRE coolant, and diphenyl, but at a given heat flux the wall superheat may lie in the range 50 per cent above to 30 per cent below that predicted by the correlation.

Burnout heat-flux data for Santowax R are correlated by the equation (reference 17, reviewed in the June 1959 issue of *Power Reactor Technology*, Vol. 2, No. 3, pages 20 and 21):

$$\left(\frac{Q}{A}\right)_c = 552\ \Delta T_{sub}\ V^{0.67} = 152{,}000$$

and for the following ranges of variables:

System pressure	91 to 109 psia
Bulk temperature (T_b)	595 to 771°F
Velocity (V)	4.9 to 15.3 ft/sec
Subcooling ($T_{sat} - T_b$)	174 to 334°F
Heat flux (Q/A_c)	0.416×10^6 to 1.287×10^6 Btu/(hr)(sq ft)
Hydraulic diameter	0.272 in. (annulus)

Reference 2 states that, in pool-boiling heat transfer, the addition of 5 per cent benzene to diphenyl has been observed to approximately double the burnout heat flux above that which would have characterized either pure diphenyl or pure benzene, and it is postulated that this effect could be used to advantage in reactor designs.

References

1. R. H. J. Gercke, Status of Organic Coolant Technology, in Proceedings of the Organic Cooled Reactor Forum, October 6–7, 1960, USAEC Report NAA-SR-5688, pp. 5–43, Atomics International, December 1960.
2. W. R. Martini, Status of Heat Transfer Development for Organic Reactors, in Proceedings of the Organic Cooled Reactor Forum, October 6–7, 1960, USAEC Report NAA-SR-5688, pp. 45–67, Atomics International, December 1960.
3. W. R. Martini, Status of Process Development for Organic Reactors, in Proceedings of the Organic Cooled Reactor Forum, October 6–7, 1960, USAEC Report NAA-SR-5688, pp. 69–87, Atomics International, December 1960.
4. H. Pearlman, Status of OMR Fuel Element Development at Atomics International, in Proceed-

ings of the Organic Cooled Reactor Forum, October 6–7, 1960, USAEC Report NAA-SR-5688, pp. 89–124, Atomics International, December 1960.

5. H. N. Royden, Current Status of OMR Experimental Physics, in Proceedings of the Organic Cooled Reactor Forum, October 6–7, 1960, USAEC Report NAA-SR-5688, pp. 125–141, Atomics International, December 1960.
6. R. O. Williams, Jr., OMRE Operating Experience, in Proceedings of the Organic Cooled Reactor Forum, October 6–7, 1960, USAEC Report NAA-SR-5688, pp. 143–170, Atomics International, December 1960.
7. W. M. Campbell, Canada's Research and Development Program for an Organic Liquid Cooled Nuclear Reactor, in Proceedings of the Organic Cooled Reactor Forum, October 6–7, 1960, USAEC Report NAA-SR-5688, pp. 171–187, Atomics International, December 1960.
8. M. R. Dusbabek, Experimental Organic Cooled Reactor, in Proceedings of the Organic Cooled Reactor Forum, October 6–7, 1960, USAEC Report NAA-SR-5688, pp. 189–210, Atomics International, December 1960.
9. E. F. Weisner, The Piqua Nuclear Power Facility, in Proceedings of the Organic Cooled Reactor Forum, October 6–7, 1960, USAEC Report NAA-SR-5688, pp. 211–224, Atomics International, December 1960.
10. Jay E. Brunings, Intermediate Size Prototype Plant, in Proceedings of the Organic Cooled Reactor Forum, October 6–7, 1960, USAEC Report NAA-SR-5688, pp. 225–253, Atomics International, December 1960.
11. R. K. Winkleblack and R. J. Gimera, 300 Mw(e) OMCR Power Plants — Present and Future, in Proceedings of the Organic Cooled Reactor Forum, October 6–7, 1960, USAEC Report NAA-SR-5688, pp. 255–274, Atomics International, December 1960.
12. J. R. Dickinson and R. F. Scarth, OCDR Power Plant Study, in Proceedings of the Organic Cooled Reactor Forum, October 6–7, 1960, USAEC Report NAA-SR-5688, pp. 275–306, Atomics International, December 1960.
13. R. H. J. Gercke and G. Asanovich, Thermo-Physical Properties of Irradiated Polyphenyl Coolants, Part I, Density and Viscosity, USAEC Report NAA-SR-4484, Atomics International, Dec. 1, 1960.
14. E. G. Lowell, unpublished letter dated Aug. 4, 1961.
15. Evaluation of the Organic Fouling Problem in the OMRE, USAEC Report TID-6882, Mar. 24, 1961.
16. C. Grove-Palmer and H. Pass, Heat-Transfer Properties of Santowax R, *Nuclear Power*, 4(44): 118-121 (December 1959).
17. T. C. Core and K. Sato, Determination of Burnout Limits of Polyphenyl Coolants, Summary Report, USAEC Report IDO-28007, Aerojet-General Corp., Feb. 14, 1958.

Section XIII

FAST BREEDERS

Recent reports have given new information on some of the more important aspects of the fast-breeder reactor: the performance of fuel elements, the neutron physics, and the relation of design variables to power-generation cost.

Reference 1 describes the results of irradiation tests of prototype Experimental Breeder Reactor No. 2 (EBR-II) fuel elements in the Argonne Research Reactor (CP-5), Materials Testing Reactor (MTR), and Engineering Test Reactor (ETR). Figure XIII-1 describes the reference design for the EBR-II fuel elements, which consist of uranium alloy pins jacketed with stainless steel, with a sodium bond. Several different test-facility designs were used in the different test reactors, but every design used exposed full-size elements (Fig. XIII-1) in a sodium environment. The power generated in the element was as high as 13.4 kw (191 kw/kg of uranium) in one of the ETR tests. The maximum central temperature of the fuel was in the range 640 to 932°F for the high-power-density runs, although central temperatures up to 1150°F were attained in exposures at lower powers. The maximum design value of central temperature in EBR-II is about 1200°F. A maximum fuel burnup of 1.56 at.% was reached in the tests.

Although the CP-5 irradiations used specimens of both uranium-zirconium and fissium alloys, made by several different processes, the MTR and ETR tests employed only fissium alloys, made by the EBR-II reference method of precision casting in Vycor tubes. Fissium is an alloy of uranium with fission-product elements that will be left in the fuel under an equilibrium recycling through the melt-refining reprocessing scheme contemplated for EBR-II. The compositions of several fissium alloys are given in Table XIII-1. The development of the melt-refining method for reprocessing fast-reactor fuel has been described in a series of papers in *Nuclear Science and Engineering*.[2–13]

Since the tests were of the nature of proof tests, the primary result of the program was to

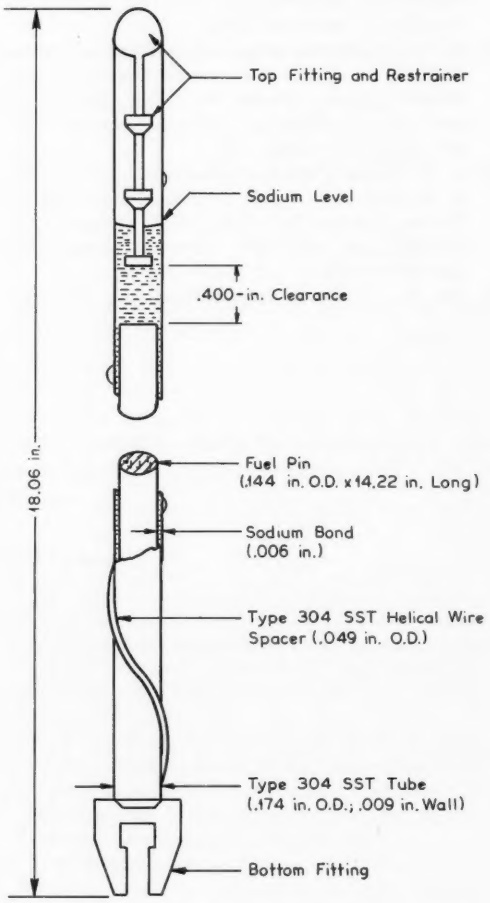

Fig. XIII-1 Reference design for EBR-II fuel element.[1]

Table XIII-1 DESIGNATION AND COMPOSITION OF FISSIUM ALLOYS[1]

Alloy designation	Composition, %						
	U	Zr	Mo	Ru	Rh	Pd	Nb
3% fissium	96.9	0.1	1.54	1.16	0.19	0.1	0.01
4% fissium	96	0.16	2	1.2	0.24	0.4	
5% fissium	95	0.2	2.5	1.5	0.3	0.5	
7.5% fissium	92.49	2.56	2.48	1.97	0.3	0.2	

establish the feasibility of the reference fuel-pin design. Although there were obvious effects of the irradiation, including some loss of density, surface roughening, and embrittlement to the point that it was very difficult to handle the irradiated fuel remotely without breakage, these effects were judged to be tolerable, and the tests were used as the basis for selecting the EBR-II fuel alloy:[1]

> ...an over-all evaluation of the data accumulated leads to the postulation that the 5 per cent fissium alloy will perform well up to 2 per cent burnup with a central metal temperature of approximately 1200°F. The major changes in the fuel will be a decrease in density, with considerable roughening of the fuel surface. Fission gas release is not expected to be troublesome. Accordingly, the 5 per cent cast fissium alloy was selected for the first core loading of EBR-II.

Postirradiation heating of samples irradiated at 794°F to 1.24 per cent burnup indicated that swelling might become severe at temperatures above about 1300°F.

The fuel alloys tested were those of interest for initial operation of EBR-II. Plutonium-bearing alloys would be required for operation on the equilibrium breeding cycle. The early irradiation tests of plutonium-bearing alloys are summarized in reference 14 and in the February 1958 issue of *Power Reactor Technology*, Vol. 1, No. 2.

In reference 15, the question of high-burnup fuels for fast reactors is considered from a more general point of view. It is claimed that the approach of using relatively high percentages of alloying materials, such as molybdenum or fissium, with the uranium-plutonium fuel has been, so far, only partially successful. It is stated that this approach has been successful only in achieving burnups in the lower end of the 1 to 5 per cent range, which is necessary for economic fast-breeder operation, and that in addition the approach appears to have the following disadvantages:

1. The achievement of high burnup appears to require that the center temperature be limited to about 600 to 650°C.
2. The alloying additions reduce thermal conductivity, thus accentuating the trend to small, expensive fuel elements.
3. The presence of the alloy degrades the nuclear performance of the reactor.
4. The presence of the alloying material increases aqueous reprocessing costs.

These shortcomings have resulted in increased interest in nonmetallic fuel elements. The reference[15] cites the use of oxide fuel in the Russian BR-5 reactor and in the French Rapsodie reactor and the plans for a cermet core of 25 vol.% UO_2 in stainless steel for the second loading of the Enrico Fermi reactor. The reference examines the basic problem of high-burnup fuel and concludes that promising possibilities remain for the metal fuel approach.

Previous theories of metallic fuel swelling at high burnup are examined, and it is concluded[15] that these are correct in the assumption that the important part of the swelling is due to the pressure of trapped fission gases, whereas a small fraction of the swelling may be attributed to the effects of solid fission-product atoms in the fuel lattice. It is pointed out that quantitatively the theories, which take the basic approach of equating the forces due to gas pressure in minute bubbles within the fuel to the tensile forces in the fuel, underestimate the swelling by a large factor. An alternate approach is recommended, based on an energy balance which equates the work done by the gas to the maximum work of deformation—to rupture—of the fuel: the basic assumption is that initially fuel deformation is by creep, under the influence of the gas-pressure stress, and that eventually a point of "runaway swelling" is reached, comparable to the occurrence of rupture in a tensile test.

The important gases are assumed to be the stable xenon and krypton isotopes, which are formed in the quantities indicated in Table XIII-2.* If it is assumed that the fuel sample contains a void volume v per unit volume of fuel and that the fission gas distributes itself uni-

* Tables XIII-2 and XIII-3 and Figure XIII-2 are reprinted here by permission from *Reactor Science and Technology, Journal of Nuclear Energy, Parts A & B.*

Table XIII-2 FISSION-PRODUCT GAS RELEASE IN U^{235} AND Pu^{239} FAST FISSION*[15]

	Gas release, (gas vol. at NTP)/(vol. of fuel completely fissioned)		
	Xe	Kr	(Xe + Kr)
U^{235}	391	53	444
Pu^{239}	428	16	444

*Deduced from: L. Burris, Jr., and I. G. Dillon, Estimation of Fission Product Spectra in Discharged Fuel from Fast Reactors, USAEC Report ANL-5742, Argonne National Laboratory, July 1957.

formly throughout the voids, the gas pressure in the voids, at temperature T°K and fractional burnup b is, for a perfect gas

$$p = 14.7 \frac{T}{273} \cdot \frac{444b}{v} = \frac{24Tb}{v} \quad \text{psi}$$

and the work done by the gas in deforming the fuel is

$$W_g = \int_{v_0}^{v} p\,dv \quad \text{in.-lb/cu in. of fuel}$$

where v_0 is the initial voidage and v is its value at burnup b. The irradiation data suggest[15] that, up to a critical burnup b_c where "runaway swelling" occurs, v is approximately proportional to b, and, hence

$$W_g = p(v - v_0)$$
$$\fallingdotseq pv = 24Tb, \text{ if } v \gg v_0$$

It is assumed that the stress in the fuel is everywhere limited to an appropriate creep stress, σ_c, and that whenever the fuel strain anywhere exceeds a limiting value, ϵ_r (similar to the strain at rupture in a tensile test), that part of the fuel is no longer capable of resisting further gas pressure by tension. Since the strain is greatest near a cavity, and least at the fuel surface, the internal regions of the fuel can be expected to reach the point of critical deformation before the surface, and it is reasonable to define the critical burnup of the fuel as a whole as that burnup at which the fuel surface reaches the point of critical deformation. If an additional approximation is made by assuming that the work-to-rupture of the internal fuel is the same as that for the surface fuel, then the critical burnup can be determined by simple relations in terms of the sample geometry and the creep properties of the surface layer.

At the point of critical burnup and critical swelling, when the surface layer of fuel ruptures, the work done by the gas is equated to the work of deformation:

$$pv_c = 24Tb_c = \sigma_c \epsilon_r \qquad (1)$$

In order to select the appropriate value for the creep stress, σ_c, it is necessary to specify the rate of strain, $\dot{\epsilon}$. The assumption of a linear variation of growth with burnup yields

$$\frac{\dot{\epsilon}}{\epsilon_r} = \frac{\dot{b}}{b_c} \qquad (2)$$

from which values of $\dot{\epsilon}$ consistent with ϵ_r, $\dot{b}$, and b_c can be determined. Finally, for a cylindrical fuel element with surface skin having the properties of a thin-walled tube,

$$v = 2\epsilon_1 + \epsilon_2 = 2.24\epsilon_1$$

where ϵ_1 is the surface hoop strain and ϵ_2 is the surface longitudinal strain. If the surface strain ϵ is identified with the hoop strain, then

$$v = 2.24\,\epsilon \qquad (3)$$

If the creep properties and the strain at rupture ϵ_r are known for the fuel, Eqs. 1, 2, and 3 can be solved iteratively for the critical burnup and the critical swelling. In the reference, the results of such calculations are given for unalloyed uranium and for uranium–10 wt.% molybdenum. The calculations utilized out-of-pile irradiation data and an assumed value of 2 per cent for the surface strain at rupture. The agreement with the results of fuel irradiation is better than the uncertainties of the analysis should warrant, and the author suggests that it is partly fortuitous.

The analysis can be extended, in a straightforward way, to the case of a fuel element with a jacket of significant strength. This is done in the reference,[15] and the resulting relations are used to estimate fuel-element lifetimes in the Dounreay and Enrico Fermi reactors.

The reference recommends the approach of utilizing a strong fuel-element jacket, or can, and of incorporating whatever additional materials are to be used for strengthening pur-

poses in the can wall rather than as alloying materials in the fuel. It estimates that this approach, along with the provision of void space within the can (into which the fuel can expand as it swells), can yield fuel elements of attractively high maximum burnup. Table XIII-3 shows the

Table XIII-3 EFFECT ON b_c AND P_c OF REDUCING CAN THICKNESS, THE VOLUME SAVED BEING USED FOR ADDITIONAL FUEL VOIDAGE*[15]

Fuel voidage Net fuel vol. (v), %	Can wall thickness (t), in.	Av. fuel temp. (T), °K	Max. burnup (b_c), %	Max. can internal press. (P_c), 1000 psi
10	0.0234	892	4.1	21
20	0.0200	883	7.1	18
30	0.0166	877	9.5	14.5
40	0.0136	875	11.3	12
50	0.0106	881	12.2	9.0
60	0.0076	896	11.8	6.3
70	0.0047	934	9.4	3.8

*Can outside diameter = 0.200 in.
Can surface heat flux = 2 kw/sq in.
Can outer surface temperature = 450°C.
Can creep stress = 80,000 lb/sq in.

results of calculations on fuel life for cylindrical elements that have the same outside diameter and the same uranium content but different initial void fractions and different can thicknesses: as the void content is increased, the can thickness is decreased to give the same uranium content for an element of constant outside diameter. The calculations indicate that the use of relatively large void fractions might be attractive. The reference points out that the void should be incorporated in some way to allow the fuel to grow freely without concentrating stresses on the can at local points and in such a way that good thermal contact is maintained between the can and the fuel. These conditions may not be easy to meet. In the calculation it was assumed that all the restriction against fuel growth was provided by the can; the fuel was assumed to swell as though it had no strength. The reference points out also that the incorporation of large void fractions in the fuel may pose a safety problem, since the fuel, if it were ever melted, could presumably densify and settle to the bottom of the fuel can, thus increasing the reactivity of the reactor. It therefore recommends some restraint in the use of void and estimates that 40 per cent void might be a reasonable compromise.

Figure XIII-2 shows the calculated behavior of two fuel elements, having different void fractions, as functions of burnup. In the 20 per cent void case, the pressure inside the fuel element rises continuously to a burnup of about 7.5 per cent while the fuel is swelling and expanding the can elastically. At higher burnups the can begins to yield, and the pressure remains constant. For the case of 40 per cent void, yielding does not occur until a burnup of about 15 per cent.

It is stated that preparations are being made to test the predictions of theory by irradiating, in the Dounreay Materials Testing Reactor, unalloyed uranium with 30 to 50 per cent void space. The irradiations will be made at 450°C can temperature and 700°C center temperature, at a specific power of 500 watts/g, or about 1 per cent burnup in 20 days.

The reference points out the possible undesirable effects of sodium leakage into fuel elements containing void spaces. These include possible blockage of the void space so that it is not available for expansion and possible rupture of the can by expansion or vaporization of the sodium. These possibilities suggest (1) that the best form of voidage would be that of distributed, noninterconnected porosity, (2) that in any case a large central void should be avoided, and (3) that operation at center temperatures above the boiling point of sodium (880°C) is undesirable. As an extreme possibility, the use of a double can with an intermediate sodium thermal bond is considered.

With regard to oxide fuels, the reference points out that the relatively high degree of fission-product retention, which is exhibited by the oxide in thermal-reactor applications, may not persist at the high irradiation levels desired in fast reactors. It suggests that it might even be best to attempt to attain 100 per cent fission-gas release and to provide space for the gas within the fuel element. The reference also points out that oxide fuels may present additional difficulties because of the high temperature at which the oxide operates—far above the sodium boiling point. Thus any sodium that leaked into the oxide element would probably boil and possibly rupture the can.

Finally, it is suggested that an attractive possibility for fast-reactor fuel may be a dispersion of UO_2-PuO_2 in unalloyed uranium, with

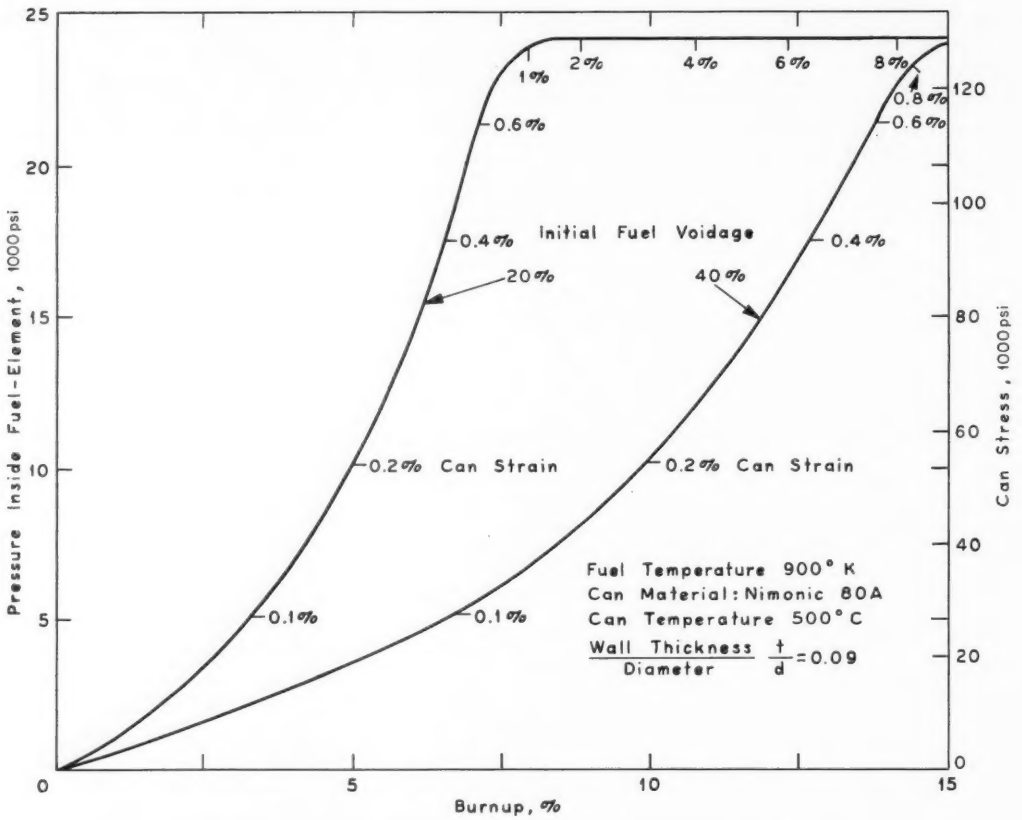

Fig. XIII-2 Variation of fuel pressure inside can with burnup.[15]

void space, contained in a strong can. It is suggested that this element may combine the good properties of both oxide and metal fuels.

In the field of fast-reactor physics, a study was recently completed which led to the formulation of a new set of group cross sections for the materials of most interest in fast-reactor design. The 16-group cross-section set was developed entirely from microscopic data. Reference 16 describes the bases on which the cross-section values were selected and tests the set against the existing integral experiments. Although the agreement is not perfect—the calculated critical masses, for example, being consistently low—the usefulness of a carefully documented set of group cross sections is obvious, both for promoting consistency in calculations and for guiding the further investigations, which may improve the agreement between microscopic and integral measurements.

In reference 17 the new cross-section set was used to calculate the neutron-physics characteristics of a set of idealized fast-breeder reactors. The general characteristics of the reactor set are similar to those investigated earlier and reported at the 1958 Geneva Conference.[18] Spherical reactors with core volumes of 800, 1500, and 2500 liters,* and with core and blanket compositions that are typical for fast-breeder reactors, were considered. A range of structural materials with metallic, oxide, and carbide fuels of various isotopic compositions was investigated. The fertile materials considered were U^{238} and thorium, used, respectively, with plutonium and U^{233} as the fissionable material. Plutonium of three dif-

* When it is considered that average power densities up to 1000 kw(t)/liter are contemplated for fast breeders, the 2500-liter case can be seen to represent a very large reactor.

Table XIII-4 REACTOR COMPOSITIONS[17]

Core volume: 800, 1500, or 2500 liters				
Core volume fractions:				
Fuel and fertile material 0.25				
Structural material 0.25				
Coolant 0.50				
Fuels	Fuel density, g/cm^3			
Pu-U^{238}	19			
PuO_2-UO_2	8.4			
PuC-UC	11.39			
U^{233}-Th	18.57 (for U^{233})			
	11.58 (for Th)			
$U^{233}O_2$-ThO_2	8.4			
U^{233}C-ThC	11.39			
Plutonium composition, at.%				
Type	Pu^{239}	Pu^{240}	Pu^{241}	Pu^{242}
A	100	0	0	0
B	74.7	10.2	12.4	2.7
C	40	10	25	25
Coolants, g/cm^3:				
Liquid sodium 0.84				
Liquid lead-bismuth eutectic (44.5 wt.% Pb–55.5 wt.% Bi) 10.46				
Structural materials:				
Stainless steel				
Titanium				
Vanadium				
Zirconium				
Niobium				
Molybdenum				
Tantalum				
Blanket thickness:				
45 cm (uranium)				
54 cm (thorium)				
Blanket volume fractions:				
U^{238} or Th 0.6				
Na or Pb-Bi 0.2				
Fe 0.2				
Reflector* thickness:				
30 cm				
Reflector volume fractions:				
Fe 0.6				
Na or Pb-Bi 0.4				

*The reflector surrounded the blanket.

ferent isotopic compositions was considered: type A, which consisted of pure Pu^{239}; type B, which consisted of an isotopic mixture typical of that discharged from a thermal-neutron reactor; and type C, which consisted of an isotopic mixture typical of plutonium that had been recycled several times in a thermal reactor. The reactor compositions investigated are summarized in Table XIII-4.†

†Table XIII-4 is reprinted here by permission from *Fast Reactor Cross Sections*.

Table XIII-5 summarizes the results of the calculations on reactors using steel as the structural material, Table XIII-6 summarizes the results of varying the structural material in the 800-liter plutonium-metal fueled reactor, and Table XIII-7 gives the results for the steel reactor using U^{233}–thorium in the metal, oxide, and carbide forms.

It is to be noted (Table XIII-5) that the "dirty" plutonium gives the higher breeding ratios, primarily because Pu^{240} is a better fertile material than U^{238} (because of its larger fission cross section) and because Pu^{241} has a lower average alpha than Pu^{239}. In computing the breeding ratios, only Pu^{239} and Pu^{241} were considered as fissionable materials; the presence of Pu^{240} and Pu^{242} is, of course, evidence of conversion losses that occurred during the previous exposure of the fuel.

The coolant-density coefficient of reactivity for the various reactor compositions was also investigated in the study. It was found that, in the larger reactor sizes, the loss of sodium causes an increase of reactivity. The dependence of this effect on the structural and fuel materials was investigated for the cases of steel and niobium. With the use of niobium as the structural material and plutonium metal as the fuel, the reactivity change upon loss of sodium was positive for core volumes greater than about 400 liters, whereas for steel structure the reactivity change was negative at a core volume of 800 liters and positive (for the plutonium-metal fueled reactors) at 1500 liters. With carbide and oxide fuels, respectively, the effect became positive in the steel core at about 2200 and 3400 liters, whereas it was positive for all 800-liter and larger cores with the niobium structure. The reference concludes that positive sodium coefficient difficulties can be anticipated for large central-station reactors having metal fuel elements jacketed in niobium, molybdenum, or other relatively strongly absorbing material and that titanium, vanadium, or zirconium is the best alternate for steel from the point of view of reactor physics. Negative reactivity changes were computed for the loss of sodium in all sizes of U^{233}–thorium systems using steel structure. Negative coolant coefficients were also calculated for plutonium–U^{238}–steel systems using lead-bismuth as coolant. The latter systems gave breeding ratios nearly the same as the

Table XIII-5 EFFECT OF ISOTOPIC COMPOSITION OF PLUTONIUM IN 800-, 1500-, AND 2500-LITER REACTORS FUELED WITH METAL, OXIDE, AND CARBIDE FUELS, AND HAVING SODIUM COOLANT AND STEEL STRUCTURE[17]

Reactor size, liters	Fuel	Pu "A"				Pu "B"					Pu "C"				
		M_c, kg				M_c, kg					M_c, kg				
		M_c, kg	IBR*	BR*	α	Total Pu	Pu^{239} + Pu^{241}	IBR	BR	$\bar{\alpha}$†	Total Pu	Pu^{239} + Pu^{241}	IBR	BR	$\bar{\alpha}$†
800	Metal	431	0.73	1.82	0.188	458	399	0.79	1.93	0.173	533	346	0.86	2.12	0.150
	Oxide	372	0.31	1.55	0.230	392	341	0.35	1.65	0.209	452	294	0.37	1.81	0.178
	Carbide	396	0.46	1.62	0.224	417	363	0.51	1.73	0.204	480	312	0.55	1.90	0.174
1500	Metal	686	0.91	1.79	0.198	729	635	0.97	1.90	0.182	849	552	1.05	2.08	0.156
	Oxide	562	0.44	1.47	0.251	590	514	0.48	1.57	0.228	680	442	0.51	1.72	0.192
	Carbide	613	0.61	1.56	0.241	645	562	0.66	1.67	0.218	743	483	0.71	1.82	0.185
2500	Metal	1025	1.04	1.76	0.205	1089	949	1.11	1.87	0.187	1269	825	1.21	2.05	0.161
	Oxide	806	0.54	1.42	0.267	845	736	0.59	1.52	0.240	973	632	0.64	1.65	0.203
	Carbide	897	0.73	1.52	0.253	943	821	0.79	1.62	0.229	1086	706	0.85	1.77	0.192

*As defined herein, the breeding ratio is the ratio of the rate at which Pu^{239} and Pu^{241} are being formed to the rate at which they are being destroyed. BR = breeding ratio = [U^{238} and Pu^{240} captures in reactor/(Pu^{239} and Pu^{241}) captures + fissions in reactor]. IBR = internal breeding ratio = (production of thermally fissionable isotopes in core/destruction of thermally fissionable isotopes in entire reactor).

†$\bar{\alpha}$ = (Pu^{239} and Pu^{241} captures/Pu^{239} and Pu^{241} fissions).

Table XIII-6 EFFECT OF VARIOUS STRUCTURAL MATERIALS ON 800-LITER PLUTONIUM-METAL FUELED REACTORS[17]
(Plutonium "A")

Structural material	Critical mass, kg	Breeding ratio	α
Fe (stainless steel)	431	1.82	0.188
Ti	425	1.92	0.180
V	456	1.68	0.222
Zr	415	1.89	0.181
Nb	494	1.51	0.169
Mo	502	1.46	0.185
T	716	1.02	0.170

Table XIII-7 PERFORMANCE OF LARGE REACTORS FUELED WITH U^{233}-THORIUM MIXTURE AS METAL, OXIDE, OR CARBIDE FUEL, HAVING SODIUM COOLANT AND STEEL STRUCTURE[17]

Reactor size, liters	Fuel	Critical mass, kg	Internal breeding ratio	Breeding ratio	α
800	Metal	453	0.38	1.29	0.085
	Oxide	371	0.27	1.23	0.099
	Carbide	410	0.38	1.26	0.096
1500	Metal	679	0.50	1.28	0.089
	Oxide	539	0.39	1.21	0.106
	Carbide	616	0.52	1.24	0.102
2500	Metal	968	0.61	1.28	0.092
	Oxide	755	0.49	1.19	0.112
	Carbide	890	0.62	1.23	0.106

corresponding systems, with sodium as coolant, and gave slightly lower critical masses.

Reference 19 reports studies parallel to those of references 16 and 17. It describes a 16-group formulation which differs from the formulation of reference 16 in that the high-energy range is treated in somewhat less detail and the low-energy range is treated in more detail. This difference, no doubt, stems from differences in the intended applications of the formulations. The reference gives a set of 16-group cross sections for U^{235}, U^{233}, U^{238}, Pu^{239}, Th^{232}, iron, and Na^{23}. The cross sections have been adjusted, within the limits of uncertainty of the microscopic data, to improve agreement between theoretical and measured critical masses, and the results are illustrated by an extensive set of experimental-theoretical comparisons in the reference.

Reference 19 also presents the results of a theoretical survey of idealized spherical fast breeders, covering a wide range of compositions made up of the materials mentioned above. The curves showing critical mass and breeding ratio as functions of the ratio of fertile-to-fissile material are particularly instructive. The curves for the Pu^{239}-U^{238} combination have been reproduced in Figs. XIII-3 and XIII-4. Figure XIII-4 shows that there is a substantial leakage of neutrons through the "standard" blanket, which was 50 cm thick, composed of

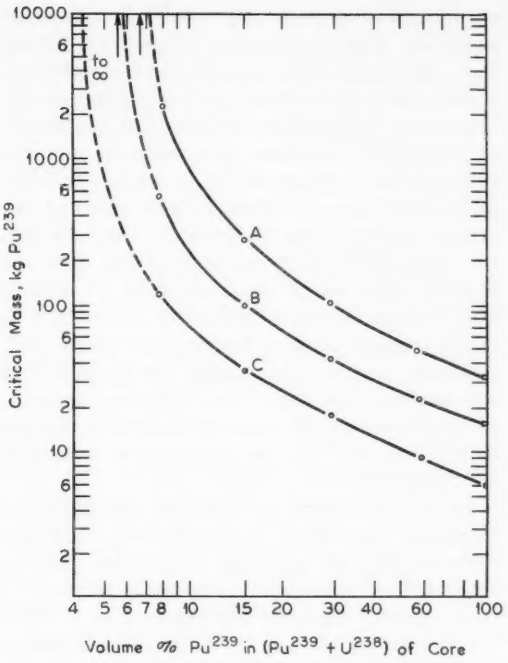

Fig. XIII-3 Computed critical masses of spherical Pu^{239}-U^{238}-Na-S.S. systems, 50-cm-thick blanket.[19] A, 50 vol.% Na, 25 vol.% S.S. in core. B, 33⅓ vol.% Na, 16⅔ vol.% S.S. in core. C, no Na, S.S. in core.

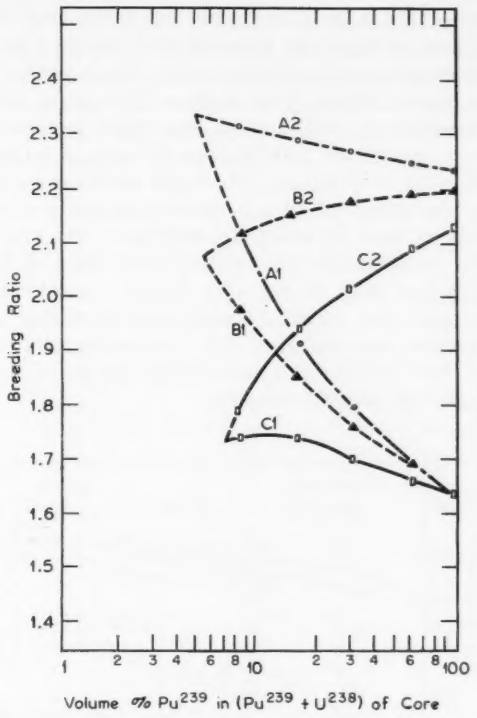

Fig. XIII-4 Computed initial breeding ratios for Pu^{239}-U^{238} systems.[19] A1, Pu^{239}-U^{238} core, standard blanket. A2, core of A1, infinite blanket. B1, 50 vol.% (Pu^{239}-U^{238}), 33⅓ vol.% Na, 16⅔ vol.% Fe core, standard blanket. B2, core of B1, infinite blanket. C1, 25 vol.% (Pu^{239}-U^{238}), 50 vol.% Na, 25 vol.% Fe core, standard blanket. C2, core of C1, infinite blanket.

40 vol.% U^{238}, 40 vol.% sodium, and 20 vol.% stainless steel. As the reactor size increases and the core leakage decreases (decreasing percentage of plutonium in the core), the breeding ratios for the reactors with standard blankets increase (curves A1, B1, and C1). For the reactors with infinite blankets, there is no loss of breeding due to leakage. For these cases, the reactors containing steel and sodium show decreasing breeding ratios as the Pu^{239}-to-U^{238} ratio is decreased (curves C2 and B2). This decrease is due to the greater fractional parasitic absorption as the neutron-energy spectrum is "softened" by the greater dilution. Owing to the increase in the U^{238} fast-fission effect, the breeding ratio in the pure Pu^{239}-U^{238} core increases slightly as the Pu^{239}-to-U^{238} ratio is decreased (curve A2).

Reference 20 reports a parametric study of an oxide-fueled fast breeder. The thermal output of the reactor was held constant at 812 Mw [300 Mw(e)] for the study, and the major variables considered were fuel-rod diameter, oxide density, and fuel-jacket thickness. The cladding and structural materials were both stainless steel. The fuel considered was a mixture of PuO_2 and $(U^{238})O_2$, whereas the fertile material in the blanket was pure $(U^{238})O_2$. The assumed composition of the feed plutonium was 60 per cent Pu^{239}, 25 per cent Pu^{240}, 12 per cent Pu^{241}, and 3 per cent Pu^{242}, characteristic of the output of a high-burnup thermal reactor. Most of the work was done on a right cylindrical core of $L/D = 1$, completely surrounded by an 18-in.-thick oxide blanket; however, some calculations were done for an annular core which did not appear to have pronounced advantages.

The size and the macroscopic composition of the core were determined by setting certain generalized thermal conditions in addition to the power capability. A peak-to-average power-density ratio of 2.5 was assumed; the thermal conductivity of the oxide was taken as 1.0 Btu/

(hr)(ft)(°F); and the temperature difference between the center and the surface of the fuel, at the position of peak power, was set at 3500°F. These assumptions fixed the total length of fuel element required in the core for any given fuel-element design. The sodium flow area was specified by fixing inlet and outlet temperatures of 750 and 1000°F, respectively, at a flow velocity of 23 ft/sec. Additional stainless steel, to the extent of 10 per cent of the fuel jacket, was allowed as additional structure. The blanket composition (volumetric) was fixed at 50 per cent UO_2, 20 per cent stainless steel, and 30 per cent sodium. Small-batch reloading of the core was assumed, with a reloading interval of four months and an average discharge exposure of 100,000 Mwd/ton.

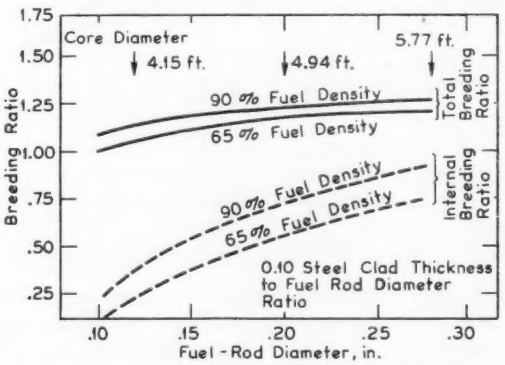

Fig. XIII-5 Variation of breeding ratio with fuel-rod diameter and fuel density: oxide-fueled fast-breeder study.[20]

Figure XIII-5 shows the effect of fuel-rod diameter on breeding ratio, for two different assumed oxide densities, and a jacket thickness equal to 10 per cent of the total fuel-rod diameter. As the size of the fuel rod is increased, the size of the core must be increased to satisfy the thermal conditions. The main effect is to decrease markedly the neutron leakage from the core and to decrease slightly the total loss of neutrons by leakage. The result is a substantial increase in internal breeding ratio and a smaller increase in total breeding ratio, as the fuel-rod diameter is increased. It should, of course, be borne in mind that the major effect is one of core size, which results from the arbitrary choice of total power rating. The important effect of the increase in internal breeding ratio is to reduce the loss of reactivity between reloading periods. The reference states that, for a 125-mil fuel-rod diameter, an excess operating reactivity of 7.5 dollars is required. This requirement drops to 2.5 dollars for a diameter of 200 mils and to 0.7 dollar for a diameter of 280 mils. As the reactor size is increased, the sodium temperature coefficient of reactivity becomes less negative and the reactor size corresponding to the upper limit of the fuel-element diameters considered becomes positive. The reference[20] suggests that an intermediate fuel-rod size of 200 mils, or slightly less, which requires about 2.5 dollars of operating excess reactivity and yields a small negative sodium temperature coefficient, would be a good compromise for a reactor of 300-Mw(e) capability. The breeding ratio is here defined as the ratio of nonfission capture in U^{238} and Pu^{240} to the fission plus capture in Pu^{239} plus Pu^{241}.

As the core size is increased, the plutonium inventory increases. This variation, along with the variation in breeding ratio (Fig. XIII-5), results in a minimum in the curve of doubling time versus fuel-rod diameter. For a plant load factor of 0.7 and for an out-of-pile inventory equal to two fuel batches, a minimum doubling time of 17 years is attained with the 90 per cent fuel density at a fuel-rod diameter of about 0.175 in. The minimum doubling time with the 65 per cent dense fuel is about 21.8 years and is achieved with a fuel-rod diameter of about 0.21 in.

The effect of varying the thickness of the fuel jacket on total breeding ratio is shown in Fig. XIII-6. If the "metallurgical" lifetime of the fuel element were known as a function of jacket thickness, curves of the type shown in Fig. XIII-6 could be used to determine an economic optimum for the jacket thickness.

A parametric study that considers various fuel-element types is reported in reference 21. Two approximate reactor sizes are considered: a size compatible with an electrical output in the 100- to 150-Mw(e) range and a size compatible with an electrical output in the 300-Mw(e) range. The Enrico Fermi plant design was used as the basis for the smaller reactor, whereas the Plutonium-Fueled Fast-Breeder Reactor (PFFBR) design* was used as the basis

* Atomic Power Development Associates, Inc. (Unpublished)

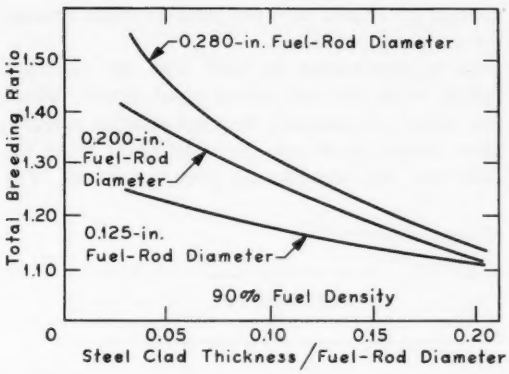

Fig. XIII-6 Effect of thickness of stainless-steel fuel cladding on breeding ratio: oxide-fueled fast-breeder study.[20]

for the larger reactor. The maximum core volume for the smaller reactor was 800 liters, whereas that for the larger reactor was 3000 liters. The radial blanket thickness was 18 in. for both reactors. Capital costs were determined for the basic Enrico Fermi and PFFBR designs, and these were adjusted to take into account the individual requirements and changes in performance characteristic of the different fuel elements considered. The major characteristics of the designs for the two different power ranges are listed in Table XIII-8.

Table XIII-8 CHARACTERISTICS OF BASIC FAST-REACTOR DESIGNS USED FOR PARAMETER STUDY[21]

	Enrico Fermi	PFFBR
Heat power output, Mw	300–400	600–800
Inlet coolant temp., °F	550–600	550–650
Outlet coolant temp., °F	800–900	1000 max.
Coolant flow rate, lb/hr	15.3×10^6 max.	25.3×10^6 max.
Core pressure drop, psi	75 max.	100 max.
Total fuel subassemblies	130 max.	200 max.
Core length, in.	24–48	30–60
Subassembly size, in.	2.7 (square)	4 (hexagon or equivalent square)
Core volume (including control), liters	800 max.	3000 max.

The major emphasis of the study was on the fuel cycle. The choice of fuel elements for consideration was influenced by two assumptions: (1) that the next few large fast reactors in the United States will be based on extensions of the technology developed by the EBR-I, the EBR-II, and the Enrico Fermi projects, and (2) that they will utilize the AEC facilities for chemical reprocessing of blanket and fuel materials. That is to say, the study was restricted to solid, shippable, fuel materials amenable to aqueous reprocessing. The parameter study included the fuel-element types listed in Table XIII-9; in addition, a partial study was made on PuO_2–stainless steel plates, PuO_2-thorium plates, and UO_2-thorium plates. The possible advantages of heterogeneous oxide pins were also investigated. These pins would incorporate the initial fissionable oxide—$(U^{235})O_2$ or PuO_2—at the periphery of the cylindrical oxide pin and would confine the fertile $(U^{238})O_2$ to the inner region of the pin. This segregation of fissionable and fertile material would reduce the central fuel temperature by a substantial amount in the new pin. It was found that, however, at the high exposure levels used, the generation of plutonium in the U^{238} eliminated much of the

Table XIII-9 FABRICATION COSTS USED IN PARAMETER STUDY[21]

	Diameter, in.	$/element	No. of elements used per year
U–10 wt.% Mo alloy pins:			
Enrico Fermi	0.216	72.7	10,500
	0.197	70.1	
	0.181	68.1	
PFFBR-2000	0.292	81.0	18,900
	0.243	74.0	
	0.212	70.1	
	0.190	67.8	
	0.172	66.0	
PFFBR-3000	0.369	95.5	18,900
	0.309	84.0	
	0.266	77.0	
	0.232	72.5	
	0.207	69.7	
U–10 wt.% Mo alloy plates	*	267.0	1,440
UO_2–stainless steel plates	*	131.0	750
	†	148.0	515
PuC–U–15 wt.% Mo plates	†	512.0	725
PuO_2-UO_2 powder pins	†	33.5	18,650

*Enrico Fermi plant design.
†PFFBR design.

benefit of the arrangement as fuel exposure increased, and it was concluded that the scheme was not economically attractive in the fast reactor.

The estimated costs and breeding ratios are given in Table XIII-10 for the larger-sized plants using the various types of fuel element.

Table XIII-10 RESULTS OF OPTIMIZATION STUDIES, LARGE PLANT (PFFBR TYPE)[21]

	U–10 wt.% Mo pins	UO_2–S.S. plates	PuC–U–15 wt.% Mo plates	PuO_2–UO_2 pins
Fixed charges on plant	5.58	5.45	5.53	5.41
Initial core fabrication	0.58	0.09	0.30	0.21
Initial blanket fabrication	0.15	0.10	0.10	0.11
Total fixed charges	6.31	5.64	5.93	5.73
Operation and maintenance	0.57	0.54	0.56	0.53
Fuel-cycle costs	3.40	3.76	3.36	2.84
UF_6 fabrication	2.03	0.84	0.63	0.35
Scrap recovery	0.003	0.14	0.20	0.02
Reprocessing	0.88	0.57	0.49	0.42
Burnup and losses	2.01	2.93		
Inventory, 4%	1.24	0.71		
Inventory, 12%			2.25	1.86
Radial blanket fabrication	0.06	0.18	0.10	0.15
Axial blanket fabrication	0.01	0.02	0.005	0.004
Blanket reprocessing	0.36	0.42	0.37	0.38
Plutonium revenue	−3.19	−2.05	−0.69	−0.34
Total power production cost	10.28	9.94	9.85	9.10

As will be noted, the core volume varies from reactor to reactor. In each case the volume selected was that which gave the lowest total power cost in the analysis, but optimization with respect to core volume was not precise; in most cases, only volumes of 2000 and 3000 liters were considered.

The table does not tell the complete story on either absolute power cost or relative power cost—for this purpose it is necessary to carefully examine the ground rules and assumptions in the original report—but it does indicate the interesting points of difference from one core type to another. It is to be noted that the ground rules for the feed fuel are different for U^{235} and plutonium. In the U^{235} case, the normal AEC burnup charges are applied, and a use charge of 4 per cent per year is charged against the core fuel inventory. All plutonium produced is sold to the AEC. In the plutonium-fueled cases, the fuel cycle is considered to be a closed one, bred plutonium being extracted from the blanket and added to the core as necessary and the excess plutonium from the blanket being sold to the AEC. In this case an inventory charge of 12 per cent per year is made against the core plutonium.

It is interesting to note that the reactors fueled with UO_2–stainless steel plates, which fall short of breeding by a substantial margin, give power costs not much different from the reactors with substantial breeding gains. The lower estimates of fixed charges and fuel fabrication for the UO_2–stainless steel plate system compensate approximately for the cost disadvantage of about 2 mills/kw-hr that may be attributed to the poor breeding performance.

It is also interesting that the differences in estimated costs between uranium and plutonium

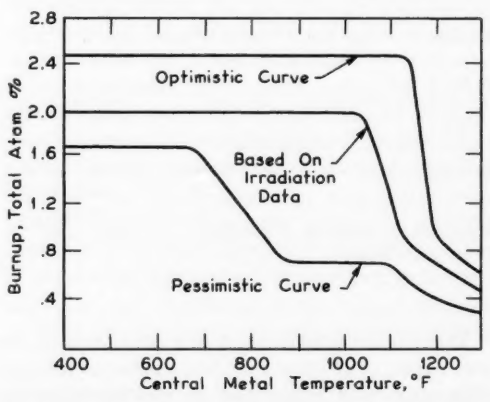

Fig. XIII-7 Burnup limitations of U–10 wt.% Mo as a function of temperature.[21]

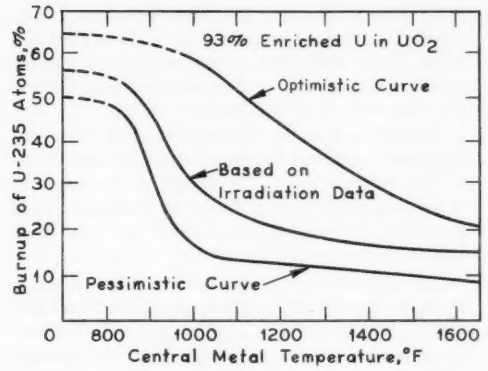

Fig. XIII-8 Burnup limitation of 30 wt.% UO_2 or PuO_2 dispersed in stainless steel.[21]

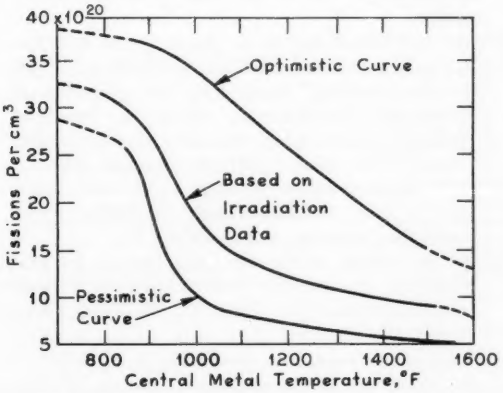

Fig. XIII-9 Burnup limitations[21] of UO_2 in stainless steel for loading up to 30 wt.% UO_2.

elements are not tremendous. The tabulated fabrication costs are based on estimates from two fuel-element manufacturers, made on the assumptions that the fuel element has been fully developed and that process development costs are not included in the fabrication cost. A more direct comparison of uranium and plutonium fabrication costs is given in the report for the case of oxide–stainless steel cermet elements. The cost per plate is estimated at $225 for the PuO_2 case versus $148 for the UO_2 case; however, by the time the plates have been assembled into 16-plate assemblies, the cost comparison per assembly is $8700 versus $6470.

The study takes a new approach to the optimization of fuel-element design in that it attempts to factor in the relation between

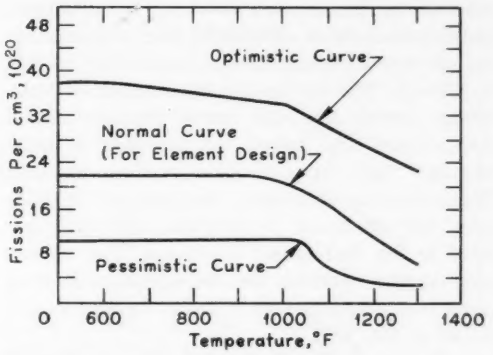

Fig. XIII-10 Burnup limitations[21] for UC-(U–15 wt.% Mo) and PuC-(U–15 wt.% Mo).

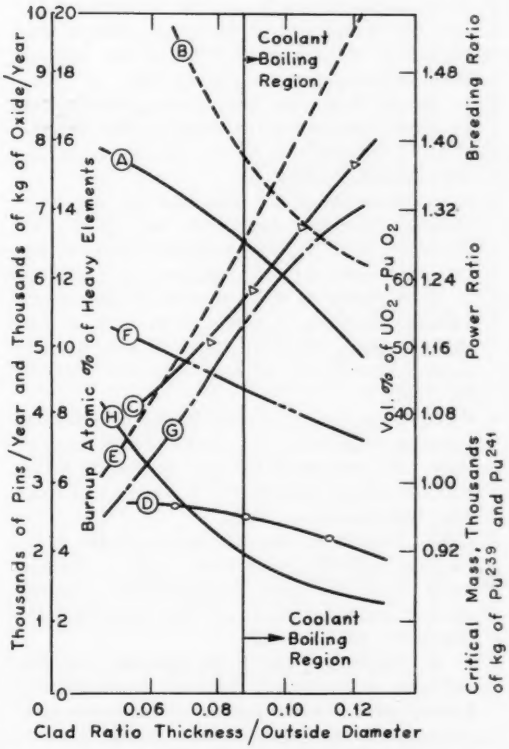
Coolant Boiling Region
Coolant Boiling Region
Thousands of Pins/Year and Thousands of kg of Oxide/Year
Burnup Atomic % of Heavy Elements
Vol. % of UO_2 - $Pu O_2$
Breeding Ratio
Power Ratio
Critical Mass, Thousands of kg of Pu^{239} and Pu^{241}
Clad Ratio Thickness/Outside Diameter

Fig. XIII-11 UO_2-PuO_2 pin performances in 2760-liter core.[21] A, breeding ratio. B, fuel pins per year. C, fresh power per equilibrium power. D, critical mass. E, throughput burnup. F, vol.% oxide. G, equilibrium burnup. H, weight of oxide per year.

central fuel temperature and maximum attainable burnup. The curves used for this purpose, along with curves showing the optimistic and

pessimistic limits, are given for the uranium-molybdenum, oxide–stainless steel dispersions, and carbide-uranium dispersions in Figs. XIII-7 to XIII-10. The curves for the uranium-molybdenum metal and the oxide–stainless steel dispersions are based on irradiation data, whereas the curve for the carbide-uranium dispersions is estimated. For the case of oxide pins, the maximum permissible burnup is related to the fuel-jacket thickness. The curves showing this relation, and the variation of other important quantities with jacket thickness, are shown in Fig. XIII-11.

References

1. J. H. Monaweck and E. S. Sowa, A Summary Report on Irradiation of Prototype EBR-II Fuel Elements, USAEC Report ANL-6010, Argonne National Laboratory, September 1960.
2. L. Burris et al., The Melt Refining of Irradiated Uranium: Application to EBR-II Fast Reactor Fuel. I. Introduction, *Nuclear Sci. and Eng.*, 6(6): 493 (December 1959).
3. G. J. Bernstein et al., The Melt Refining of Irradiated Uranium: Application to EBR-II Fast Reactor Fuel. II. Experimental Furnaces, *Nuclear Sci. and Eng.*, 6(6): 496 (December 1959).
4. D. C. Hampson et al., The Melt Refining of Irradiated Uranium: Application to EBR-II Fast Reactor Fuel. III. Preparation of Experimental Alloys, *Nuclear Sci. and Eng.*, 6(6): 501 (December 1959).
5. C. L. Rosen et al., The Melt Refining of Irradiated Uranium: Application to EBR-II Fast Reactor Fuel. IV. Interaction of Uranium and Its Alloys with Refractory Oxides, *Nuclear Sci. and Eng.*, 6(6): 504 (December 1959).
6. G. A. Bennett et al., The Melt Refining of Irradiated Uranium: Application to EBR-II Fast Reactor Fuel. V. Yield of Fissionable Material upon Pouring, *Nuclear Sci. and Eng.*, 6(6): 511 (December 1959).
7. V. G. Trice, Jr., and N. R. Chellew, The Melt Refining of Irradiated Uranium: Application to EBR-II Fast Reactor Fuel. VI. The Behavior of Plutonium in the Melt-Refining Process, *Nuclear Sci. and Eng.*, 9(1): 55 (January 1961).
8. A. Schneider and N. R. Chellew, The Melt Refining of Irradiated Uranium: Application to EBR-II Fast Reactor Fuel. VII. The Evolution of Xenon and Krypton, *Nuclear Sci. and Eng.*, 9(1): 59 (January 1961).
9. N. R. Chellew et al., The Melt Refining of Irradiated Uranium: Application to EBR-II Fast Reactor Fuel. VIII. The Behavior of Rare Earths, Yttrium, Barium, Strontium, and Cesium, *Nuclear Sci. and Eng.*, 9(1): 64 (January 1961).
10. J. Wolkoff and A. A. Chilenskas, The Melt Refining of Irradiated Uranium: Application to EBR-II Fast Reactor Fuel. IX. Sorption and Retention of Sodium and Cesium Vapor on Stationary Beds at Elevated Temperature, *Nuclear Sci. and Eng.*, 9(1): 71 (January 1961).
11. N. R. Chellew and V. G. Trice, The Melt Refining of Irradiated Uranium: Application to EBR-II Fast Reactor Fuel. X. The Behavior of Zirconium, *Nuclear Sci. and Eng.*, 9(1): 78 (January 1961).
12. N. R. Chellew and M. Ader, The Melt Refining of Irradiated Uranium: Application to EBR-II Fast Reactor Fuel. XI. Behavior of Iodine in Melt Refining, *Nuclear Sci. and Eng.*, 9(1): 82 (January 1961).
13. N. R. Chellew and G. A. Bennett, The Melt Refining of Irradiated Uranium: Application to EBR-II Fast Reactor Fuel. XII. The Behavior of Ruthenium, Molybdenum, Palladium, Rhodium, Technetium, Antimony, Cadmium, and Tellurium, *Nuclear Sci. and Eng.*, 9(1): 87 (January 1961).
14. J. R. Dietrich and W. H. Zinn, *Solid Fuel Reactors*, p. 118, Addison-Wesley Publishing Company, Inc., Reading, Mass., 1958.
15. L. R. Blake, Achieving High Burnup in Fast Reactors, *Reactor Sci. and Technol., J. Nuclear Energy, Parts A & B*, 14(1): 31–48 (April 1961).
16. S. Yiftah et al., *Fast Reactor Cross Sections*, Pergamon Press, Inc., New York, N. Y., 1960.
17. S. Yiftah and D. Okrent, Some Physics Calculations on the Performance of Large Fast Breeder Power Reactors, USAEC Report ANL-6212, Argonne National Laboratory, December 1960.
18. W. B. Loewenstein and D. Okrent, The Physics of Fast Power Reactors; A Status Report, *Proceedings of the Second United Nations International Conference on the Peaceful Uses of Atomic Energy, Geneva, 1958*, Vol. 12, pp. 16–37, United Nations, New York, 1958.
19. W. H. Roach, Computational Survey of Idealized Fast Breeder Reactors, *Nuclear Sci. and Eng.*, 8(6): 621 (December 1960).
20. P. Greebler et al., Fast Oxide Breeder—Reactor Physics. Part 1. Parametric Study of 300(e) MW Reactor Core, USAEC Report GEAP-3287, General Electric Co., Atomic Power Equipment Dept., Nov. 15, 1959.
21. Fast Reactor Core Design Parameter Study, USAEC Report APDA-133, Atomic Power Development Associates, Inc., March 1960.

Index

VOLUME 4

Included in this issue is the index for Volume 4 of *Power Reactor Technology*. Future indexes for this quarterly will be prepared annually and will appear in the final (Number 4) issue. Here the bold numbers denote issues, and the other numbers denote pages.

A

A-nickel alloy, corrosion by carbon monoxide, carbon monoxide–carbon dioxide systems, and carbon monoxide–hydrogen systems, **3**: 43–4
A1W Reactor
  See Reactor (A1W)
Accidents, Los Alamos Scientific Laboratory criticality accident, August 1945, **2**: 29
  Oak Ridge National Laboratory criticality accident, May 1954, **2**: 29
  Y-12 Plant criticality accident, June 1958, **2**: 29
Acetone, reactions with uranium carbides, **1**: 47
Acids, reactions with uranium carbides, **1**: 47
Advanced Gas-Cooled Reactor
  See Reactor (Advanced Gas-Cooled)
Advanced Organic-Moderated Reactor
  See Reactor (Advanced Organic-Moderated)
Advanced Sodium Graphite Reactor
  See Reactor (Advanced Sodium Graphite)
AGN-201M Reactor
  See Reactors (AGN-201)
AGR Reactor (UK)
  See Reactor (Advanced Gas-Cooled) (UK)
Air, reactions with uranium carbides, **1**: 46–7
Alco Products Critical Facility
  See Reactor (Alco Products Critical Facility)
Alkalies, reactions with uranium carbides, **1**: 47
Allis-Chalmers Manufacturing Company, nuclear superheater research, **3**: 82
Alpha radiation
  See Radiation (alpha)
ALPR
  See Reactor (SL-1)
Aluminum, compatibility with steel, **1**: 1–2
  corrosion by carbonic acid, **3**: 45
  corrosion by water, **1**: 2; **3**: 46
  criticality effects of tubes, **2**: 11
  reactions with uranium carbides, **1**: 45
Aluminum alloys, corrosion by water, **1**: 2
Aluminum–lithium-6 alloys, reactivity worth, **4**: 40
Aluminum-molybdenum-uranium alloys
  See Uranium-molybdenum-aluminum alloys
Aluminum-plutonium alloys
  See Plutonium-aluminum alloys
Aluminum-uranium alloys
  See Uranium-aluminum alloys
Ammonia, hydrazine synthesis from, **3**: 1–2
  reactions with uranium carbides, **1**: 47
Ammonium citrate process, corrosion of reactor materials, **3**: 45
Analytical methods, reactor kinetics, **2**: 28–30
Annuli, burnout, **3**: 21–4
  cooling with solid-gas systems, **3**: 16–17
  forced-convection heat transfer, **2**: 13–15
Antimony, shielding applications, **2**: 34
APDA fast-breeder reactor
  See Reactor (Enrico Fermi Fast-Breeder)
Approach-to-critical experiments, NRU Reactor, **2**: 11
APS-1 Reactor (USSR)
  See Reactor (APS-1)(USSR)
Argonne Low-Power Reactor
  See Reactor (SL-1)
Argonne National Laboratory, nuclear superheater research, **3**: 82–3
ASME *Boiler and Pressure Vessel Code*
  See Boiler codes
ASTM boiler codes
  See Boiler codes
Atomic power
  See Nuclear power
Atomic power plants
  See Power plants (nuclear)
Atomics International, Division of North American Aviation, Inc., nuclear superheater research, **3**: 83
AVR Reactor (West Germany)
  See Reactor (AVR)(West Germany)

B

Benzene, reactions with uranium carbides, **1**: 47
Berkeley Reactors (UK)
  See Reactors (Berkeley)(UK)
Beryllium, neutron reflection, **3**: 10
  radiation effects, **1**: 65
  reactions with uranium carbides, **1**: 46
Beryllium-moderated reactors
  See Reactors (beryllium-moderated)
Beryllium oxide–uranium dioxide systems
  See Uranium dioxide–beryllium oxide systems
Beryllium-uranium alloys
  See Uranium-beryllium alloys
Bismuth, reactions with uranium carbides, **1**: 46
BN-50 Reactor (USSR)
  See Reactor (BN-50)(USSR)
Bohunice Reactor (Czechoslovakia)
  See Reactor (Bohunice)(Czechoslovakia)
Boiler codes, ASME specifications for boilers and pressure vessels, **2**: 44–8
  ASTM specifications for reactor pressure vessels, **4**: 50–1
  British specifications for reactor pressure vessels, **4**: 51–4
Boiling, bubble formation, **2**: 26
  burnout, **3**: 21–4; **4**: 25–8
  heat transfer, **2**: 15–18; **3**: 24–6
  transient experiments, **2**: 26–7
Boiling (bulk), heat transfer with terphenyl, **4**: 82
Boiling (nucleate), departure from, **3**: 24–5
  heat transfer, **1**: 27–9
  heat transfer with terphenyl, **4**: 82
  hydrodynamic factors, **3**: 25
  in spray cooling, **4**: 22
Boiling songs, in rectangular channels, **1**: 29
Boiling-water reactors
  See Reactors (boiling-water)
BONUS Reactor
  See Reactor (BONUS)
Boral, shielding properties, **2**: 36
BORAX Reactors
  See Reactors (BORAX)
Borides
  See also specific borides
  corrosion, **4**: 42–3, 44
  radiation effects, **4**: 42–3, 44
Boron, corrosion by steam, **4**: 44
  radiation effects, **4**: 44
  reactivity-worth burnup, **4**: 41
  solubility in boiling water, **4**: 43
Boron carbide, corrosion by steam, **4**: 44
  radiation effects, **4**: 44
  reactivity worth, **4**: 40, 41
  solubility in boiling water, **4**: 43
Boron glass, reactivity worth, **4**: 40
Boron nitride, corrosion by steam, **4**: 44
  solubility in boiling water, **4**: 43
Boron–stainless steel systems, failure in control rods, **4**: 43, 45–6
  poisoning properties, **2**: 10
Boron steel
  See Steel (boron)

Boundary layer, heat-transfer effects, **2**: 16–17
BR-3 Reactor
See Reactor (BR-3)(Belgium)
BR-5 Reactor (USSR)
See Reactor (BR-5)(USSR)
Bradwell Reactors (UK)
See Reactors (Bradwell)(UK)
Breeding, **1**: 5–9
factors in uranium-238–plutonium-239 systems, **4**: 91–4
nuclear superheaters, **3**: 83
uranium carbides, ratios, **1**: 51–2
uranium-molybdenum alloys, **1**: 51–2
Bromine, reactions with uranium carbides, **1**: 47
Bubbles, formation, **3**: 24
formation by nucleation, **2**: 26
Bulk Shielding Reactors
See Reactors (Bulk Shielding)
Burners, for high-boiling fractions from Piqua Power Reactor, **2**: 83–4
Burnout, **3**: 17–24; **4**: 25–8
BORAX-I Reactor, **1**: 38
effect of flow and pressure drop, **2**: 18
free convection conditions, **2**: 17–18
SPERT-I Reactor, **1**: 38
TREAT Reactor, **1**: 40–1
Butterfly valves
See Valves (butterfly)
Byeloyarsk Reactor (USSR)
See Reactor (Byeloyarsk)(USSR)

C

Cables (coaxial)
See Coaxial cables
Cadmium, flux hardening effects, **1**: 11–12
reactivity-worth burnup, **4**: 41–2
Cadmium-covered gold foils
See Foils (gold)
Cadmium-indium-silver alloys, control-rod applications, **3**: 48–50
reactivity-worth burnup, **4**: 42
Cadmium–silver alloys, reactivity worth, **4**: 40
Calandria, sodium graphite reactors, **3**: 88, 89–91
Calcium hexaboride, corrosion by steam, **4**: 44
radiation effects, **4**: 44
solubility in boiling water, **4**: 43
Calder Hall Reactors (UK)
See Reactors (Calder Hall)(UK)
Canada, coal reserves, **2**: 1–2
CANDU Reactor (Canada)
See Reactor (CANDU)(Canada)
Canned moderators
See Moderators (canned)
Carbon dioxide, corrosion of iron alloys, **3**: 43
corrosion of nickel alloys, **3**: 43
reactions with uranium carbides, **1**: 47
Carbon dioxide–carbon monoxide systems, corrosion of A-nickel, chromium-molybdenum steel, copper, Inconel, Inconel 702, Inconel X, molybdenum, Monel, niobium, niobium-titanium alloys, niobium-zirconium alloys, and stainless steel, **3**: 43–4
Carbon monoxide, corrosion of A-nickel, chromium-molybdenum steel, copper, Inconel, Inconel 702, Inconel X, molybdenum, Monel, niobium, niobium-titanium alloys, niobium-zirconium alloys, and stainless steel, **3**: 43–4
corrosion of iron alloys, **3**: 43
corrosion of nickel alloys, **3**: 43
Carbon monoxide–carbon dioxide systems
See Carbon dioxide–carbon monoxide systems
Carbon monoxide–hydrogen systems, corrosion of A-nickel, chromium-molybdenum steel, copper, Inconel, Inconel 702, Inconel X, molybdenum, Monel, niobium, niobium-titanium alloys, niobium-zirconium alloys, and stainless steel, **3**: 43–4
Carbon steel
See Steel (carbon)
Carbon tetrachloride, reactions with uranium carbides, **1**: 47
Carbon-uranium systems
See Uranium-graphite systems
Carbonic acid, corrosion of aluminum, **3**: 46
Carolinas-Virginia Power Reactor
See Reactor (Parr Shoals Power)
Carrier Vessel Reactor
See Reactor (A1W)
Centrifugal pumps
See Pumps (centrifugal)
Cesium chloride–lithium chloride–rubidium chloride–sodium chloride systems, fuel cell applications, **3**: 2
CETR
See Reactor (Indian Point Power)
Channels, void static distribution in boiling, **2**: 28
Channels (circular)
See also Tubes
hydrodynamic characteristics, **1**: 59
superheated-steam heat transfer, **2**: 19–20
Channels (fuel), spacing measurement methods, **1**: 32
temperature determination methods, **1**: 30
Channels (rectangular), boiling songs, **1**: 29
burnout, **3**: 17–21
flow distribution determination, steady state, **1**: 32
superheated-steam heat transfer, **2**: 19–20
Channels (square), hydrodynamic characteristics, **1**: 59
Chapelcross Reactors (UK)
See Reactors (Chapelcross)(UK)
Chemonuclear reactors
See Reactors (chemonuclear)
Chlorine, reactions with uranium carbides, **1**: 47
Chromium, cooling with mercury, **3**: 15
Chromium-molybdenum steel
See Steel (chromium-molybdenum)
Circular fuel channels
See Channels (circular)
Coal, Canadian reserves, **2**: 1–2
European reserves, **2**: 1–2
U. S. reserves, **2**: 1–3
Coaxial cables, **4**: 36
COD(S-4) process, corrosion of reactor materials, **3**: 45
reactor decontamination, effectiveness, **3**: 45
Columbium
See Niobium
Combustion Engineering–General Nuclear Engineering Corp., nuclear superheater research, **3**: 76–82
Commonwealth Edison Reactor
See Reactor (Dresden Power)
Concrete
See also specific types of concrete, e.g., Limonite, etc.
shielding properties at elevated temperatures, **2**: 34–5
shielding properties, water loss effects on, **2**: 35
Conduction (thermal)
See Thermal conductivity
Conferences, Reactor Kinetics Conference, Sun Valley, Idaho, Oct. 12–14, 1960, **2**: 22–30
Consolidated Edison Thorium Reactor
See Reactor (Indian Point Power)
Construction practices, **2**: 44–51
Containment, **2**: 31–3
Dresden Power Reactor, **4**: 66–7
Yankee Power Reactor, **3**: 55
Containment vessels, heat transfer after cooling-system rupture, **2**: 31–2
pressure suppression, **2**: 32–3
Control materials, **4**: 39–46
Control rods, boiling-water reactors, **3**: 87
cadmium-indium-silver alloys, **3**: 48–51
Dresden Power Reactor, **4**: 43, 45–6, 59
failure of boron–stainless steel systems, **4**: 43, 45–6
failure in Experimental Boiling-Water Reactor, **4**: 43, 45–6
nuclear superheaters, **3**: 79, 82
Organic-Moderated Reactor Experiment, **4**: 45
Shippingport Pressurized-Water Reactor, **4**: 45
Sodium Modular Reactor, **3**: 93, 95
Vallecitos Boiling-Water Reactor, **4**: 45
Yankee Power Reactor, **3**: 48–50
Convection (forced), in annuli, **2**: 13–15
burnout, **3**: 24
coefficients in superheated steam, **2**: 19
in spray cooling, **4**: 22
Convection (free), boiling heat transfer, **2**: 17
burnout, **2**: 17–18; **3**: 17–21
Conventional power plants
See Power plants (conventional)
Coolant flow, BONUS Reactor, **3**: 76–82
organic-cooled and -moderated reactors, **1**: 59
Pathfinder Power Reactor, **3**: 82
sodium graphite reactors, **3**: 90
Sodium Modular Reactor, **3**: 93, 94
supercritical water reactors, **2**: 79–80
Coolant radioactivity, Experimental Boiling-Water Reactor, **3**: 65–9
Coolants, helium, **1**: 63
decomposition of organic in Organic-Moderated Reactor Experiment, **4**: 76, 80, 82
purification of organic, **2**: 82–3
Cooling (spray)
See Spray cooling
Cooling systems, design modifications in Sodium Reactor Experiment, **4**: 73
Dresden Power Reactor, **4**: 61–2, 63–6
heat transfer during rupture of pressurized water, **2**: 31–2
Yankee Power Reactor, **3**: 50–2, 54
Copper, cooling with mercury, **3**: 15
corrosion by carbon monoxide, carbon monoxide–carbon dioxide systems, and carbon monoxide–hydrogen systems, **3**: 43–4
neutron absorption cross section, **1**: 19
Copper (chrome-plated), cooling with mercury, **3**: 15
Copper–europium hexaboride systems
See Europium hexaboride–copper systems
Corrosion inhibitors, hydrogen peroxide–carbonate solutions, **3**: 44–6
Coupled reactors
See Reactors (coupled)
Critical assemblies
See Reactor (name of critical assembly)
Critical experiments, **3**: 4–12; **4**: 11–13
BR-3 Reactor, **1**: 22
High-Temperature Test Facility, **1**: 23–4
plutonium-graphite systems, **1**: 23
plutonium-Plexiglas systems, **1**: 23
Thorium Uranium Physics Experimental Program, **1**: 22–3
uranium-zirconium alloys (zirconium-clad), **1**: 23–4
uranyl nitrate–water systems, **1**: 23
Yankee Power Reactor, **1**: 21–2
Criticality
See as subheading under specific reactor, alloys, etc.

D

Dancoff integral, **1**: 16
Decontamination, carbon steel, **2**: 49–50
  water in pressurized-water reactors, **3**: 44–6
Departure from nucleate boiling, **3**: 24
  heat transfer from horizontal tubes, **1**: 27–9
Deuterium oxide
  See Heavy water
DIMPLE pile oscillator
  See Reactor (DIMPLE)
DNB
  See Departure from nucleate boiling
Doppler effect, in thermal reactors, **4**: 14–17
Doppler temperature coefficients, **1**: 12–14
Dounreay Fast-Breeder Reactor (UK)
  See Reactor (Dounreay Fast-Breeder)(UK)
Dowtherm A, thermal-neutron diffusion, **1**: 16–17
Dragon Reactor (UK)
  See Reactor (Dragon)(UK)
Dresden Power Reactor
  See Reactor (Dresden Power)
Ducts, design for gas-cooled reactors, **1**: 65–7
Dungeness Reactors (UK)
  See Reactors (Dungeness)(UK)
Dysprosium, reactivity-worth burnup, **4**: 42
Dysprosium oxide, reactivity worth, **4**: 41

E

EBWR
  See Reactor (Experimental Boiling-Water)
Economics of nuclear power, **4**: 1–10
  See also specific power reactors
  Enrico Fermi Fast-Breeder Reactor fuel-fabrication costs, **4**: 93
  heavy-water reactors, **2**: 62–4, 67, 68, 69–73
  Plutonium-Fuel Fast-Breeder Reactor, **4**: 93, 94
  remote power stations, **2**: 4–9
  seed-blanket reactors, **3**: 38–41
  sodium graphite reactors, **3**: 92; **4**: 8, 9
EDF Reactors (France)
  See Reactors (EDF)(France)
EGCR
  See Reactor (Experimental Gas-Cooled)
EL-4 Reactor (France)
  See Reactor (EL-4)
Elk River Power Reactor
  See Reactor (Elk River)
ELPHR
  See Reactor (Experimental Low-Temperature Process-Heat)
Energy, available from coal, **2**: 2–3
  available from uranium, **2**: 2–3
Engineering Test Reactor
  See Reactor (Engineering Test)
Enriched uranium
  See Uranium (enriched); Uranium (highly enriched)
Enriched uranium dioxide
  See Uranium dioxide (enriched)
Enrico Fermi Fast-Breeder Reactor
  See Reactor (Enrico Fermi Fast-Breeder)
Epoline-n (boron carbide impregnated), moderating properties, **3**: 5
Erbium, reactivity-worth burnup, **4**: 42
Erbium oxide, reactivity worth, **4**: 40
Ethanol, reactions with uranium carbides, **1**: 47
Ethylene glycol, reactions with uranium carbides, **1**: 47
  synthesis from methanol, **3**: 1
ETR
  See Reactor (Engineering Test)
Europe, coal reserves, **2**: 1–2
Europium, reactivity-worth burnup, **4**: 42
Europium hexaboride, corrosion by steam, **4**: 44
  radiation effects, **4**: 44
  solubility in boiling water, **4**: 43
Europium hexaboride–copper systems, reactivity worth, **4**: 39, 40
Evaluation, **1**: 1–2
Experimental Boiling-Water Reactor
  See Reactor (Experimental Boiling-Water) (EBWR)
Experimental Breeder Reactors
  See Reactors (Experimental Breeder) (EBR)
Experimental Gas-Cooled Reactor
  See Reactor (Experimental Gas-Cooled) (EGCR)
Experimental Low-Temperature Process-Heat Reactor
  See Reactor (Experimental Low-Temperature Process-Heat)
Experimental Organic-Cooled Reactor
  See Reactor (Experimental Organic-Cooled)
Exponential experiments, **4**: 11–13

F

Fast-breeder reactors
  See Reactors (fast-breeder)
Federal regulations, radiation-protection standards, **1**: 43–4
Fermi Fast-Breeder Reactor
  See Reactor (Enrico Fermi Fast-Breeder)
Ferrophosphorus concrete, shielding properties, **2**: 34
  shielding properties at elevated temperatures, **2**: 35
Ferrous alloys
  See Iron alloys; Stainless steel; Steel; specific iron alloys
Finned fuel elements
  See Fuel elements (finned)
Fission-gas release, BORAX-IV Reactor, **1**: 54
  Experimental Boiling-Water Reactor, **1**: 52–54
  Shippingport Pressurized-Water Reactor, **1**: 54
  temperature effects on rates, **1**: 54
  uranium, **1**: 54–5
  uranium dioxide fuel elements, **1**: 65
  uranium dioxide–thorium oxide systems, **1**: 52–3
  Vallecitos Boiling-Water Reactor, **1**: 54
Flanges, leaks in Calder Hall Reactors, **3**: 69–70
Florida Power Reactor
  See Reactor (Florida Power)
Fluid flow, **1**: 27–33; **3**: 13–28; **4**: 19–30
  effect of rate on burnout, **2**: 18
  heat-transfer effects on stability, **2**: 17
  hydrodynamic instability, **2**: 27–8
Fluid flow (turbulent), boiling heat transfer, **2**: 15–18
Fluid flow (two-phase), **4**: 28–9, 31
  boiling heat transfer, **2**: 15–18
  slip-velocity determination, **2**: 26
  transients, **3**: 24
Fluid-fuel reactors
  See Reactors (fluid-fuel)
Fluorine, reactions with uranium carbides, **1**: 47
Foils (gold), neutron-attenuation measurements, **2**: 34
Foils (sulfur), neutron-attenuation measurements, **2**: 34
Forced convection
  See Convection (forced)
Free convection
  See Convection (free)
Freeze seals
  See Seals (freeze)
Fuel cells, cesium chloride–lithium chloride–rubidium chloride–sodium chloride systems, **3**: 2
  in combination with reactors, **3**: 2–3
  lithium hydride, **3**: 2–3
Fuel channels
  See Channels (fuel)
Fuel conversion ratio, **1**: 5–9
Fuel cycles, **1**: 3–10; **3**: 38–41; **4**: 37–8
Fuel development, **2**: 38–43
Fuel elements, Advanced Organic-Moderated Reactor, **1**: 61–2
  burnup, **1**: 61–2
  CANDU Reactor, **2**: 65–6, 74
  comparison of various dispersions, **1**: 61
  criticality of Puerto Rico Nuclear Center Research Reactor, **3**: 7
  design for fast-breeder reactors, **4**: 84–96
  development, **1**: 45–56
  Enrico Fermi Fast-Breeder Reactor, **1**: 51–2; **4**: 85, 93
  Experimental Gas-Cooled Reactor, **1**: 63-5; **3**: 6
  exponential experiments in uranium, **2**: 10
  Hallam Power Reactor, **1**: 51
  NPD-2 Reactor, **2**: 65
  nuclear superheater, **3**: 76–80
  organic-moderated and -cooled reactors, **1**: 58–62
  Piqua Power Reactor, **1**: 58, 60–1
  sodium graphite reactors, **3**: 88, 90
  spray-cooled reactors, **1**: 75–6
  temperature determination methods, **1**: 30
  thermal conductivity of uranium dioxide, **2**: 38–43
  uranium-aluminum alloys, **1**: 58, 61
  uranium-beryllium alloys, **1**: 61–2
  uranium carbide–plutonium carbide systems, **1**: 51
  uranium carbides, **1**: 52; **3**: 91
  uranium dioxide, **1**: 75–8; **4**: 85
  uranium dioxide–thorium oxide systems, radiation effects, **1**: 52–4
  uranium-graphite systems, **1**: 61–2
  uranium-magnesium alloys, **1**: 61
  uranium-molybdenum-aluminum alloys (aluminum-clad, finned), **1**: 60
  uranium-niobium alloys, **1**: 61–2
  uranium-zirconium alloys, **1**: 61–2
  Variable Moderator Reactor, **1**: 77–8
Fuel elements (finned), fabrication, **1**: 60
  heat transfer in organic reactors, **1**: 58
Fuel elements (pins), application in Plutonium-Fuel Fast-Breeder Reactor, **4**: 94
  radiation effects, **4**: 84–5
Fuel elements (plates), application in Plutonium-Fuel Fast-Breeder Reactor, **4**: 94
  buckling measurements on uranium, **2**: 11–12
  burnout, **1**: 38
  heat transfer, **4**: 19–20
  uranium-molybdenum alloys, **1**: 58
Fuel elements (rods), boiling-water reactors, **3**: 86–7
  buckling measurements on uranium, **2**: 11–12
  buckling measurements on uranium dioxide, **2**: 11
  criticality of plutonium-aluminum alloys, (Zircaloy-2-clad), **3**: 6
  design modifications in Sodium Reactor Experiment, **4**: 73–4
  design of rods and assemblies for Dresden Power Reactor, **4**: 56–9
  Doppler effect, **4**: 14
  fast-fission factors, **3**: 4–5
  flux hardening effects, **1**: 11–12
  heat transfer, **2**: 20

Fuel elements (rods) (Continued)
heat transfer by gas, **1**: 29–30
nuclear measurements, **3**: 5
Fuel elements (thimbles), sodium graphite reactors, **3**: 88–9
Sodium Modular Reactor, **3**: 93–4
Fuel elements (tubes), criticality of uranium dioxide (aluminum-clad), **3**: 4
Heavy-Water Components Test Reactor, **2**: 65
NPD-2 Reactor, **2**: 65
uranium dioxide (Zircaloy-2-clad), **2**: 65, 67–70
uranium-zirconium alloys (Zircaloy-clad), **2**: 65
Yankee Power Reactor, **3**: 47–8
Fuel elements (Zircaloy-clad), autoclave testing, **2**: 49
Fuel handling, Dresden Power Reactor, **4**: 65–6
Yankee Power Reactor, **3**: 54–5
Fuel pins
See Fuel elements (pins)
Fuel plates
See Fuel elements (plates)
Fuel-processing plants, nuclear safety, **4**: 14
Fuel resources, **2**: 1–3
Fuel rods
See Fuel elements (rods)
Fuel thimbles
See Fuel elements (thimbles)
Fuel tubes
See Fuel elements (tubes)
Fuel washing systems, design modifications in Sodium Reactor Experiment, **4**: 74
Furfural, moderating properties, **3**: 4
Furfuryl alcohol, moderating properties, **3**: 4

G

Gadolinium, flux hardening effects, **1**: 11–12
Gamma radiation
See Radiation (gamma)
Gas-cooled heavy-water reactors
See Reactors (gas-cooled heavy-water-moderated)
Gas-cooled reactors
See Reactors (gas-cooled)
Gas-Cooled Reactor Experiments
See Reactors (Gas-Cooled, Experiment)
Gas disposal, **2**: 87–8
from Piqua Power Reactor, **2**: 24–8
Gas flow, determination methods, **1**: 29
duct design, **1**: 65–7
Gas-solid systems
See Solid-gas systems
Gaseous diffusion process, cost factors, **1**: 3–5
GCRE
See Reactors (Gas-Cooled, Experiment)
General Electric Company, nuclear superheater research, **3**: 72–5
General Electric Test Reactor
See Reactor (General Electric Test)
General Nuclear Engineering Corp.–Combustion Engineering
See Combustion Engineering–General Nuclear Engineering Corp.
Glands, leaks in Calder Hall Reactors, **3**: 69–70
Glass (boron)
See Boron (glass)
GLEEP Reactor
See Reactor (GLEEP)
Godiva Critical Facility
See Reactor (Godiva Critical Facility)
Godiva Reactors
See Reactors (Godiva)
Gold, neutron absorption cross section, **1**: 19
reactivity worth, **4**: 39, 40
Gold foils
See Foils (gold)
Graphite, moderating properties, **3**: 6–7
neutron absorption cross sections, **1**: 19–20
Graphite-moderated reactors
See Reactors (graphite moderated)
Graphite-plutonium systems
See Plutonium-graphite systems

H

Hafnium diboride, corrosion by steam, **4**: 44
radiation effects, **4**: 44
solubility in boiling water, **4**: 43
Half-fast reactors
See Reactors (coupled)
Hallam Power Reactor
See Reactor (Hallam Power)
Hanford Production Reactors
See Reactors (Hanford Production)
Hanford Test Reactor
See Reactor (Hanford Test)
Heat transfer, **1**: 27–33; **2**: 13–21; **3**: 13–28; **4**: 19–30
mathematical analysis, **3**: 26–7
Heavy water, recovery in Experimental Boiling-Water Reactor, **2**: 59
Heavy-water boiling reactors
See Reactors (heavy-water boiling)
Heavy-Water Components Test Reactor
See Reactor (Heavy-Water Components Test)
Heavy-water-cooled organic-moderated reactors
See Reactors (Organic-cooled heavy-water-moderated)
Heavy-water-moderated reactors
See Reactors (heavy-water)
Heavy water–uranyl nitrate systems
See Uranyl nitrate–heavy water systems
Helium, corrosion problems caused by impurities, **3**: 43–4
reactor cooling, **1**: 63
Heterogeneous reactors
See Reactors (heterogeneous)
High-Flux Isotope Reactor
See Reactor (High-Flux Isotope)
High-Temperature Test Facility
See Reactor (High-Temperature Test Facility)
Hinkley Point Reactors (UK)
See Reactors (Hinkley Point)(UK)
HIPPO
See Reactor (HIPPO)
Homogeneous Reactor Experiments
See Reactors (Homogeneous, Experiment)
Homogeneous reactors
See Reactors (homogeneous)
Horizontal tubes
See Tubes (horizontal)
Hot-channel factors, **1**: 30–2
HTTF
See Reactor (High-Temperature Test Facility)
Humboldt Bay Reactor
See Reactor (Humboldt Bay Power)
Hunterston Reactors (UK)
See Reactors (Hunterston)(UK)
Hydraulic effects, **2**: 26–8
Hydrazine, synthesis from ammonia, **3**: 1–2
Hydrogen, corrosion of iron alloys, **3**: 43
corrosion of nickel alloys, **3**: 43
reactions with uranium carbides, **1**: 47
Hydrogen–carbon monoxide systems
See Carbon monoxide–hydrogen systems
Hydrogen peroxide–carbonate solution, corrosion inhibition applications, **3**: 44–6
Hydrogen sulfide, reactions with uranium carbides, **1**: 47

I

Inconel alloy, corrosion by carbon monoxide, carbon monoxide–carbon dioxide systems, and carbon monoxide–hydrogen systems, **3**: 43–4
Inconel 702 alloy, corrosion by carbon monoxide, carbon monoxide–carbon dioxide systems, and carbon monoxide–hydrogen systems, **3**: 43–4
Inconel X alloy, corrosion by ammonium citrate process solutions, **3**: 45
corrosion by carbon monoxide, carbon monoxide–carbon dioxide systems, and carbon monoxide–hydrogen systems, **3**: 43–4
corrosion by sodium bisulfate process solutions, **3**: 44
Indian Point Power Reactor
See Reactor (Indian Point Power)
Indium, flux hardening effects, **1**: 11–12
Indium-cadmium-silver alloys
See Cadmium-indium-silver alloys
Instrumentation, **4**: 34–6
Shippingport Pressurized-Water Reactor, **2**: 52, 56; **4**: 35
Yankee Power Reactor, **3**: 53–4
Iodine, reactions with uranium carbides, **1**: 47
Iron, shielding properties, **2**: 35
Iron alloys, corrosion by carbon dioxide, **3**: 43
corrosion by carbon monoxide, **3**: 43
corrosion by hydrogen, **3**: 43

J

JAPC Reactor (Japan)
See Reactor (JAPC)(Japan)
Jezebel Plutonium Critical Facility
See Reactor (Jezebel Plutonium Critical Facility)
JPDR Reactor (Japan)
See Reactor (JPDR)(Japan)

K

Kahl Reactor (West Germany)
See Reactor (Kahl)(West Germany)
Kerosene, reactions with uranium carbides, **1**: 47
KEWB
See Reactors (Kinetic Experiment on Water Boilers)
Kinetic Experiment on Water Boilers
See Reactors (Kinetic Experiment on Water Boilers)(KEWB)

L

Latina Reactor (Italy)
See Reactor (Latina)(Italy)
Lead, reactions with uranium carbides, **1**: 46
Leaks, Calder Hall Reactors, **3**: 69–70
Experimental Boiling Water Reactor, **3**: 56
Limonite concrete, shielding properties at elevated temperatures, **2**: 34–5
Liquid-metal-cooled reactors
See Reactors (liquid-metal-cooled)
Liquid-metal pumps
See Pumps (liquid-metal)
Liquid metals
See Metals (liquid)
Lithium-aluminum alloys
See Aluminum-lithium alloys
Lithium chloride–cesium chloride–rubidium chloride–sodium chloride systems
See Cesium chloride–lithium chloride–rubidium chloride–sodium chloride systems

Lithium hydride, fuel cell applications, **3**: 2–3
Lithium-6–magnesium alloys, reactivity worth, **4**: 40
instabilities in boiling pentane, **3**: 27
Los Alamos Scientific Laboratory, criticality accident, August 1945, **2**: 29
Loss-of-coolant accidents, **1**: 38–9
experiments in ZEEP, **2**: 11
Lutetium, flux hardening effects, **1**: 11–12
reactivity-worth burnup, **4**: 42

M

Magnesium-lithium alloys
See Lithium-magnesium alloys
Magnesium-uranium alloys
See Uranium-magnesium alloys
Magnetite concrete, shielding properties at elevated temperatures, **2**: 34
Magnetite limonite concrete, shielding properties at elevated temperatures, **2**: 34–5
Marine reactors
See Reactors (marine)
Maritime Gas-Cooled Reactor
See Reactor (Maritime Gas-Cooled)
McMurdo Sound Reactor
See Reactor (McMurdo Sound)
Mercury, heat transfer, **3**: 15–17
Metal-water reactions, rates, **1**: 39–40
Metals (liquid)
See also specific metals and alloys
flow partitioning with variable orifices, **4**: 19
heat transfer, **3**: 15–17
pumping, **2**: 59–61
Methanol, ethylene glycol synthesis from, **3**: 1
MGCR
See Reactor (Maritime Gas-Cooled)
ML-1 Reactor
See Reactor (ML-1)
Moderators (canned), sodium graphite reactors, **3**: 89
Sodium Modular Reactor, **3**: 93, 95
Molybdenum, corrosion by carbon dioxide–carbon monoxide systems, carbon monoxide, and carbon monoxide–hydrogen systems, **3**: 43–4
reactions with uranium carbides, **1**: 46
Molybdenum-aluminum-uranium alloys
See Uranium-molybdenum-aluminum alloys
Molybdenum-silicon-uranium systems
See Uranium-molybdenum-silicon systems
Molybdenum-uranium alloys
See Uranium-molybdenum alloys
Monel alloy, corrosion by ammonium citrate process solutions, **3**: 45
corrosion by carbon dioxide–carbon monoxide systems, carbon monoxide, and carbon monoxide–hydrogen systems, **3**: 43–4

N

NaK
See Sodium-potassium alloys (liquid)
Natural convection
See Convection (free)
Neuglobsow Reactor (East Germany)
See Reactors (Neuglobsow)(East Germany)
Neutron-activation distribution measurements, High-Temperature Test Facility, **1**: 23–4
uranium-zirconium alloys (zirconium-clad), **1**: 23–4
Neutron economy, in heavy-water reactors, **2**: 64
Neutron radiation
See Radiation (neutron)
Neutrons, attenuation in zirconium, **2**: 36
background source in new reactors, **1**: 17–19
penetration through iron slabs, **2**: 35
production per fission of uranium-235 in uranium-238, average, **1**: 19
reflection by beryllium, **3**: 10
Neutrons (thermal), capture spectra, **2**: 34
diffusion in Dowtherm A, **1**: 16–17
diffusion in water, **1**: 16–17
penetration through boral, **2**: 36
New Production Reactor
See Reactor (New Production)
Nichrome V alloy, reactions with uranium carbides, **1**: 46
Nickel, cooling with mercury, **3**: 15
Nickel (chrome-plated), cooling with mercury, **3**: 15
Nickel alloys
See also specific nickel alloys
corrosion by carbon dioxide, **3**: 43
corrosion by carbon monoxide, **3**: 43
corrosion by hydrogen, **3**: 43
Niobium, corrosion by carbon monoxide, carbon monoxide–carbon dioxide systems, and carbon monoxide–hydrogen systems, **3**: 43–4
reactions with uranium carbides, **1**: 46
Niobium-titanium alloys, corrosion by carbon monoxide, carbon monoxide–carbon dioxide systems, and carbon monoxide–hydrogen systems, **3**: 43–4
reactions with uranium carbides, **1**: 46
Niobium-uranium alloys
See Uranium-niobium alloys
Niobium-zirconium alloys, corrosion by carbon monoxide, carbon monoxide–carbon dioxide systems, and carbon monoxide–hydrogen systems, **3**: 43–4
Nitric acid process, corrosion of reactor materials, **3**: 45
Nitrogen, reactions with uranium carbides, **1**: 46–7
NPD Reactors
See Reactors (NPD)(Canada)
NRU Reactor
See Reactor (NRU)(Canada)
N.S. *Savannah* Reactor
See Reactor (N.S. *Savannah*)
Nuclear power, economics, **2**: 4–9
Nuclear power plants
See Power plants (nuclear)
Nuclear safety guide, **4**: 13–14
Nuclear superheaters
See Superheaters (nuclear)
Nucleate boiling
See Boiling (nucleate)

O

Oak Ridge National Laboratory, criticality accident, **2**: 29
OCDRE
See Reactor (Organic-Cooled Deuterium, Experiment)(OCDRE)
OMRE
See Reactor (Organic-Moderated, Experiment)(OMRE)
Oralloy
See Uranium (highly enriched)
Organic coolants
See Coolants
Organic-Cooled Deuterium Reactor Experiment
See Reactor (Organic-Cooled Deuterium, Experiment)(OCDRE)
Organic-cooled heavy-water-moderated reactors
See Reactors (organic-cooled heavy-water-moderated)
Organic materials
See specific organic materials
Organic-Moderated Reactor Experiment
See Reactor (Organic-Moderated, Experiment)(OMRE)
Organic-moderated reactors
See Reactors (organic-cooled and -moderated)
ORNL Critical Experiments Facility
See Reactor (ORNL Critical Experiments Facility)
Oxalic acid process, corrosion of reactor materials, **3**: 45
Oxygen, reactions with uranium carbides, **1**: 46–7

P

Pajarito Critical Assemblies Facility
See Reactors (Pajarito Critical Assemblies Facility)
Parr Shoals Reactor
See Reactor (Parr Shoals Power)
Pathfinder Reactor
See Reactor (Pathfinder Power)
PCTR
See Reactor (Physical Constants Testing)
Pentane, instabilities in boiling loops, **3**: 27
Permanganate solutions, corrosion film oxidation, **3**: 44
PFFBR
See Reactor (Plutonium-Fuel Fast-Breeder)
Phenanthrenes, alkyl-, evaluation as reactor coolants, **4**: 79
radiation effects, **4**: 79
Phosphoric acid process, corrosion of reactor materials, **3**: 45
Physical Constants Testing Reactor
See Reactor (Physical Constants Testing)
Pins (fuel)
See Fuel elements (pins)
Pipes, steam-line corrosion, **3**: 65–6
Piqua Reactor
See Reactor (Piqua Power)
PL-2 Reactor
See Reactor (PL-2)
Plexiglas, moderating properties, **3**: 5
Plexiglas-plutonium systems
See Plutonium-Plexiglas systems
Plutonium, criticality, **3**: 8, 9
neutron multiplication measurements, **3**: 5
Plutonium-239, alpha activities, specific, **1**: 19
breeding ratios, **1**: 9
flux hardening effects, **1**: 11–12
radiation effects, **4**: 86
resonance fission integrals, **4**: 13
Plutonium-240, alpha activities, specific, **1**: 19
Plutonium-241, flux hardening effects, **1**: 11–12
resonance fission integrals, **4**: 13
Plutonium-aluminum alloys, fuel-element applications in organic reactors, **1**: 58
Plutonium-aluminum alloys (Zircaloy-2-clad), criticality, **3**: 6
Plutonium carbide–uranium systems
See Uranium–plutonium carbide systems
Plutonium carbide–uranium carbide systems
See Uranium carbide–plutonium carbide systems
Plutonium carbides, physical properties, **1**: 48
Plutonium dioxide–uranium dioxide systems
See Uranium dioxide–plutonium dioxide systems
Plutonium-Fuel Fast-Breeder Reactor
See Reactor (Plutonium-Fuel Fast-Breeder)
Plutonium-fuel reactors
See Reactors (plutonium-fuel)

Plutonium-graphite systems, criticality measurements, **1**: 23
Plutonium-Plexiglas systems, criticality measurements, **1**: 23
Plutonium Recycle Test Reactor
See Reactor (Plutonium Recycle Test)
Plutonium-uranium alloys
See Uranium-plutonium alloys
PM-1 Reactor
See Reactor (PM-1)
PM-2A Reactor
See Reactor (PM-2A)
Polyphenyls
See also Terphenyl
gas removal, **2**: 84–8
purification, **2**: 82–3
Popsy Critical Assembly
See Reactor (Popsy Critical Assembly)
Potassium-sodium alloys (liquid)
See Sodium-potassium alloys (liquid)
Power excursions, research, **2**: 22–5
Power plants (conventional), economics of remote, **2**: 4–9
Power plants (nuclear), economics of remote, **2**: 4–9
Power plants (remote), **2**: 4–9
cooling with mercury, **3**: 15–16
Power reactors
See Reactors (power)
Preamplifiers, **4**: 36
Pressure drop, effect on burnout, **2**: 18
Pressure tube reactors
See Reactors (pressure tube)
Pressure vessels, ASME codes for design and construction, **2**: 44–8
ASTM specifications for reactor, **4**: 50–1
British specifications for reactor, **4**: 51–4
design for Advanced Gas-Cooled Reactor, **4**: 52, 54
design for Berkeley Reactors, **4**: 52, 54
design for Bradwell Reactors, **4**: 52, 54
design for Calder Hall Reactors, **4**: 52, 54
design for Chapelcross Reactors, **4**: 54
design for Dragon Reactor, **4**: 52
design for Dresden Power Reactor, **4**: 62
design for Hunterston Reactors, **4**: 52, 54
design for Latina Reactor, **4**: 52, 54
nuclear superheaters, **3**: 79
radiation effects, **2**: 46
sodium graphite reactors, **3**: 90
Yankee Power Reactor, **3**: 52–3
Pressure waves, propagation in steam-water systems, **4**: 31
Pressurized Critical Assembly
See Reactor (Pressurized Critical Assembly
Pressurized-water reactors
See Reactors (pressurized-water)
Process Development Pile
See Reactor (Process Development Pile)
Process heat reactors
See Reactors (process heat)
PRTR
See Reactor (Plutonium Recycle Test)
Puerto Rico Nuclear Center Research Reactor
See Reactor (Puerto Rico Nuclear Center Research)
Puerto Rico Reactor
See Reactor (BONUS)
Pumps, Dresden Power Reactor, **4**: 64–5
leakage in heavy-water reactors, **4**: 70–3
SL-1 Reactor, **1**: 69
Pumps (centrifugal), liquid-metal pumping, **2**: 59–61
Pumps (liquid-metal), Hallam Power Reactor, **2**: 59–61
sodium graphite reactors, **3**: 90
PWR
See Reactor (Shippingport Pressurized-Water)

R

Radiation (alpha), specific activities in plutonium-239, **1**: 19
specific activities in plutonium-240, **1**: 19
Radiation (gamma), materials for shielding, **3**: 36
penetration through iron slabs, **2**: 35
from uranium-239 decay at 74 kev, **1**: 16
Radiation (neutron), penetration through iron slabs, **2**: 35
Radiation (thermal)
See Thermal radiation
Radiation chemistry, ethylene glycol synthesis from methanol, **3**: 1
hydrazine synthesis from ammonia, **3**: 1
Radiation effects, alkylphenanthrenes, **4**: 79
beryllium, **1**: 65
borides, **4**: 42–3, 44
boron, **4**: 44
boron carbide, **4**: 44
fuel pins in Experimental Breeder Reactor-II, **4**: 84–5
organic coolants, **4**: 76, 79, 82
plutonium-239, **4**: 86
pressure vessels, **2**: 46
uranium, **1**: 54–5
uranium-235, **4**: 86
uranium-239, **4**: 84–5
uranium alloys, **4**: 84–5
uranium carbides, **1**: 48–50
uranium dioxide–thorium oxide systems, **1**: 52–4
uranium-molybdenum alloys, **1**: 60
uranium-molybdenum-aluminum alloys, **1**: 60
uranium-molybdenum-silicon systems, **1**: 60
Zircaloy-2 tubing, **3**: 42–3
Radiation protection, regulations, **1**: 43–4
Radioisotopes, nuclear properties, **4**: 32–3
Rapsodie Reactor (France)
See Reactor (Rapsodie)(France)
Reactivity excursions, **1**: 37–8
fast-breeder reactors, **4**: 86–96
Reactor containment
See Containment
Reactor control
See also Control rods
Dresden Power Reactor, **4**: 61, 62–3, 67
sodium graphite reactors, **3**: 92–3
Yankee Power Reactor, **3**: 53–4, 55
Reactor fuel elements
See Fuel elements
Reactor instrumentation
See Instrumentation
Reactor physics, **1**: 11–26; **2**: 10–12; **3**: 4–12; **4**: 11–18
Reactor safety, criticality hazards, **4**: 13–14
Experimental Boiling-Water Reactor, **3**: 59
metal-water reactions, **1**: 37–42
radiation from power reactors, **4**: 33
Yankee Power Reactor, **3**: 47
Reactor shielding
See Shielding (biological)
Reactor transfer functions, **2**: 25–6
Reactors, ASME specifications for pressure vessels, **2**: 44–8
ASTM specifications for pressure vessels, **4**: 50–1
British specifications for pressure vessels, **4**: 51–4
in combination with fuel cells, **3**: 2–3
core instrumentation, **4**: 34–6
decontamination by COD(S-4) process, **3**: 45
design, **2**: 44–51; **4**: 50–68
dynamics, **1**: 34–6; **3**: 29–35
hazards, **1**: 37–42
kinetics, **2**: 22–30
operating experience, **3**: 56–70; **4**: 69–75
spray cooling, **4**: 20–5
Reactor (A1W), carbon steel applications, **2**: 49
Reactor (Advanced Gas-Cooled)(UK), pressure-vessel design, **4**: 52, 54
steam-cycle efficiency, **4**: 48
Reactor (Advanced Organic-Moderated), fuel-element development, **1**: 61–2
Reactor (Advanced Sodium Graphite), design, **3**: 91–3
Reactors (AGN-201), radiation chemistry applications of AGN-201M, **3**: 2
Reactor (AGR)(UK)
See Reactor (Advanced Gas-Cooled)(UK)
Reactor (Alco Products Critical Facility), critical experiments, **3**: 7–8
Reactor (APS-1)(USSR), steam-cycle efficiency, **4**: 48
Reactor (Argonne Low-Power)
See Reactor (SL-1)
Reactor (AVR)(West Germany), steam-cycle efficiency, **4**: 48
Reactors (Berkeley)(UK), pressure-vessel design, **4**: 52, 54
steam-cycle efficiency, **4**: 48
Reactors (beryllium-moderated)
See also Reactor (General Electric Test) (GETR)
breeding ratios, **1**: 8
economics, **4**: 3, 4, 5
steam-cycle efficiency, **4**: 48
Reactor (BN-50)(USSR), steam-cycle efficiency, **4**: 48
Reactor (Bohunice)(Czechoslovakia), steam-cycle efficiency, **4**: 48
Reactors (boiling-water), **1**: 68-70
See also Reactor (BONUS); Reactors (BORAX); Reactor (Byeloyarsk)(USSR); Reactor (Dresden Power); Reactor (Elk River Power); Reactor (Experimental Boiling-Water); Reactor (Humboldt Bay Power); Reactor (JPDR)(Japan); Reactor (Kahl)(West Germany); Reactors (Kinetic Experiment on Water Boilers); Reactor (Pathfinder Power); Reactor (PL-2); Reactor (SENN)(Italy); Reactor (SL-1); Reactor (Vallecitos Boiling-Water); Reactor (Variable Moderator)
applications for remote power stations, **2**: 4–9
control rods, **3**: 87
dynamics, **3**: 29–33
economics, **4**: 8, 9
marine applications, **3**: 86–7
stability, **1**: 34–5
Reactor (BONUS), bibliographies, **1**: 57
development, **3**: 76–82
economics, **4**: 3, 4, 5
steam-cycle efficiency, **4**: 48
Reactors (BORAX), fission-gas release in BORAX-IV, **1**: 54
reactivity excursions in BORAX-I, **1**: 38
stability, **1**: 34
step tests on BORAX-IV, **2**: 25
superheated-steam heat transfer in BORAX-V, **2**: 19–20
superheater design for BORAX-V, **1**: 71–3
superheater development for BORAX-V, **3**: 82–3
water analysis in BORAX-IV, **3**: 63
Reactor (BR-3)(Belgium), critical experiments, **1**: 22
steam-cycle efficiency, **4**: 48
Reactor (HR-5)(USSR), fuel materials, **4**: 85
Reactors (Bradwell)(UK), pressure-vessel design, **4**: 52, 54
steam-cycle efficiency, **4**: 48
Reactors (Bulk Shielding), $1/\rho$ measurements in BSR-I, **2**: 25
$1/\beta$ measurements in BSR-II, **2**: 25
criticality experiments, **3**: 7
Reactor (Byeloyarsk)(USSR), steam-cycle efficiency, **4**: 48

Reactors (Calder Hall)(UK), duct design, I: 66–7
leak testing, 3: 69–70
pressure-vessel design, 4: 52, 54
resonance integrals, I: 15
Reactor (CANDU)(Canada), design, 2: 65–6, 74; 4: 65
economics, 4: 3, 4
steam-cycle efficiency, 4: 48
Reactor (Carolinas-Virginia Power) *See* Reactor (Parr Shoals Power)
Reactors (Chapelcross)(UK), pressure-vessel design, 4: 54
Reactors (chemonuclear), 3: 1–2
Reactor (Commonwealth Edison) *See* Reactor (Dresden Power)
Reactors (coupled), 2: 29
Reactor (DIMPLE)(UK), Doppler temperature coefficients measurement on, I: 12–13
resonance integrals, I: 19
Reactor (Dounreay Fast-Breeder)(UK), steam-cycle efficiency, 4: 49
Reactor (Dragon)(UK), pressure-vessel design, 4: 52
Reactor (Dresden Power), control, 4: 61, 62–3, 67
control-rod composition, 4: 46
control-rod failure, 4: 43, 45–6
core instrumentation, 4: 35
design details, 4: 56–68
fuel-fabrication costs, 4: 5
spatial power distribution stability, 2: 26
steam-cycle efficiency, 4: 48
Reactors (Dungeness)(UK), steam-cycle efficiency, 4: 48
Reactors (EDF)(France), steam-cycle efficiency, 4: 48
Reactor (EL-4)(France), 2: 74
Reactor (Elk River Power), bibliographies, I: 57
economics, 4: 3, 4, 5
steam-cycle efficiency, 4: 48
Reactor (Engineering Test), control-rod experience, 4: 45
Reactor (Enrico Fermi Fast-Breeder), bibliographies, I: 57
Doppler effect, 4: 16–17
economics, 4: 3, 4, 5
fuel elements, I: 51–2; 4: 85
fuel-fabrication costs, 4: 93
fuel materials, 4: 85
steam-cycle efficiency, 4: 49
Reactor (Experimental Boiling-Water)(EBWR), control-rod failure, 4: 43, 45–6
core instrumentation, 4: 35
dynamics, 3: 29–33
economics, 4: 3
fission-gas release, I: 52–4
fuel elements, radiation effects, I: 52–4
heavy-water recovery, 2: 59
inspection after operation, 3: 56–69
operating experience, 3: 65–69
stability, I: 34
steam contamination, I: 54
steam-cycle efficiency, 4: 48
step tests, 2: 25
superheater experiments, 3: 82–3
vapor-recovery system testing, 2: 59
test-report list, 3: 62–3
Reactors (Experimental Breeder)(EBR), core design of EBR-I, I: 35
economics of EBR-II, 4: 3, 5
radiation effects on fuel pins in EBR-II, 4: 84–5
steam-cycle efficiency of EBR-II, 4: 49
Reactor (Experimental Gas-Cooled)(EGCR), I: 63–5
cooling system, I: 29–30
core instrumentation, 4: 35
economics, 4: 3, 5
fuel-element critical experiments, 3: 6
lattice-parameter measurements, I: 23
steam-cycle efficiency, 4: 48
temperature coefficient of reactivity, I: 15
test loops, 3: 6
Reactor (Experimental Low-Temperature Process-Heat), design, I: 1–2
Reactor (Experimental Organic-Cooled)(EOCR), design, 4: 76
Reactors (fast-breeder), 4: 84–96
See also Reactor (BN-50)(USSR); Reactor (BR-5)(USSR); Reactor (Dounreay Fast-Breeder)(UK); Reactor (Enrico Fermi Fast-Breeder); Reactors (Experimental Breeder); Reactor (Plutonium-Fuel Fast-Breeder); Reactor (Rapsodie)(France); Reactor (ZEBRA)(UK); Reactor (ZPR-3)
applications for remote power stations, 2: 4
economics, 4: 8, 9
Reactor (Florida Power), bibliographies, I: 57
design, 2: 73–6
economics, 4: 3, 4, 5
steam-cycle efficiency, 4: 48
Reactors (fluid-fuel), applications for remote power stations, 2: 4
Reactors (gas-cooled), I: 63–7
See also Reactor (Advanced Gas-Cooled)(UK); Reactor (AVR)(West Germany); Reactors (Berkeley)(UK); Reactor (Bohunice)(Czechoslovakia); Reactors (Bradwell)(UK); Reactors (Calder Hall)(UK); Reactors (Chapelcross)(UK); Reactor (Dragon)(UK); Reactors (Dungeness)(UK); Reactors (EDF)(France); Reactor (Experimental Gas-Cooled)(EGCR); Reactor (Gas-Cooled, Experiment)(GCRE); Reactor (GLEEP)(UK); Reactor (Hanford Test); Reactors (Hinkley Point)(UK); Reactors (Hunterston)(UK); Reactor (JAPC)(Japan); Reactor (Latina)(Italy); Reactor (ML-1); Reactor (Maritime Gas-Cooled); Reactor (Neuglobsow)(East Germany); Reactors (Sizewell)(UK); Reactors (Trawsfynydd)(UK); Reactor (TREAT)
applications for remote power stations, 2: 4
cooling systems, I: 29–32
Reactors (Gas-Cooled, Experiment)(GCRE), core instrumentation of GCRE-I, 4: 35
Reactors (gas-cooled heavy-water-moderated) *See* Reactor (EL-4)(France); Reactor (Florida Power)
Reactor (General Electric Test)(GETR), control-rod failure, 4: 43, 45–6
superheater tests, 3: 72
Reactor (GLEEP), neutron absorption cross-section measurements, I: 20
Reactors (Godiva), power excursion in Godiva-I, 2: 29
power excursions in Godiva-II, 2: 24
Reactor (Godiva Critical Facility), 3: 8–9
Reactors (graphite-moderated)
See also Reactors (sodium graphite); Reactor (Advanced Gas-Cooled)(UK); Reactor (APS-1)(USSR); Reactor (AVR)(West Germany); Reactors (Berkeley)(UK); Reactor (Bohunice)(Czechoslovakia); Reactors (Bradwell)(UK); Reactors (Calder Hall)(UK); Reactors (Chapelcross)(UK); Reactor (Dragon)(UK); Reactors (Dungeness)(UK); Reactors (EDF); Reactor (Experimental Gas-Cooled)(EGCR); Reactor (Gas-Cooled, Experiment)(GCRE); Reactor (GLEEP)(UK); Reactor (Hanford Test); Reactors (Hinkley Point)(UK); Reactors (Hunterston)(UK); Reactor (JAPC)(Japan); Reactor (Latina)(Italy); Reactor (Neuglobsow)(East Germany); Reactor (New Production); Reactor (Physical Constants Testing); Reactors (Sizewell)(UK); Reactor (Thermal Test); Reactors (Trawsfynydd)(UK); Reactor (TREAT)
breeding ratios, I: 8
Reactor (Hallam Power), bibliographies, I: 57
core II, 3: 91
economics, 4: 3, 4, 5
flow orifices, 4: 19
freeze seals, 4: 55
fuel elements, I: 51; 3: 91
pumps, liquid-metal, 2: 59–61
seals, 2: 60–1
steam-cycle efficiency, 4: 49
valve design, 4: 54–6
Reactors (Hanford Production), core instrumentation, 4: 35
Reactor (Hanford Test), neutron absorption cross-section measurements, I: 19–20
Reactors (heavy-water), 2: 62–77
See also Reactor (CANDU)(Canada); Reactor (DIMPLE)(UK); Reactor (Florida Power); Reactor (Heavy-Water Components Test); Reactor (HIPPO)(Canada); Reactor (NPD)(Canada); Reactor (NRU)(Canada); Reactor (Parr Shoals); Reactor (Plutonium Recycle Test); Reactor (Process-Development Pile); Reactor (Spectral Shift Control); Reactor (ZEEP)(Canada); Reactor (Zoé)(France)
applications for remote power stations, 2: 4
breeding ratios, I: 8
physics, 2: 11
pump leakage, 4: 70–3
supercritical water reactors, 2: 78–81
valve leakage, 4: 70–3
Reactors (heavy-water boiling), design, 2: 65–6
Reactor (Heavy-Water Components Test), burnout, 3: 21
carbon steel applications, 2: 49
design, 2: 74
fuel elements, 2: 65
Reactors (heavy-water-moderated organic-cooled) *See* Reactors (organic-cooled heavy-water-moderated)
Reactors (heterogeneous)
See also specific reactors
flux hardening effects, I: 11–12
Reactor (High-Flux Isotope), burnout, 3: 17–21
criticality studies on mockup, 3: 7
Reactor (High-Temperature Test Facility), criticality measurements, I: 23–4
neutron-activation distribution measurements, I: 23–4
Reactors (Hinkley Point)(UK), steam-cycle efficiency, 4: 48
Reactor (HIPPO)(Canada), temperature coefficient of reactivity, 2: 11
Reactors (homogeneous)
See also Reactor (Gas-Cooled, Experiment)(GCRE); Reactors (Homogeneous, Experiment)(HRE); Reactor (TREAT)
critical experiments, 3: 7
Reactors (Homogeneous, Experiment)(HRE), fuel instability in HRE-II, 2: 26
Reactor (Humboldt Bay Power), economics, 4: 3, 4, 5
pressure suppression during cooling-system rupture, 2: 32–3
steam-cycle efficiency, 4: 48
Reactors (Hunterston)(UK), pressure-vessel design, 4: 52, 54
steam-cycle efficiency, 4: 48
Reactors (hydride-moderated) *See* Reactor (Maritime Gas-Cooled); Reactor (SNAP Experimental)
Reactor (Indian Point Power), core instrumentation, 4: 35
critical experiments, I: 22–3
economics, 4: 3, 4
steam-cycle efficiency, 4: 48
Reactor (JAPC)(Japan), steam-cycle efficiency, 4: 48

Reactor (Jezebel Plutonium Critical Facility), **3**: 8
Reactor (JPDR)(Japan), steam-cycle efficiency, **4**: 48
Reactor (Kahl)(West Germany), steam-cycle efficiency, **4**: 48
Reactors (Kinetic Experiment on Water Boilers)(KEWB), power excursions, **2**: 23–4
  transfer-function measurements, **3**: 33
Reactor (Latina)(Italy), pressure-vessel design, **4**: 52, 54
  steam-cycle efficiency, **4**: 48
Reactors (liquid-metal-cooled)
  See also Reactors (sodium graphite); Reactor (BN-50)(USSR); Reactor (BR-5)(USSR); Reactor (Dounreay Fast-Breeder)(UK); Reactor (Enrico Fermi Fast-Breeder); Reactors (Experimental Fast-Breeder); Reactor (Plutonium-Fuel Fast-Breeder); Reactor (Rapsodie)(France); Reactor (SNAP Experimental); Reactor (ZEBRA)(UK); Reactor (ZPR-3)
  economics, **4**: 8, 9
Reactor (McMurdo Sound), fuel-fabrication costs, **4**: 5
  steam-cycle efficiency, **4**: 48
Reactor (ML-1), criticality experiments on ML-1-1B, **4**: 12
  design parameters, **2**: 7
Reactors (marine)
  See also Reactor (Maritime Gas-Cooled); Reactor (N.S. *Savannah*)
  boiling-water reactors, **3**: 86–7
Reactor (Maritime Gas-Cooled), corrosion problems, **3**: 43–4
Reactor (Neuglobsow)(East Germany), steam-cycle efficiency, **4**: 48
Reactor (New Production), carbon steel applications, **2**: 49
Reactors (NPD)(Canada), buckling measurements on fuel rods of NPD-1, **2**: 11
  design of NPD-2, **2**: 64–5, 74
  steam-cycle efficiency of NPD-2, **4**: 48
Reactor (NRU)(Canada), approach-to-critical experiments, **2**: 11
  temperature coefficient of reactivity, **2**: 11
Reactor (N.S. *Savannah*), core instrumentation, **4**: 35
  shielding, **3**: 36
Reactors (organic-cooled and -moderated), **1**: 58–62; **4**: 76–83
  See also Reactors (organic-cooled heavy-water-moderated); Reactor (Advanced Organic-Moderated); Reactor (Experimental Organic-Cooled)(EOCR); Reactor (Organic-Moderated, Experiment)(OMRE); Reactor (Piqua Power)
  applications for remote power stations, **2**: 4, 6
  criticality experiments in USSR, **1**: 23
Reactor (Organic-Cooled Deuterium, Experiment)(OCDRE), design, **2**: 76
Reactors (organic-cooled heavy-water-moderated)
  See also Reactor (Organic-Cooled Deuterium, Experiment)(OCDRE)
  design, **4**: 76
  economics, **4**: 8, 9
Reactor (Organic-Moderated, Experiment)(OMRE), control-rod experience, **4**: 45
  core instrumentation, **4**: 35
  design, **1**: 58; **4**: 76–83
Reactor (ORNL Critical Experiments Facility), critical experiments on highly enriched uranium, **3**: 7
Reactors (Pajarito Critical Assemblies Facility), **3**: 9–10
Reactor (Parr Shoals Power), bibliographies, **1**: 57
  design, **2**: 73, 74
  economics, **4**: 3, 4, 5
  steam-cycle efficiency, **4**: 48
Reactor (Pathfinder Power), bibliographies, **1**: 57
  economics, **4**: 3, 4, 5
  steam-cycle efficiency, **4**: 48
  superheater development, **3**: 82
Reactor (Physical Constants Testing), Experimental Gas-Cooled Reactor fuel-element testing, **3**: 6
  graphite moderating properties measurement, **3**: 6–7
  neutron absorption cross-section measurements, **1**: 19–20
  temperature coefficient of reactivity, **1**: 15
Reactor (Piqua Power), auxiliary systems, **2**: 82–8
  bibliographies, **1**: 57
  core instrumentation, **4**: 35
  design, **4**: 76
  economics, **4**: 3, 4, 5
  fuel elements, **1**: 58, 60–1
  steam-cycle efficiency, **4**: 49
Reactor (PL-2), design parameters, **2**: 7
  economics at remote locations, **2**: 6–8
Reactors (plutonium-fuel)
  See also Reactor (BN-50)(USSR); Reactor (BR-5)(USSR); Reactor (Jezebel Plutonium Critical Facility); Reactor (Plutonium-Fuel Fast-Breeder); Reactor (Plutonium Recycle Test); Reactor (Rapsodie)(France)
  breeding ratios, **1**: 7–8
  reactivity factors, **4**: 86–96
Reactor (Plutonium-Fuel Fast-Breeder), fuel-element design, **4**: 94
  fuel-fabrication costs, **4**: 93
Reactor (Plutonium Recycle Test), core instrumentation, **4**: 35
  design, **2**: 73–4
  pump design, **4**: 71–3
Reactors (PM), core instrumentation in PM-1, **4**: 35
  design parameters in PM-1, **2**: 7
  design parameters in PM-2A, **2**: 7
Reactor (Popsy Critical Assembly), **3**: 8
Reactors (power)
  See also specific power reactors
  breeding ratios, **1**: 5–9
  heat transfer, **2**: 20
  radiation from, **4**: 33
Reactors (pressure-tube), **2**: 65–7
  See also Reactor (Byeloyarsk)(USSR); Reactor (CANDU)(Canada); Reactor (New Production); Reactor (Parr Shoals Power)
Reactor (Pressurized Critical Assembly), criticality studies, **2**: 10
Reactors (pressurized-water)
  See also Reactor (A1W); Reactor (APS-1)(USSR); Reactor (BR-3)(Belgium); Reactor (Experimental Low-Temperature Process-Heat); Reactor (High-Temperature Test Facility); Reactor (Indian Point Power); Reactor (McMurdo Sound); Reactor (N.S. *Savannah*); Reactors (PM); Reactor (Pressurized Critical Assembly); Reactor (Saxton Power); Reactor (SELNI)(Italy); Reactor (Shippingport Pressurized-Water); Reactors (SM); Reactor (Spectral Shift Control); Reactors (SPERT); Reactor (Ulyanovsk)(USSR); Reactor (Veronezh)(USSR); Reactor (Yankee Power)
  applications for remote power stations, **2**: 4–9
  economics, **4**: 8, 9
  heat transfer during cooling-system rupture, **2**: 31–2
  thermal analysis, **1**: 32
  water decontamination, **3**: 44–6
Reactor (Process Development Pile), buckling measurements, **2**: 11–12
  thermal-neutron distribution measurements, **2**: 10–11
Reactors (process heat)
  See also Reactor (Low-Temperature Process-Heat)
  evaluation, **1**: 1–2
Reactor (Puerto Rico)
  See Reactor (BONUS)
Reactor (Puerto Rico Nuclear Center Research), fuel-element criticality, **3**: 7
Reactor (Rapsodie)(France), fuel materials, **4**: 85
Reactors (Savannah River), step tests, **2**: 25
Reactor (Saxton Power) bibliographies, **1**: 57
  fuel-fabrication costs, **4**: 5
  steam-cycle efficiency, **4**: 48
Reactors (seed-blanket), economic potentials, **3**: 38–41
Reactor (SELNI)(Italy), economics, **4**: 3, 4
  steam-cycle efficiency, **4**: 48
Reactor (SENN)(Italy), economics, **4**: 3, 4, 5
  steam-cycle efficiency, **4**: 48
Reactor (Shippingport Pressurized-Water), control-rod experience, **4**: 45
  core design, **2**: 52–3
  core modifications, **2**: 58
  economics, **4**: 3, 5
  fission-gas release, **1**: 54
  fuel cycle, **3**: 38–41
  fuel-element thermal conductivity, **2**: 41
  instrumentation, **2**: 52, 56; **4**: 35
  refueling, **2**: 52–8
  steam-cycle efficiency, **4**: 48
  step tests, **2**: 25
Reactors (Sizewell)(UK), steam-cycle efficiency, **4**: 48
Reactor (SL-1), **1**: 68–70
Reactors (SM), control-rod failure of SM-1, **4**: 43, 45–6
  critical experiments on SM-2, **3**: 7–8
  economics of SM-1, **4**: 3
  economics of SM-2 at remote locations, **2**: 6–8
  nuclear measurements on SM-1, **3**: 8
  steam-cycle efficiency of SM-1, **4**: 48
  pressure suppression during cooling-system rupture of SM-1, **2**: 33
Reactors (small power)
  See also Reactor (AVR)(West Germany); Reactor (BONUS); Reactor (Dounreay Fast-Breeder)(UK); Reactor (Experimental Boiling-Water)(EBWR); Reactors (Experimental Breeder); Reactor (Kahl)(West Germany); Reactor (McMurdo Sound); Reactor (ML-1); Reactor (Piqua Power); Reactors (PM); Reactor (Saxton Power); Reactor (SL-1); Reactors (SM); Reactor (Sodium, Experiment)(SRE); Reactor (Vallecitos Boiling-Water)
  invitation to bid on 22,000 kw(e), **1**: 1
Reactor (SNAP Critical Assembly), critical measurements, **3**: 4
Reactor (SNAP Experimental), criticality experiments, **4**: 12
Reactor (Sodium, Experiment)(SRE), control-rod experience, **4**: 45
  core instrumentation, **4**: 35
  design modifications, **4**: 73–4
  economics, **4**: 3, 5
  oscillation measurements, **3**: 33–4
  steam-cycle efficiency, **4**: 49
Reactors (sodium graphite), **3**: 89–96
  See also Reactor (Advanced Sodium Graphite); Reactor (Hallam Power); Reactor (Sodium, Experiment)(SRE); Reactor (Sodium Modular)
  applications for remote power stations, **2**: 4
  economics, **3**: 92; **4**: 8, 9
  pressure vessels, **3**: 90
Reactor (Sodium Modular), **3**: 93–6
Reactor (Spectral Shift Control), criticality experiments, **4**: 12

Reactors (SPERT), hydrodynamic instabilities in SPERT-IA, 2: 27–8
oscillator program in SPERT-I, 2: 25
power excursions in SPERT-I, 2: 22–3
reactivity excursions in SPERT-I, 1: 38
stability, 1: 34
steam voids in SPERT-IA, 2: 27
Reactors (spray-cooled), 1: 74–7
Reactors (supercritical-water), 2: 78–81
Reactors (superheater)
See Superheaters (nuclear); Reactor (BONUS); Reactor (Byeloyarsk)(USSR); Reactor (Elk River Power); Reactor (Pathfinder)
Reactors (thermal), Doppler effect, 4: 14–17
Reactor (Thermal Test), neutron multiplication and exponential experiments, 3: 6
Reactor (Topsy Critical Facility), 3: 8
Reactors (Trawsfynydd)(UK), steam-cycle efficiency, 4: 48
Reactor (TREAT), burnout, 1: 40–1
kinetics, 3: 34
power excursions, 2: 24–5
Reactor (Ulyanovsk)(USSR), steam-cycle efficiency, 4: 48, 49
Reactor (Vallecitos Boiling-Water), control-rod experience, 4: 45
fission-gas release, 1: 54
fuel-fabrication costs, 4: 5
SADE loop superheater experiments, 3: 74–5
stability, 1: 34
steam-cycle efficiency, 4: 48
Reactor (Variable Moderator), 1: 77–8
critical assemblies, 3: 4
Reactor (Veronezh)(USSR), steam-cycle efficiency, 4: 48
Reactors (water-cooled)
See Reactors (water-cooled and -moderated); Reactor (ML-1); Reactor (New Production); Reactor (Thermal Test)
Reactors (water-cooled and -moderated)
See also Reactors (boiling-water); Reactors (pressurized-water); Reactor (Alco Products Critical Facility); Reactors (Bulk Shielding); Reactor (Engineering Test); Reactor (General Electric Test)(GETR); Reactors (Homogeneous, Experiment) (HRE); Reactor (ORNL Critical Experiments Facility)
breeding ratios, 1: 6–8
metal-water reaction studies, 1: 37
power distribution, 1: 17
critical experiments, 1: 21–2
nuclear constants measurements, 1: 21
Reactor (Yankee Power), 3: 47–55
bibliographies, 1: 57
core instrumentation, 4: 35
critical experiments, 1: 21–2
economics, 4: 3, 4, 5, 6
operating experience, 4: 69–70
power distributions in critical experiments, 1: 17
steam-cycle efficiency, 4: 48
Reactor (ZEBRA)(UK), buckling measurements, 2: 11
Reactor (ZEEP)(Canada), reactivity, 2: 11
Reactor (Zoé)(France), neutron absorption cross-section measurements, 1: 20
Reactor (ZPR-3), step tests, 2: 25
Rectangular channels
See Channels (rectangular)
Refueling, Shippingport Pressurized-Water Reactor, 2: 52–8
Sodium Modular Reactor, 3: 94
Rods
See Fuel elements (rods)
Remote power plants
See Power plants (remote)
Rubidium chloride–cesium chloride–lithium chloride–sodium chloride systems
See Cesium chloride–lithium chloride–rubidium chloride–sodium chloride systems

S

SADE loop, superheater studies, 3: 74–5
Saline water conversion, reactor application, 1: 2
Samarium, flux hardening effects, 1: 11–12
reactivity-worth burnup, 4: 42
Samarium hexaboride, corrosion by steam, 4: 44
radiation effects, 4: 44
Santowax OMB
See also Polyphenyls
gas removal, 2: 84–8
purification, 2: 82–3
Santowax R
See Terphenyl
Savannah River production reactors
See Reactors (Savannah River)
Saxton Power Reactor
See Reactor (Saxton Power)
Seals, BORAX-V superheater, 3: 83
Hallam Power Reactor, 2: 60–1
leakage in Calder Hall Reactors, 3: 69–70
Seals (freeze), Hallam Power Reactor, 2: 60; 4: 55
Seed-blanket reactors
See Reactors (seed-blanket)
SELNI (Italy) Power Reactor
See Reactor (SELNI)(Italy)
SENN (Italy) Power Reactor
See Reactor (SENN)(Italy)
Shielding (biological), 2: 34–7; 3: 36–7; 4: 32–3
Dresden Power Reactor, 4: 67–8
SL-1 Reactor, 1: 68
Yankee Power Reactor, 3: 54
Shippingport Pressurized-Water Reactor
See Reactor (Shippingport Pressurized-Water)
Shutdown, Yankee Power Reactor, 3: 47
Silicon, reactions with uranium carbides, 1: 46
Silicon-molybdenum-uranium systems
See Uranium-molybdenum-silicon systems
Silver-cadmium alloys
See Cadmium-silver alloys
Silver-indium-cadmium alloys
See Cadmium-indium-silver alloys
Sizewell Reactors (UK)
See Reactors (Sizewell)(UK)
SL-1 Reactor
See Reactor (SL-1)
Slip velocity, determination, 2: 26
SM Reactors
See Reactors (SM)
Small power reactors
See Reactors (small power)
SNAP Critical Assembly)
See Reactor (SNAP Critical Assembly)
SNAP Experimental Reactor
See Reactor (SNAP Experimental)
Sodium bisulfate process, corrosion of reactor materials, 3: 44
Sodium chloride–cesium chloride–lithium chloride–rubidium chloride systems
See Cesium chloride–lithium chloride–rubidium chloride–sodium chloride systems
Sodium graphite reactors
See Reactors (sodium graphite)
Sodium (liquid), reactions with uranium carbides, 1: 46
valve design for containing, 4: 54–6
Sodium Modular Reactor
See Reactor (Sodium Modular)
Sodium-potassium alloys (liquid), reactions with uranium carbides, 1: 46
Sodium Reactor Experiment
See Reactor (Sodium, Experiment)
Solid-gas systems, heat transfer, 3: 16–17
Spectral Shift Control Reactor
See Reactor (Spectral Shift Control)
SPERT Reactors
See Reactors (SPERT)
Spray-cooled reactors
See Reactors (spray-cooled)
Spray cooling, 4: 20–5
Square fuel channels
See Channels (square)
SRE
See Reactor (Sodium, Experiment)
Stainless steel, applications in supercritical water reactors, 2: 81
corrosion by ammonium citrate process solutions, 3: 45
corrosion by carbon monoxide, carbon monoxide–carbon dioxide systems, and carbon monoxide–hydrogen systems, 3: 43–4
corrosion by oxalic acid process solutions, 3: 45
corrosion by phosphoric acid process solutions, 3: 45
corrosion by sodium bisulfate process solutions, 3: 44
reactions with uranium carbides, 1: 46
Stainless steel–boron systems
See Boron–stainless steel systems
Stainless steel–uranium dioxide cermets
See Uranium dioxide–stainless steel cermets
Stationary Low-Power Plant No. 1
See Reactor (SL-1)
Steam
See also Water vapor
contamination in Experimental Boiling-Water Reactor, 1: 54
corrosion of borides, 4: 43, 44
corrosion of boron, 4: 44
corrosion of boron carbide, 4: 44
corrosion of boron nitride, 4: 43, 44
corrosion of pipes, 3: 65–6
corrosive effects in nuclear superheaters, 3: 72–4
reactions with uranium carbide–zirconium carbide systems, 1: 52
reactions with Zircaloy, 1: 38–9
reactions with zirconium, 1: 38–9
separation from water, 3: 81, 82
superheater cooling, 3: 13–15
Steam (superheated), heat transfer, 2: 19–20
thermal conductivity, 2: 19
viscosity, 2: 19
Steam cycles, efficiency, 4: 47–9
Steam plants, Dresden Power Reactor, 4: 66
Steam-water systems, flow, 4: 28–9, 31
pressure-wave propagation, 4: 31
Steel, compatibility with aluminum, 1: 1–2
corrosion by water, 1: 2
radiation effects in pressure vessels, 2: 46
reactions with uranium carbides, 1: 46
Steel (boron), impact tests, 4: 46
Steel (carbon), corrosion by ammonium citrate process solutions, 3: 45
corrosion by COD(S-4) process solutions, 3: 45
corrosion by nitric acid process solutions, 3: 45
corrosion by oxalic acid process solutions, 3: 45
corrosion by phosphoric acid process solutions, 3: 45
corrosion rates, 2: 49–50
corrosion by sodium bisulfate process solutions, 3: 44
decontamination, 2: 49–50
reactor applications, 2: 49–50
Steel (chromium-molybdenum), corrosion by carbon monoxide, carbon monoxide–carbon dioxide systems, and carbon monoxide–hydrogen systems, 3: 43–4
Steel (stainless)
See Stainless steel

Stellite alloy, corrosion by nitric acid process solutions, **3**: 45
Subcritical assemblies
See Reactor (name of subcritical assembly)
Sulfur foils
See Foils (sulfur)
Supercritical water, technology, **2**: 80–1
Supercritical-water reactors
See Reactors (supercritical-water)
Superheater reactors
See Superheaters (nuclear)
Superheaters (nuclear), **1**: 71–3; **2**: 19–20; **3**: 71–85
See also Reactor (BONUS); Reactor (Byeloyarsk)(USSR); Reactor (Elk River Power); Reactor (Pathfinder Power)
shutdown, **3**: 13–15
spray-cooled reactors, **1**: 75–6; **4**: 24–5

T

Tankers, nuclear propulsion, **3**: 87
Tantalum, reactions with uranium carbides, **1**: 46
Terbium oxide, reactivity worth, **4**: 40
Terphenyl, boiling heat transfer, **4**: 82
properties, **4**: 77–8
reactions with uranium carbides, **1**: 47
Thermal conductivity, mathematical analysis, **2**: 13
perforated solids, **4**: 19–20
Shippingport Pressurized-Water Reactor fuel elements, **2**: 41
superheated steam, **2**: 19
thorium oxide, **1**: 53
uranium-aluminum alloys, **1**: 61
uranium carbides, **1**: 50
uranium dioxide, **1**: 50; **2**: 38–43
uranium-graphite systems, **1**: 61–2
uranium-magnesium alloys, **1**: 61
Thermal effects, **2**: 26–8
Thermal expansion, uranium carbides, **1**: 50
uranium dioxide, **1**: 50
Thermal-neutron diffusion parameters, **1**: 16–17
Thermal neutrons
See Neutrons (thermal)
Thermal radiation, heat transfer, **2**: 20
Thermal reactors
See Reactors (thermal); specific reactors
Thermal Test Reactor
See Reactor (Thermal Test)
Thimbles (fuel)
See Fuel elements (thimbles)
Thorium, Doppler coefficients, **1**: 12–14; **4**: 15–16
Thorium (irradiated), radioactivity, **4**: 37
reactivity, **4**: 37–8
Thorium carbides, physical properties, **1**: 48
Thorium oxide, Doppler coefficients, **4**: 15–16
thermal conductivity, **1**: 53
Thorium oxide–uranium dioxide systems
See Uranium dioxide–thorium oxide systems
Thorium oxide–uranium systems
See Uranium–thorium oxide systems
Thorium Uranium Physical Experimental Program, critical experiments, **1**: 22–3
Tin, shielding applications, **2**: 34
Tin (liquid), reactions with uranium carbides, **1**: 46
Titanium, reactions with uranium carbides, **1**: 46
Titanium diboride, corrosion by steam, **4**: 44
radiation effects, **4**: 44
solubility in boiling water, **4**: 43
Titanium-niobium alloys
See Niobium-titanium alloys
Topsy Critical Facility
See Reactor (Topsy Critical Facility)
Transient analysis, **2**: 28–30
Trawsfynydd Reactors (UK)
See Reactors (Trawsfynydd)(UK)
TREAT Reactor
See Reactor (TREAT)
Tubes
See also Channels (circular) and Fuel elements (tubes)
burnout, **3**: 21–4; **4**: 28
cooling with mercury, **3**: 15–16
criticality effects of aluminum, **2**: 11
criticality effects of Zircaloy-2, **2**: 11
fabrication of Zircaloy-2, **3**: 42
Tubes (horizontal), heat transfer, **1**: 27–9
Tungsten alloys, neutron reflection, **3**: 10
TUPE
See Thorium Uranium Physical Experimental Program
Turbines, inspection of Experimental Boiling-Water Reactor, **3**: 56–7
SL-1 Reactor, **1**: 69
Yankee Power Reactor, **3**: 55
Two-phase flow
See Fluid flow (two-phase)

U

Ulyanovsk Reactor (USSR)
See Reactor (Ulyanovsk)(USSR)
United States, coal reserves, **2**: 1–3
Uranium, background neutron source in new reactors, **1**: 17–19
buckling measurements on plates, **2**: 11–12
buckling measurements on rods, **2**: 11–12
Canadian reserves, **2**: 1–2
criticality studies on beryllium oxide moderated, **2**: 10
Doppler coefficients, **4**: 14–15
Doppler temperature coefficient, **1**: 12–14
European reserves, **2**: 1–2
fission-gas release, **1**: 54–5
neutron reflection, **3**: 10
prices, official AEC, **4**: 1–2
radiation effects, **1**: 54–5
reactions with water, **1**: 40–1
resonance integrals, **1**: 16
thermal-neutron distribution in heavy-water-moderated, **2**: 10–11
U. S. reserves, **2**: 1–3
Uranium (depleted), neutron reflection, **3**: 9–10
Uranium (enriched), background neutron source in Zircaloy-2-clad, **1**: 17–19
cost factors, **1**: 3–5
critical configurations, **3**: 9
neutral reflection, **3**: 10
prices, official AEC, **4**: 1–2
Uranium (highly enriched), criticality, **3**: 7
Uranium (Lucite-clad), buckling measurements, **3**: 5
Uranium-233, breeding ratio, **1**: 7–8
neutron age to indium resonance measurements in water, isoamyl alcohol, cyclohexanone, benzyl alcohol, toluene, formic acid, and a mixture of organic compounds, **1**: 20–1
Uranium-235, flux hardening effects, **1**: 11–12
neutron production per fission in uranium-238, average, **1**: 19
nuclear properties, **3**: 4
radiation effects, **4**: 86
resonance fission integrals, **4**: 13
Uranium-238, cadmium ratios of wire, **2**: 11
neutron production per fission of uranium-235 atom, average, **1**: 19
nuclear properties, **3**: 4
resonance capture, **1**: 16
resonance capture integrals, **4**: 13
Uranium-239, gamma activity from decay at 74 kev, **1**: 16
breeding ratios, **4**: 91–4
fabrication costs, **4**: 5
radiation effects, **4**: 84–5
Uranium alloys, radiation effects, **4**: 84–5
Uranium-aluminum alloys, fuel-element applications in organic reactors, **1**: 58
physical properties, **1**: 61
Uranium-aluminum alloys (aluminum-clad), burnout, **1**: 38
Uranium-beryllium alloys, physical properties, **1**: 61–2
Uranium carbide–plutonium carbide systems, fuel-element applications, **1**: 51
heat-transfer characteristics, **1**: 51
Uranium carbide–zirconium carbide systems, reactions with water and steam, **1**: 52
Uranium carbides, breeding ratios, **1**: 51–2
criticality studies, **1**: 51
development for reactor fuels, **1**: 45–56
fabrication, **1**: 50–1
Hallam Power Reactor fuel elements, **3**: 91
mechanical properties, **1**: 48
physical properties, **1**: 48
preparation, **1**: 50–1
radiation effects, **1**: 48–50
reactions with acetone, **1**: 47
reactions with acids, **1**: 47
reactions with air, **1**: 46–7
reactions with alkalies, **1**: 47
reactions with aluminum, **1**: 45
reactions with ammonia, **1**: 47
reactions with benzene, **1**: 47
reactions with beryllium, **1**: 46
reactions with bismuth, **1**: 46
reactions with bromine, **1**: 47
reactions with carbon dioxide, **1**: 47
reactions with carbon tetrachloride, **1**: 47
reactions with chlorine, **1**: 47
reactions with ethanol, **1**: 47
reactions with ethylene glycol, **1**: 47
reactions with fluorine, **1**: 47
reactions with hydrogen, **1**: 47
reactions with hydrogen sulfide, **1**: 47
reactions with iodine, **1**: 47
reactions with kerosene, **1**: 47
reactions with lead, **1**: 46
reactions with molybdenum, **1**: 46
reactions with Nichrome V alloy, **1**: 46
reactions with niobium, **1**: 46
reactions with niobium-titanium alloys, **1**: 46
reactions with nitrogen, **1**: 46–7
reactions with oxygen, **1**: 46–7
reactions with silicon, **1**: 46
reactions with sodium (liquid), **1**: 46
reactions with sodium-potassium alloys (liquid), **1**: 46
reactions with stainless steel, **1**: 46
reactions with steel, **1**: 46
reactions with tantalum, **1**: 46
reactions with terphenyl, **1**: 47
reactions with tin, **1**: 46
reactions with titanium, **1**: 46
reactions with uranium carbides, **1**: 46
reactions with water vapor, **1**: 47
reactions with xylene, **1**: 47
reactions with zinc (liquid), **1**: 46
reactions with Zircaloy-2 alloy, **1**: 46
reactions with zirconium, **1**: 46
reactions with Zyglo solution, **1**: 47
thermal conductivity, **1**: 50
thermal expansion, **1**: 50
Uranium dioxide, application as fuel in BR-5 Reactor (USSR), **4**: 85
application as fuel in Rapsodie Reactor (France), **4**: 85
breeding ratio, **1**: 7
buckling measurements, **2**: 11
criticality constants of cylinders in water lattices, **4**: 11–12
Doppler coefficients, **4**: 15–16
fabrication costs, **4**: 5
fission-gas release, **1**: 65

Uranium dioxide (Continued)
fuel-element applications, **1**: 75–8; **4**: 85
radiation effects, **1**: 65; **2**: 41
resonance capture, **1**: 16
thermal conductivity, **1**: 50; **2**: 38–43
thermal expansion, **1**: 50
Yankee Power Reactor fuel elements, **3**: 47–8
Uranium dioxide (aluminum-clad), criticality, **3**: 4
Uranium dioxide (enriched), temperature coefficient of reactivity for 7-rod cluster, **1**: 15
Uranium dioxide (stainless-steel-clad), criticality, **2**: 10; **3**: 5
Uranium dioxide (Zircaloy-2-clad), fabrication, **2**: 67–70
NPD-2 Reactor fuel elements, **2**: 65
Uranium dioxide–beryllium oxide systems, criticality experiments on Hastelloy-X-clad, **4**: 12
Uranium dioxide–plutonium dioxide systems, application in Plutonium-Fuel Fast-Breeder Reactor, **4**: 94
criticality studies, **1**: 51–2
Uranium dioxide–stainless steel cermets, application as fuel in Enrico Fermi Fast-Breeder Reactor, **4**: 85
Uranium dioxide–thorium oxide systems, criticality studies, **3**: 7
fission-gas release, **1**: 52–3
radiation effects, **1**: 52–4
Uranium-graphite systems, buckling measurements, **3**: 5
mechanical properties, **1**: 48
physical properties, **1**: 61–2
Uranium-magnesium alloys, physical properties, **1**: 61
Uranium-molybdenum alloys, application in Plutonium-Fuel Fast-Breeder Reactor, **4**: 94
breeding ratios, **1**: 51–2
criticality studies, **1**: 51
fuel-element applications in organic reactors, **1**: 58
heat-transfer characteristics, **1**: 51
radiation effects, **1**: 60
reactions with water, **1**: 40–1
sodium graphite reactor fuel elements, **3**: 90
Uranium-molybdenum-aluminum alloys, radiation effects, **1**: 60
Uranium-molybdenum-aluminum alloys (aluminum-clad, finned), fabrication, **1**: 60
Uranium-molybdenum-silicon systems, radiation effects, **1**: 60
Uranium-niobium alloys, physical properties, **1**: 61–2
Uranium-plutonium alloys, criticality experiments, **4**: 12–13
Uranium–plutonium carbide systems, application in Plutonium-Fuel Fast-Breeder Reactor, **4**: 94
Uranium-238–plutonium-239 systems, breeding effects, **4**: 91–4
Uranium–stainless steel alloys, application in Plutonium-Fuel Fast-Breeder Reactor, **4**: 94
Uranium–thorium oxide systems, fabrication costs, **4**: 5
heat transfer, **4**: 19–20
Uranium-zirconium alloys, physical properties, **1**: 61–2
Uranium-zirconium alloys (Zircaloy-clad), Heavy-Water Components Test Reactor fuel elements, **2**: 65
Uranium-zirconium alloys (zirconium-clad), burnout, **1**: 38
criticality measurements, **1**: 23–4
neutron-activation distribution measurements, **1**: 23–4
Uranyl nitrate–heavy water systems, criticality, **3**: 7
Uranyl nitrate–water systems, criticality measurements, **1**: 23

V

Vallecitos Boiling-Water Reactor
See Reactor (Vallecitos Boiling-Water)
Valves, design for Hallam Power Reactor, **4**: 54–6
design for liquid-sodium applications, **4**: 54–6
leakage in Calder Hall Reactors, **3**: 69–70
leakage in heavy-water reactors, **4**: 70–3
Valves (butterfly), gas-cooled reactor applications, **1**: 66–7
Vanadium diboride, corrosion by steam, **4**: 44
solubility in boiling water, **4**: 43
Vapor-recovery systems, Experimental Boiling-Water Reactor, **2**: 59
Variable Moderator Reactor
See Reactor (Variable Moderator)
Vena contracta, effect on heat-transfer coefficient, **2**: 20
Veronezh Reactor (USSR)
See Reactor (Veronezh)(USSR)

W

Water, corrosion by
See Material corroded
decontamination in pressurized-water reactors, **3**: 44–6
moderating properties, **3**: 4
reactions with uranium, **1**: 40–1
reactions with uranium carbide–zirconium carbide systems, **1**: 52
reactions with Zircaloy, **1**: 37
separation from steam, **3**: 81, 82
thermal-neutron diffusion, **1**: 16–17
Water-cooled and -moderated reactors
See Reactors (water-cooled and -moderated)
Water purification systems, Dresden Power Reactor, **4**: 65
Water vapor
See also Steam
reactions with uranium carbides, **1**: 47
Wolfram
See Tungsten

X

Xylene, reactions with uranium carbides, **1**: 47

Y

Y-12 Plant, criticality accident, June 1958, **2**: 29
Yankee Power Reactor
See Reactor (Yankee)
Ytterbium hexaboride, corrosion by steam, **4**: 44
radiation effects, **4**: 44
solubility in boiling water, **4**: 43
Yttrium hexaboride, corrosion by steam, **4**: 44
radiation effects, **4**: 44
Yttrium tetraboride, corrosion by steam, **4**: 44
radiation effects, **4**: 44

Z

ZEBRA
See Reactor (ZEBRA)
ZEEP Reactor
See Reactor (ZEEP)
Zinc (liquid), reactions with uranium carbides, **1**: 46
Zircaloy alloy, reactions with steam, **1**: 38–9
reactions with water, **1**: 37
Zircaloy-2 alloy, autoclave testing, **2**: 48–9
corrosion by ammonium citrate process solutions, **3**: 45
corrosion by sodium bisulfate process solutions, **3**: 44
criticality effects of tubes, **2**: 11
fabrication into tubing, **3**: 42
heat transfer, **4**: 19–20
radiation effects in tubing, **3**: 42–3
reactions with uranium carbides, **1**: 46
reactions with water, **1**: 40–1
Zirconium, corrosion by nitric acid process solutions, **3**: 45
reactions with steam, **1**: 38–9
reactions with uranium carbides, **1**: 46
shielding properties, **2**: 36
Zirconium carbide–uranium carbide systems
See Uranium carbide–zirconium carbide systems
Zirconium diboride, corrosion by steam, **4**: 44
radiation effects, **4**: 44
solubility in boiling water, **4**: 43
Zirconium hydride, moderator for nuclear superheaters, **3**: 83
Zirconium-niobium alloys
See Niobium-zirconium alloys
Zirconium-uranium alloys
See Uranium-zirconium alloys
Zyglo solution, reactions with uranium carbides, **1**: 47
Zoé Reactor
See Reactor (Zoé)
ZPR-3 Critical Assembly
See Reactor (ZPR-3)

LEGAL NOTICE

This document was prepared under the sponsorship of the U. S. Atomic Energy Commission. Neither the United States, nor the Commission, nor any person acting on behalf of the Commission:

A. Makes any warranty or representation, expressed or implied, with respect to the accuracy, completeness, or usefulness of the information contained in this report, or that the use of any information, apparatus, method, or process disclosed in this report may not infringe privately owned rights; or

B. Assumes any liabilities with respect to the use of, or for damages resulting from the use of any information, apparatus, method, or process disclosed in this report.

As used in the above, "person acting on behalf of the Commission" includes any employee or contractor of the Commission, or employee of such contractor, to the extent that such employee or contractor of the Commission, or employee of such contractor prepares, disseminates, or provides access to, any information pursuant to his employment or contract with the Commission, or his employment with such contractor.

NUCLEAR SCIENCE ABSTRACTS

The U. S. Atomic Energy Commission, Division of Technical Information, publishes *Nuclear Science Abstracts (NSA)*, a semimonthly journal containing abstracts of the literature of nuclear science and engineering.

NSA covers (1) research reports of the U. S. Atomic Energy Commission and its contractors; (2) research reports of government agencies, universities, and industrial research organizations on a world-wide basis; and (3) translations, patents, books, and articles appearing in technical and scientific journals.

Complete indexes covering subject, author, source, and report number are included in each issue. These are cumulated quarterly, semiannually, and annually providing a detailed and convenient key to the literature.

Availability of *NSA*

SALE *NSA* is available on subscription from the Superintendent of Documents, U. S. Government Printing Office, Washington 25, D. C., at $22.00 per year for the semimonthly abstract issues and $15.00 per year for the four cumulated-index issues. Subscriptions are postpaid within the United States, Canada, Mexico, and all Central and South American countries, except Argentina, Brazil, British and French Guiana, Surinam, and British Honduras. Subscribers in these Central and South American countries, and in all other countries throughout the world, should remit $27.50 per year for subscriptions to semimonthly abstract issues and $17.50 per year for the four cumulated-index issues.

EXCHANGE *NSA* is also available on an exchange basis to universities, research institutions, industrial firms, and publishers of scientific information. Inquiries should be directed to the Division of Technical Information Extension, U. S. Atomic Energy Commission, P. O. Box 62, Oak Ridge, Tennessee.

TECHNICAL PROGRESS REVIEWS may be purchased from Superintendent of Documents, U. S. Government Printing Office, Washington 25, D. C. for $2.00 per year for each subscription or for $0.55 per issue. The use of the coupon below will facilitate the handling of your order.

POSTAGE AND REMITTANCE: Postpaid within the United States, Canada, Mexico, and all Central and South American countries except as hereinafter noted. Add $0.50 per year, or $0.15 per single issue, for postage to all other countries, including Argentina, Brazil, British and French Guiana, Surinam, and British Honduras. Payment should be by check, money order, or document coupons, and MUST accompany order. Remittances from foreign countries should be made by international money order, or draft on an American bank, payable to the Superintendent of Documents, or by UNESCO book coupons.

order form

SUPERINTENDENT OF DOCUMENTS
U. S. GOVERNMENT PRINTING OFFICE
WASHINGTON 25, D. C.

Enclosed:
document coupons ☐ check ☐ money order ☐

Charge to Superintendent of Documents No._____

Please send a one-year subscription to

☐ REACTOR CORE MATERIALS
☐ POWER REACTOR TECHNOLOGY
☐ NUCLEAR SAFETY
☐ REACTOR FUEL PROCESSING

(Each subscription $2.00 a year; $0.55 per issue.)

SUPERINTENDENT OF DOCUMENTS
U. S. GOVERNMENT PRINTING OFFICE
WASHINGTON 25, D. C.

(Print clearly)

Name_____

Street_____

City_____ Zone____ State_____